The Effect of Moisture Gradients on the Stiffness and Strength of Yellow-Poplar

by

Terrance Edward Conners

Dissertation submitted to the Faculty of the
Virginia Polytechnic Institute and State University
in partial fulfillment of the requirements for the degree of
DOCTOR OF PHILOSOPHY
in
Forestry and Forest Products

APPROVED:

T. E. McLain, Chairman

G. Ifju

J. N. Reddy

C. Skaar

E. M. Wengert

July, 1985
Blacksburg, Virginia

THE EFFECT OF MOISTURE GRADIENTS ON THE STIFFNESS AND STRENGTH OF YELLOW-POPLAR

by

Terrance Edward Conners

Committee Chairman: Thomas E. McLain

Forest Products

(ABSTRACT)

Wood with a uniform moisture distribution is known to have different mechanical properties compared to wood with a non-uniform moisture distribution. Moisture gradients are likely to develop in full-size members tested in the In-Grade Testing Program and might therefore affect the test results. The purpose of this study was to mathematically model the effect of desorption moisture gradients on the stiffness and strength of yellow-poplar beams. An additional objective was to experimentally determine gradient effects in yellow-poplar beams.

Three-dimensional finite-element modeling was employed and several subsidiary models were developed. Among these was a three-parameter segmented model for fitting digitized tension and compression stress-strain curves. Unlike

previous models (such as the Ramberg-Osgood model), this model has a linear slope up to the point approximately corresponding to the proportional limit. A methodology was also devised whereby most hardwood and softwood elastic constants can be estimated at any moisture content. Data are required at one moisture content.

Equilibrated uniaxial testing was conducted at four moisture contents to acquire data for the finite-element model. It was found that the longitudinal Young's moduli in tension and compression were approximately equal at 6% and 18% moisture content; the compression modulus was greater at 12%, but the tension modulus was greater for green specimens. Intersection points for tension and compression mechanical properties may be different.

Tests of small clear yellow-poplar beams indicated that moisture gradients induced at 12% equilibrium moisture content had little effect on the modulus of rupture up to 19% average moisture content. At higher moisture contents, gradient-containing beams were significantly stronger than equilibrated beams when comparisons were made at identical moisture contents. Modulus of elasticity data exhibited a similar trend, although differences between equilibrated and non-equilibrated beams were observed below 19% moisture content.

The finite-element program was moderately successful in predicting the effects of moisture gradients on the strength and stiffness of yellow-poplar beams. Computer time and storage constraints limited the accuracy of the solutions. Predicted trends were verified by the experimental data. Modeling of full-size lumber indicated that significant moisture gradients will likely influence the stiffness and strength of higher quality lumber.

ACKNOWLEDGEMENTS

I would like to extend my sincere thanks to those many individuals who generously contributed their time and advice towards the completion of this study. I am especially grateful to and Tom McLain for their guidance and insightful comments throughout the course of this work. I would also like to thank Dr. J. N. Reddy for his help with the finite-element program. Drs. Geza Ifju, Chris Skaar and Gene Wengert made many suggestions which contributed to this dissertation, and their discussions are greatly appreciated.

I would also like to thank several fellow graduate students for their technical assistance. explained how to modify his CPAL program for this study, and made numerous suggestions during the writing of the finite-element programs used in this study. totally rewired the controls of the conditioning chamber. , , technicians at the Brooks Forest Products Center at Virginia Tech, all gave generously of their time to help with the log acquisition and sawing. Harold Vandivort deserves special thanks for making the LVDT holder used for the tension tests.

My deepest appreciation is extended to my wife, Without her love, encouragement and support this study could not have been completed.

TABLE OF CONTENTS

LIST OF TABLES

LIST OF FIGURES

Chapter I

INTRODUCTION

Wood is a natural material with a wide range of physical and mechanical characteristics. The usefulness of a piece of wood depends on these characteristics, such as its density, moisture content, the number, type, and position of growth defects, and other traits. Historically, wood technologists and engineers have sought to describe the strength and stiffness of wood in structural sizes by adjusting the results of tests on small clear specimens to account for the characteristics present in the larger pieces (Tiemann, 1906). It has long been recognized, for example, that strength properties for straight-grained, defect-free wood increase as it dries from its green condition to some dry state (Bauschinger, 1887). The best-known description of this relationship is now known as the United States Forest Products Laboratory (USFPL) "exponential formula" (U. S. Forest Products Laboratory, 1974). This equation describes how strength properties vary with moisture content according to a curvilinear relationship over a range from approximately six to thirty percent moisture content (MC). It has been used extensively in the United States to predict the mechanical performance of wood at various moisture contents based on tests at a single moisture content.

In the early years of this century, H. D. Tiemann (1906) inadvertently prepared small clear chestnut beams and compression samples with moisture gradients and found that this material was stiffer and stronger than similar material uniformly seasoned to the same average moisture content. Although Tiemann verified that the core of the material was wetter than the shell, he made no attempt to measure the moisture distribution or to quantify the effect of various gradient severities on the mechanical properties. Wilson (1932) did measure one-dimensional moisture gradients in some specially-prepared specimens, and he also found that specimens with dry outer edges and moist centers could be stronger than similar equilibrated specimens at the same average moisture content (Figure 1).

Wilson's attempts to predict the effect of moisture gradients on the modulus of rupture (MOR) for chestnut were unsuccessful, but his findings are in agreement with the parallel-axis theorem (Popov, 1976). This theorem states that a dry extreme fiber region (with a higher modulus of elasticity (MOE)) would significantly increase the stiffness (EI) of a beam. Uniaxial specimens would be less affected. The locations of the drier areas should not influence the strength and stiffness properties in the same manner as in beams, and it would be more appropriate to apply the Rule of

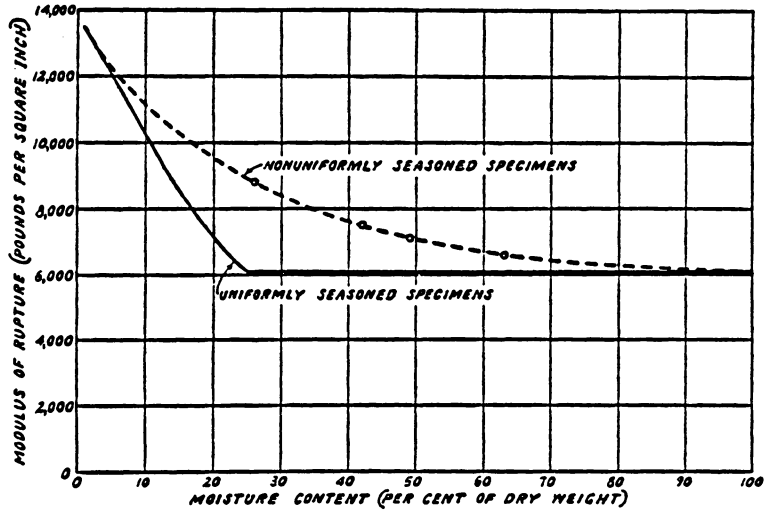

Figure 1: Effect of non-uniform moisture distribution on MOR. (From Wilson, 1932).

Mixtures to predict the stiffness properties than the parallel-axis theorem (Jones, 1975).

The potential effect that moisture gradients could have on mechanical tests of wood has been of little importance historically due to the predominance of tests on small equilibrated specimens. Recent tests indicate, however, that this effect may be significant in tests of full-size lumber. In the mid-1960's, several researchers questioned the philosophy of assigning design stresses to lumber based on hypothetical adjustment factors and began studies to test lumber in structural sizes. As those initial full-size testing studies progressed, the scope of the research was expanded to investigate the influence of moisture content and the manner in which it interacts with the quality of the material. Based upon the analysis of small clear specimens by Tiemann and Wilson, it had been assumed for many years that the strength and stiffness of full-size lumber would also increase as the lumber became drier (Markwardt and Wilson, 1935). The results of the full-size tests indicated, however, that this assumption might not apply to all species and to all grades of lumber (Gerhards, 1968, 1970; Madsen, 1975; Brynildsen, 1977; Hoffmeyer, 1978; Madsen, et al., 1980).

Several studies by various laboratories showed that different grades of green material had varying degrees of changes in the strength properties after drying. The higher grades of wood had the highest degree of stiffness and strength improvement. However, there was significant variation noted among the reported results, especially for the amount of improvement observed for the lower grades investigated. Hoffmeyer attributed the variation to the fact that different procedures were used to bring the lumber to the desired moisture contents and suggested that the discrepancies among the various data sets might be due to the presence of moisture gradients in some of the test material (Hoffmeyer, 1978). Madsen (1975), for example, tested his material while it was drying, and moisture gradients were almost certainly present. In later tests, Madsen, et al. (1980), observed only slight differences between equilibrated and gradient-containing wood (at the same average moisture content) at twenty-two and twelve percent average moisture contents. They did not, however, present any data about the severity of the moisture gradients present in their tests. Without this information, it is impossible to quantitatively assess the effect various moisture gradients might have upon the results of mechanical tests. Aside from Wilson's work in 1932, this aspect of

moisture-strength relations does not appear to have been investigated.

Moisture gradients are also likely to develop in wood under service conditions due to seasonal (or even daily) fluctuations in temperature and relative humidity conditions to which the wood is exposed. Structural members treated with hygroscopic fire-retardant salts are known to develop moisture gradients as well, although in this instance the extreme fiber regions are wetter than the core. The lack of knowledge regarding the effect these gradients have on mechanical properties, and especially the possible benefits to beam tests in the In-Grade Testing Program (Galligan, et al., 1980) is the motivation for this research.

1.1 OBJECTIVES AND SCOPE

Although T. R. C. Wilson (1932) attempted to account for the effects of a one-dimensional moisture content gradient on the mechanical properties of wood, it is likely that two- and three-dimensional moisture gradients are more common both in actual use situations and in previous tests of full-size lumber. Based on this assumption, it appears that a study of the effects of a two-dimensional moisture gradient would be the simplest investigation which might be of practical benefit. Therefore, the primary objective of this

dissertation was to mathematically model and quantify the effects of a two-dimensional desorption moisture gradient (within the cross-section) on the moduli of rupture and elasticity in bending of small clear specimens. Bending analyses were emphasized since beams may be more sensitive to gradients, but the model should be applicable to axial force members as well. The model was experimentally calibrated and verified using test data on yellow-poplar (Liriodendron tulipifera), but the results should be applicable to other reasonably homogeneous species. Due to complicating factors such as defects and the depth effect, full-size tests were not considered in this analysis except in an exploratory manner.

Chapter II

LITERATURE REVIEW

To quantitatively determine how moisture gradients influence the strength and stiffness properties of wood, it is first necessary to know the type of gradients expected. It is also desirable to know what effects of moisture gradients have been observed in previous studies, and how researchers tried to account for the effects of moisture gradients on mechanical properties. This review includes descriptions of previous efforts to form a predictive model of the strength of equilibrated wooden beams as well. It will be shown why these models are inapplicable to beams with moisture gradients, and why a numerical approach to the problem might succeed. Any numerical approach, however, requires more than a description of the expected form of the moisture gradient. Descriptions of the variation of the elastic and strength properties with moisture content are required as well. It must also be decided whether drying history or specific gravity are likely to influence these properties significantly enough that these factors must be accounted for in the experimental design or in a numerical model. The known effects of these factors are reviewed in the final sections of this chapter.

2.1 THE INFLUENCE OF MOISTURE GRADIENTS ON STRENGTH PROPERTIES

2.1.1 The Form of Moisture Gradients

Although both adsorption and desorption gradients are possible, the desorption gradients associated with wood drying are most frequently cited in the forest products literature. These gradients are usually assumed to be parabolic, with the driest portion of the wood lying in the edges of the piece of wood (Hart, 1968; Kawai, et al., 1979; Bramhall, 1979) (Figure 2).

A number of articles have been published that cite experimental evidence for the parabola-shaped gradient. The shape of the gradient was usually determined by oven-drying successive slices across the width of the piece of wood being dried (Wilson, 1932; Sonnleithner, 1933; Bateman, et al., 1939; Krischer, 1942; McMillen,1955a,b; Cech, 1964; Kollmann and Cote, 1968; Moschler and Martin, 1968; Wengert, 1975; Rosen, 1976; Sandoe, et al., 1982). Fernow (1898) and Schaffner (1981) cite data illustrating that the gradient is approximately parabolic in two dimensions, both across the width and the depth of a cross-section.

There is some evidence to suggest that the shape of the moisture content profile may not follow a smooth parabola from the drier edges inwards if the piece of wood being dried has been water-soaked (Bateman, et al., 1939). The

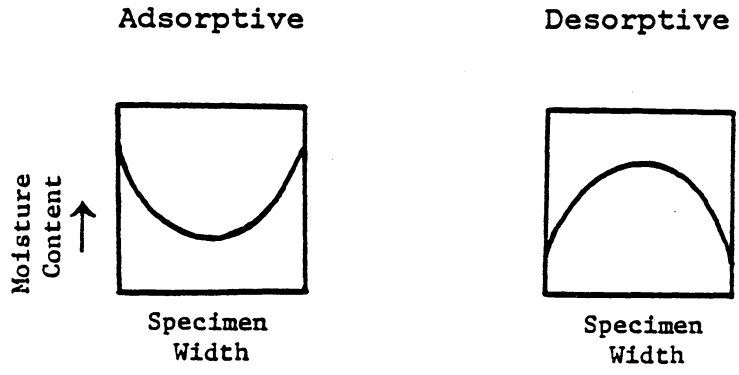

Figure 2: Diagrams of adsorptive and desorptive moisture gradients

slope of the curve increases sharply as it reaches the moisture content on the cross-section approximately corresponding to the fiber saturation point (Figure 3).

Evidence also exists to show that the diffusion coefficients for heartwood and sapwood may be different. This could possibly affect the smoothness of the parabolic moisture content curve in pieces of wood which contain both heartwood and sapwood. The diffusion coefficient values reported by Choong and Fogg (1968) for yellow-poplar do not seem to show any significant differences between heartwood and sapwood, especially for lateral flow. However, lateral flow data for yellow-poplar from Choong and Skaar (1969) appear to be different for heartwood and sapwood; the sapwood diffusion coefficients are greater by approximately twenty percent. The aforementioned articles also stated that the radial diffusion coefficients are greater than the tangential diffusion coefficients by as much as eighty-five percent. This would seem to indicate that wood cross-sections will not dry symmetrically even under ideal conditions. An additional factor which could interfere with a parabolic moisture content distribution is the angle of the longitudinal cell axis to the longitudinal specimen axis (Wengert, 1975; Wengert and Skaar, 1978) According to these authors, moisture movement will likely occur primarily along

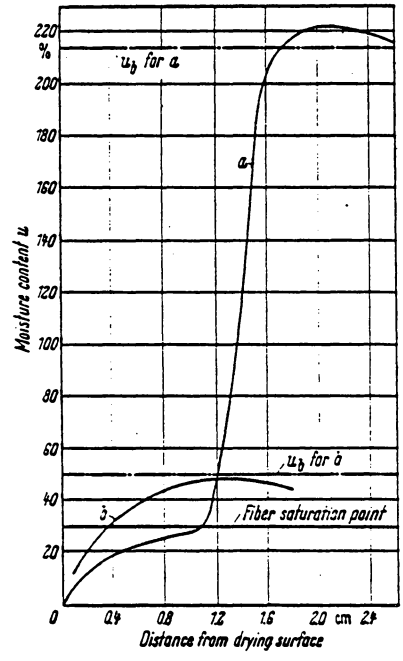

Figure 3: Moisture gradient in tangential drying of Sitka spruce. Curve a: water saturated wood. Curve b: green wood. Ub: original MC before drying. (From Kollmann and Cote, 1968).

the longitudinal cell axis unless especial care is taken to cut the wood perfectly parallel to the grain. Therefore, the differences between the lateral diffusion coefficients alone may be of secondary importance in the formation of an idealized, two-dimensional moisture content gradient.

2.1.2 Strength Property-Moisture Gradient Interactions

Fernow (1896, 1897) appears to have been the first to recognize that non-uniform moisture distribution might affect the results of bending tests. Tiemann (1906) also noted this problem during his attempts to determine the fiber saturation point for chestnut, and he conducted a special study to determine "the relation of casehardening (sic) to the moisture-strength law". His experiments with chestnut demonstrated that, when the shell is drier than the core, the strength properties are greater than those measured for uniformly-seasoned specimens at the same average moisture content. The percentage increase (compared to uniformly-seasoned wood) appears to have been about the same for bending and compression specimens at the same average moisture contents. It should be noted that these data were taken from specimens with a three-dimensional parabolic gradient, as can be seen from the photographs of chestnut cross-sections included as Plate IV, Figure 2 in Tiemann's 1906 report.

Wilson (1932) also induced moisture gradients in various species as part of his investigations, and tested pieces of wood in bending to determine the effect that moisture gradients have on strength. After reviewing the results, he decided that the effect was somewhat species-dependent. It is believed, however, that this conclusion was based upon inadequate data. Figure 4, after Wilson (1932), shows the effect of moisture gradients on two by four chestnut beams with a one-dimensional moisture gradient (through the depth only). The curve for uniformly-seasoned specimens was derived through analysis of equilibrated specimens; it depicts a semi-logarithmic relationship of the modulus of rupture with moisture content up to a moisture content (defined as M_p) at which the strength is equal to the green modulus of rupture. Compared to this curve, the gradient-containing specimens are much stronger on an equal average moisture content basis. His data (Table 1) show that the moisture content (on average) was below his estimated M_p for the outer three-quarters of an inch of the beam. It is assumed that this three-quarters of an inch of drier wood was symmetrical, equalling a total of three square inches out of the eight square inches of cross-sectional area.

In contrast to the chestnut data, Wilson's loblolly pine data (Figure 5) show that there is no apparent effect of

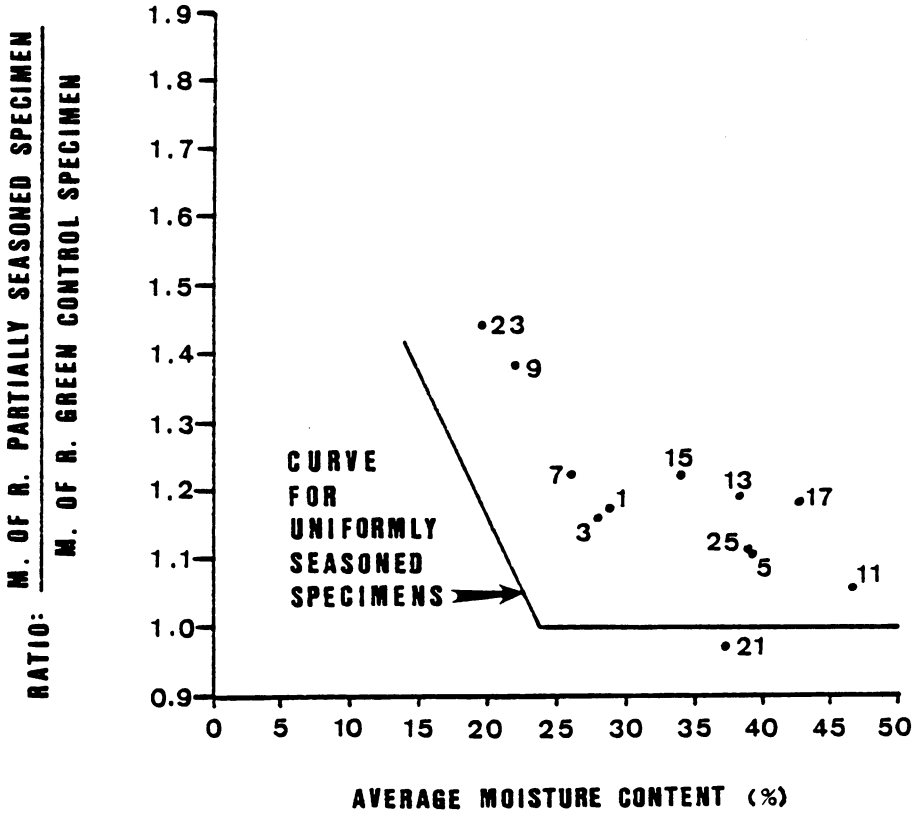

Figure 4: Results of the determination of the modulus of rupture of nonuniformly seasoned 2 by 4 inch specimens of chestnut. (After Wilson, 1932). Labels indicate specimen numbers.

TABLE 1

Moisture distribution data for nonuniformly seasoned 2 by 4 inch specimens of chestnut plotted in Figure 1. (From Wilson, 1932)

Specimen	Moisture Content of Successive Slices From Compression Face of Static Bending Specimen				
	First 1/8"	Second 1/8"	Second 1/4"	Third 1/4"	Fourth 1/4"
1	12.7	15.8	18.3	22.3	26.2
3	12.6	16.0	18.1	20.4	25.0
5	8.4	12.5	14.9	19.3	27.1
7	13.1	15.8	18.3	21.1	24.7
9	13.7	16.2	18.0	19.7	21.7
11	11.5	15.3	21.4	39.8	102.4
13	9.7	12.2	15.1	22.2	33.7
15	13.8	16.5	19.0	23.0	29.0
17	13.8	16.0	19.8	25.5	33.6
19	11.1	13.3	19.5	30.0	50.5
21	11.4	14.8	17.8	22.2	29.2
23	9.6	11.6	13.8	16.0	18.1
25	12.4	15.4	18.1	23.6	31.6

moisture gradients on the modulus of rupture. It should be noted, however, that the value of M_p is lower for loblolly pine (21%) than it is for chestnut (24%). Therefore, all loblolly pine specimens but one have a moisture content at or above M_p in the second one-quarter inch from the extreme fiber, and six specimens have moisture contents above M_p in the second one-eighth inch (Table 2). Based on these data, it would be unlikely that this group of loblolly pine beams would demonstrate the degree of strength difference that the chestnut did. It was on this basis, however, (and on that of unpublished "intermediate" results), that Wilson deduced that the effect of moisture gradients was species-dependent.

2.1.3 Attempts to Predict the Effect of Moisture Gradients on Strength

Wilson was the first to attempt to predict the results of non-uniform moisture distributions. He induced a parabolic moisture gradient through the depth of a two inch by four inch beam, tested it, then sliced a cross-section into horizontal layers (as in Tables 1 and 2). After determining the moisture content for each slice, he calculated what the approximate modulus of rupture would have equalled for those layers. His formula for the expected modulus of rupture was:

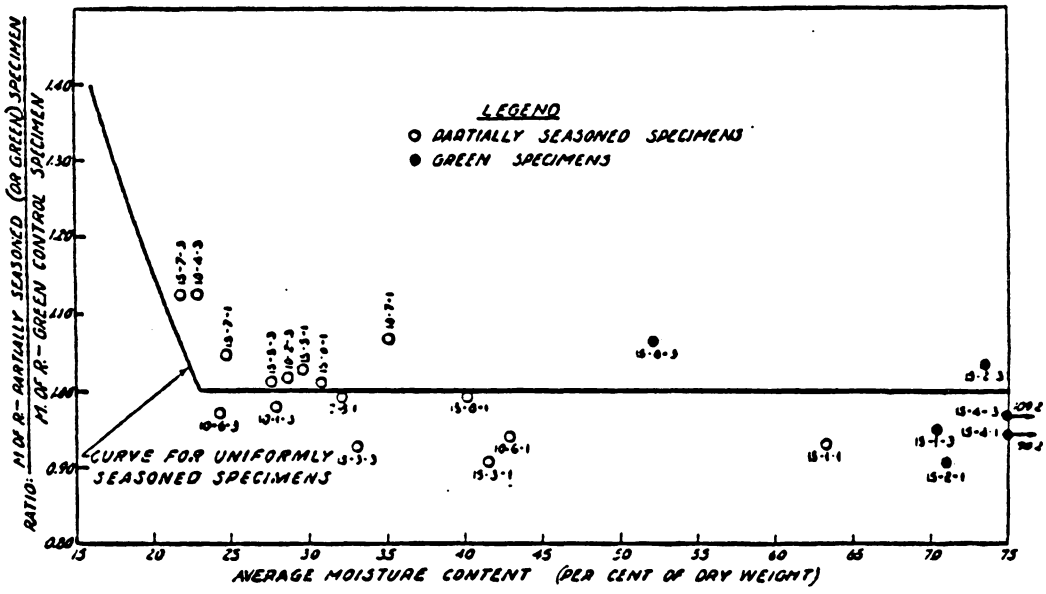

Figure 5: Results of the determination of the modulus of rupture of nonuniformly seasoned 2 by 4 inch specimens of loblolly pine. (From Wilson, 1932). Labels indicate specimen numbers.

TABLE 2

Moisture distribution data for nonuniformly seasoned 2 by 4 inch specimens of loblolly pine plotted in Figure 2. (From Wilson, 1932).

Specimen	Moisture Content of Successive Slices From Compression Face of Static Bending Specimen				
	First 1/8"	Second 1/8"	Second 1/4"	Third 1/4"	Fourth 1/4"
10-1-3	12.7	16.8	22.9	25.7	27.9
10-2-3	14.1	18.1	23.3	25.6	27.1
10-4-3	12.0	17.8	22.6	25.2	----
10-6-1	17.2	45.6	43.4	59.4	55.8
10-6-3	14.1	16.0	20.6	24.1	26.0
10-7-1	14.7	17.7	23.0	36.7	56.8
10-8-1	13.1	16.9	20.7	24.6	28.9
15-1-1	17.4	21.7	26.9	25.3	36.6
15-3-1	12.6	17.0	20.6	26.9	33.6
15-3-3	20.0	30.8	44.0	57.2	50.6
15-5-1	15.4	19.1	21.5	23.2	24.5
15-5-3	17.9	28.6	31.7	35.6	29.0
15-6-1	22.4	26.2	29.0	29.8	31.2
15-7-1	12.9	15.9	21.6	27.5	34.3
15-7-3	14.2	16.0	18.3	21.6	24.0
15-8-1	20.8	28.4	29.4	46.0	43.6

$$MOR = \frac{\Sigma (MOR_i \times I_i)}{\Sigma I_i} \qquad [2.1]$$

where "i" indicates the i-th layer and "I" the moment of inertia. This procedure did not yield numbers that agreed with the beam tests, probably because the modulus of rupture is a ficticious stress based on the assumption of elasticity beyond the proportional limit stress for the extreme fiber in compression.

A similar procedure to predict the observed modulus of elasticity based on the use of transformed sections has been used with good success for both wood-composite and non-wood beams (Mark, 1961; Bryan, 1962; Koch and Bohannan, 1966; Gurfinkel, 1973; Popov, 1976; Marx and Moody, 1981a,b; Bodig and Jayne, 1982). As Popov (1976) states, "the transformation of a section is accomplished by changing dimensions of a cross-section parallel to the neutral axis in the ratio of the elastic moduli of the materials". For wood containing a one-dimensional moisture gradient, this would involve computing the modulus of elasticity for each layer, dividing each by the value for a reference modulus of elasticity, and multiplying the resulting values by the actual section widths in order to get the effective section widths in terms of the reference modulus. The moment of inertia would then be calculated for each layer using the transformed width, and these values would be multiplied by

the corresponding values for modulus of elasticity. The effective modulus of elasticity for the cross-section containing a moisture gradient would then be:

$$MOE = \frac{\Sigma (E_i \times I_i)}{\Sigma I_i} \qquad [2.2]$$

where "i" indicates the i-th layer.

The above procedure would have to be slightly modified to work for a cross-section with moisture gradients across the width and through the depth, as might commonly be encountered in actual drying situations. In this case, each horizontal layer would in turn be broken into smaller pieces, so that the effective width for each layer would be the sum of the effective widths of the smaller pieces. The accuracy of the method will improve as the number of blocks and/or layers increases. To the best of the author's knowledge, no studies have been published which have reported the application of this procedure to wood beams. It seems reasonable to suggest that the elastic constants of the beam outer layer(s) would be the determining factors for beam stiffness; the expression "outer layer" is vague and has no quantitative meaning, but the exact definition of this term is not necessary to this discussion. By whatever arbitrary measure is applied, beams with shallow moisture

gradients would have a reasonably thick outer layer at moisture contents close to the EMC and beams with steep moisture gradients would have thinner layers at the same moisture condition. Assuming that the longitudinal modulus is of primary importance and that increases in the moisture content result in decreases in the longitudinal Young's modulus, the parallel axis theorem would suggest that lower MOEs should be observed as the moisture gradient increases at higher average moisture contents.

A similar and equally simple approach can be used to determine an approximate effective modulus of elasticity for uniaxial specimens. The Rule of Mixtures was originally proposed for composites, and is defined as:

$$E \leq \Sigma(E_i \times V_i) \qquad [2.3]$$

where V_i is the fractional volume of the piece associated with E_i (Jones, 1975). This formula describes an upper bound for the effective modulus of elasticity, and is not necessarily exact. For a piece of wood that has the identical moisture gradient at every point of the cross-section along its length, this equation could be changed to:

$$E \leq \Sigma(E_i \times A_i) \qquad [2.4]$$

where A_i is the fractional area on the cross-section associated with E_i. Within the limitations of the formulation, the accuracy of this approximation will also improve as the cross-section is further sub-divided.

2.1.4 Summary

Moisture gradients may be commonly found in drying lumber, and it appears that they may be characterized as being simultaneously parabolic along all three axes. Possible procedures for calculating an effective modulus of elasticity for such (composite) beams exist in the literature, but no procedure has been successfully used to predict the strength of such material.

2.2 METHODS USED TO PREDICT MECHANICAL PROPERTIES

There are three methods in the literature which have been used to predict the strength of a piece of wood which might be applied to material containing moisture gradients. The first method is to predict the strength as a simple function of some measured property such as specific gravity or modulus of elasticity at a given moisture level (U. S. Forest Products Laboratory, 1974). There appears to be no information in the literature about attempts to relate specific gravity (or any other physical or mechanical

property) to the ultimate strength of wood with a moisture gradient.

The second method is to develop a theoretical basis for the prediction of ultimate strength as has been done for equilibrated beams. Several authors have proposed models, but most of them have been been shown to yield unsatisfactory strength estimates (Bazan, 1980). Perhaps the greatest problem with many of these theories is that they are not formulated with an adequate description of the stress distribution within a beam as it nears failure. It has long been known that the neutral axis shifts downwards due to compression failure in the extreme fiber region (Tiemann, 1906), and most theories acknowledge this fact. Most theories also assume that the stress in the tensile region increases linearly from the neutral axis to the extreme fiber region. However, there are several versions of the stress representation within the compression region, as discussed elsewhere (Dietz, 1942; Robinson and Cooper, 1958; Ethington, 1960; Moe, 1961; Ramos, 1961; Mazur, 1965; Nwokoye, 1972; Zakic, 1976; Bazan, 1980; Malhotra and Bazan, 1980; Anderson, 1981). There are two major problems with applying these ultimate strength theories to wood with a moisture gradient: (1) numerical complexity, and (2) they do not appear to be adaptable for situations where the moisture

may vary through the width and/or length, not just the depth.

The third method in the literature, numerical techniques, comprises piece-wise modeling approaches such as finite differences and finite elements (Zienkiewicz, 1973, 1977; Cook, 1981; Reddy, 1984). Each has been used to successfully solve complex problems in the forest products discipline. The strengths of these methods lie in their ability to predict physical changes from a mathematical model, but successful modeling is dependent upon the inclusion of correct values for mechanical properties in the computer program. Another reason for the popularity of numerical techniques is that they can model non-linear behavior using iterative techniques. For these reasons, numerical techniques (especially finite elements) have been most frequently used in problems associated with wood mechanics or wood drying (Al-Dabbagh, 1970; Al-Dabbagh, et al., 1970; Maghsood, 1970; Wengert, 1975; Fernandez and Polensek, 1979; Thomas, et al., 1980; Wilkinson and Rowlands, 1981 a,b; Schaffner, 1981; Phillips, et al., 1981; Morgan, et al., 1982; Gerhardt, 1982)

Although the accuracy of a mathematical model is quite dependent upon the suitability of the mathematical formulation and solution process used, a numerical procedure

which relies on a piece-wise approach appears to be the best technique available to solve this problem. No attempts to use these procedures on the moisture gradient-strength problem have been reported in the literature. In order to use these techniques, however, it is first necessary to determine the variation of the mechanical properties with moisture content.

A number of investigations have firmly established that, up to the fiber saturation point, strength properties generally decline as the moisture content of a piece of wood is increased. Investigations have also shown that the values of the elastic constants vary with moisture content. Several research projects were conducted to quantify these changes with moisture content around the turn of this century. Whether strength and stiffness properties were envisioned *a priori* to have identical relationships with moisture is unknown. In any event, the effect of moisture on strength and stiffness properties was invariably described by the same type of relationship. With the exception of the very earliest efforts in this area, researchers have, for the most part, chosen to use either linear or semi-logarithmic equations to describe their data. Probably because the semi-logarithmic relationship was formulated and adopted by workers at the USFPL, this so-

called "exponential formula" has become the standard among modern investigators and engineers. However, fifty years have passed since this relationship was first published, and it would be worthwhile to re-examine the basis for the present-day use of this type of equation.

Numerous investigators have individually made significant contributions to the study of moisture-wood strength relations. The following subsections will chronologically detail these individual achievements.

2.2.1 Early Moisture Content-Strength Studies

One of the earliest attempts to discover the effect that moisture content has on the mechanical properties of wood was made by Bauschinger (1883, 1887). Bauschinger represented his data for ultimate compression strength in Scotch pine by a hyperbola (Figure 6). This curve appears to become approximately asymptotic below eight percent and above forty-five percent MC, showing that a point exists beyond which an increase in moisture content has no deleterious effect on compression strength.

Janka (1904) described the moisture content-ultimate strength relationship somewhat differently from Bauschinger and Fernow. Janka's data for spruce affirmed the horizontal trend noted by Bauschinger for wood strength at high

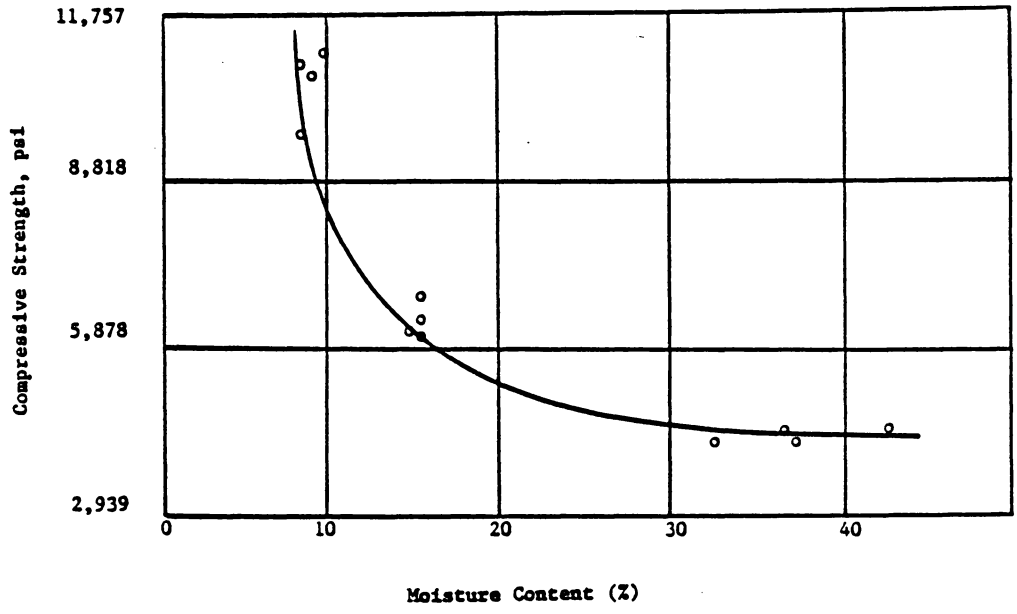

Figure 6: Variation of compressive strength for varying percentages of moisture. Results on Scotch Pine timber. (After Bauschinger, 1887(?), via Fernow, 1893).

moisture contents, but contradicted previous indications about wood strength at low moisture contents. Instead of being asymptotic, the slope of the moisture content-strength curve tended to decrease as the moisture content fell below about seven percent (Figure 7).

The U.S. Forest Service apparently initiated the first United States study to investigate the wood strength-moisture content relationship in cooperation with Professor J.B. Johnson at the laboratories of Washington University at St. Louis (Fernow 1892, 1893). This project, which began in 1891, analyzed the results of over 2000 tests on longleaf pine before being discontinued in 1896 because of a lack of Federal funding. Tests were apparently conducted only at moisture contents between ten and fifty percent , but the results were similar to those reported by Bauschinger (Figure 8). One difference was that the Forest Service MC-strength curves did not become asymptotic as moisture content increased.

2.2.2 Tiemann

Under the direction of Professor J. W. Toumey and Dr. W. Kendrick Hatt, a civil engineer with the Forest Service, H. D. Tiemann began in 1903 to study the influence that moisture content had on the various mechanical properties of

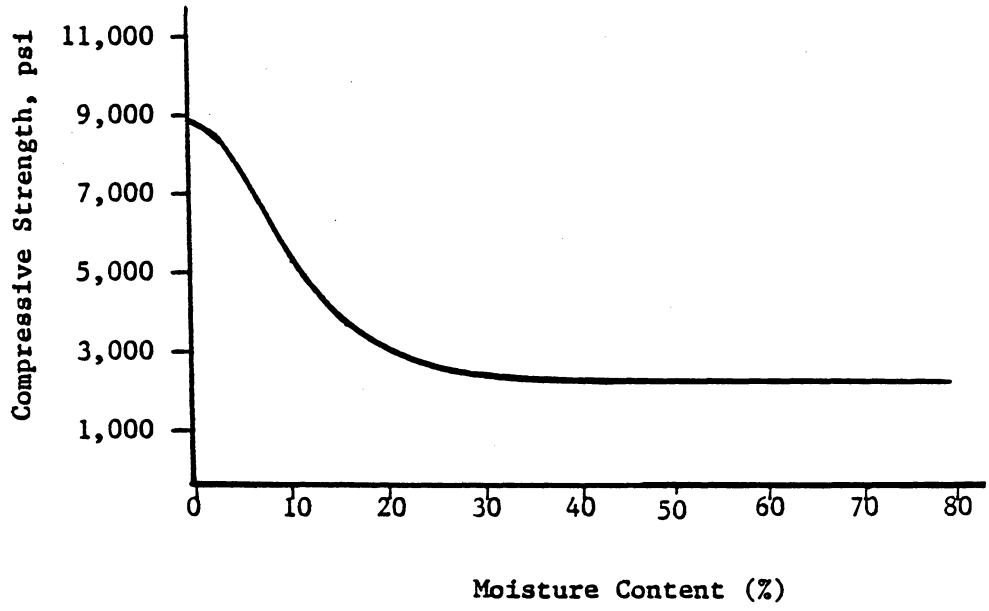

Figure 7: Moisture-strength curve obtained by Janka (1904) from tests of spruce in compression parallel to the grain. (After Tiemann, 1906).

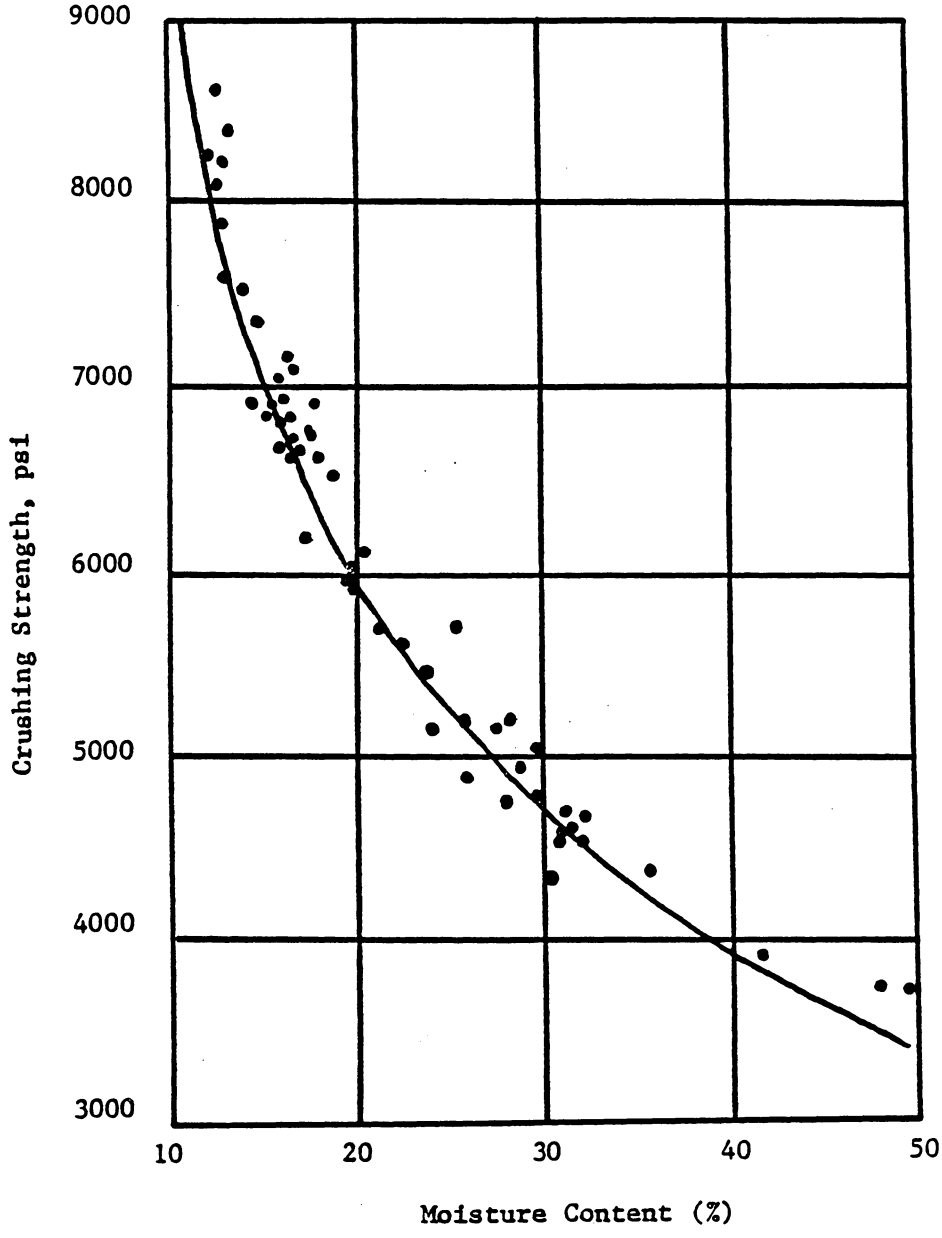

Figure 8: Diagram showing the increase in crushing strength endwise with decrease in moisture content in longleaf pine. (Redrawn from Fernow, 1893).

wood (Tiemann, 1906). At the Yale Forest School he determined various strength properties from bending, compression and shear tests over a wide range of moisture contents, and also calculated the MOE and Young's modulus parallel to the grain from the bending and compression data (Tiemann, 1906, 1907).

Tiemann worked with groups of matched small clear specimens, which he called "series". Each specimen ("block") in a series had been subjected to a different drying treatment so that there would be a range of moisture contents in the set. Tiemann drew separate curves for each series for each type of test, and then averaged the individual series curves from each kind of test to obtain generalized curves for each test/species combination under investigation. His curves differed from Janka's in two ways: (1) Tiemann's curves show smooth increases in strength at low moisture contents; (2) Tiemann's curves show that wood specimens with moisture contents as low as seventeen to thirty-five percent can have the same strength and stiffness properties as green wood (Figure 9). Although Tiemann cautioned that his curves were not to be relied upon to predict the strength properties of untested wood specimens, his reports (1906, 1907) include tables of strength reduction factors to estimate the strength property of a

given piece of wood at various moisture contents when the desired property is known at another moisture content.

It should be noted that Tiemann claimed to be the first to recognize the concept of a point beyond which increases in moisture content do not influence strength or stiffness. He called this point the "fiber saturation point" (FSP) and defined it as "the exact point where the strength first begins to increase during the drying of green or wet wood". He envisioned that the cell walls at the FSP were saturated with water, and that free water would not be present within the cell lumens. Tiemann believed that this point should most accurately be determined by tests on small clear specimens, primarily due to the greater likelihood of uniform seasoning with the relatively crude apparatus then available, and because the wood anatomy would be expected to be more uniform in a small specimen. The fiber saturation points which he determined from these tests appeared to be species-, temperature-, and test-dependent, however.

It should be noted that Tiemann usually had only a few data values in the vicinity of his fiber saturation points (Figure 10). This is probably due to his acknowledged difficulty in obtaining uniformly seasoned specimens at moisture contents around twenty to twenty-five percent.

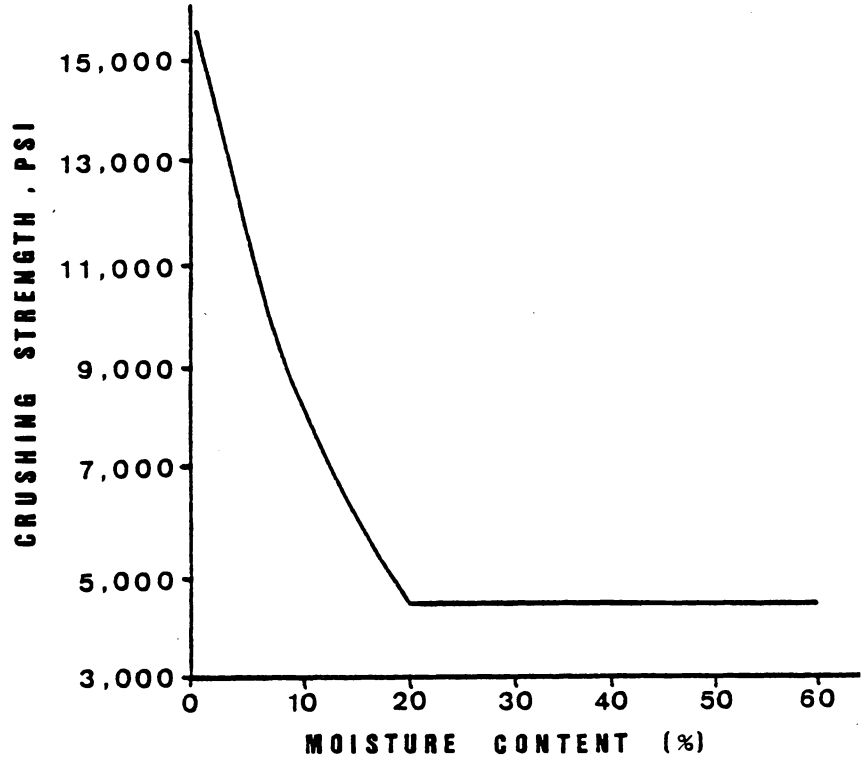

Figure 9: Variation of strength with moisture in compression parallel to the grain for longleaf pine. (Redrawn from Tiemann, 1906).

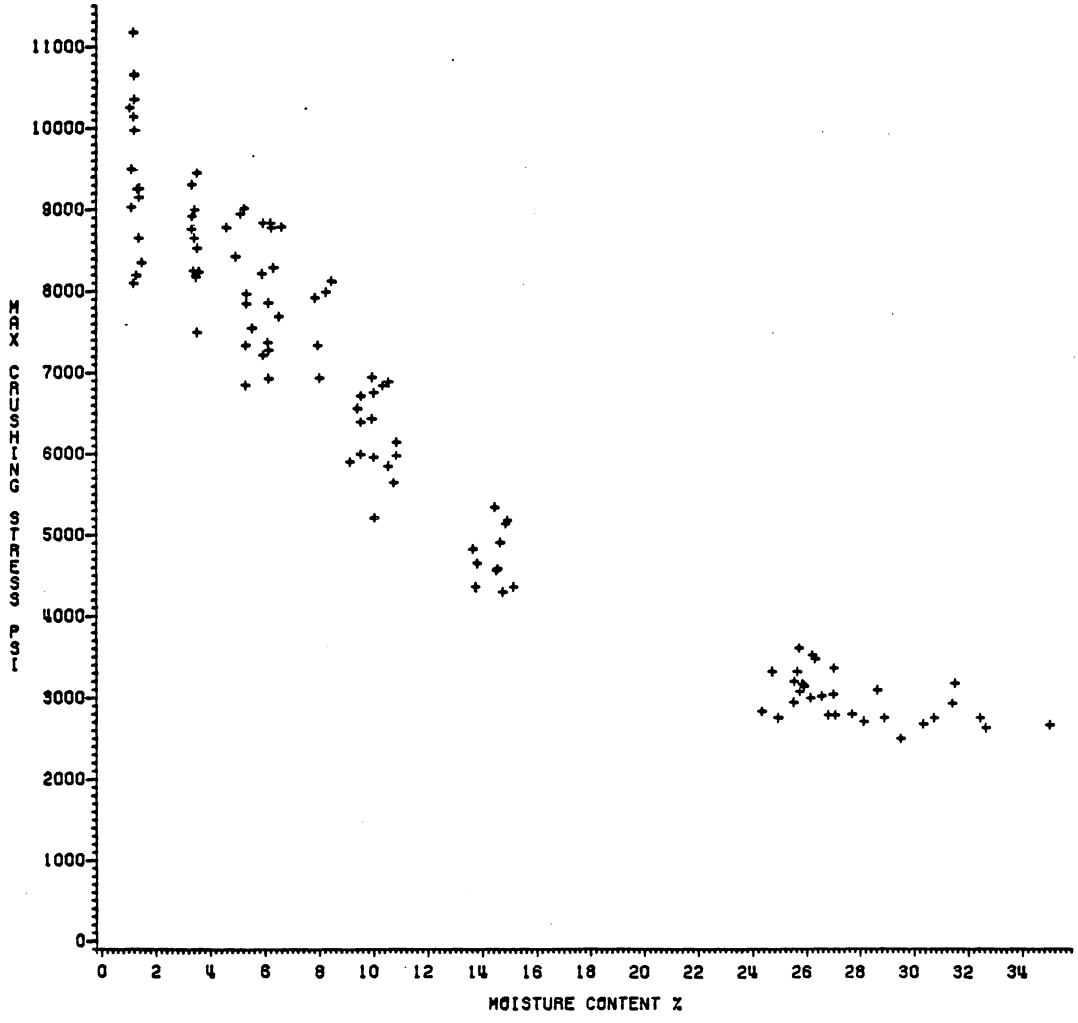

Figure 10: Tiemann's crushing strength data for spruce. Drawn from desorption data in 1906 report.

Tiemann also had to contend with the possibility that some of his data were obtained from wood specimens with non-uniform moisture contents (dry shell, moist core). This was particularly likely at moisture contents close to the actual fiber saturation points. Tiemann noted that moisture gradients were found in many of his chestnut specimens, and he did not knowingly include the results of these gradient-containing specimens in his moisture content-strength property curves.

As an historical reflection, it is likely that Tiemann's analysis was influenced by Bauschinger, Fernow and Janka; he probably expected to find a curvilinear relationship and fit curves to his data accordingly. As noted above, these curves were determined by averaging the curves determined by "connecting the dots" for each series (Figure 11). It appears from his report that he did not consider any other type of relationship, although his data suggest that a linear relationship could often have been drawn instead if the entire data set had been considered (Figure 12). Statistical inference techniques were in their infancy, and a least-squares analysis was not performed on the data.

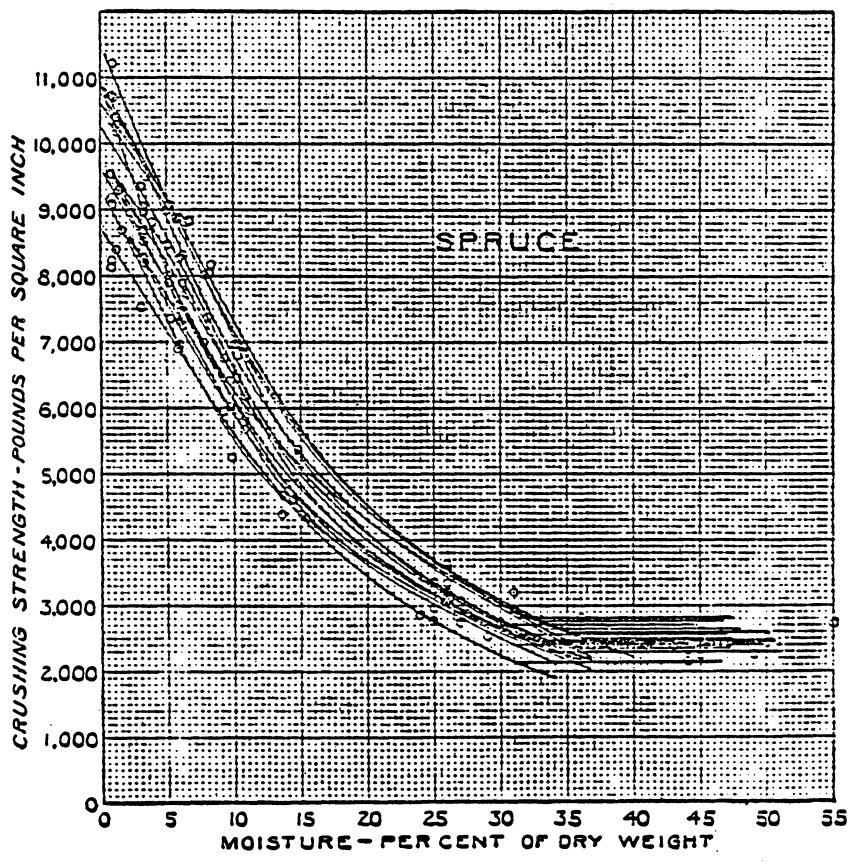

Figure 11: Individual moisture-strength curves for 16 series of spruce tested in compression parallel to the grain. (From Tiemann, 1906).

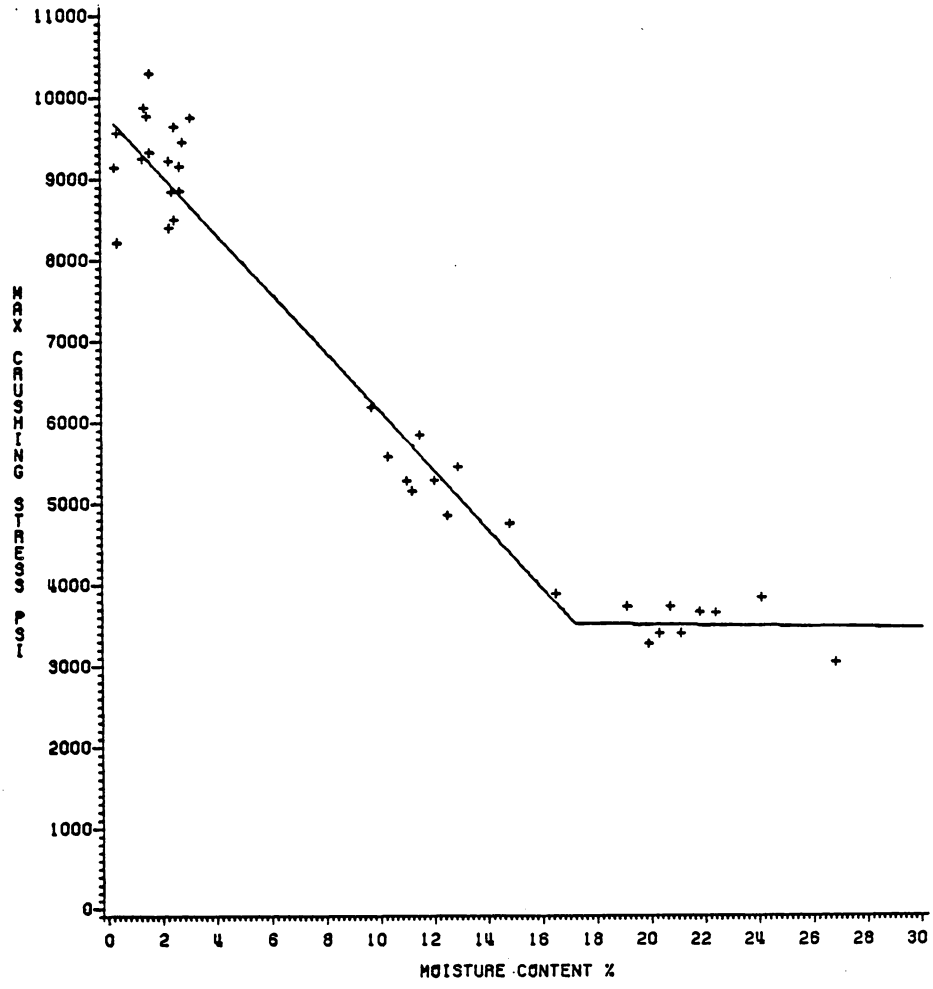

Figure 12: Tiemann's crushing strength data for chestnut overlaid by best bi-linear regression lines from TWOLINE program. (See Appendix).

2.2.3 Carrington

Following Tiemann's studies, Carrington (1922) undertook the study of the variation in the elastic constants with accompanying changes in wood moisture content. Using only six matched pieces of spruce, he determined elastic constants over a range of moisture contents by alternately drying and re-wetting the same six specimens to get flexure and torsion data at moisture contents ranging from one or two percent to about 100 percent. According to his description of his experiment, he began his tests with spruce previously dried to twelve percent moisture content. He then tested the specimens (below the proportional limit), further dried them at 102 degrees Celsius until close to oven-dry, and repeated his tests. Following these tests, he induced the wood to re-adsorb moisture by exposing the specimens first to room conditions, then to a humid atmosphere and he tested the specimens at various stages of moisture sorption. Carrington then soaked the pieces and allowed them to dry, again testing them at various moisture contents. It is likely that Carrington's specimens contained moisture gradients at moisture contents below the FSP as a result of his procedure.

Carrington found that straight lines overlaid on graphs of his data at moisture contents below the apparent fiber

saturation point appeared to fit the data fairly well, although a few data suggest that some minimum moisture content exists at around five or ten percent MC, below which point further decreases in the moisture content have little or no effect on the elastic constants (Figure 13). With the exception of the Poisson's ratios ν_{rt} and ν_{tr}, the value of every elastic constant decreased as the wood moisture content increased; the values for ν_{rt} and ν_{tr} increased.

The fiber saturation points from Carrington's beam and torsion tests were determined graphically from the intersection of two straight lines and ranged from about twenty-four to thirty-seven percent, depending on the specimen. Carrington did not discuss this variation, but it is possible that some of it might be due to the (probable) moisture gradients in his specimens. It is also possible that some of the variation is due to the hand-fitting of the lines through the data. It should be noted, however, that his data were obtained at a greater number of intervals between the oven-dry and green moisture contents than Tiemann used. Although the total number of data points is smaller than Tiemann's, the resultant trend is more clear than that presented by Tiemann's approach. The clarity of this trend is not a guarantee of its correctness, but Carrington believed that Tiemann's curvilinear relationships

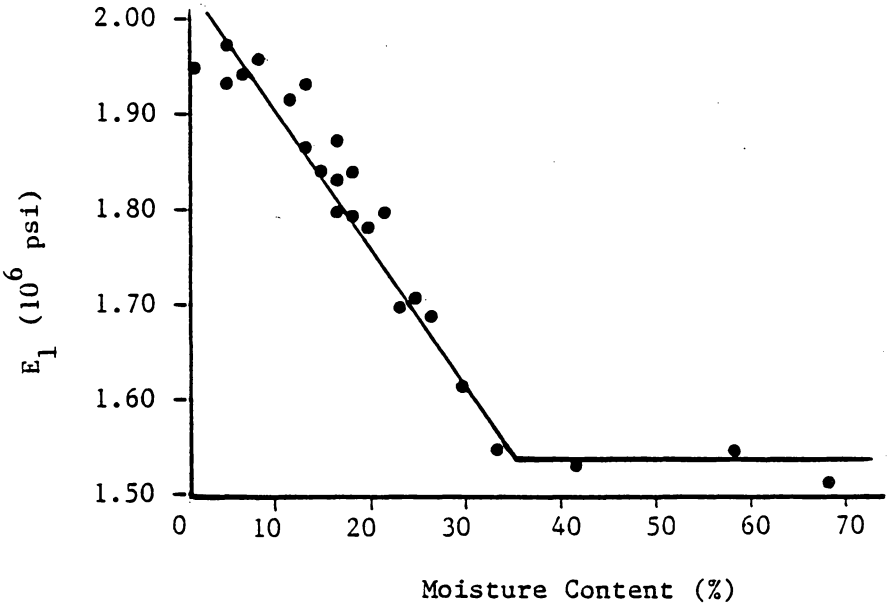

Figure 13: Variation of the longitudinal Young's modulus for spruce. (Redrawn from graph of specimen No. 3, Carrington, 1922).

resulted from averaging the data from many sets of matched specimens instead of varying the moisture content and testing identical specimens.

2.2.4 Wilson

In contrast to Tiemann and Carrington, the primary purpose of T. R. C. Wilson's work at the USFPL was to determine a mathematical relationship between moisture content and the various mechanical properties which would be valid for all species (Wilson, 1932). Wilson first approached the problem by examining the data averages from Tiemann's averaged curves to ascertain whether or not a straight line was appropriate to describe the moisture content-strength relationship. Examination of these data led him to reject this hypothesis. Neither the raw data nor the means by which they were obtained appear to have been critically examined.

Wilson was apparently unaware of Carrington's study since it is not listed among his references, and there is no other evidence to indicate that he knew of its existence.

Wilson then found that "within certain limits the relation between the logarithm of the strength value and the moisture content could be quite adequately represented by a straight line" (Figure 14). He recorded that this line did

not always intersect with the horizontal line indicating green strength at the identical moisture content Tiemann had used for the fiber saturation points. (These fiber saturation points had been deduced from curve averaging rather than from a rigorous analysis of the raw data). Therefore, to distinguish between the two points, Wilson named the point where the lines joined the "intersection point". The moisture content at this intersection point was designated as M_p, and the strength value at that point (the green wood strength) was designated as S_p.

The "exponential formula" that Wilson proposed for moisture strength adjustments is:

$$\log S = \log S_p + K(M_p - M) \qquad [2.5]$$

where:

K = the arithmetic opposite of the slope of the inclined line, i.e.,

$$K = \frac{\log S_1 - \log S_2}{MC_1 - MC_2} \qquad [2.6]$$

To test this equation, Wilson applied this formula both to Tiemann's data and to a larger body of data which he gathered especially for this study. (The constants were fit by performing least-squares computations on the averaged

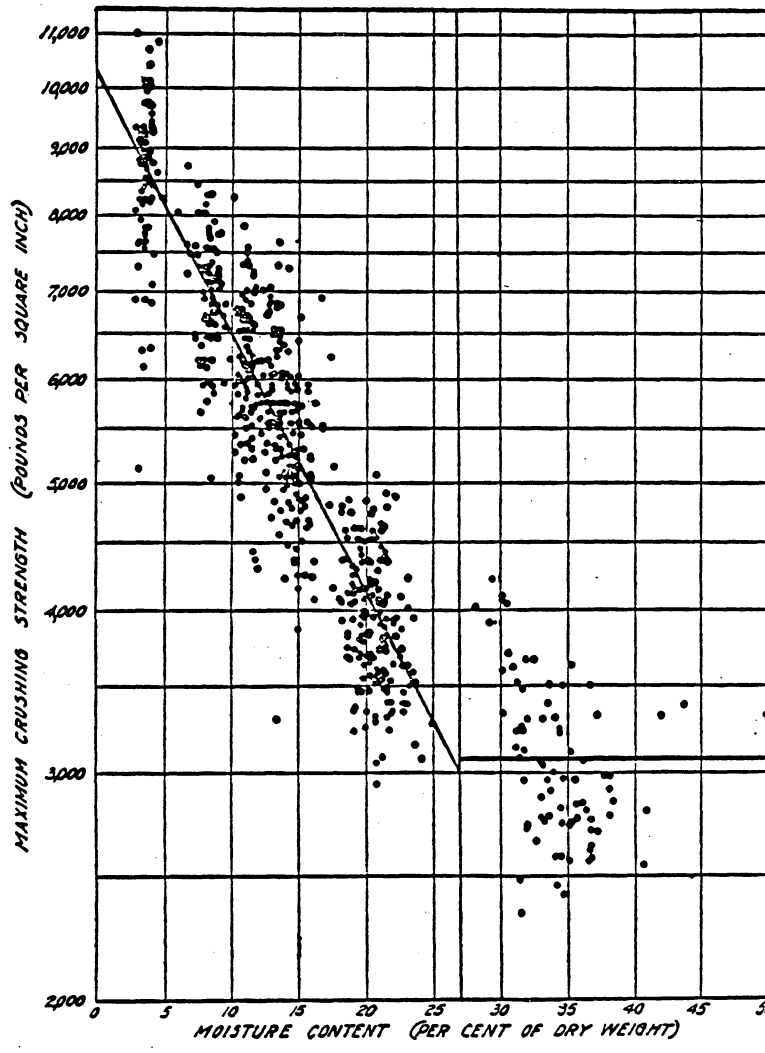

Figure 14: Variation of the maximum crushing strength with moisture content for Sitka spruce. (From Wilson, 1932).

points for various moisture contents, subject to the constraint that M_p had to be a whole number.) In both cases, the exponential formula was successfully compared to averages of the data for various tests at defined moisture content classes. Data available to him included ultimate strength values for the various tests, longitudinal Young's moduli, and the MOE values for bending tests. He also used this equation for average values of a modulus of rigidity for Sitka spruce at several moisture contents. Deviations of the data from the predicted values were attributed to (1) non-uniform moisture distribution, (2) varying amounts of extractives, and (3) the variability normally inherent in wood (such as varying densities).

Like Tiemann, Wilson noted that the moisture content at the intersection point depended upon the species and (apparently) even upon the kind of test. Wilson thought that the latter difficulty was due to imperfect specimen matching, as he had depended upon "a fairly large number of specimens rather than individual matching...to provide data in which the influence of factors other than the differences in moisture content would be averaged out". He apparently expected variation in M_p due to differences in the percentage of latewood present and other factors. He also compared his M_p values for several species with the

corresponding fiber saturation points; these were determined both from electrical conductivity tests and from extrapolation of EMC values at various RH conditions to that EMC which would exist at 100 percent RH. Wilson wrote that

> the intersection points...are not true fiber saturation points of the respective species. However, it has been shown that a straight-line relationship exists between percentage moisture, within a range somewhat below the intersection point or the fiber saturation point, and the logarithm of the strength property. Failure of the intersection point to coincide with the true fiber saturation point does not vitiate this relation nor render invalid its application in adjusting strength values for differences in moisture content.

The modulus of rigidity values noted above perhaps deserve special mention at this point. These data were originally collected by Trayer and March (1929) on twelve matched Sitka spruce specimens, and it appears that their study was the first to use Wilson's relationship to describe the moisture content-elastic constant relationship. Trayer and March used the semi-logarithmic relationship to describe the changes in shear strength with moisture content as well.

2.2.5 U.S. Forest Products Laboratory

Following Wilson's 1932 paper, the semi-logarithmic curve for strength properties at various moisture contents became commonly accepted both in the United States and abroad. Although Wilson had demonstrated the usefulness of his

formula for numerous strength properties, the only elastic constant he had investigated was the modulus of elasticity measured in bending and compression tests. Therefore, as part of an investigation to determine the elastic properties of a number of woods used in aircraft, the USFPL performed a series of limited tests to determine the relationship of the various elastic constants with moisture content. In work on Sitka spruce and Douglas-fir, researchers found that the longitudinal Young's modulus, E_l, was less sensitive to variations in the moisture content than the Young's moduli in the radial and tangential directions (E_r, E_t) (Drow and McBurney, 1946a; McBurney and Drow, 1956). They found that the data averages for defined moisture content classes appeared to fit the exponential formula, and they did not make any attempt to describe the data by alternative expressions.

The USFPL performed only a small study to determine the effects of moisture content on the shear moduli (Doyle, McBurney and Drow, 1946). Moisture content was only varied from about six to twelve percent, and it was found that the shear moduli behaved similarly to the Young's moduli. The range of moisture contents tested, however, was insufficient to determine if the relationships of these moduli to moisture content followed the exponential expression.

The relationships between moisture content and the Poisson's ratios is less clear in these studies than it is for the other elastic constants (Drow and McBurney, 1946a; McBurney and Drow, 1956). Data summaries from these studies show that the averages of the measured Poisson's ratios varied considerably between groups of test specimens at the moisture contents used. It is, therefore, uncertain whether any trends can be said to be present in these data. It is very possible that the Poisson's ratios do change with moisture content, however; using the assumption that orthotropic elasticity applies to wood, if the Young's moduli are affected by moisture then the Poisson's ratios must also change in order to preserve the symmetry of the compliance matrix.

2.2.6 Youngs

Youngs (1957) determined E_r, E_t, and G_{tr} at three moisture contents and at three temperatures as part of a drying study on red oak. He did not attempt to reduce his data to algebraic expressions, nor did he compare his data to the values predicted from the linear or semi-logarithmic equations used by previous researchers. His values do, however, follow the same general MC-strength property trends noted by others. Increasing temperatures reduced the

magnitude of the data observed, but did not materially affect the shape of the MC-elastic constant relationship. Young's figures show, however, that temperature can have a significant affect on these properties. The effect of a 50 degree Fahrenheit increase in temperature (from 80 to 130 degrees F.) was roughly equivalent to a ten percent increase in moisture content at 80 degrees F..

2.2.7 Kollmann and Krech

Kollmann and Krech (1960) investigated the relationship of the dynamic longitudinal Young's modulus with variations in moisture content. They found that the moisture content-Young's modulus relationship was essentially linear over the range of eight to twenty-two percent moisture content. Although specimens were not tested at moisture contents between about twenty-two and thirty-two percent, Kollmann and Krech chose to fit this portion of the moisture content relationship by a curve (Figure 15). Their results were similar to Carrington's in that their E_1 data do not steadily increase as moisture content is decreased; at moisture contents below about eight percent, E_1 may remain constant or even decrease.

It should be noted that Kollmann and Krech's plots suggest fiber saturation points in excess of forty percent

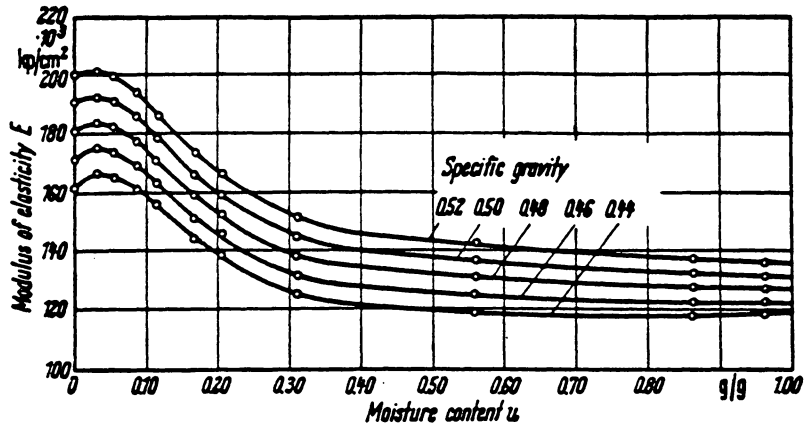

Figure 15: Effect of moisture content on the modulus of elasticity parallel to the grain of spruce. (From Kollmann and Krech, 1960).

for both oak and spruce; the data appear to show that the modulus is always decreasing with increasing moisture content, even up to ninety percent. This trend appears to be more significant for the denser material within a species. These data appear to be contrary to those from other laboratories.

2.2.8 Byvshykh

As part of a study on stress formation during drying, Byvshykh (1959) studied several elastic and material properties as they varied with temperature and moisture. He found that E_t for pine decreased in a curvilinear fashion as moisture content was varied from six to twenty-four percent at fifty degrees C., and that this curvilinear relationship became nearly linear as temperatures were increased to 100 degrees Celsius. Byvshykh also found that the maximum load in tension in the tangential direction declined with decreasing moisture content. His graphs indicate that the maximum load changed only slightly with moisture contents between zero and twelve percent MC, and that the most significant changes occur between twelve and eighteen percent moisture content. Increasing temperatures did not alter the form of this relationship, although the magnitude of the data appeared to be inversely proportional to the temperature at which they were collected.

2.2.9 Mark, et al.

Mark, et al., (1970) reported on determinations of yellow-poplar and Virginia pine shear moduli at various moisture contents. In contrast to most previous researchers, they obtained data at a large number of different moisture contents (presumably equilibrated) between zero and forty (plus) percent. Their results were presented in graphical form only, and the trends observed from these data were fairly well defined due to the large number of moisture contents used. The data were not compared to any mathematical models, but it appears from the graphs that a straight-line relationship would be more appropriate than a semi-logarithmic curve, particularly between about five percent and the green-moduli intersection points (Figure 16). Between zero and five percent moisture content, some of the data show a leveling-off similar to the trend observed by Kollmann and Krech and Carrington.

2.2.10 Tang, et al.

In 1971, Tang, et al., performed plate tests to determine the shear moduli for scarlet oak. These researchers, having tested specimens at a large number of moisture contents, chose to fit each data set by a straight line from below the intersection point to about four percent moisture content

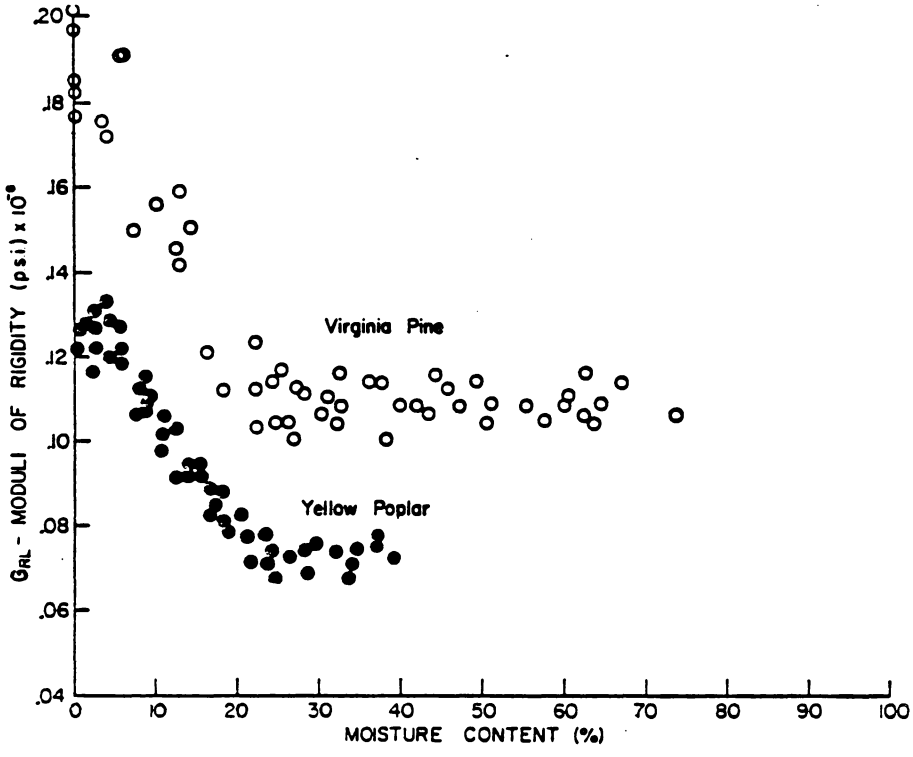

Figure 16: Variation of the modulus of rigidity G_{lr} with moisture content for yellow-poplar and Virginia pine specimens. (From Mark, et al., 1970).

(Figure 17). Below this point, changes in moisture content appear to have little or no effect.

2.2.11 Tang and Hsu

Like Kollmann and Krech, Tang and Hsu (1972) observed the response of the dynamic Young's modulus to variation in moisture content. The major difference in the two data sets appears to be that Tang and Hsu's data (on scarlet oak and yellow-poplar) indicate definite intersection points between twenty-five and thirty percent moisture content (Figure 18). Judging from their raw data for yellow-poplar, it is apparent that they did not observe any continuing decline in the modulus as the moisture content was increased from about twenty-five percent to forty-eight percent. The yellow-poplar data points also show a leveling-off as moisture content decreases from five percent to zero percent; the oak data do not. Because only a relatively small number of data were obtained, any statement about linear or semi-logarithmic relationships would be speculative; neither relationship, however, appears to be excludable.

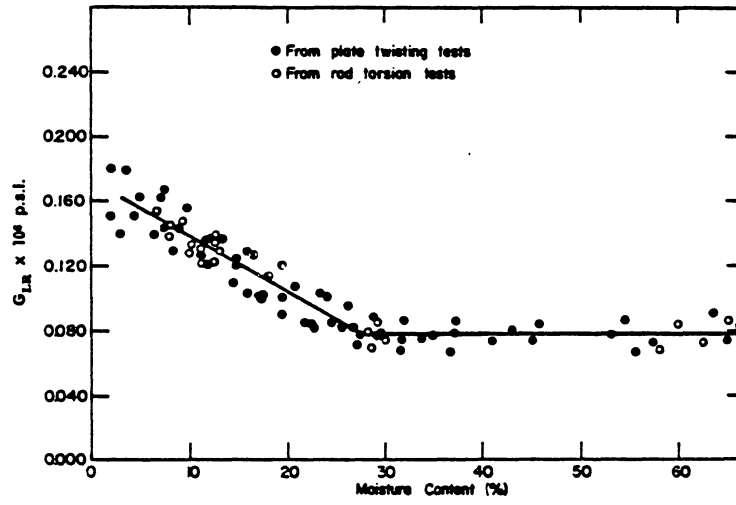

Figure 17: Variation of modulus of rigidity G_{lr} with moisture content. (From Tang, et al., 1971).

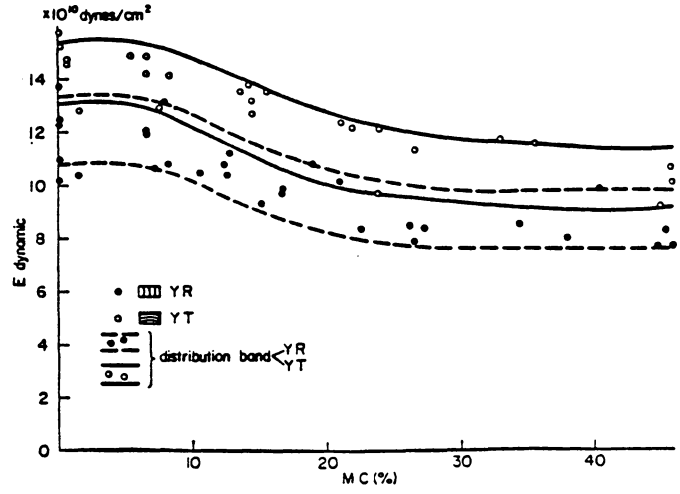

Figure 18: Dynamic Young's modulus versus moisture content for yellow-poplar. (From Tang and Hsu, 1972).

2.2.12 Drow, Samek and Bohlen

Interest in the modeling of the MC-strength relationship has not been restricted to solid wood. Drow (1957) used Wilson's formula to correct plywood strength properties for small changes in moisture content, and Samek (1970) later re-checked the validity of this adjustment using matched specimens at two moisture contents. Samek found that the exponential formula overestimated the loss in compression strength when going from a low to a higher moisture content, but he could not derive an alternative adjustment based on data at only two moisture levels. Bohlen (1975) believed that it would be more useful to be able to apply a more reliable adjustment formula, so he conditioned matched plywood specimens to several moisture contents and tested them in compression. He found that a linear adjustment formula was more accurate than the exponential formula for both large and small moisture content adjustments.

2.2.13 Palka

Palka has not published original data to indicate how moisture affects the elastic constants, but he has examined other data and made suggestions about how to model this relationship. One suggestion has been to use linear approximations to estimate elastic constants (for softwoods)

when values exist for only one moisture content (Palka, 1973). Palka indicated that the semi-logarithmic model for the moisture content-strength property relationship was probably more correct, and noted that some error would likely result from the use of this approximation method. No testing was performed to justify this assertion, however.

More recently, Palka (1982) has proposed an exponential model for plywood which could describe a curvilinear moisture content-strength property curve from zero moisture to the soaked condition. Provided that the four parameters are correctly determined, the equation is capable of describing the apparent decline in strength properties which sometimes occurs below about five percent moisture content (Figure 19). Palka's equation was expressed as

$$Y = A + B \exp(-C(x-D)^2) \qquad [2.7]$$

where: A = mechanical property in soaked condition,
B = difference between the maximum value of the mechanical property and the mechanical property in the soaked condition,
C = the scale (slope) parameter,
D = the moisture content at the maximum value of the mechanical property,
x = the moisture content (%), and

Y = the mechanical property at moisture content, x.

When the mechanical property (Y_0) is known at some reference moisture content (x_0), the equation can take this form

$$Y = Y_0 + B(\exp(-C(x-D)^2 - \exp(-C(x_0-D)^2) \quad [2.8]$$

These equations have apparently not been used in any published research, nor have they been compared to published data for either the strength properties or the elastic constants. They offer great flexibility in describing the moisture content-strength property relationship, however.

2.2.14 Summary

Very little substantive work has been done on modeling wood strength property-moisture content relationships in the past fifty years. Studies to date have made no distinction between the wood strength-moisture content relationship and the wood elastic constant-moisture content relationship. Only Wilson (1932) has attempted to model some of the elastic constants and the strength properties for the same species. Based on this work alone, it appears possible that the elastic constants and the strength values may have the

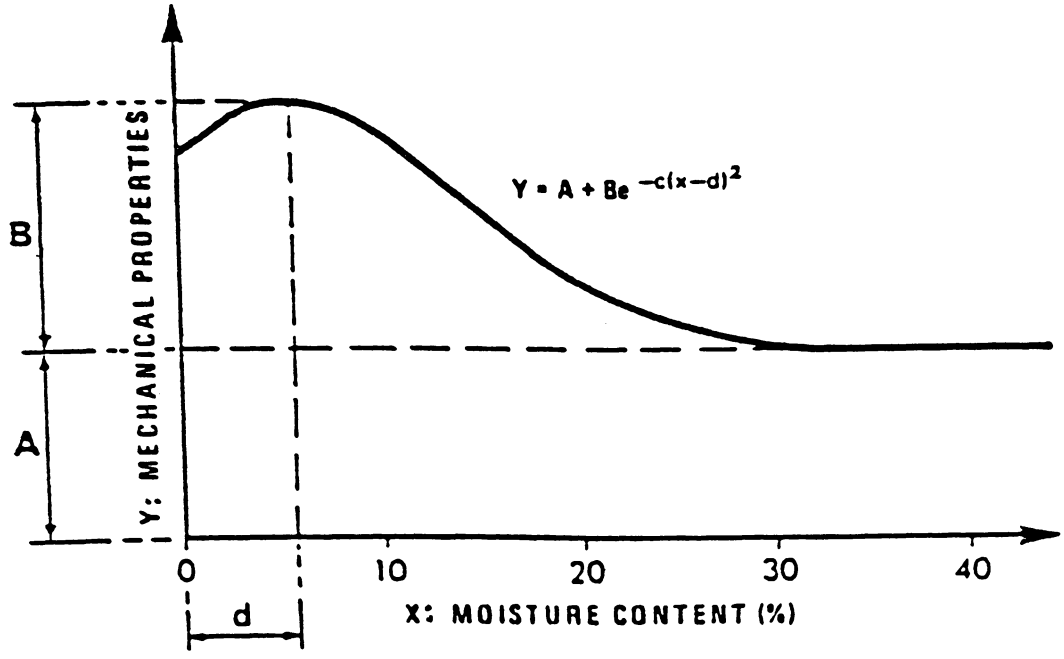

Figure 19: Graph of Palka's mixed exponential equation. (From Palka, 1982).

same form of mathematical relationship with changing moisture contents. Wilson did not consider elastic constants other than E_1 and a shear modulus, however, so a definitive statement about the similarities of these relationships can not be made.

Although Wilson's study indicates that the relationships with moisture are fit well by his semi-logarithmic formula, the raw data he collected were not subjected to rigorous statistical comparisons with this model. Data collected by other researchers suggest that a linear relationship might fit equally well or better (at least for certain properties), and it is possible that the type of relationship may be test- and/or species-specific. Palka's complex exponential formula might be able to be used to advantage under these conditions.

2.3 THE EFFECT OF MOISTURE CONTENT HISTORY ON STRENGTH PROPERTIES

It is well-known that the drying of wood can result in some degree of permanent microstructural damage. The effect that these induced flaws have on mechanical properties has mostly been assessed for drying processes which use temperatures in excess of 212 degrees Fahrenheit, and the results of these studies have been somewhat ambiguous (Salamon, 1963; Salamon, 1969; Gerhards and McMillen, 1976; Huffman, 1977).

Some species appear to have up to twenty percent strength decreases compared to specimens dried at more conventional temperatures, while other species had negligible losses.

It appears that only a few investigators have determined the degree of damage resulting from less severe drying conditions. In most cases, the degree of damage was determined by resoaking dried specimens and comparing the strength data against undried green controls. This procedure is similar to the experimental methods apparently used by researchers such as Carrington (1922). It is important to be aware of the potential changes in wood strength properties which can result from such cyclic moisture conditions. The studies summarized below illustrate the importance of using wood with a single drying history in any study where the mechanical properties of a single species are to be compared.

2.3.1 Tiemann

Tiemann (1906, 1907) is apparently the first investigator to discover that wood has less than its original strength after it has been dried and re-wet. In bending, shear, and compression tests on matched specimens of longleaf pine, spruce and chestnut, he found that the severity of the drying treatment affected the strength loss. Strength

losses of ten to fifteen percent (determined upon re-wetting) were caused by drying at temperatures as low as 130 degrees F., while more severe drying treatments resulted in strength losses of up to fifty percent. In preliminary tests, Tiemann could not determine whether any additional strength losses occurred due to a second or third drying/re-wetting cycle. Tiemann later published similar information for tests on different species conducted at about the same time (Tiemann, 1942).

2.3.2 Carrington

Carrington (1922) attributed the loss of strength observed by Tiemann to flaws in the specimens induced by the various drying processes. Carrington claimed that the severity of the flaws induced was a function of the specimen's size, and he wrote that he had minimized this problem in his study by using small specimens. He inferred that he had not, upon re-wetting, observed any strength loss due to drying. Carrington did not identify individual data in his report for the purpose of comparison, but it should be noted that he could only have compared the effect of drying on the elastic properties at twelve percent moisture content.

2.3.3 Khookriansky

Khookriansky (1936) found that pieces of wood which were oven-dried to about five percent moisture content before being re-wet to sixteen percent moisture content and tested had lower strength properties than wood which had been dried to sixteen percent moisture content as the only treatment.

2.3.4 Covington

Covington (1965) reported that the degree of strength loss was a function of the moisture content to which the wood was dried. He found that the strength of Scots pine was reduced twice as much when it was first dried to twelve percent and re-wet than it was when it was first dried to twenty percent. Covington did not record any information about the effect of repeated drying and re-wetting cycles.

2.3.5 Youngs

Youngs' 1957 study on the mechanical properties of red oak related to drying confirmed the observation that permanent strength loss occurs when wood is heated at temperatures below 212 degrees Fahrenheit. He found that strength losses were more pronounced for wood dried at 180 degrees F. than for wood dried at 130 degrees F..

2.3.6 Keith

Keith's work (1960) is perhaps the most comprehensive of the various studies on this topic. By performing longitudinal shear tests on several species he found that the number of drying and re-wetting cycles affected a specimen's final strength. The initial drying and re-wetting cycle caused the most noticeable strength decrease. Strength continued to decrease with the number of treatment cycles, but at a decreasing rate. Some specimens lost up to sixty percent of their original green strength after twenty-five oven-drying cycles.

Keith also performed microscopic inspections of the wood he tested. He attributed strength deterioration to structural changes such as "internal checking and microscopic separations". He also found that uniform-structured woods suffered less structural deterioration than woods like red oak, and that these uniform-structured woods also exhibited the least strength loss. Keith worked with relatively small specimens in order to minimize possible stresses from different drying rates within each specimen. He ascribed the greater deterioration in non-uniform woods to the differences in shrinkage and swelling of the various wood tissues, especially the earlywood/latewood layers.

2.3.7 Summary

Overall, it appears that wood strength properties are affected both by the severity of the drying treatment and by the number of times the wood is dried. It seems that much of this strength loss is due to differential shrinkage and swelling, causing failures to form in the resulting shear planes. The effect appears to be most significant for larger specimens and for species with non-uniform anatomy.

The relevance of this information to the present study is clear. To minimize drying defects caused by even mild drying conditions, it would be best to use a diffuse-porous species for the mechanical tests. Severe moisture gradients can best be imposed in wet wood, and since water-soaked specimens do not dry with a smooth parabolic gradient the gradients should be formed in green wood being dried for the first time. All other tests performed to measure mechanical properties for some numerical model must also, therefore, be conducted on wood which has not been dried previously.

2.4 THE EFFECT OF SPECIFIC GRAVITY ON THE STRENGTH AND STIFFNESS PROPERTIES OF WOOD

Specific gravity has long been thought to be a major factor in predicting the strength and stiffness properties of individual wood specimens, but early studies differed greatly as to the amount of influence to ascribe to this

factor. Bauschinger (1887) found that strength was proportional to specific gravity. Tests by the Division of Forestry also indicated that strength increased with increasing specific gravity, but at a less than proportional rate (Fernow, 1892). Janka thought that wood strength increased as a function of the square of the specific gravity (Fernow, 1892, 1893; Tiemann 1906). Tiemann (1906) found that the maximum crushing strength of longleaf pine was proportional to the specific gravity, and he thought that this relationship held over the entire moisture content range. These early tests can not be relied upon for accurate trends, however, as it was apparently common to test wood specimens at various moisture conditions as the wood dried down from the green state. This procedure was explicitly stated to have been followed in at least one study (Fernow, 1892, 1893). Specific gravity was also calculated on the basis of current weight divided by current volume in at least two studies (Fernow, 1893; Tiemann, 1906); calculation of specific gravity on some moisture content-independent basis (such as ovendry or green volumes) would have been preferable.

Possibly because of the conflicting results noted above, Newlin and Wilson (1919) attempted to uncover the relationship between various strength properties and

specific gravity by studying the available data for numerous species with widely differing density ranges. They reported that it had been commonly assumed up to this time that the modulus of rupture and strength in compression parallel to the grain were properties which were proportional to density, and that this relationship held "between pieces of the same species, between pieces of different species, and between average results of strength tests on different species". It was recognized that other properties did not vary linearly with specific gravity, but the relationships had not been established.

After studying the data to which they had access, Newlin and Wilson found that the previously held assumptions were incorrect, and they proposed instead to describe the average strength-specific gravity relationship among species by an equation of the form

$$P = KG^{x} \qquad [2.9]$$

where P is the strength property of interest,
K is a constant,
G is the specific gravity
(ovendry weight/current volume),
and x is an exponent specified for each
kind of test.

The among-species relationships which they derived for green and air-dry material are listed in Table 3. The authors emphasized that these are only useful as approximate average relationships among different species, and they included tables of correction factors for more accurate estimations of the strength properties of individual species. They did not propose an equation to be used for within-species adjustments.

It should be noted that the term "air-dry" took on a rather flexible meaning in this report. Air-dry data for modulus of rupture and maximum strength in compression parallel to the grain were adjusted to twelve percent moisture content using unspecified methods, but the authors stated that the relationships of other properties to moisture content had not been studied in detail. Other properties were left unadjusted, and the remaining specific gravity-strength relationships for air-dry wood were derived from specimens which had moisture contents ranging from eight to eighteen percent. The potential consequences of analyzing these unadjusted data were not discussed.

Newlin and Wilson's paper was a significant contribution to the literature when it was published, but it did not provide for an adjustment of strength values within a given species, nor did it provide information about how density

TABLE 3

Newlin and Wilson's specific gravity-strength functions

Property	SG-Strength Relation[1] Green Wood	Air Dry Wood[2]
Static Bending:		
Fiber Stress at Elastic Limit	10300 $G^{1.25}$	19000 $G^{1.25}$
Modulus of Elasticity	2500000 G	3000000 G
Modulus of Rupture	18500 $G^{1.25}$	26200 $G^{1.25}$
Work to Maximum Load	42.7 G^{2}	38.9 G^{2}
Work to Elastic Limit	3.51 G^{2}	9.00 G^{2}
Impact Bending:		
Fiber Stress at Elastic Limit	23500 $G^{1.25}$	35000 $G^{1.25}$
Height of Drop Causing Failure	140 G^{2}	111 G^{2}
Work to Elastic Limit	15.1 G^{2}	25.0 G^{2}
Compression Parallel to Grain:		
Fiber Stress at Elastic Limit	6800 $G^{1.25}$	11000 $G^{1.25}$
Maximum Crushing Strength	6900 G	12000 G
Compression Perpendicular to Grain:		
Fiber Stress at Elastic Limit	2900 $G^{2.25}$	5200 $G^{2.25}$
Hardness:		
End	3700 $G^{2.25}$	4800 $G^{2.25}$
Side	3300 $G^{2.25}$	3700 $G^{2.25}$
Shearing Strength:	2650 $G^{1.33}$	3815 $G^{1.33}$
Tension Perpendicular to Grain:	2120 G^{2}	2250 G^{2}

[1] G represents the specific gravity of ovendry wood, based on the volume at the moisture condition indicated.

[2] 12% MC

influences elastic constants other than the modulus of elasticity in bending. This was not unusual. In the paper advancing his exponential formula, Wilson (1932) noted that the maximum strength of longleaf pine was positively correlated to specific gravity, but he did not use these data to determine a within-species adjustment factor; neither did he attempt to use the among-species adjustment factors (previously derived) for his within-species data. Markwardt (1930) reviewed Newlin and Wilson's equations for among-species adjustments and revised the constants for the among-species relation to specific gravity which had been published in the earlier paper (Table 4). Again, no mention was made of adjustments within species. Markwardt and Wilson (1935) appear to have been the first to propose a method whereby adjustments for specific gravity could be made among individual pieces of a single species. No special study appears to have been performed to determine the relationship of specific gravity to strength properties within a given species, but the authors noted that the among-species relationship could be used if the power of the exponent from the between-species relationship was increased slightly. The amount of this slight increase was not tabulated, but the specific gravity exponent for the modulus of rupture was increased from 1.25 to 1.50 in the example presented.

TABLE 4

Specific gravity-strength relations (Markwardt,1930). Revised from Newlin and Wilson, 1919.

Property	SG-Strength Relation[1] Green Wood	Air Dry Wood[2]
Static Bending:		
Fiber Stress at Elastic Limit	10200 $G^{1.25}$	16700 $G^{1.25}$
Modulus of Rupture	17600 $G^{1.25}$	25700 $G^{1.25}$
Work to Maximum Load	35.6 $G^{1.75}$	32.4 $G^{1.75}$
Total Work	103 G^{2}	72.7 G^{2}
Modulus of Elasticity	2360 G	2800 G
Impact Bending:		
Fiber Stress at Elastic Limit	23700 $G^{1.25}$	31200 $G^{1.25}$
Modulus of Elasticity	2940 G	3380 G
Height of Drop	114 $G^{1.75}$	94.6 $G^{1.75}$
Compression Parallel to Grain:		
Fiber Stress at Elastic Limit	5250 G	8750 G
Maximum Crushing Strength	6730 G	12200 G
Modulus of Elasticity	2910 G	3380 G
Compression Perpendicular to Grain:		
Fiber Stress at Elastic Limit	3000 $G^{2.25}$	4630 $G^{2.25}$
Hardness:		
End	3740 $G^{2.25}$	4800 $G^{2.25}$
Radial	3380 $G^{2.25}$	3720 $G^{2.25}$
Tangential	3460 $G^{2.25}$	3820 $G^{2.25}$

[1] G represents the specific gravity of ovendry wood, based on the volume at the moisture condition indicated.

[2] 12% MC

Further studies in this area were apparently not conducted until it became desirable to have this information for use in aircraft design during World War II. One study performed on yellow-poplar (Luxford and Wood, 1944) found that the among-species specific gravity exponent should be increased by 0.25 for nearly every property in order to make adjustments or predictions of strength for this species. Other studies published near this time also reported on the effect of specific gravity, but the conclusions were more tentative. Stern (1943, 1944b) attempted to show the effect of specific gravity on the longitudinal modulus of elasticity and some strength properties for yellow-poplar and red spruce, but his data variability was too great to show convincing relationships within species. Stern was more successful in demonstrating the effect of specific gravity on the proportional limit stress and moduli of elasticity in compression perpendicular to the grain for several hardwood species (Stern, 1944a). He compared his stress at proportional limit data to the among-species relationship for this property published by the USFPL (Markwardt, 1930) and noted that the equation fit the data fairly well for many, but not all, of the species he tested. These results are consistent with those reported by Newlin and Wilson (1919). The modulus of elasticity data followed

a similar trend, but no effort was made to describe the results mathematically because of the limited number of data.

About the same time Stern was publishing his studies, the USFPL was conducting similar investigations of its own with particular emphasis on the elastic constants of wood. Their studies showed that the longitudinal Young's modulus appears to be positively correlated with specific gravity, but they did not attempt to determine a specific gravity exponent which would best represent the data for all species according to the formula proposed by Markwardt. Longitudinal Young's moduli for Sitka spruce were plotted against a curve using 1.25 as the exponent, while yellow-poplar data were described using a linear relationship (Drow and McBurney, 1946a, b). The hypothesized relationship for Sitka spruce in particular is unconvincing, and if actually present is weak at best. The remaining Young's moduli for both Sitka spruce and yellow-poplar may also have a weak correlation with specific gravity, but these data indicate that (at least for these species) the trend may be considered to be nonexistent for all practical purposes. Comparisons of the moduli of rigidity for these woods to the corresponding specific gravities appeared to show negligible trends as well, although it was thought that yellow-poplar

might have demonstrated a better correlation if individual data points had been plotted instead of the averages for each of the logs tested (Doyle, McBurney and Drow, 1946; Drow and McBurney, 1946b). Slightly different results were obtained in tests on khaya and mahogany. No significant trend was observed for the correlation of the longitudinal Young's moduli with specific gravity, but the remaining Young's moduli and shear moduli appeared to increase with specific gravity (Doyle and Drow, 1946).

Some additional data regarding the effect of specific gravity on mechanical properties have been collected independently of the USFPL. Draffin and Muhlenbruch (1937) found that the relationship between the moduli of elasticity in bending and compression and specific gravity was linear for balsa specimens. Kollmann and Krech (1960) obtained dynamic Young's modulus measurements for oak and spruce, and it appeared that these trends were linear as well. These authors also determined that the relationship of the shear moduli to specific gravity apparently depended on the species tested. Spruce shear moduli were apparently constant regardless of the specific gravity, while the oak shear moduli increased with density. Kellogg and Ifju (1962), working with twenty-one species representing a specific gravity range from 0.22 to 1.18, found that both

the ultimate tensile strength and the longitudinal Young's modulus in tension were linearly related to specific gravity. James (1964) found that specific gravity was linearly correlated with both compression strength parallel to the grain and modulus of rupture data for Douglas-fir for a range of moisture contents between two and twenty-eight percent. Wengert (1979) found that average toughness data for 17 species had a curvilinear dependency with specific gravity. Most of the above trends are similar to the linear relationships noted above for the USFPL observations on observations of the ultimate compressive strength and the moduli of elasticity in compression and bending. Currently, the American Society for Testing and Materials (1983) recommends that a linear relationship be determined between specific gravity and the property of interest for any group of specimens in a testing program (ASTM D-2555).

2.4.1 Summary

Other studies could be referenced at this point, but this writer believes that they would not significantly clarify the situation or augment the reader's understanding of how specific gravity influences the strength and stiffness of wood. It is apparent that, among species overall, specific gravity is positively correlated with most strength and

elastic properties, but the relationship of specific gravity to these properties within a given species is less certain. This can possibly be attributed to the relatively narrow specific gravity range for individual species and the (for the most part, non-statistical) methods which have been applied to analyze the available data. On the basis of the information available, this writer believes that a (weak) linear specific gravity relationship probably exists for most mechanical properties within a given species. The longitudinal Young's modulus is likely to be included in this category, but this is , perhaps, species- or material organization-specific. Other elastic constants appear to be relatively insensitive to specific gravity differences within a given species.

Chapter III

RESEARCH METHODOLOGY

In order to quantify the effects of a moisture content gradient on the strength and stiffness properties of wood, it is necessary that some model be formulated and employed which would be capable of modeling the load-deformation relationship (for either beam or uniaxial models) up to the point of failure. This model should ideally be flexible enough that the effects of various moisture gradients could be predicted for various domains without reformulating the model. The finite-element method is a numerical modeling technique which is capable of fulfilling these requirements. A brief description of the finite-element method follows this introduction.

It should be recognized, however, that the mere use of the finite-element method (FEM) does not automatically result in an accurate answer to a particular problem. It is an approximation technique which relies on certain assumptions to solve "a continuum mechanics problem with an accuracy acceptable to engineers" (Cook, 1981). The solution of non-linear mechanics problems (such as the prediction of ultimate compression strength) is accomplished using multiple steps and requires that a model for

mechanical behavior be incorporated into the computer program for the FEM solution. Obviously, then, the finite-element method cannot be expected to provide exact answers to complex problems if the mechanical behavior model used is too simplistic or unrealistic, or if the behavior being modeled is highly dependent upon random factors in real life. Three models which are relevant to predictions of mechanical behavior need to be incorporated into the finite-element program and are described in this chapter. The first describes the distribution of moisture within a wood specimen under varying relative humidity-temperature (EMC) conditions. The second model quantifies the effect of moisture content on the elastic constants of equilibrated material. The third model defines the stress-strain relationship in both tension and compression. This last model is required to predict mechanical behavior beyond the proportional limit for either beam or uniaxial finite-element models.

3.1 EXPERIMENTAL PLAN

The overall plan for this study is outlined in Figure 20. Experimental testing is required in several instances:

1. Uniaxial data need to be collected to form a data base to calibrate the models of uniaxial stress-strain behavior.

2. These same data are needed to form a model for the variation of the longitudinal Young's moduli with moisture content; as is discussed in another section, the accurate estimation of these constants is very important.
3. Data are required to verify the finite-element method solution for moisture gradient effects.

3.1.1 Mechanical Testing

Previous tests on yellow-poplar indicate that the longitudinal Young's modulus is significantly different in compression and in tension for wood at around 9% moisture content (Stern, 1944b). Comparable yellow-poplar data are not available for other moisture contents, but these data alone indicate that both tension and compression tests should be conducted for a range of moisture contents to accurately predict beam stiffness at different moisture contents using a finite-element model.

Four moisture content levels were selected for the uniaxial test material: six, twelve, eighteen percent moisture content, and green. The three lower moisture contents were chosen because

1. They exceed the moisture content value (approximately 4% MC) where the moisture content-strength property relationship appears to change.

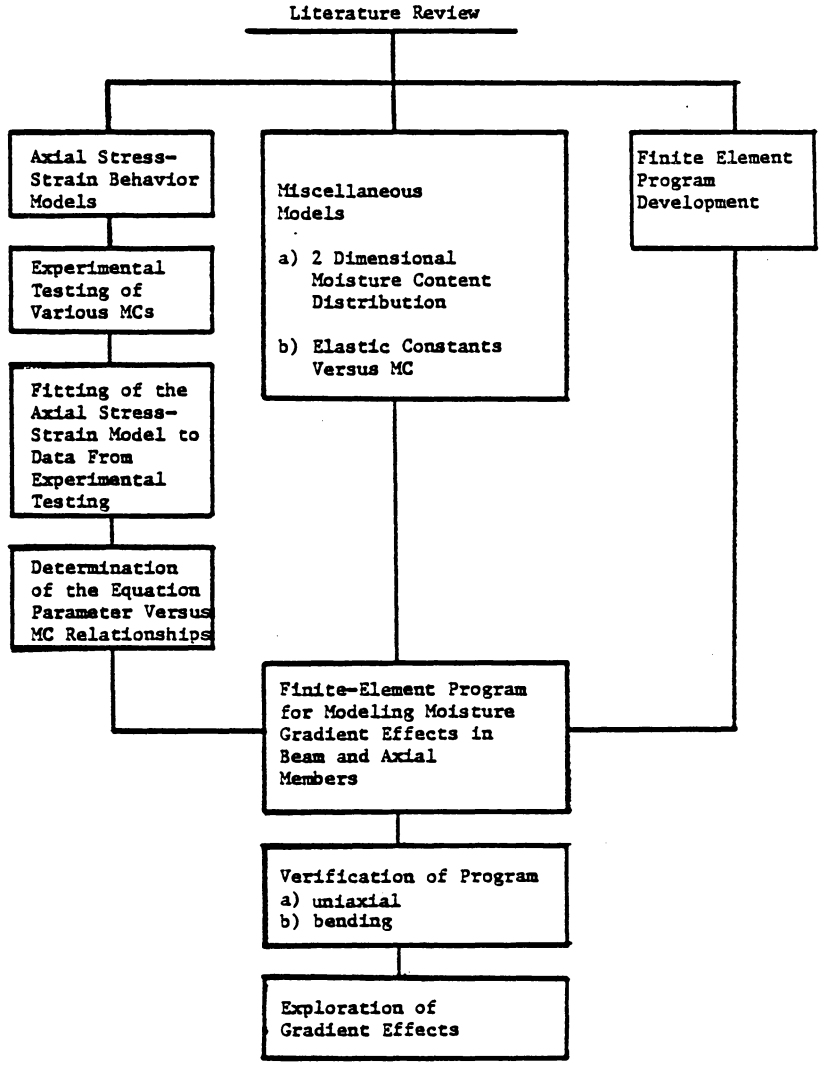

Figure 20: Outline of experimental plan.

2. These three moisture contents are equally spaced and well below the fiber saturation point, and
3. Three moisture contents are the minimum number required to differentiate a curvilinear moisture content-mechanical property relationship from a linear moisture content-mechanical property relationship.

Green specimens were tested to obtain the mechanical properties and to aid in establishing a reference value for estimating an intersection point. Specific gravity is a possible confounding factor in analyzing the results of any mechanical tests, so its effect was minimized by planning to use only a few trees from a single site for all the tests. (A second group of logs had to be used to acquire sufficient specimens for the beam tests, however; the comparison of this material to the original specimens is described in a later section). It was also decided to take specific gravity measurements on a green volume basis to eliminate any influence of the drying treatment(s) on volume.

3.1.2 Reasons for Selecting Yellow-Poplar

Although moisture gradients are hypothesized to affect all species similarly, it is not within the scope of this dissertation to test enough species to verify this

assumption. Therefore, yellow-poplar (Liriodendron tulipifera) was chosen as the sole species tested in this study. The choice of this species was motivated by several factors:

1. The tree grows locally and fresh-cut logs are easy to obtain,
2. The wood has a fairly straight grain and a uniform cell structure (diffuse-porous), thereby minimizing the effects of material inhomogeneity, and
3. Some data are available in the literature regarding the elastic constants.

Heartwood was excluded from this investigation for two reasons. First, there is evidence that the diffusion coefficients are different for the heartwood and the sapwood of yellow-poplar (Choong and Fogg, 1968; Choong and Skaar, 1969). A simple model for a moisture gradient (as described earlier) would be less likely to have significant errors. The second consideration was the fact that wood is actually a material with conical orthotropy, although it is traditionally considered to have rectangular orthotropy. By selecting only the sapwood from large trees, the error involved in using this traditional assumption can be minimized (Figure 21). That yellow-poplar sapwood and heartwood are easily distinguishable by color is an added convenience.

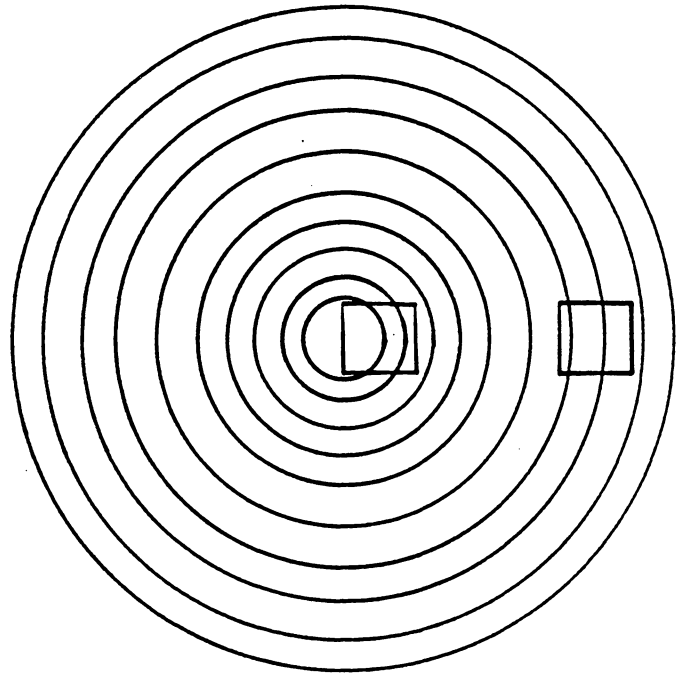

Figure 21: Cross-section of a tree showing how growth ring curvature is minimized in sapwood

3.1.3 Use of the Finite-Element Model

The foregoing are the data required to make the finite-element model a useful tool; the specific experimental procedures are presented in another chapter. Once the data have been resolved into models for the finite-element program, the program must be verified. This can be achieved to a certain extent by comparing the uniaxial data already collected to the program predictions of uniaxial behavior. The correctness of these analyses, however, does not guarantee that beam behavior will be predicted with equal accuracy, so a number of beam tests are required for verification of the beam model. Both equilibrated and non-equilibrated beams must be tested at various average moisture contents to provide data to be compared to the finite-element program output. Subsequent exploration of gradient effects is possible once the satisfactory performance of the model has been established.

3.2 THE FINITE-ELEMENT MODEL

3.2.1 Overview of Finite Elements

The finite element method is a numerical technique developed in the mid-1950s to solve differential equations with complex domains or boundary conditions. In very general terms, the use of this method follows this procedure (Reddy, 1984):

1. Discretization of the domain into elements
2. Derivation of the element equations
3. Assembly of the element equations
4. Imposition of the boundary equations
5. Solution of the equations
6. Postprocessing the solution

For the benefit of the reader without previous exposure to the finite-element method, these steps will be briefly discussed below. For more details, the reader is encouraged to refer to the books by Zienkiewicz (1973, 1977), Cook (1981) and Reddy (1984).

3.2.1.1 Discretization of the Domain into Elements

Because the finite-element method is a piece-wise approximation to the solution of a continuum problem, the domain of the problem must first be broken up into sub-domains called elements. These elements may be uniform shapes and need not exactly represent the domain of the problem, although this improves the accuracy of the solution. Note that the circular domain in Figure 22 has been broken into triangular elements. This is not the only element which could have been chosen for this diagram. Differently-shaped elements such as squares could also have been used, although the boundary approximation error (white

space in Figure 22) would likely have been greater in this instance unless additional elements were used. An additional distinction which should be made between these two elements is that square elements have four corners at which solutions (loads or displacements) can be calculated, as opposed to three corners for the triangular elements. These points at which solution values can be determined are called nodes. It should be emphasized at this point that nodes need not be solely restricted to corners. A more complex element may also have interior nodes and/or nodes spaced along the boundary.

3.2.1.2 Derivation of the Element Equations

As previously mentioned, nodes are points at which values of the solution are determined. These values for the solution are determined by setting up a series of simultaneous equations for each element in matrix form. For static loading in the absence of temperature and/or body forces, these equations take the form

$$[K]\ \{u\} = \{F\} \qquad [3.1]$$

The symmetric [K] matrix (stiffness matrix) is derived from the equilibrium equations which mathematically describe the load-displacement relationship for the problem, while {u}

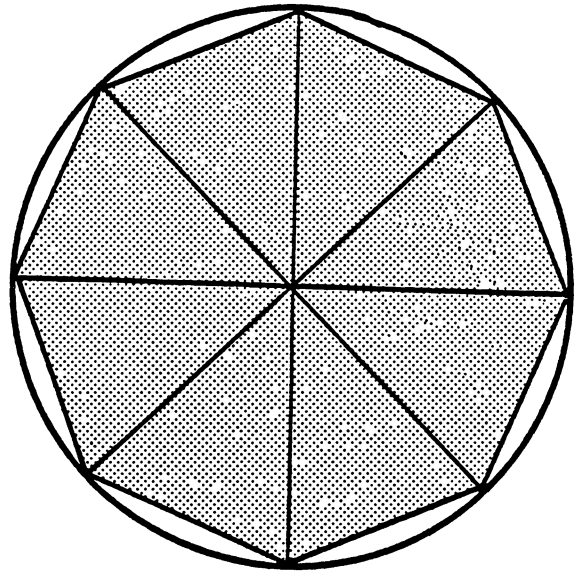

Figure 22: Finite-element discretization of a circular domain. (After Reddy (1984)).

and {F} are the nodal displacement and force vectors, respectively. The number of rows in these matrices will equal the number of nodes times the number of degrees of freedom. For example, a line element with one degree of freedom at each of two nodes will have two equations. The solution of the equilibrium equations for individual elements is made possible by incorporating an assumed function for the displacements within the elements into the mathematical formulation of the problem. This function, called a shape or interpolation function, is derived for the type of element being used. Consequently, several types of elements can be used together, as the shape functions change only the numerical values involved in the solution, not the mathematical statement of the problem (Figure 23).

3.2.1.3 Assembly of the Element Equations

Following the derivation of the element equations for each element, the equations are assembled into a system of matrix equations representing the mathematical model for the discretized domain. This is accomplished by adding the contribution of adjacent elements at shared nodes and by including lines to account for the nodes which are not shared by two or more elements (Figure 23). Note that both the stiffness matrix and the force vector for each element must be manipulated.

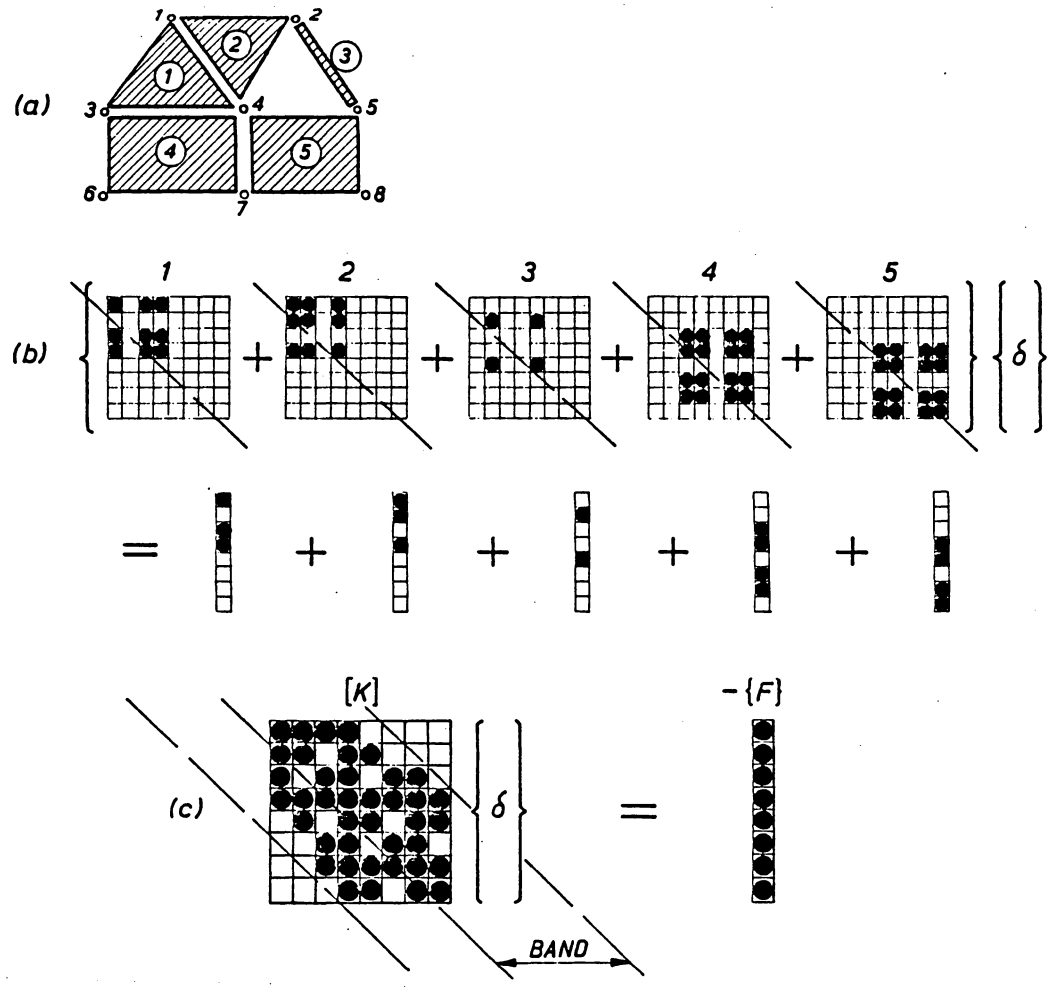

Figure 23: Arbitrary assemblage of elements. The circled numbers designate the number of the element, the numbered points between elements are the nodes. (From Zienkiewicz, 1977).

3.2.1.4 Solution of the Problem

It is not sufficient to assemble the equations and to specify the known nodal forces, because an infinite number of solutions can be found unless the system of equations is also restricted by the specification of a number of displacements to prevent rigid body motion. This fixes conditions at additional nodes, because when a force is known the displacement can be determined, and vice versa. Following the imposition of all the boundary conditions, the [K] matrix becomes non-singular and procedures such as Gaussian elimination may be used to solve for the remaining unknowns. Because the stiffness matrix is symmetric, it may be stored in banded form to save on computer storage requirements, as in the example from Zienkiewicz presented in the previous subsection. This will not necessarily affect the choice of a solution method, although it will make the programming of the solution routine rather more complex.

3.2.1.5 Postprocessing the Solution

"Postprocessing the solution" means determining the strains and stresses once the unknown forces and displacements are calculated. Strains are calculated for points within the elements using the nodal displacements and the assumed

displacement function (shape function) mentioned previously. Stresses are then obtained by multiplying the element strain vector by the symmetric material stiffness matrix from the theory of elasticity.

3.2.2 Review of Suitable Elements

When making a finite-element analysis, it is often possible to take advantage of material uniformity to reduce the modeled structure to an assemblage of planar or even linear elements. In the present study, however, the presence of a moisture gradient in the wood will create a material which has different material properties through both its thickness and its depth. This material nonhomogeneity requires the use of three-dimensional elements in any finite-element analysis.

Three-dimensional analyses are infrequently reported in the literature because they require significantly more computer storage and execution time than two-dimensional models. Even for an orthotropic material such as wood, planar models are most commonly used for mechanical analyses (Maghsood, 1970; Krueger and Sandberg, 1974; Gopu and Goodman, 1974, 1975; Fernandez and Polensek, 1979; Gopu, 1980; Wilkinson, et al., 1981; Wilkinson and Rowlands, 1981a, b; Gerhardt, 1982). Three-dimensional finite-element

models have occasionally been used for wood mechanics problems, however, and the experience of these investigators, plus those who have worked on two-dimensional problems, suggests that three different brick-type elements should be given the most consideration (Al-Dabbagh, 1970; Al-Dabbagh, et al., 1972). These brick-type elements are especially attractive for the present study because they will exactly represent the rectangular domain of the wooden beams.

3.2.2.1 Eight-node Linear Brick-type Element

Eight-node brick elements are also known as three-dimensional linear elements because of the linear displacement function with which they are associated (Figure 24). These elements will enable the solution of the differential equation governing axial deformation of a bar to be exact at the nodes, but in general, linear elements are too "stiff" to model more complex behavior, such as the bending of beams (Zienkiewicz, 1977; Cook, 1981; Gerhardt, 1982). Reasonable solutions for beams can be obtained with this element, but these require the use of a considerable number of elements along the longitudinal axis of the beam (Al-Dabbagh, 1970; Gerhardt, 1982). In most cases, it is usually recommended that higher order elements be used for bending analyses.

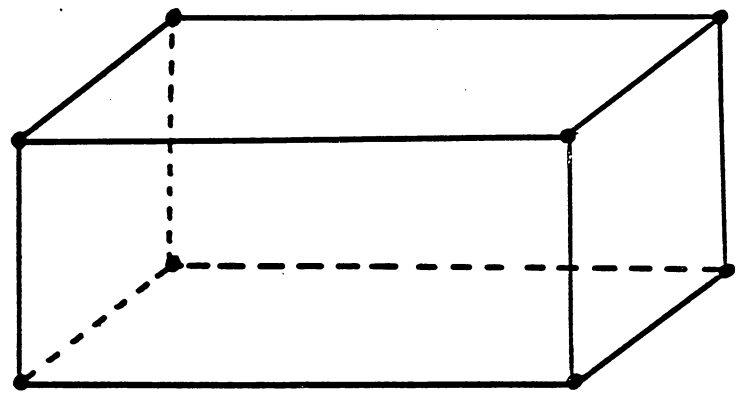

Figure 24: Eight-node linear brick-type element

3.2.2.2 Twenty-node Quadratic Brick-type Element

Twenty-node quadratic elements are considerably more flexible than the linear elements because they permit parabolic displacements along their edges (Figure 25). Two-dimensional analogues of three-dimensional linear and quadratic elements have shown that the same numbers of quadratic elements and linear elements yield cantilever-tip deflections which are within 99% and 65% of the exact solution, respectively (Zienkiewicz, 1977). It also appears as though the computer storage and time requirements needed for good answers might be similar for simple beams modeled by either linear or quadratic elements. Al-Dabbagh (1970), for example, required a three-dimensional (3-D) mesh of twenty by five by one (l x d x w) linear elements to approach to within three percent of the theoretical solution for a cantilever beam, while Maghsood (1970) was able to get equivalent accuracy with a (two-dimensional) four by six (l x d) element mesh of quadratic elements for a comparable problem (one-half of a symmetrical beam subjected to third-point loading).

3.2.2.3 Thirty-two-node Cubic Brick-type Element

This element is capable of representing beam displacements exactly (Zienkiewicz, 1977), but at the expense of

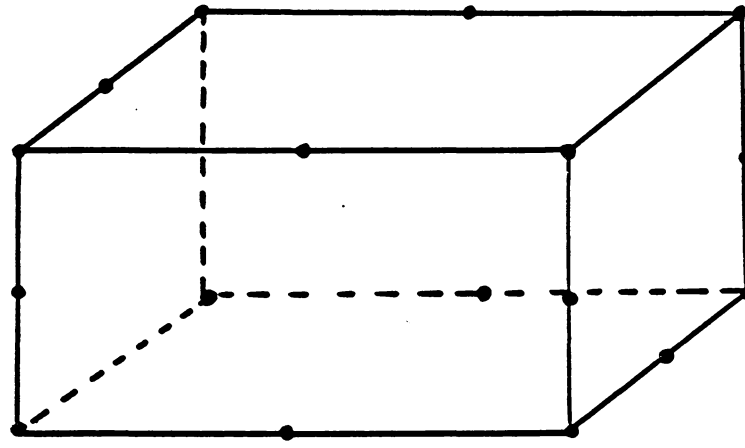

Figure 25: 20-node quadratic brick-type element

considerably more computation time and storage than is required even for the quadratic elements (Figure 26). It is seldom used in 3-D finite element analyses for this reason, especially since quadratic elements often yield reasonable results.

3.2.3 Analyses Beyond the Elastic Limit

Finite-element texts describe several methods for performing analyses where stress-strain modeling is required beyond the elastic limit of the material (Zienkiewicz, 1977; Cook, 1981; Reddy, 1984). In general, these problems are solved in a number of discrete steps, with each step approximating a portion of the stress-strain diagram by one of several methods (linear step-by step, Newton-Raphson, modified Newton-Raphson, et cetera). The Newton-Raphson and the modified Newton-Raphson methods are more accurate than the linear step-by-step procedure, but the accuracy is obtained at the expense of several iterations per load or displacement increment added to the model. On the other hand, the linear step-by-step method has been known to yield answers which are correct to within a few percent if the loads or displacements are imposed in small increments (Maghsood, 1970). Since the material properties of wood with a nonuniform moisture gradient vary in three dimensions

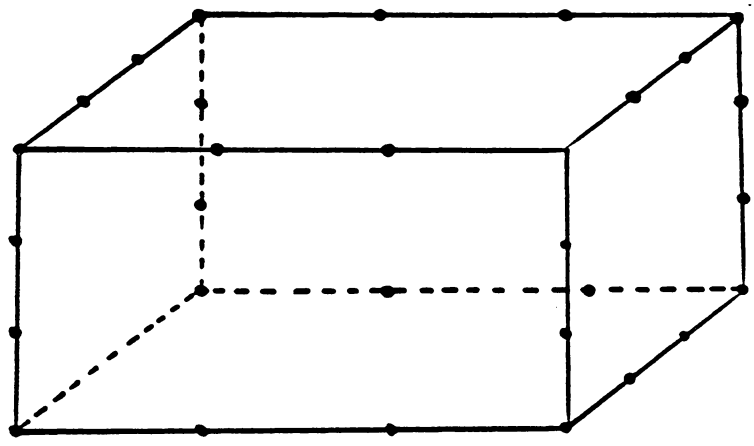

Figure 26: 32-node cubic brick-type element

as it is tested to failure, the element stiffness matrices would have to be updated not only along the axis of the modeled specimen, but also across the cross-section. For these reasons an iterative type of model would likely be prohibitively expensive and time-consuming. Since the linear step-by-step procedure appeared to be more practical, this procedure was selected for use in this study even though it was realized that some degree of accuracy was being sacrificed. A brief description of this method follows this subsection, and a description of the method used to determine the elastic constants at various points along the stress-strain curve is included as well.

3.2.3.1 Linear Step-by-Step Method for Analyses Beyond the Elastic Limit

This is perhaps the simplest of the various methods, but it is subject to the greatest amount of potential inaccuracy. In this incremental scheme, the stiffness matrix is originally defined using the initial elastic constants. (These elastic constants are equal to the initial slope of some mechanical response model (e.g., stress-strain diagram) for each elastic constant at zero strain). The solution of the initial finite-element equations results in the determination of particular strain values for each element; the slopes of the mechanical response models at these strain

values are used to determine the appropriate elastic constants for the next step. This procedure is repeated over and over until the desired number of steps is completed. The accuracy of this method improves as more steps are taken in the analysis (Figure 27). Bookkeeping must be used to keep track of the displacements, stresses, and strains, as these are additive.

3.2.3.2 Estimation of Elastic Constants Beyond the Elastic Limit

Methods are described later in this chapter for estimating elastic constants based on variation of moisture content. The Young's modulus parallel to the grain also changes under load as the stress and/or strain exceeds certain limits (i.e., the "proportional limit"), and the modeling of this response is detailed in a following section. Much less is known about the concomitant changes in the other elastic constants.

One approach which might be utilized would be to assume that all the elastic constants are proportional to the longitudinal Young's modulus at every point on the stress-strain curve. There appears to be no evidence for this, however, and it seems unlikely that the proportional limit stress would be reached for the perpendicular to the grain Young's moduli (for example) in a uniaxial test when the primary stress is along the longitudinal axis.

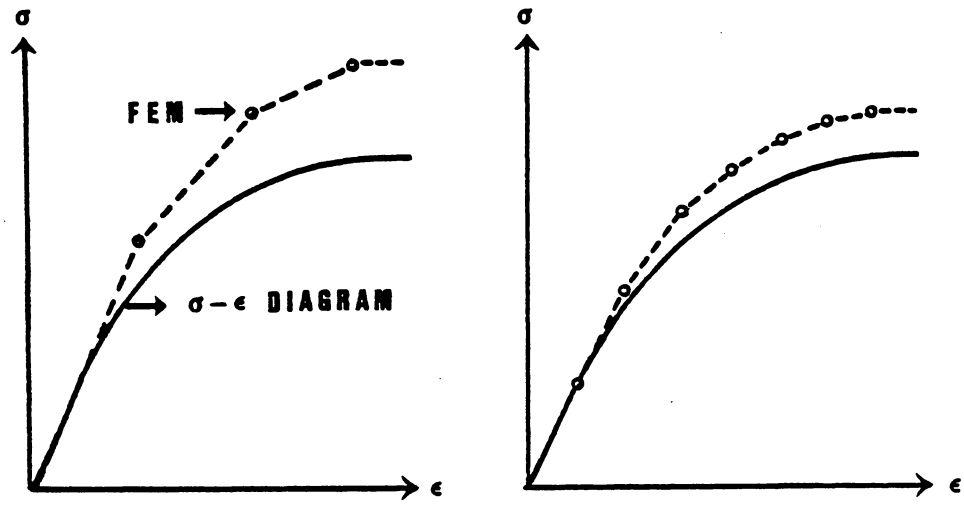

Figure 27: Examples of stress-strain diagrams modeled by differing numbers of steps in the finite-element analysis.

Maghsood (1970) used a two-dimensional finite-element model for beam analysis and found that "it was not necessary to modify any ... moduli" except E_l (i.e., E_r, G_{lr}, and the Poisson's ratios ν_{lr} and ν_{rl}), "since the corresponding stresses did not exceed their proportional limits" determined from testing. These findings may be true for most of the elastic constants, but two Poisson's ratios should change along with the longitudinal Young's modulus if the assumption of orthotropic elasticity is valid. As can be seen from an examination of the simple elastic constant relationship

$$\frac{\nu_{ij}}{E_i} = \frac{\nu_{ji}}{E_j} \qquad [3.2]$$

if E_i were to decrease by some factor (x), then ν_{ij} would have to decrease by the same proportional amount. For example,

$$\frac{\nu_{12}}{E_1} = \frac{\nu_{21}}{E_2} \xrightarrow{E_1' = 0.8E_1} \frac{0.8\nu_{12}}{E_1'} = \frac{\nu_{21}}{E_2} \qquad [3.3]$$

$$\frac{\nu_{13}}{E_1} = \frac{\nu_{31}}{E_3} \xrightarrow{E_1' = 0.8E_1} \frac{0.8\nu_{13}}{E_1'} = \frac{\nu_{31}}{E_3} \qquad [3.4]$$

Therefore, ν_{12} and ν_{13} are the only Poisson's ratios that should change as E_1 changes with stress/strain. For the most part, the remaining elastic constants will remain solely dependent upon moisture content for the purposes of this study. Slight adjustments to this rule become necessary when an element fails in longitudinal tension or compression.

First of all, it must be recognized that no element in an analysis of this type can be allowed to have a modulus equal to zero, which is what essentially happens at failure during an actual test. Some positive, non-zero modulus is necessary in order to prevent numerical difficulties during the matrix solution of the stiffness equations. In this study, failures in longitudinal compression were modeled by decreasing the principal Young's modulus, ν_{12} and ν_{13} to pre-determined minimal values, but it was decided to retain the initial values for the other elastic constants in view of the fact that no physical discontinuity actually results. Failures in tension result in a physical rupture, however, and all elastic constants must be reduced. These points are of minimal importance during the modeling of uniaxial tests; failure of a single element usually indicates failure of the whole. Beam tests are different, however, and it is for this reason that the previous points have been addressed.

3.3 MATHEMATICAL DESCRIPTION OF MOISTURE DISTRIBUTION

Drying wood is commonly presumed to have a parabolic moisture gradient (Kollmann and Cote, 1968). This assumption is based to a considerable extent upon one-dimensional experiments (Sonnleithner, 1933; Bateman, et al., 1939; Krischer, 1942; McMillen, 1955a,b; Cech, 1964), and also upon the results of mathematical solutions to the differential equation for diffusion (Moschler and Martin, 1968; Bramhall, 1979). A related assumption is that the outer edges of a wood specimen come to near-immediate equilibrium with the conditions to which the wood is exposed (Bateman, et al., 1933; Comstock, 1963; Hart, 1968; Siau, 1971; Simpson, 1974). Some studies indicate, however, that this assumption is not correct during the initial drying period. Bramhall's model for lumber drying reveals that the surface of green alpine fir should require approximately twenty-five hours to attain equilibrium with the exposure conditions, and Moschler and Martin's data for yellow-poplar support this prediction (Bramhall, 1979; Moschler and Martin, 1968). Therefore, this restriction must be recognized, but it does not invalidate the basic parabolic moisture gradient for the majority of the drying cycle.

Extending the one-dimensional parabolic model to a two-dimensional surface, it seems reasonable to assume that the

moisture content gradient could be represented by a paraboloid over the two-dimensional cross-section (Figure 28). This assumption is supported by the aforementioned data of Fernow (1898) and Schaffner (1981). Since the diffusion coefficients for the radial and tangential directions are usually unequal (although this may be species-dependent), this hypothesis is not likely to be exactly correct (Choong and Fogg, 1968; Choong and Skaar, 1969). Nonetheless, discrepancies between the actual moisture content distribution and that from the simple paraboloid model are not likely to be significant enough to warrant a more complex model.

The model for the two-dimensional moisture distribution chosen for this investigation, therefore, is the simple two-dimensional (2-D) paraboloid. The model for a desorption gradient can be represented mathematically for a rectangular domain by[1]

$$MC = 2.25 \times (MCBAR-EMC) \times (1-k_1X^2) \times (1-k_2Y^2) + EMC \qquad [3.5]$$

where X = horizontal distance from the center

Y = vertical distance from the center

MCBAR = average moisture content (%)

---

[1] This equation was furnished to the author through the courtesy of Dr. C. Skaar.

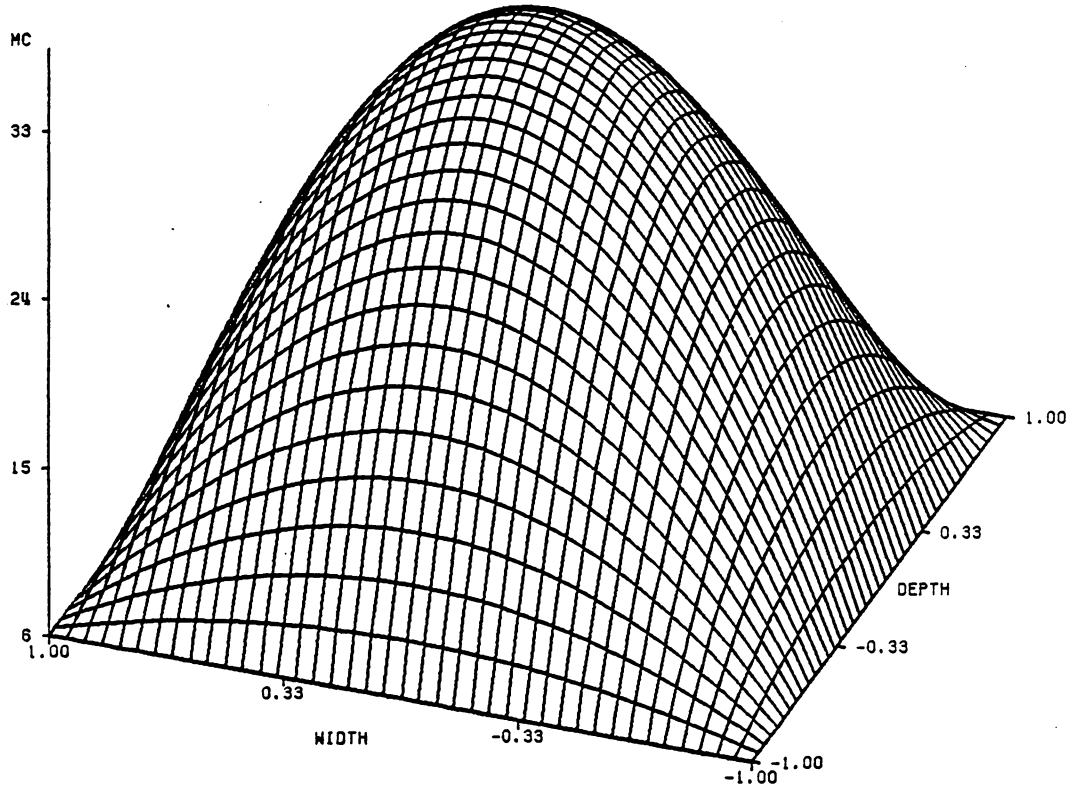

Figure 28: Hypothetical moisture distribution over a square cross-section. Average MC=18 percent, EMC=6 percent.

EMC = equilibrium moisture content (%)

k_1 = 1/(w/2)squared

k_2 = 1/(d/2)squared

w = width of the rectangular domain (cross-section)

d = depth of the rectangular domain (cross-section)

3.4 MATHEMATICAL DESCRIPTION OF THE VARIATION OF SOME MECHANICAL PROPERTIES WITH MOISTURE CONTENT

To predict strength properties of wooden beams with a finite elements program, it is necessary to know both the strength properties and the elastic constants for wood in uniaxial stress. Previous studies employing finite-elements have found that the mechanical properties parallel to the grain (MOE and the maximum stresses in tension and compression) were of greatest importance in successfully modeling beam behavior (Krueger and Sandberg, 1974; Fernandez and Polensek, 1979). The effect of inaccuracies in the estimation of the other elastic constants was found to be of only minor significance. Therefore, it was decided that only the longitudinal properties would be obtained by direct testing and that the remaining parameters would be estimated.

3.4.1 Estimation of the Elastic Constants at Various Moisture Contents

In reviewing the available literature on the variation of the elastic constants (other than E_l) with moisture content, it was noted that all the trends appeared to be substantially linear (Carrington, 1922; Mark, et al., 1970; Tang, et al., 1971). Therefore, it was assumed that the elastic constants (with the exception of E_l) could be approximated by linear functions between the minimum and maximum property values over an appropriate moisture content range. Unfortunately, no data are available for E_r, E_t and the Poisson's ratios for yellow-poplar except at eleven percent moisture content (Drow and McBurney, 1946b). (Shear moduli data are available in the literature for a wide range of moisture contents (Mark, et al., 1970)). Data from other species were examined to determine if there are inter-species similarities which might be useful in forming approximate relationships for the elastic constants with moisture content. Several important points were noted. First of all, investigators often chose to study elastic constants at a few discrete moisture contents instead of using a wide range of moisture contents (Doyle, McBurney and Drow, 1946 ; Drow and McBurney, 1946a; McBurney and Drow, 1956; Youngs, 1957). These data are useful in that they show a given amount of change for a given moisture content

range, but their usefulness is limited by the range of the moisture contents studied. Certain other investigations were conducted using specimens at many moisture contents between approximately zero and sixty-five (plus) percent (Carrington, 1922; Mark, et al., 1970; Tang, et al., 1971). These studies affirm T. R. C. Wilson's observation that not all mechanical properties for the same species exhibit identical intersection points, although these are usually within two percent MC of each other. Limited data also indicate that the measurements of the elastic constants appear to be more variable between zero and about four percent MC, and that the elastic constants may be more or less unchanging within this range (on the average). The longitudinal modulus of elasticity in particular has been noted for this type of relationship by several researchers, and most of the elastic constants are at a maximum at some moisture content close to this range (see Literature Review). Because this (approximately four percent) moisture content will be referred to subsequently, it will be called the "maximum value moisture content" or MVMC for convenience.

The problem of finding a linear relationship for the elastic constants over a moisture content range can now be restated in terms of finding a linear relationship for these

constants between some intersection point and the MVMC. (Because this intersection point does not result from a semi-logarithmic relationship it is conceptually different from Wilson's M_p). One approach would be to pick a starting property value and add or subtract (as appropriate) some percentage of this value to the original number for each one percent change in moisture content. Because some data sets (noted above) do not bracket the intersection point, the property value at the MVMC was used for the starting point. Like the intersection points, the values of the MVMCs are also subject to some uncertainty, but it was believed that the MVMCs could be more closely estimated, thereby decreasing subsequent errors. The process of estimating the elastic constants at some MVMC for yellow-poplar involved several steps.

First, an MVMC value was determined for each elastic constant. Yellow-poplar-specific MVMC values were found only for the shear moduli (Mark, et al., 1970). These values ranged from 0.0 percent to 4.0 percent and averaged 1.9 percent. This average MVMC value appeared to be consistent with the scanty data available for shear moduli of other species. Corresponding MVMC values were lacking for the remaining elastic constants (E_r, E_t, ν_{ij}), so 1.9 percent was used as the MVMC estimate for these properties.

The elastic constant corresponding to this MVMC was then estimated. Using data available in the literature, a rate of change for each property (relative to the MVMC value) per one percent change in the moisture content was calculated as PROPDEL, where

$$\text{PROPDEL} = \frac{\dfrac{(\text{value at high MC} - \text{value at lower MC})}{(\text{the high MC} - \text{the lower MC})}}{\text{Value at the MVMC}} \qquad [3.6]$$

PROPDEL values specific for yellow-poplar could only be calculated for the shear moduli, but there is substantial agreement among other species for each of the other properties (Tables 5 through 13). Therefore, it was decided that the average PROPDEL values for several species would probably serve as reasonable estimates of the remaining yellow-poplar PROPDEL values. This hypothesis was checked by comparing the specific PROPDEL values for yellow-poplar shear moduli against the values obtained for the shear moduli of other species. A certain amount of variability was evident, but the yellow-poplar values agreed fairly well with the values from other species.

The next step was to approximate the elastic constants at the MVMCs for yellow-poplar. If this information was known from a previous study, an elastic constant at some unspecified moisture level could be calculated from

TABLE 5

Collected data and rates of change for E_r. MVMC = 1.9%

Species	E_r min. (psi)	MC%, min.	E_r max. (psi)	MC%, max.	PROPDEL
Red oak[1]	110500	22.2	248500	5.7	-.02984
Sitka spruce[2]	73600	22.7	155300	6.6	-.02831
Douglas-fir[3]	106600	20.8	207300	7.3	-.03013
Spruce[4]	54300	26.2	127000	5.0	-.02492
			Average:		-.02830

[1]Youngs (1957)

[2]Drow and McBurney (1964a)

[3]McBurney and Drow (1956)

[4]Carrington (1922)

TABLE 6

Collected data and rates of change for E_t. MVMC = 1.9%

Species	E_t min. (psi)	MC%, min.	E_t max. (psi)	MC%, max.	PROPDEL
Red oak tension[1]	64800	19.6	123700	5.4	-.03001
Red oak compression[1]	63800	20.8	123000	5.4	-.02817
Sitka spruce[2]	41400	22.7	91500	6.6	-.02931
Douglas-fir[3]	67800	20.8	154900	7.3	-.03400
Spruce[4]	27700	27.2	78300	5.0	-.02670
			Average:		-.02960

[1]Youngs (1957)

[2]Drow and McBurney (1946a)

[3]McBurney and Drow (1956)

[4]Carrington (1922)

TABLE 7

Collected data and rates of change for G_{lr}. MVMC = 1.7%

Species	G_{lr} min. (psi)	MC%, min.	G_{lr} max. (psi)	MC%, max.	PROPDEL
Yellow-poplar[1]	72000	22.6	128000	1.7	-.02093
Virginia pine[1]	109000	24.8	188000	0.0	-.01745
Scarlet oak[2]	80000	27.4	160000	3.7	-.02024
Spruce[3]	72000	33.0	117500	0.0	-.01197

[1]Mark, et al. (1970)

[2]Tang, et al. (1971)

[3]Carrington (1922)

TABLE 8

Collected data and rates of change for G_{lt}. MVMC = 0.0%

Species	G_{lt} min. (psi)	MC%, min.	G_{lt} max. (psi)	MC%, max.	PROPDEL
Yellow-poplar[1]	53000	20.0	85000	0.0	-.01882
Virginia pine[2]	94000	26.7	157000	0.0	-.01503
Scarlet oak[2]	60000	26.7	120000	3.7	-.02011
Spruce[3]	58000	30.0	71000	5.0	-.00706

[1]Mark, et al. (1970)

[2]Tang, et al. (1971)

[3]Carrington (1922)

TABLE 9

Collected data and rates of change for G_{rt}. MVMC = 4.0%

Species	G_{rt} min. (psi)	MC%, min.	G_{rt} max. (psi)	MC%, max.	PROPDEL
Yellow-poplar[1]	11000	22.0	23000	4.0	-.02899
Virginia pine[1]	15000	18.1	30000	12.1	-.04975
Scarlet oak[2]	26000	28.3	48000	3.3	-.01857
Spruce[3]	21200	33.0	38800	2.0	-.01505

[1]Mark, et al. (1970)

[2]Tang, et al. (1971)

[3]Carrington (1922)

TABLE 10

Collected data and rates of change for ν_{lr}. MVMC = 1.9%

Species	ν_{lr}, min.	MC%, min.	ν_{lr}, max.	MC%, max.	PROPDEL
Spruce[1]	0.218	36.3	0.362	7.2	-.01275
Douglas-fir[2]	0.267	20.8	0.308	7.3	-.00936
				Average:	-.01105

[1]Carrington (1922)

[2]McBurney and Drow (1956)

TABLE 11

Collected data and rates of change for ν_{lt}. MVMC = 1.9%

Species	ν_{lt}, min.	MC%, min.	ν_{lt}, max.	MC%, max.	PROPDEL
Spruce[1]	0.520	7.0	0.746	27.4	+.02390
Douglas-fir[2]	0.431	7.3	0.515	20.8	+.01566
Sitka spruce[3]	0.425	6.6	0.534	22.7	+.01722
			Average:		+.01893

[1]Carrington (1922)

[2]McBurney and Drow (1956)

[3]Drow and McBurney (1946a)

TABLE 12

Collected data and rates of change for ν_{rt}. MVMC = 1.9%

Species	ν_{rt}, min.	MC%, min.	ν_{rt}, max.	MC%, max.	PROPDEL
Spruce[1]	0.487	5.7	0.670	25.5	+.02198

[1]Carrington (1922)

TABLE 13

Collected data and rates of change for ν_{tr}. MVMC = 1.9%

Species	ν_{tr}, min.	MC%, min.	ν_{tr}, max.	MC%, max.	PROPDEL
Spruce[1]	0.245	3.1	0.378	26.4	+0.02396
Douglas-fir[2]	0.356	7.3	0.401	20.8	+0.00986
				Average:	+0.01691

[1]Carrington (1922)

[2]McBurney and Drow (1956)

$$\text{Elastic Constant (MC)} = \text{MVMC property} + (\text{MC} - \text{MVMC}) \times \text{PROPDEL} \times (\text{MVMC value}) \qquad [3.7]$$

where MVMC value is the elastic constant at the MVMC.

As noted previously, complete yellow-poplar data are available at eleven percent moisture content. If eleven percent is substituted for the moisture content in [3.7], and if the elastic constant at eleven percent (PROP11) is substituted for Elastic Constant (MC), then the above equation can be arranged to produce a mathematical definition of the elastic constant at the MVMC:

$$\text{MVMC value} = \frac{1.0}{\frac{(11-\text{MVMC}) \times \text{PROPDEL}}{\text{PROP11}} + 1/\text{PROP11}} \qquad [3.8]$$

The value of every elastic constant can now be calculated for yellow-poplar at the MVMC. With the exception of ν_{rl} and ν_{tl}, these values and the corresponding PROP11 values used for yellow-poplar are listed in Table 14.[2]

Values for yellow-poplar elastic constants at other moisture contents can be calculated by substituting the values for the property at the MVMC and the PROP11 (Table

---

[2] The Poisson's ratios ν_{rl} and ν_{tl} are usually not measured and are calculated (once E_l is known) using the assumption of orthotropic elasticity. E_l has not yet been defined, so these constants are not included in the table.

TABLE 14

Values of the elastic constants for yellow-poplar at the selected MVMCs

Elastic Constant	MVMC	PROP11[1]	Elastic Constant at MVMC
E_r	1.9	129000 psi	173700 psi
E_t	1.9	60000 psi	82200 psi
G_{lr}	1.7	105000 psi	130400 psi
G_{lt}	0.0	97000 psi	122300 psi
G_{rt}	4.0	16000 psi	20100 psi
ν_{lr}	1.9	0.318	0.354
ν_{lt}	1.9	0.392	0.334
ν_{rt}	1.9	0.703	0.586
ν_{tr}	1.9	0.329	0.285

[1]Drow and McBurney (1946b)

14) and the PROPDEL value for yellow-poplar (or the average PROPDEL value) (Tables 5 through 13) into equation [3.7], above. The elastic constants are assumed to be unchanging at moisture contents below the MVMC and above the intersection point. One study shows that the yellow-poplar intersection points for G_{lr}, G_{lt} and G_{rt} are at approximately 22.6, 20.0 and 22.0 percent moisture content, respectively, (Mark, et al., 1970). Intersection points for most of the other yellow-poplar elastic constants do not appear in the literature; a limited number of data for E_l show intersection points around twenty-five to thirty percent (Tang and Hsu, 1972). To approximate the unknown intersection points, the available intersection point values were averaged with the intersection point obtained from analysis of the uniaxial specimens tested for this study. Discussion of how this point was determined is deferred.

3.5 MODELING STRESS-STRAIN BEHAVIOR IN COMPRESSION

3.5.1 Previously Proposed Models

To fulfill the objectives of this dissertation, it was necessary to describe the stress-strain behavior of yellow-poplar in both tension and compression for a range of moisture contents up to the green state. Because modeling the stress-strain diagram for wood tests in compression has

been tried by many previous investigators, this aspect of the problem was chosen for the initial modeling trials. Most researchers involved with modeling the stress-strain diagram for wood in compression have applied their work to predicting the ultimate bending strength in beams. Many have simplified the stress-strain diagram in compression behavior in beams by assuming that either an elastic-perfectly plastic model (Figure 29) or a parabola would be adequate for their purposes (Neely, 1898; Ros, 1936; Thunell, 1939, 1940; Suenson, 1941; Ivanov, 1949; Bechtel and Norris, 1952; Ethington, 1960; Ramos, 1961; Moe, 1961; Mazur, 1965; Nwokoye, 1972; Zakic, 1976). Krueger and Sandberg (1974) improved these models somewhat by idealizing the stress-strain diagram as a tri-linear function (Figure 30). Bazhenov, et al. (1953) thought of using a three-part model consisting of a linear, quadratic, and linear regions to describe the stress-strain diagram of wood tested perpendicular to the grain (Figure 31). The shape of the stress-strain curve in compression perpendicular to the grain is dissimilar to that obtained in testing parallel to the grain; it is evident, however, that a similar linear, quadratic, linear model might be applied to compression parallel diagrams with good results (Figure 32).

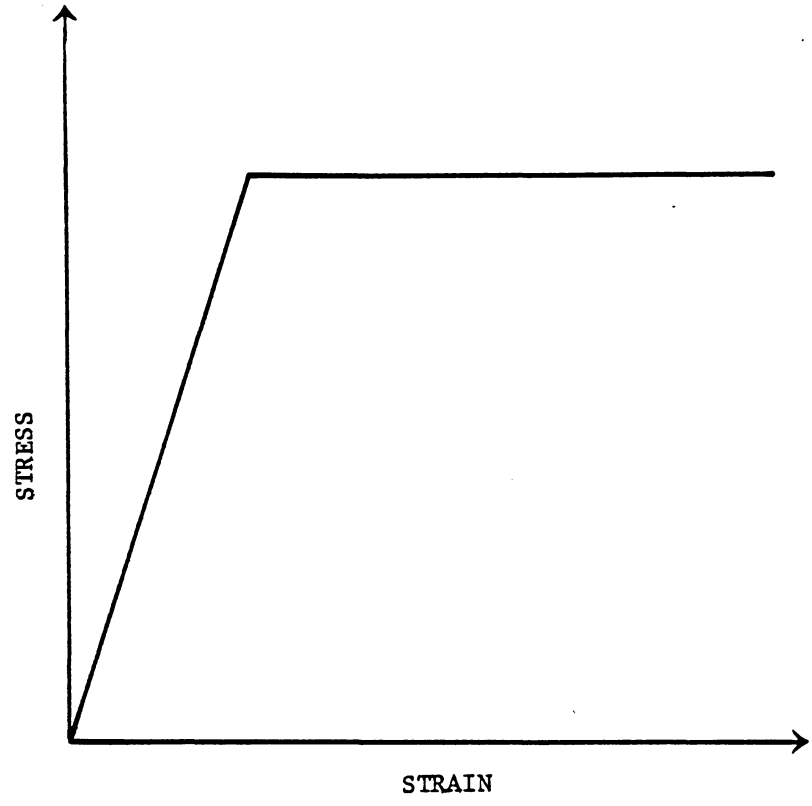

Figure 29: Elastic-perfectly plastic simplification of compression stress-strain diagram.

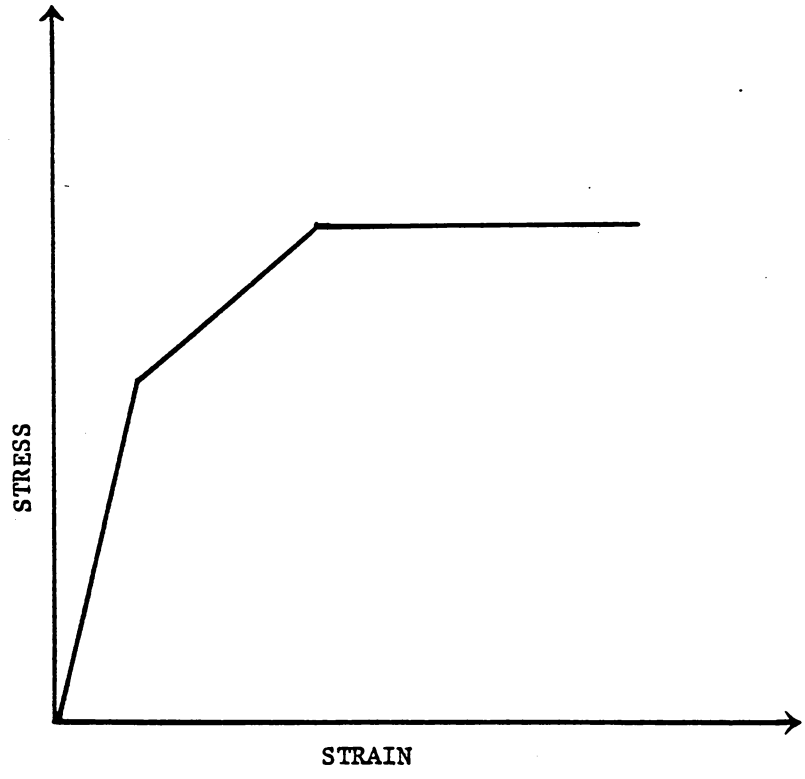

Figure 30: Tri-linearized stress-strain diagram. (After Krueger and Sandberg, 1974).

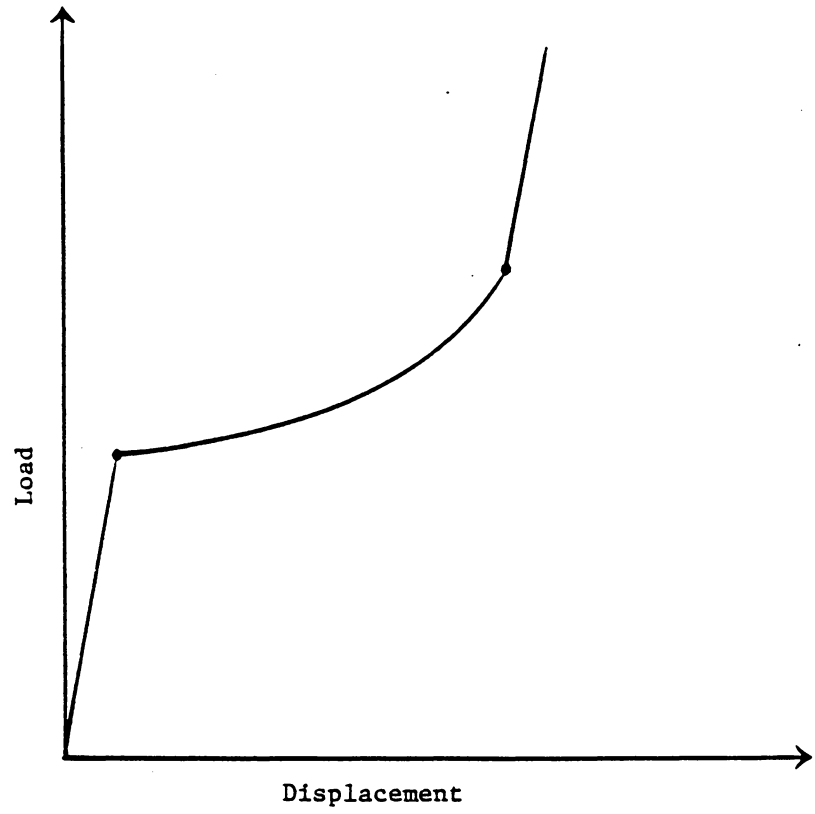

Figure 31: Three-part compression perpendicular to the grain stress-strain diagram. (After Bazhenov, et al., 1953).

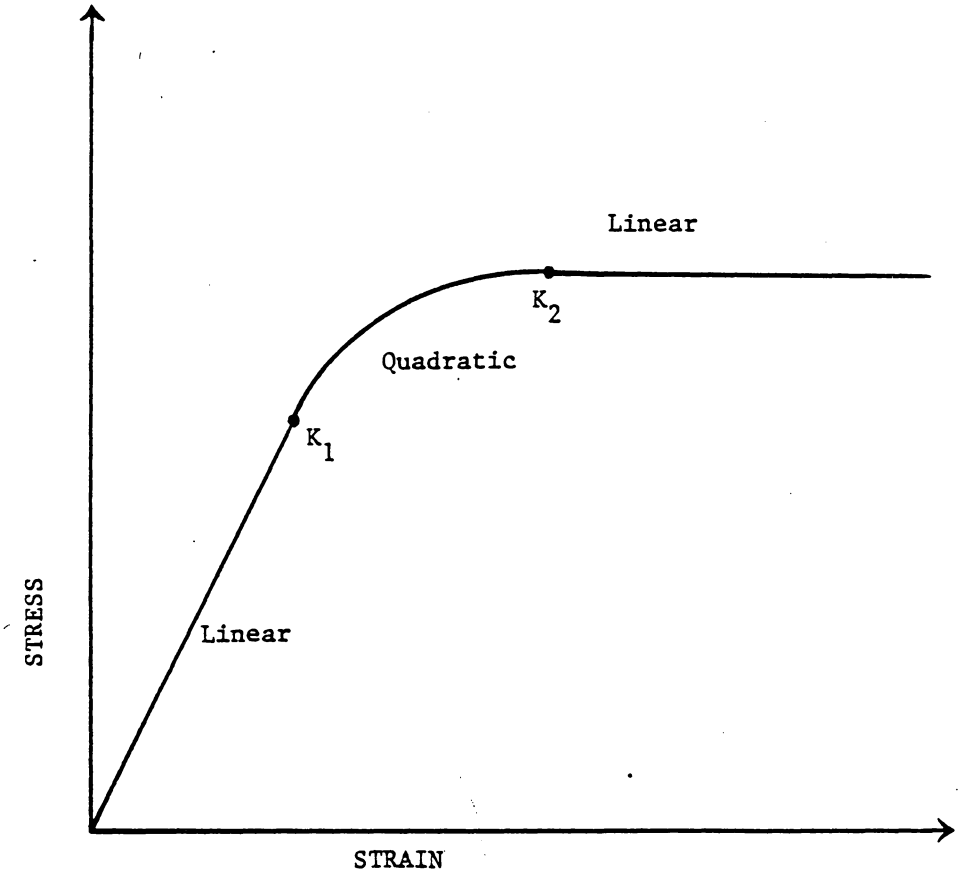

Figure 32: Idealized compression parallel-to-the-grain stress-strain diagram consisting of a linear, a quadratic and a linear segment. K_1 and K_2 are join points.

Most of the above-mentioned models were not described in the literature in such a way that they could be applied to an individual stress-strain diagram. This is a great hindrance to their potential usefulness. The parabolic model is an obvious exception, as it needs no further procedural description to be used.

Ramberg and Osgood (1943) proposed an equation which has been widely used to describe nonlinear stress-strain behavior of various materials (Laufenberg, 1983). This equation, however, is only approximately linear for low strain values, and it is unknown to what extent this nonlinearity might affect the outcome of a finite-element analysis beyond the elastic limit. The assumption might be made that the resulting difference between the Ramberg-Osgood equation and a linear function would be slight for small strains, but it is possible for the cumulative differences to be more significant at the end of a stepwise procedure. An additional difficulty with this equation is its inability to model a constant ("plateau") stress defined beyond a given strain. The Ramberg-Osgood model was therefore eliminated from further consideration.

O'Halloran (1973) reviewed a number of empirical equations to determine if any of them could successfully model stress-strain behavior in compression. He decided

that a variation of the Ramberg-Osgood formula would best fit his digitized stress-strain data, but he noted that this equation had a negative slope beyond the maximum load (Figure 33). It should be recognized that, while O'Halloran's equation might be used to successfully model a stress-strain diagram from a compression test, the data comprising this curve might not accurately reflect the actual mechanical behavior. It is more likely that the real stress-strain response in compression should be depicted as a horizontal plateau beyond the maximum load, and that indications to the contrary are due to bending or end-crushing of the specimen under test. This point is of especial importance in predicting compression stresses in a beam beyond the proportional limit, as compression strains far in excess of the strain at maximum load commonly occur before the beam fails. Another drawback to O'Halloran's equation is the lack of a truly linear slope. Examples presented in his dissertation show that the slope of this equation only equals the modulus of elasticity at zero strain and proceeds to decrease as strains increase. Some model with a better-defined linear region would more closely depict observed data. For this reason, and because of the failure of the model to predict a plateau stress, the use of O'Halloran's revised Ramberg-Osgood formula was rejected.

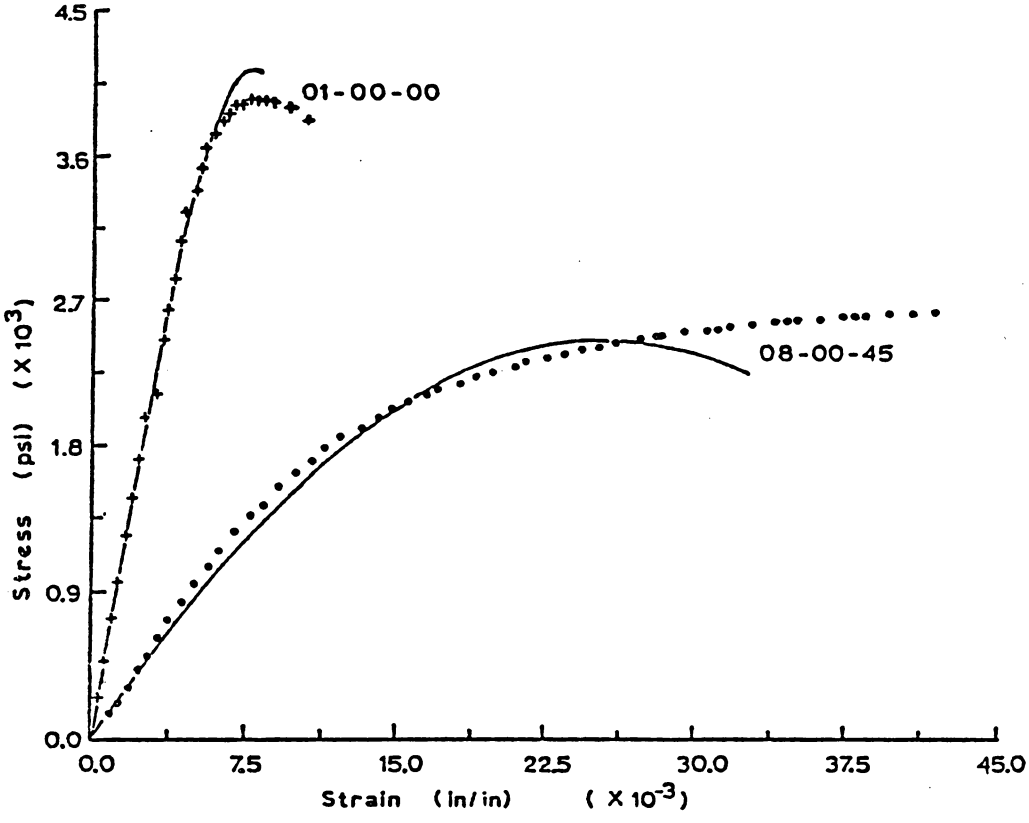

Figure 33: Diagram showing actual stress-strain data and the best fit from the modified Ramberg-Osgood equation. (From O'Halloran, 1973)

Another model for a stress-strain (σ-ε) curve has been recently proposed by Urbanik (1982). His two-parameter model is represented by

$$\sigma = C1 \tanh[C2(\varepsilon+\delta)/C1] \qquad [3.9]$$

where C1 and C2 are the shape parameters for the curve; δ is a dummy variable used to shift data towards the origin if necessary. This model can portray a plateau near the maximum stress, but it is only approximately linear at small strains and becomes increasingly nonlinear as strain increases. Urbanik's model was rejected for this reason.

3.5.2 New Model for Compression Stress-Strain Diagrams

Having eliminated O'Halloran's model from consideration for use in this dissertation, the author was forced to seek another model. The most suitable appeared to be the tri-segment model (Figure 32). This model includes features that others lack, namely an initial linear slope and a plateau stress beyond a designated strain value. This model can be stated mathematically by several equations. The initial linear segment (for strains up to the point where the linear equation joins the quadratic equation, K_1) is stated as

$$\sigma = A0 + B1 \times \varepsilon \qquad [3.10]$$

In this equation, A0 (the intercept) is defined as zero, since the model curve must begin at the origin; e represents strain. The B1 parameter is equal to the longitudinal Young's modulus obtained previously from linear regression analysis. K_1 is roughly equivalent to the strain at the proportional limit.

The second portion of the model is a parabolic function from the first join point, K_1, up to the second join point, K_2. It is stated as

$$\sigma = A1 + B2 \times \varepsilon + B3 \times \varepsilon^2 \qquad [3.11]$$

Since we wish to specify that stress is a continuous function of these two equations, and that the slopes are equal at K_1, then

$$B1 \times \varepsilon = A1 + B2 \times \varepsilon + B3 \times \varepsilon^2 \qquad [3.12]$$

$$B1 = B2 + 2 \times B3 \times \varepsilon \qquad [3.13]$$

where ε is equal to K_1. By substituting [3.13] into [3.12], A1 can be defined as

$$A1 = B3 \times K_1^2 \qquad [3.14]$$

By re-arranging [3.13], K_1 can be defined as

$$K_1 = \frac{B1 - B2}{2 \times B3} \quad \text{or} \quad \frac{E_1 - B2}{2 \times B3} \qquad [3.15]$$

The third portion of the compression model is a flat line at the plateau stress. It is applicable from K_2 on; K_2 is therefore approximately equal to the strain at maximum stress. This segment of the model is mathematically stated as

$$\sigma = A2 + B4 \times \varepsilon \qquad [3.16]$$

where B4 is equal to zero by definition. If the continuity and smoothness restrictions are imposed between [3.16] and [3.11], then

$$A1 + B2 \times \varepsilon^2 = A2 + B4 \times \varepsilon \qquad [3.17]$$

$$B2 + 2 \times B3 \times \varepsilon = B4 \qquad [3.18]$$

where $\varepsilon = K_2$. Equation [3.18] can be rearranged to yield

$$K_2 = \frac{B4 - B2}{2 \times B3} \qquad [3.19]$$

and

$$A2 = B3 \ (K_1^2 - K_2^2) \qquad [3.20]$$

results from substituting [3.18] for B4 in [3.17] and applying some algebraic manipulation. The parameters B2 and B3 are not explicitly defined in terms of other parameters and are the only parameters left undetermined at this point. The determination of these parameters will be discussed in another section.

3.6 MODELING STRESS-STRAIN BEHAVIOR IN TENSION

Stress-strain diagrams for tension tests of wood specimens are usually considered to be essentially linear almost to failure, especially for dry wood (Dietz, 1942; Stern,1944b; Bach, 1965; Mazur, 1965). King (1957) found that this relationship was actually non-linear, but concluded (1961) that "the non-proportional increase in strain relative to the increase in stress is ... so small that it does not significantly affect the essential linearity of the coarsely-measured load-strain relationship". The yellow-poplar data acquired for this report are in general agreement with these earlier studies, but a visual comparison of the data to a ruled line indicated that the stress-strain diagrams can only be described as linear to about fifty percent of the failure strain. Significant departure from a ruled line is usual beyond this point.

3.6.1 The Model

The model chosen to fit the tension data was a variation of the compression model stated previously. In this instance, the data do not have a smooth transition to a plateau stress due to the physical rupture of the specimens at failure. It was appropriate, therefore, to employ only the first two segments of the compression stress-strain model and to have

an abrupt transition to a zero slope at maximum strain. Only one join point, K_1, is defined in terms of the regression parameters. Equations [3.10] and [3.11] describe this model.

Chapter IV

MATERIALS AND METHODS

4.1 DATA ACQUISITION

4.1.1 Uniaxial Specimen Preparation

Four twelve- to sixteen-foot logs were selected from three trees cut on a single site at the Reynolds Homestead, Critz, Virginia. Fast-grown trees with few visible defects were chosen to maximize the potential yield of sapwood from each log. Large diameter logs were taken to minimize the number of logs; the average log diameter was seventeen inches at the butt. Only straight logs with a uniform growth ring curvature were selected to minimize the amount of tension wood present. These logs were then transported to the sawmill at the Brooks Forest Products Center at Virginia Tech, Blacksburg, Virginia, where the sapwood was slabbed off. The slabs were marked for knots and then sawn into shorter, clear lengths of thirty to forty inches. The sapwood was then wrapped in heavy plastic and stored in a refrigerator at approximately thirty-six degrees Fahrenheit to simultaneously keep it green and free of fungal growth until it was cut into smaller specimens for testing.

To obtain the greatest number of specimens from the material, and also to take advantage of the available

testing apparatus, the 1 x 1 x 4 inch compression specimen described in ASTM standard D 143 (ASTM, 1983) was used. This cross-section is identical to that specified for the tension test specimens as well. Therefore, the slabs were sawn and planed into 1.125 x 1.125 inch as well as 2.25 x 2.25 inch pieces running the length of the slab; the larger pieces were reserved for beam specimens. The slabs were marked on the end-grain with a clear plastic template before cutting to ensure that the growth rings would be aligned with the specimen axes as closely as possible, and a scriber was used to help make the cuts parallel to the fiber direction. The sticks were left unnumbered, wrapped in several layers of household plastic wrap and returned to the refrigerator to await selection for testing.

Ideally, in a study of this nature, series of compression and tension specimens would be perfectly matched (e.g., from the same stick) over the entire moisture content range. Because of the limited size and amount of the material, however, this matching plan was dropped. For each moisture content, sufficient 1.125 x 1.125 inch pieces were chosen from those available such that approximately fifteen compression and fifteen tension specimens could be fabricated. Most of the time this resulted in planning for one or more compression specimens and a tension specimen to

be cut from the same stick, but sometimes a given stick had to be marked for cutting in a different manner to avoid minor defects.

With the exception of the pieces reserved for testing in the green condition, the (previously undried) sticks were dried to the desired moisture content before being cut into specimens. First, however, a wafer was taken from the end of each piece to be used for specific gravity determinations on an oven-dry weight, green volume basis. Drying took place in a conditioning chamber at 100 degrees Fahrenheit and either eighty, sixty, or thirty-two percent relative humidity (RH), depending on whether the target moisture content was eighteen, twelve, or six percent. The relative humidity measurements were made using a gauge with a manufacturer-stated accuracy of plus or minus three percent. The specification of these relative humidities was determined by placing the green specific gravity wafers in the chamber with the specimens. The RH was lowered every two days, and a wafer was removed from the chamber at intervals as a check on the equilibrium moisture content (EMC) conditions. The temperature was chosen to enable the conditioning chamber to maintain the six percent equilibrium moisture content condition and also to slightly hasten the drying of the specimens. At the same time, this temperature

was considered to be low enough that temperature gradients induced by exposure to room conditions would not create a confounding influence when the tests were conducted (Schaffer, 1980). After every stick had maintained a constant weight for about a week, each stick was planed to one-inch thickness, cut to the appropriate specimen length, numbered as to stick of origin and specimen number, and replaced in the conditioning chamber.

Compression specimen preparation was complete at this point, but the tension specimens had not yet been machined to the final shape. Both bandsaws and routers were tried in attempts to machine the sticks to the shape specified by ASTM standard D 143 (ASTM, 1983), but the first of these produced fairly rough surfaces and the second was both slow and resulted in slightly glazed (and probably drier) surfaces. Alternatively, it was found that the sticks could be shaped by passing them back and forth between stops at right angles to the arbor on a table saw with the guard removed. A sixteen-inch, sixty-tooth carbide-tipped combination blade was used with the height set at either 0.3125 inch or 0.40625 inch to cut the three-eighths inch or three-sixteenths inch thick cross-sections, respectively. This procedure reduced the radius of curvature from the seventeen and one-half inches specified to eight inches and

was also extremely dangerous, but it resulted in a reduced cross-section which was truly centered; it also resulted in smooth surfaces for the central, uniform thickness portion of the specimen, and regular, well-defined smooth curvatures closer to the ends (Figure 34). The rectangular ends for the tension grips were also cut using stops on the table saw in order to ensure that the grip surfaces were collinear. The tension specimens were then returned to the conditioning chamber to await testing.

Specimens to be tested green were treated only slightly differently. Machining took place as previously described, but these specimens were occasionally dipped in water to prevent the surface from drying. After machining, the specimens were re-wrapped with household plastic wrap and placed in the refrigerator. Still wrapped, they were placed in the conditioning chamber about a day before testing. This assured that the green specimens would be tested under the same temperature conditions as the other pieces.

4.1.2 Uniaxial Specimen Testing

4.1.2.1 Compression Tests

Compression testing was conducted in accordance with the specifications of ASTM standard D 143 (ASTM, 1983) and also with the recommendations for this test in the literature

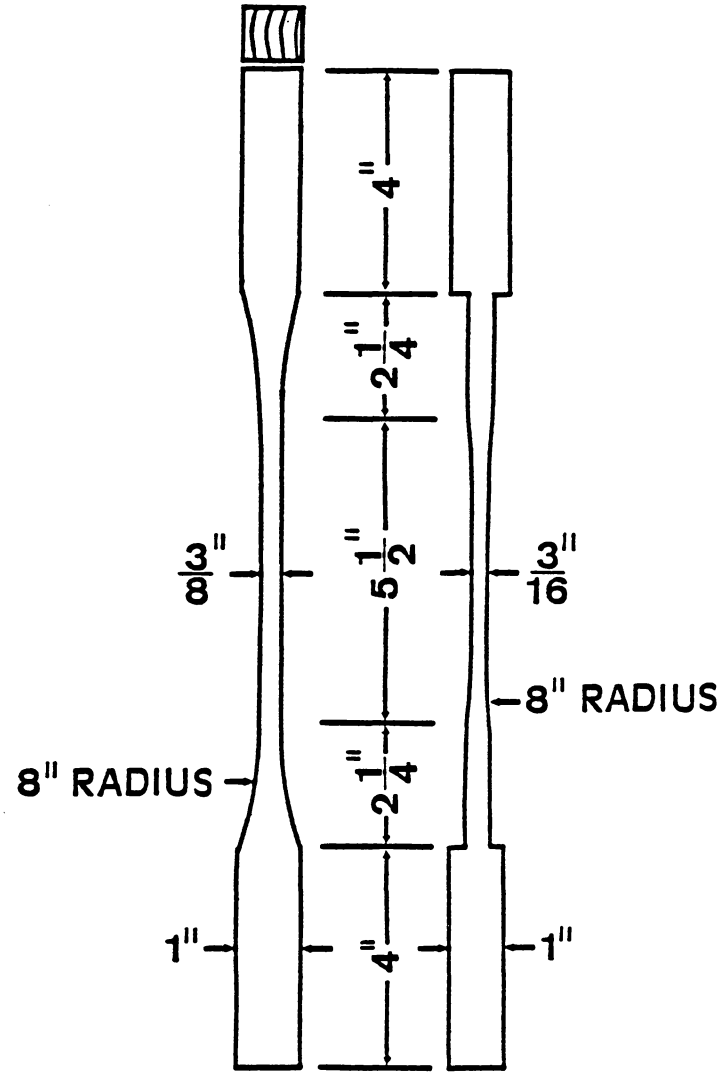

Figure 34: Tension specimen used in this study.

(Bodig and Goodman, 1969). To minimize the effect of potential temperature gradients, specimens were removed from the conditioning chamber one at a time and tested; total setup time prior to testing was usually no more than ten minutes. Prior to testing, the specimen's weight and dimensions were recorded. The specimen was then fitted with a re-usable clip-type strain gauge harness manufactured by MTI of Palo Alto, California to measure the longitudinal displacement over the central two-inch gauge length (Figure 35).

Both the strain gauge harness and the 20,000 pound load cell used for these tests were interfaced with a Radio Shack TRS-80 Model I minicomputer to digitally acquire the load-deformation diagrams for subsequent analysis. A modified version of the BASIC program CPAL (Fagan, 1982) was used to translate amplified voltage signals into meaningful units and to control the timing of the data acquisition process. This apparatus was shown to be accurate for both load and deformation during calibration trials. The precision for these measurements was normally plus or minus ten pounds and plus or minus 0.0001 inches, respectively, but this precision was somewhat less on occasion due to random electrical noise caused by the fans and compressors in the building. Measurements were generally recorded at six- or

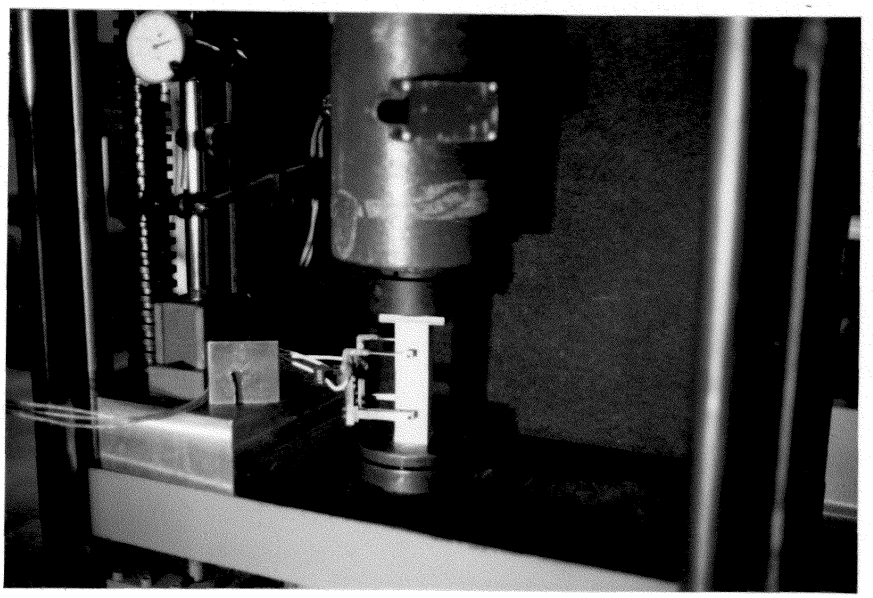

Figure 35: Compression specimen and strain gauge harness used in this study.

eight-second intervals. Fagan (1982) determined that this timing apparatus was 99.7 percent accurate. The analog signals were also recorded on an x-y plotter as a backup for each test.

After the strain gauge apparatus was clipped to the specimen, it was checked to ensure that it was centered and parallel to the specimen axis. The specimen was then placed between two metal plates with spherically-ground seats, vertically aligned, and loaded in compression using a BLH screw-type testing machine. The crosshead speed under load was set to 0.012 inches per minute; this speed was verified to plus or minus approximately 0.001 inches per minute using a timer and a dial gauge on about ten specimens. This speed did not appear to vary during testing. The entire specimen was dried at the end of each test to determine the moisture content.

4.1.2.2 Tension Tests

The general procedures used for the compression tests were followed as closely as possible for the tension testing. Specimens were withdrawn from the conditioning chamber one at a time and measured for the minimum cross-sectional area. Each specimen was then fitted with a pair of LVDTs in a lightweight aluminum yoke to measure the longitudinal

deformation (Figure 36) and tested immediately. It should be noted that this yoke attached to the specimens by slightly pressing small nail points into the specimen; this created four stress concentration points, but only one or two out of the fifty-six test specimens fractured at these locations. It should also be noted that all the specimens except those at twelve percent moisture content received a thin coating of petroleum jelly prior to testing. This was applied to prevent moisture gradients in these specimens while awaiting testing at ambient room conditions (approximately ten percent EMC). This set-up time to the start of test was usually about fifteen minutes. At the end of the test, a moisture content specimen was taken from the central section (if uncoated) or from both the (wiped) central section and from the thicker part of the specimen. The moisture content specimens in the latter instance usually agreed to within approximately 0.1 percent.

The pair of LVDTs and the 10,000 pound load cell used in the tension tests were interfaced with the same Radio Shack TRS-80 Model I minicomputer used for the compression tests. The accuracy of these devices was demonstrated during calibration trials. The precision for the longitudinal measurements was about the same as for the compression tests (plus or minus approximately 0.0001 inches), but the load

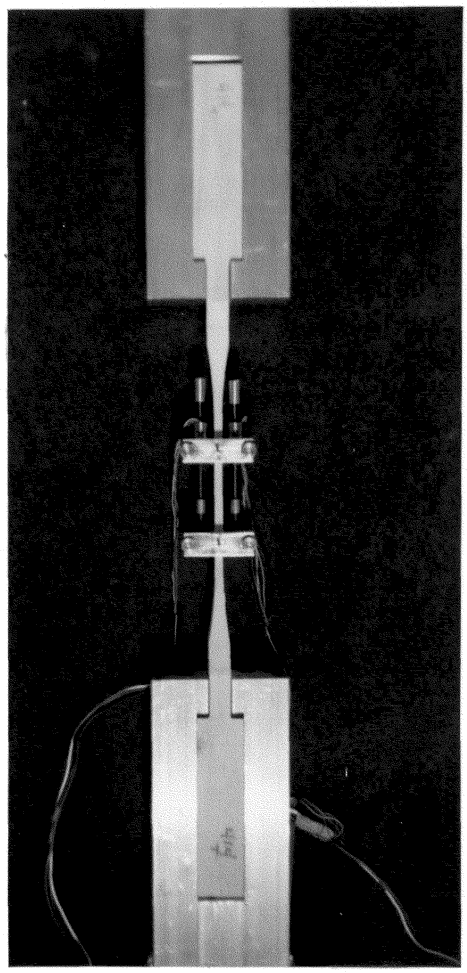

Figure 36: Photograph showing the LVDT arrangement for tension testing.

cell measurement precision was improved to plus or minus approximately four pounds. These precisions were also influenced on occasion by random electrical noise in the surrounding building. Measurements were generally recorded at ten-second intervals. The analog signals were recorded on an x-y recorder for these tests as well.

As noted earlier, the tension specimens tested were slightly at variance with ASTM D 143 (ASTM, 1983). The radius of curvature for each specimen was eight inches instead of the seventeen and one-half inches specified, but this did not cause any observed problems with the tests. Additionally, the crosshead speed used was increased over that specified to 0.012 inches per minute. The strain rates in tension and compression are equal in beam testing, and it is well known that the rate of loading affects the observed strength properties (Tiemann, 1908; Markwardt and Wilson, 1935; Brokaw and Foster, 1952; Liska, 1950; James, 1962; Sugiyama, 1967; Sliker, 1973). For this reason, it was thought that the strength properties in tension and compression should be obtained using the same crosshead speed. It was believed that this would result in similar strain rates for the compression and tension specimens as the data were acquired over a two-inch gauge length in each case, and there was a uniform cross-section at each end of

the gauge of either 1.0 or 1.5 inches in length, respectively.

4.1.3 Beam Specimen Preparation

After sufficient yellow-poplar had been sawn for the uniaxial tests, only enough material remained to fashion a total of twenty beam specimens with cross-sections two and one-quarter inches square that were free of defects. It was obvious that it would be more practical to re-saw these sticks into sixteen-inch (minimum) lengths with 1 x 1 inch cross-sections, but most of the pieces were only long enough to yield four beam specimens each for a total of forty specimens. These specimens were cut and numbered for matching purposes. Believing this sample size to be too small for adequate comparisons to be made to the results of the finite-element program, two additional green yellow-poplar logs similar in size and quality to the first were purchased from a log home builder in Shawsville, Virginia. These logs were sawn in the same fashion as the original material, first into approximately twenty pieces 2 x 2 x 40 inches, then into pieces approximately 1 x 1 x 18 inches. Approximately 120 beam specimens were prepared, and these specimens were also numbered for matching purposes. Both these specimens and the original material were wrapped in

several layers of household plastic wrap and placed in the refrigerator to await testing.

The newer material was intended to be tested first due to the greater number of specimens, so this group was divided into six different moisture categories. These were

1. 12% moisture content, no gradient
2. 18% moisture content, no gradient
3. green, no gradient
4. 15% average moisture content exposed to a 12% EMC
5. 25% average moisture content exposed to a 12% EMC
6. 35% average moisture content exposed to a 12% EMC

These choices were influenced by several factors. First, an examination of the uniaxial Young's modulus data indicated that the values measured at twelve percent moisture content were greater than those measured at six percent moisture content (see next chapter). This implied a change in the MC-Young's modulus relationship between these two moisture contents, and it seemed logical that the region within which the longitudinal Young's modulus could most accurately be predicted lay between the twelve percent and green moisture contents. The obvious approach was to split the specimens into two matched groups, one-half of which was reserved for testing with gradients. The second half was in turn divided into three side- or end-matched sub-groups such that every

group contained one stick from each two-inch by two-inch by forty-inch piece of sapwood. These three groups were allocated for testing at twelve percent, eighteen percent and green moisture contents for direct comparison to the finite-element model beam predictions at moisture contents where essentially no interpolation is required. The reasons for the moisture content specifications for the beams which were reserved for testing with moisture gradients were equally simple. Twelve percent was selected as the EMC condition to be used to create the gradients because this moisture content had the greatest Young's modulus values (and thereby the greatest influence in the extreme fiber region of beams), and also because the Young's moduli at lower moisture contents could only be modeled with uncertainty due to the moisture content-Young's modulus relationship noted earlier. Wilson (1932) observed that beams with moisture content gradients can have MOE values greater than those of green beams even though the average moisture content might be forty percent or more. Inspection of the uniaxial data suggested that the intersection point for yellow-poplar was around twenty-five percent moisture content, so the average moisture contents of fifteen, twenty-five and thirty-five percent were chosen to bracket this value.

The original material, matched to the uniaxial specimens, was apportioned into four groups. These were

1. green, no gradient
2. 22% moisture content, no gradient
3. 22% average moisture content exposed to a 12% EMC
4. 35% average moisture content, exposed to a 12% EMC

These choices were decided upon after viewing the results of the first and larger group of beam tests. The green moisture content condition, however, was included specifically so that the properties of the two groups of wood could be compared.

4.1.3.1 Moisture Content Conditioning of Beam Specimens

All beam specimens were equilibrated at 100 degrees Fahrenheit to be comparable to the uniaxial specimens. The specimens chosen to have a uniform moisture content were conditioned at the same relative humidities as their uniaxial counterparts until constant weights were achieved. The twenty-two percent equilibrated specimens, which had no uniaxial counterparts, were conditioned at 100 degrees Fahrenheit and 90 percent relative humidity. They were then removed from the conditioning chamber, planed to one-inch thickness and returned to the chamber for a couple of days before testing.

Imposing the prescribed moisture gradients proved to be considerably more difficult. Originally, plans had been made to monitor the average moisture content of drying specimens with a resistance moisture meter, but preliminary studies showed that green yellow-poplar does not always dry evenly from all sides. It was also recognized that only slight differences in the electrode penetration depth might result in considerable variation in the average moisture content readings, especially for relatively small specimens with steep gradients such as are used in the present study. Alternatively, it was decided to remove a wafer from one end of each specimen for an initial moisture content determination. These moisture contents, together with the initial weights of the remainder of the specimen, were then used to predict the weight of the beam specimen at the average target moisture content.

Prior to being placed in the conditioning chamber at twelve percent EMC, the ends of each specimen were dipped in paraffin to preclude end-drying and the subsequent formation of three-, rather than two-dimensional moisture gradients. The paraffin weight was then added to the target weight for each specimen. After the specimens were placed in the conditioning chamber they were removed at intervals to monitor the beam weights. Drying to the calculated target

weights took between twenty-four and seventy-two hours, depending on the average moisture content level to be reached. Each beam was removed and tested immediately once its target weight was reached.

4.1.4 Beam Testing

The general procedures outlined in the secondary methods of ASTM standard D 143 (1983) for the testing of small beams were followed with a few changes. As specified, the nominal 1 x 1 x 16 inch specimens were loaded at the center of a fourteen-inch span between two roller supports. The load was applied through a maple block to a tangential face which was usually selected at random (Figure 37). Certain specimens, however, especially among those not matched to the uniaxial specimens, had some fuzzy grain on one tangential surface. Since fuzzy grain is one indicator of tension wood, and since tension wood is considered to have abnormal (usually lower) tensile strength (Kollmann and Cote, 1968; Panshin and de Zeeuw, 1980), these specimens had the fuzzy grain located on the compression face during testing.

The rate of crosshead movement was changed significantly from that specified by the standard (0.05 inches per minute). It was thought that the strain rate in the extreme

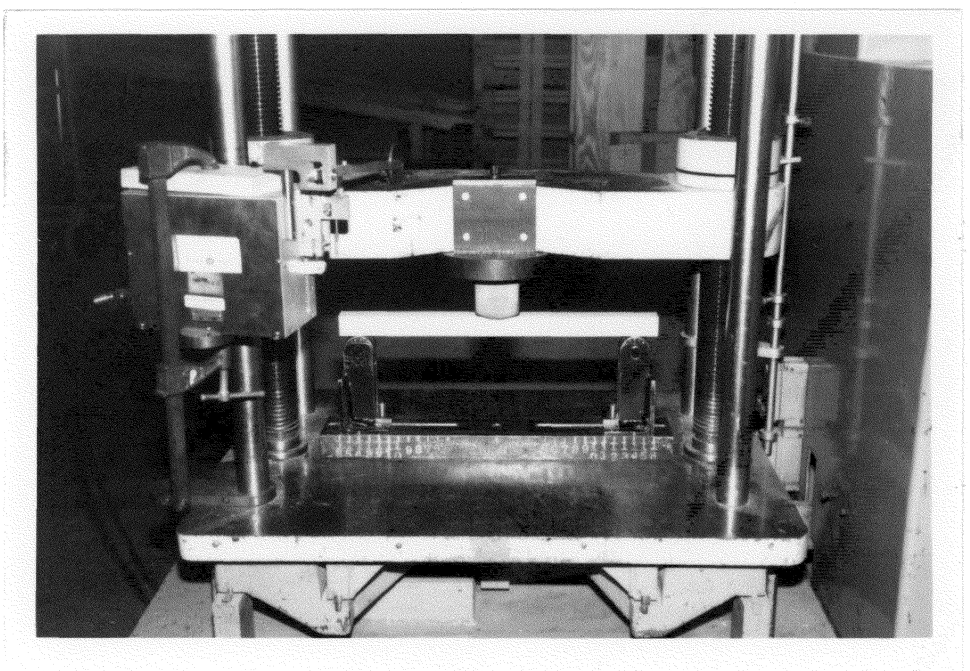

Figure 37: Setup for beam testing.

fiber region of the beams should closely match the nominal strain rate used in the uniaxial tests to preclude confounding of the results due to the influence of strain rate on strength (Tiemann, 1908; Markwardt and Wilson, 1935; Brokaw and Foster, 1952; Liska, 1950; James, 1962; Sugiyama, 1967; Sliker, 1973). For this reason the following equation from ASTM standard D 1037 (1983) was used to determine the appropriate rate of crosshead travel. If the unit rate of fiber strain of outer fiber length per minute (z) is specified as 0.012 in

$$N = zL^2/6d \qquad [4.1]$$

where N equals the rate of crosshead motion in inches per minute, L equals the span in inches (14 inches) and d equals the specimen depth (one inch), then the rate of crosshead motion to be used is 0.392 inches per minute. This degree of precision is not obtainable on the Tinius-Olsen testing machine used for these tests, but the speed control was set as close to this value as was practical.

Beams were removed from the conditioning chamber one at a time and kept wrapped in plastic while awaiting testing. Immediately prior to testing, the cross-sectional area of each beam was measured with a pair of calipers to the nearest 0.001 inch. Some problems were noted in making this

measurement on the beams containing moisture gradients, however. Due to nonuniform drying, these beam cross-sections were not truly rectangular and the distance between midpoints on opposite faces was greater than the distance between the corners on opposite faces. The measurements recorded for subsequent MOE and MOR calculations were obtained by averaging these two values.

A load-displacement diagram was drawn to the point of maximum load during each test using a deflectometer and the built-in load cell on the testing machine. Because of the measurement apparatus available, the displacements were measured from the crosshead travel during the tests.

Following testing, the central three-inch portion was cut from each beam to be used as a moisture content sample. Each beam containing a moisture gradient had a second, one-inch slice removed about two inches from one of the supports. This was used to check for significant moisture gradients along the grain. Originally, plans had been made to take two of these secondary moisture content samples (one near each support), but the observed moisture gradients along the grain proved to be minimal (less than one percent difference) for nearly every specimen. It was also noted that the moisture gradients (when present) were symmetric about the beam's midpoint. In view of these observations,

it was thought that only one sample would suffice, thereby preserving the remainder of the beam undamaged. One out of every four beams with moisture gradients was also randomly selected to have an additional one-inch wafer cut for examination of the moisture gradient. This wafer was cut from the beam immediately adjacent to the center moisture content section. The cross-section of each wafer was marked into a four by four grid of approximately one-quarter-inch squares and cut along the grain by using a weighted rubber mallet to drive a microtome knife through the specimen. This technique had been previously tried with southern pine and had been found to result in minimal moisture loss.

4.1.4.1 Correction of the Beam Displacement Values

After most of the beams had been tested, it was noted that the calculated MOE values for the equilibrated beams were significantly lower than expected based on the uniaxial test results. It seemed likely that the problem lay in not accounting for extraneous (i.e., other than mid-plane) displacements occurring in the test procedure (Fischer, et al., 1981). These displacements can arise from roller and crosshead indentation of the specimen during testing, as well as from machine flexibility. To test this hypothesis, seven pieces of wood at each of three moisture contents

(12%, 18%, green) were removed from the refrigerator where they had been stored after being wrapped in plastic to prevent changes in their moisture contents. These pieces consisted of some previously-untested compression specimens as well as some one inch by one inch by four inch ends from broken tension specimens. Pieces of the actual beams tested at 22% moisture content had also been stored in similar fashion, and these were removed from the refrigerator as well. After coming to room temperature, two tests were conducted on each specimen. In the first test, the crosshead and maple loading block were brought to bear on a tangential face of each specimen as it lay directly upon the bed of the testing machine. For the second test the loading block was removed, and the space between the supports of the roller support device used in the beam tests was changed to approximately two and one-half inches to accommodate the shorter length of these specimens. Each specimen was placed atop the rollers on a tangential face and was loaded directly by the crosshead. A load-crosshead displacement diagram was recorded for each test. The average slopes for both tests were then combined for the twelve percent, eighteen percent and the green specimens; the slopes for each individual specimen were combined for the twenty-two percent specimens. These slopes varied depending on the

moisture content, with the average slope of the green specimens approximately one-half that of the twelve percent specimens. The slope at the appropriate moisture content was then used to correct the displacement used in the MOE calculation for each equilibrated or green specimen. Due to the methodology used in this procedure, the correction is only approximately correct for any single twelve percent, eighteen percent or green specimen. The assumption was also made that the correction factors applied with equal validity to each of the two batches of wood used in this project.

The gradient-containing beams had their MOE values corrected in similar fashion. Green specimens were dried at the twelve percent EMC conditions used to create the gradients. These specimens were removed from the conditioning chamber at frequent intervals and tested according to the procedures outlined above. The average slope at the appropriate average beam moisture content was then estimated from these data, and this average slope was used to correct the original load-displacement diagram for each specimen.

4.2 THE FINITE-ELEMENT PROGRAM

Two finite-element programs were written for this project. Each incorporated the same mathematical model for three-dimensional mechanical behavior, but one used eight-node, linear elements in contrast to the other which used twenty-node quadratic elements (see Appendix). (These programs are the result of substantial modifications to a linear elastic, linear element, three-dimensional fluid flow program furnished to the author through the courtesy of Dr. J. N. Reddy). The linear element was known to be suited to modeling uniaxial behavior, but it was believed that large assemblages of these elements might yield acceptable results in beam modeling. The quadratic elements program was written to provide a more flexible standard against which linear element beam models might be compared. Both programs were written to use in-core storage (up to 5 megabytes is currently available at Virginia Tech) to speed execution, but it was not known initially how (or if) this choice might restrict the choice of mesh and element type to be used for a given problem, nor was it known to what degree these factors might influence the accuracy of the analyses. The practical implications of various meshes and elements are discussed in another chapter.

The programs used in this study incorporate the models described in the previous chapter. The program logic is independent of the element selected, so a single flow diagram can be used to describe both programs (Figure 38).

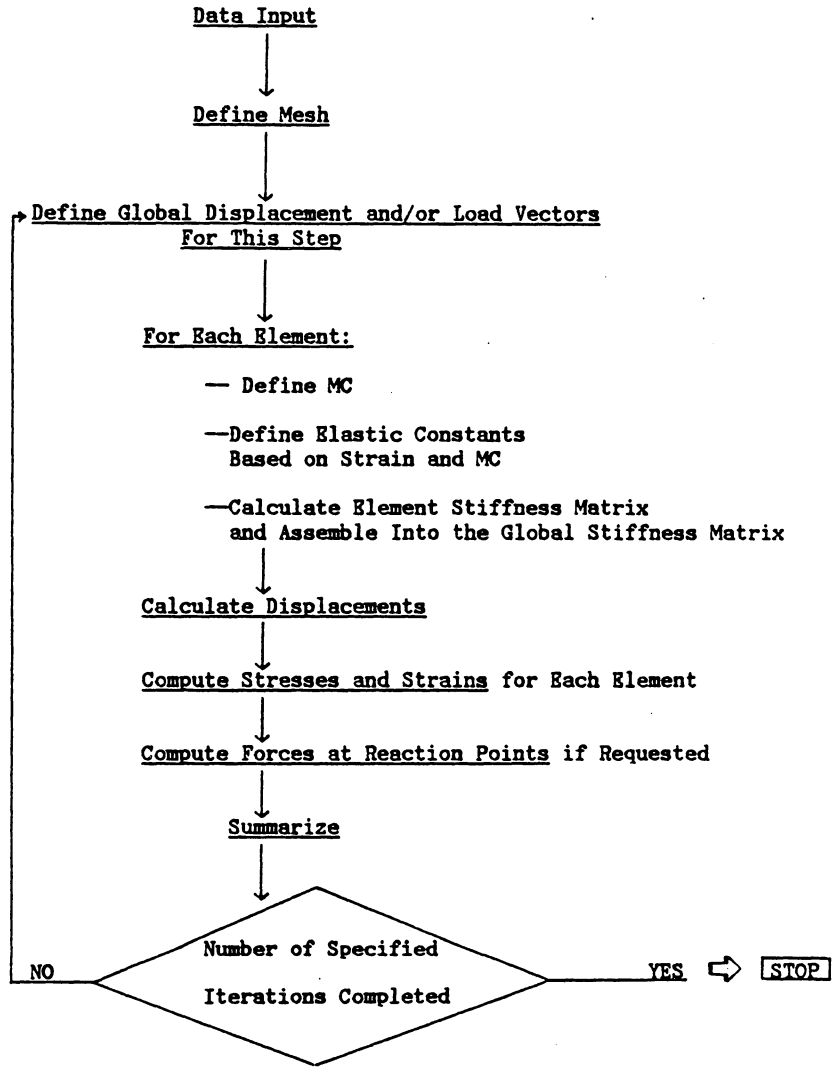

Figure 38: Flow diagram of finite-element program logic.

Chapter V

EXPERIMENTAL RESULTS AND DISCUSSION

5.1 RESULTS OF UNIAXIAL TESTS

The raw data acquired for each test were transferred from the TRS-80 Model I minicomputer to the Virginia Tech IBM mainframe computer using appropriate software. The data were then reviewed for obviously inaccurate values attributable to either electrical noise during acquisition or to the transfer process; approximately twenty such points were found among the hundreds of data values for the sixty-five compression and fifty-six tension tests conducted as part of this study. More nearly correct values for these points were estimated from the surrounding data, and these replaced the spurious values in the data sets. The load-deformation data were then re-calculated as stress-strain data and plotted for each test. Representative plots of compression and tension tests for each moisture content category are included in this report as Figures 39 and 40.

The longitudinal Young's moduli were calculated by conducting linear regressions on the appropriate data for each test. The maximum stresses at failure were calculated from the digitized data for both the compression and the tension tests, and the strains at failure for the tension

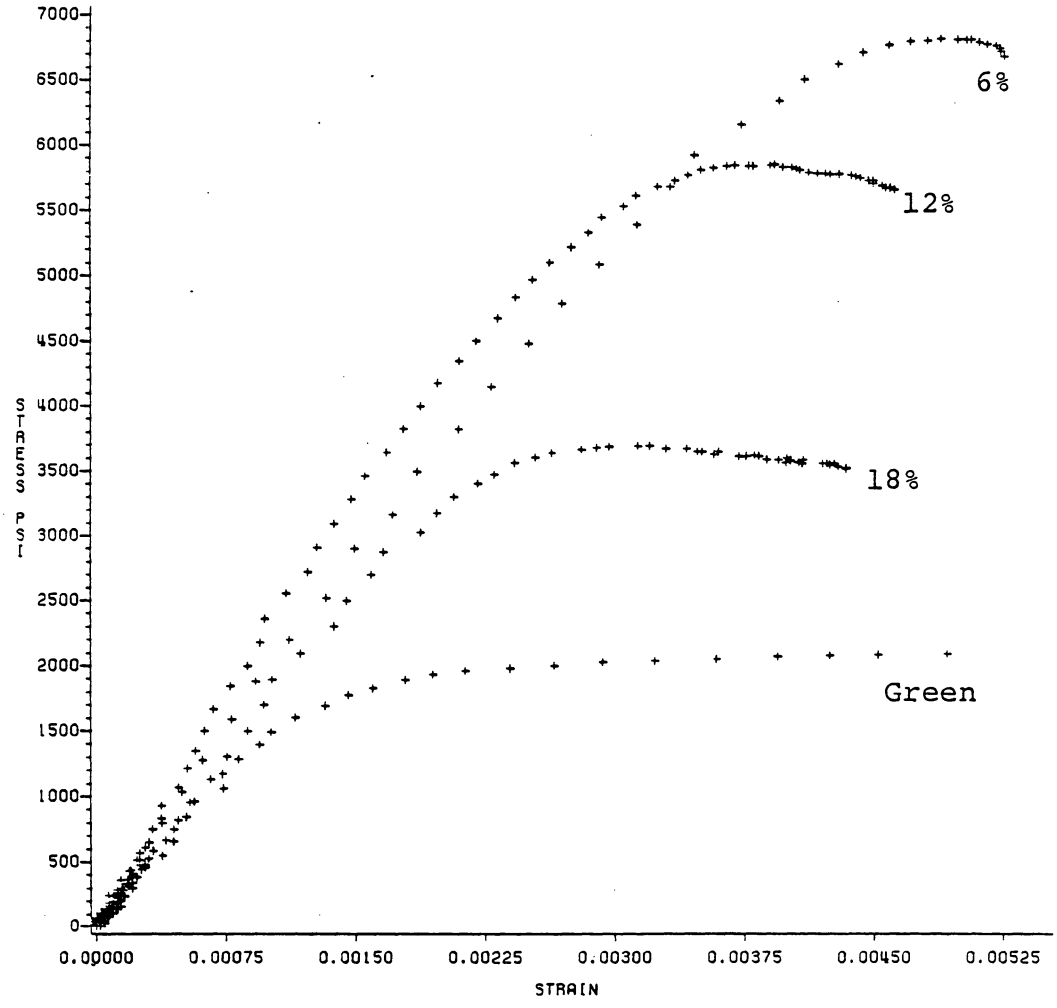

Figure 39: Examples of digitized data acquired for 6, 12, 18% MC and green compression specimens.

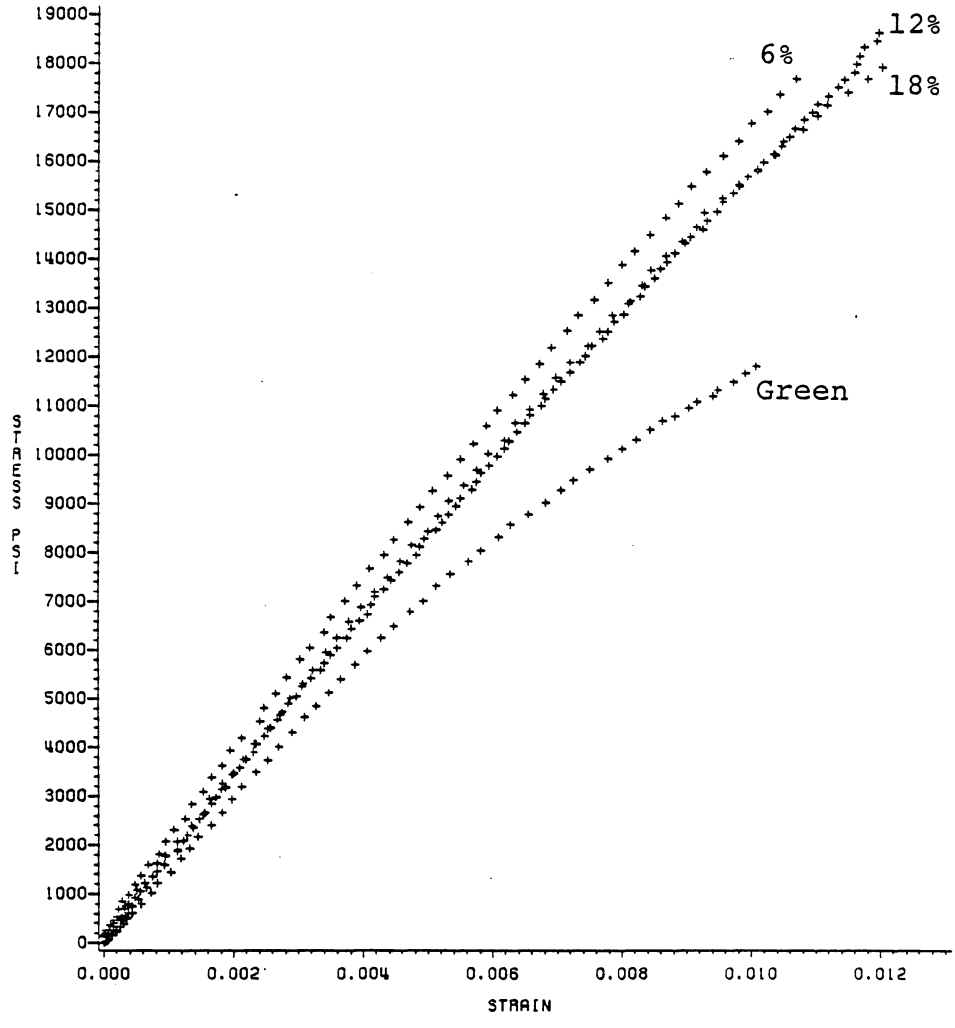

Figure 40: Examples of digitized data acquired for 6, 12, 18% MC and green tension specimens.

tests were also calculated. These data are depicted in Figures 41 through 45.

5.1.1 Stress-Strain Modeling of Digitized Compression Data

Although the segmented stress-strain model proposed earlier can be clearly stated mathematically, a methodology needed to be found to

1. locate the optimum join points, and
2. perform the appropriate regression on the digitized data in each segment.

Iterative, non-linear regression techniques readily solved these difficulties. A SAS non-linear regression program, Proc NLIN (SAS, 1982), was used to make trial analyses of several data sets with this model.

Prior to analysis, data points representing initial support settlement were removed from each of the trial data sets. Also, although the model was developed for compression data with a plateau region, it was noted that some of the data sets for individual specimens exhibited decreasing loads beyond the maximum load. This was attributed to test-related factors rather than to material properties, and is consistent with the criticism previously directed at O'Halloran's model. In order to remedy this situation and to help the procedure achieve consistent

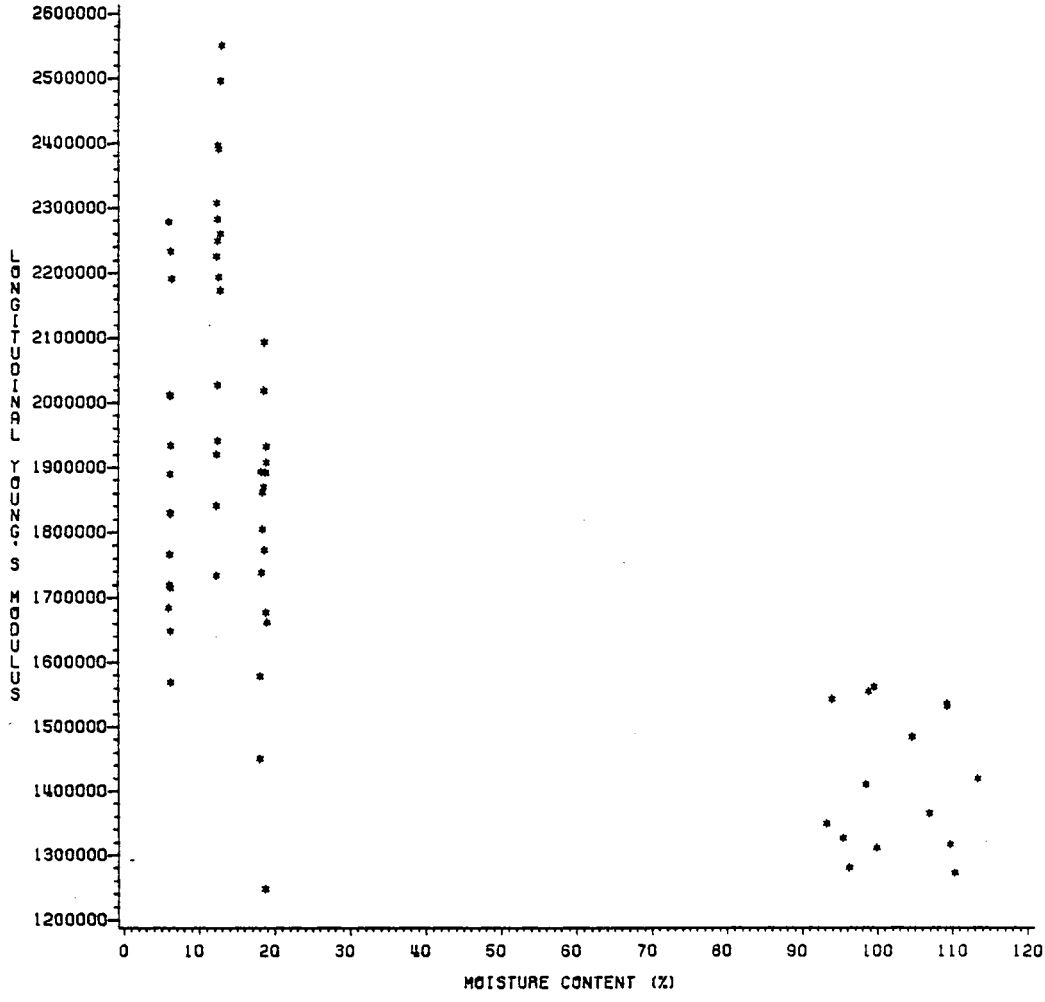

Figure 41: Data for longitudinal Young's modulus in compression.

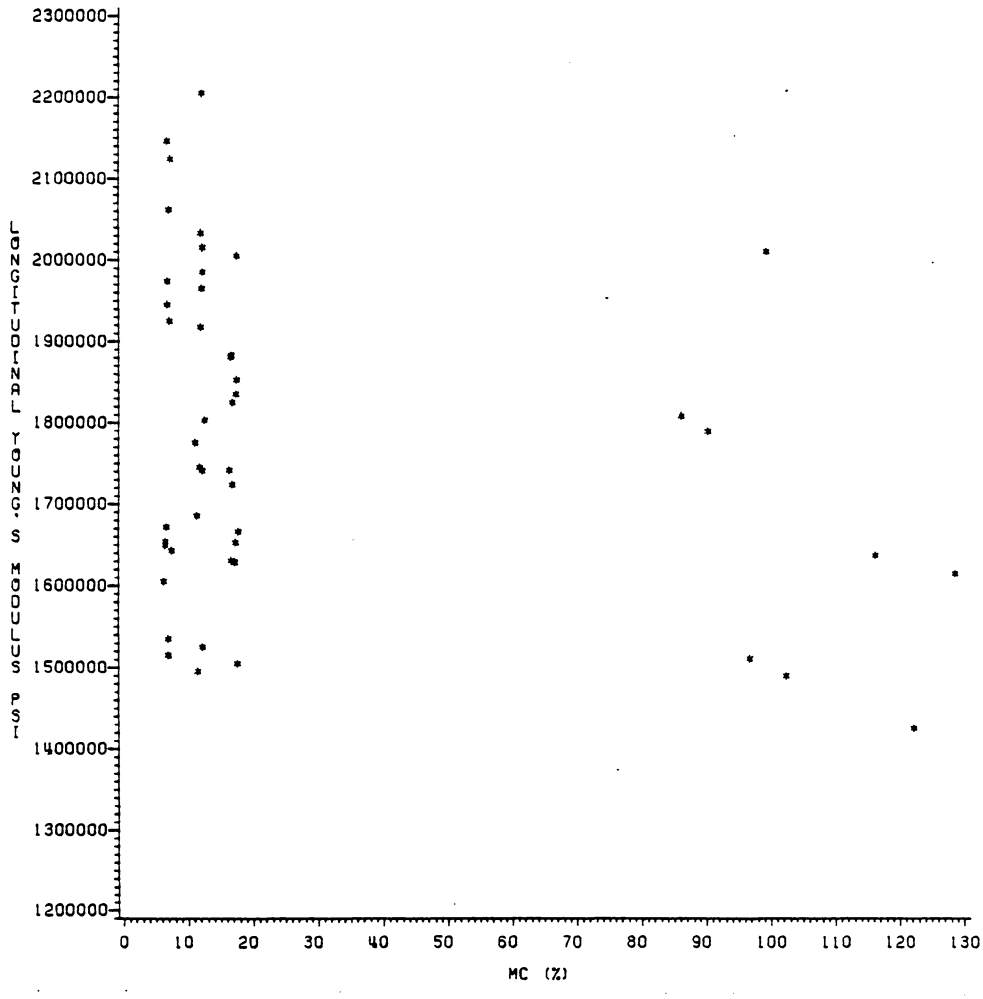

Figure 42: Data for longitudinal Young's modulus in tension.

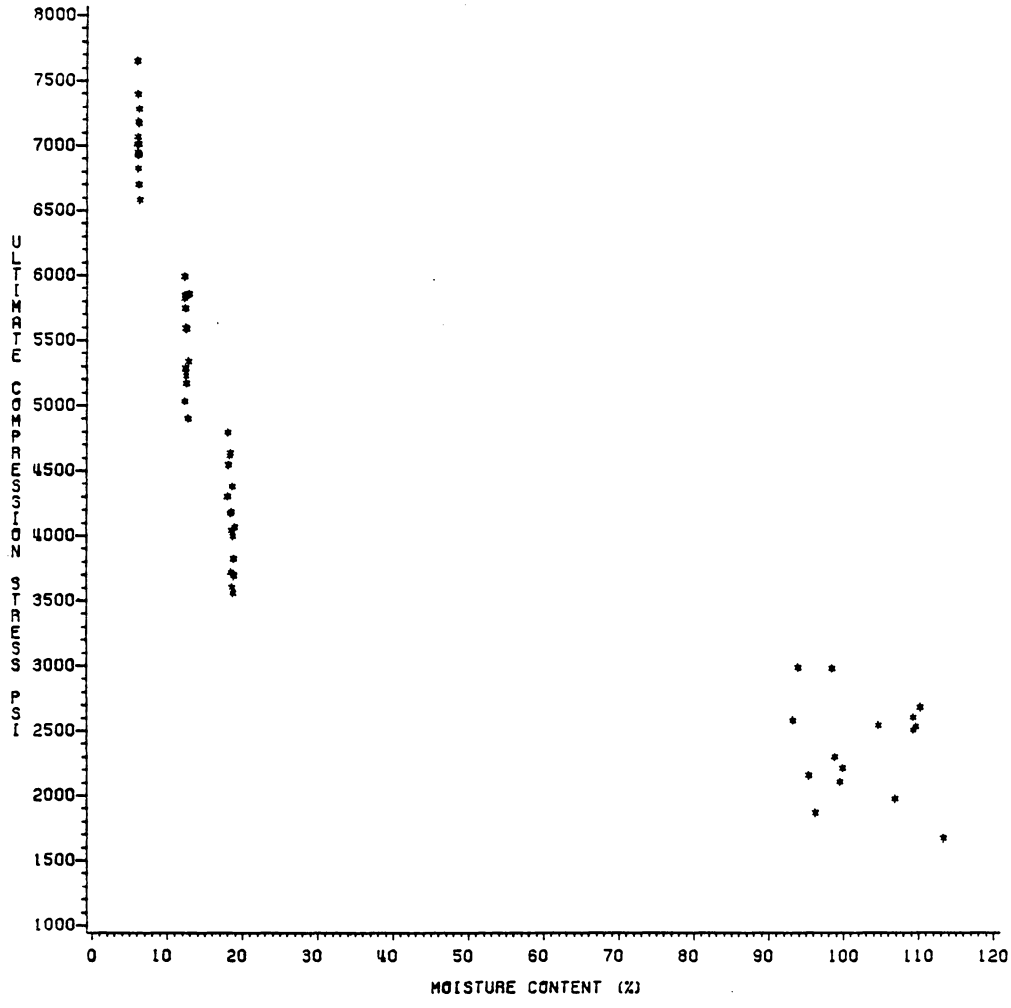

Figure 43: Data for maximum crushing strength parallel to the grain.

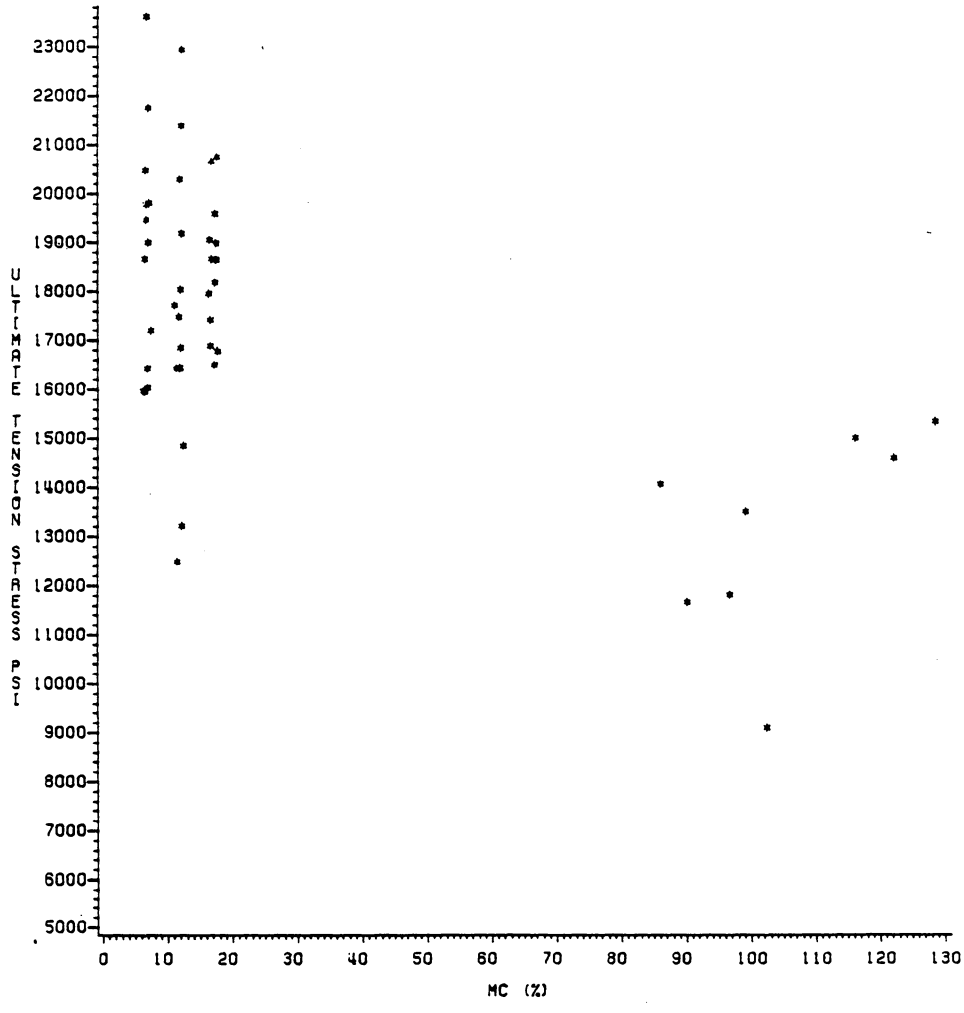

Figure 44: Data for ultimate tensile strength parallel to the grain.

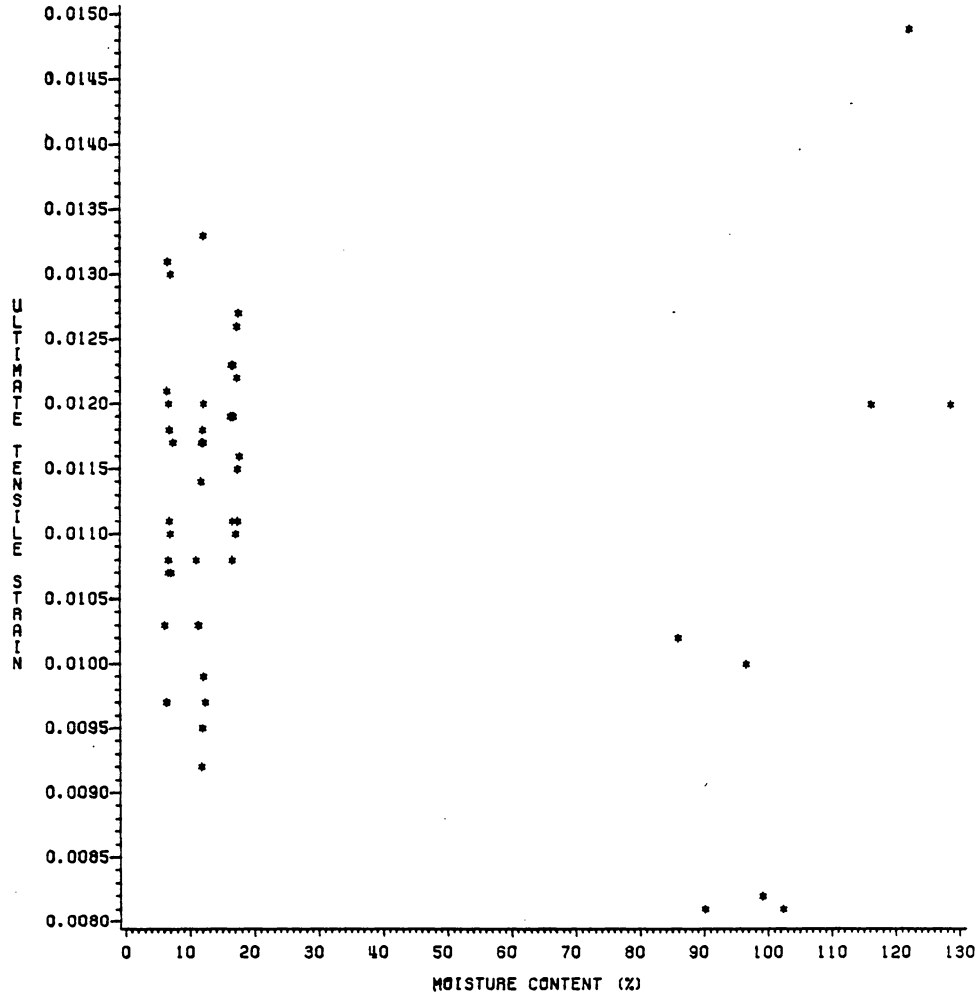

Figure 45: Data for ultimate tensile strain.

results, data points were adjusted and/or added as necessary to form a plateau region of 0.002 strain at the maximum load for each data set. The trial data sets were then analyzed. Stresses and strains were taken as positive for these analyses.

The SAS procedure was able to successfully apply the model to the trial data sets, usually with R^2 values in excess of 0.99. Every compression data set was then analyzed in this fashion. An example of the ability of the model to represent actual data is depicted by the overlay of the data and the predicted points for specimen C107-1 in Figure 46.

5.1.1.1 Compression Regression Parameters and Join Points

The digitized data for the compression specimens, when analyzed with Proc NLIN according to the previously stated model, yielded various values for the B2 and B3 parameters. (B1 equals the longitudinal Young's modulus by definition, as noted previously). These are plotted versus the corresponding test moisture contents in Figures 47 and 48. The B2 parameter appeared to have a definite relationship with moisture content, but the B3 relationship did not appear to be as strong. The join points K_1 and K_2 calculated from these parameters are plotted in Figures 49

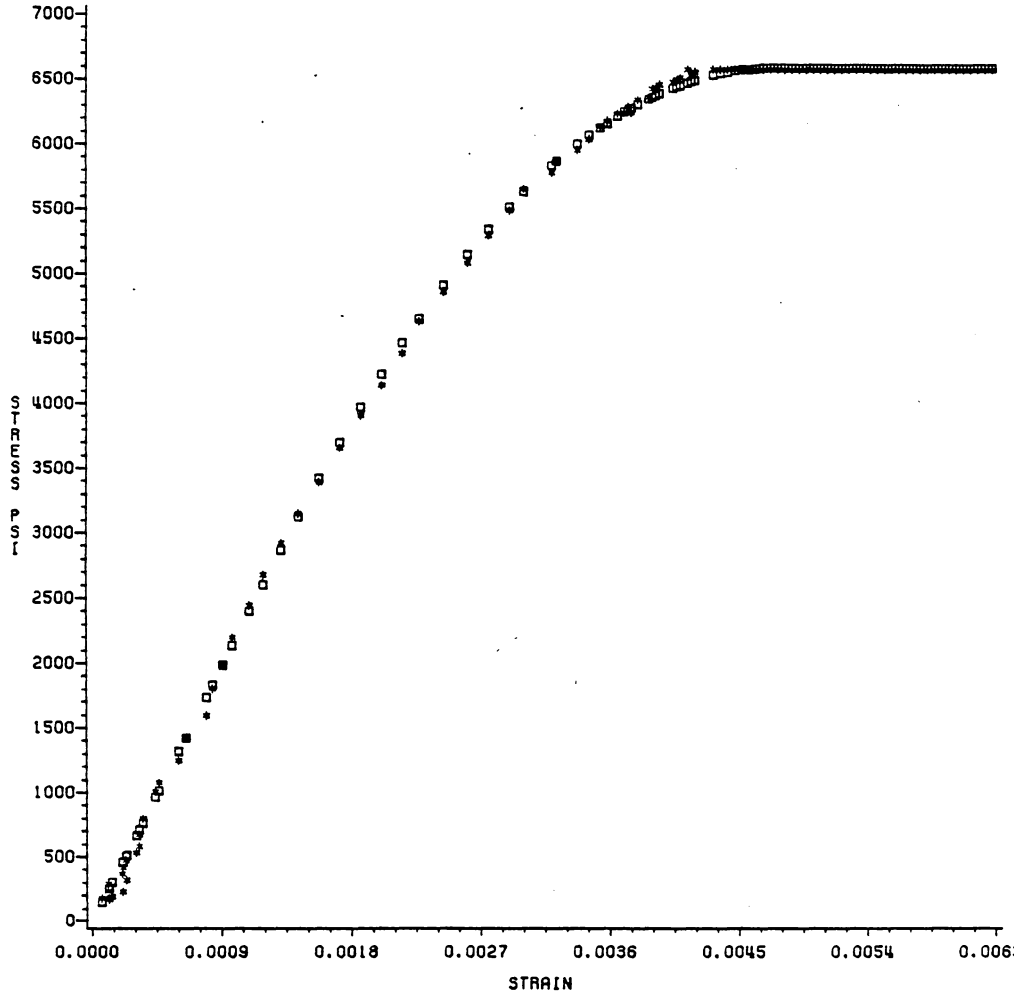

Figure 46: Overlay of predicted observations on the actual data for specimen C107-1. Data=asterisks, predicted points=squares.

and 50. Both join points appeared to be influenced by moisture content. It is interesting to note that a few of the specimens in the 12 and 18% MC categories had negative values for the join point K_1. This indicates an absence of a linear region, as the data were (statistically) better fitted solely by a quadratic function up to K_2. Ivanov (1941, 1949) thought that stress-strain curves for wood would be entirely curvilinear, but the vast majority of the data gathered for this study negate this hypothesis for short-term tests in compression parallel to the grain.

5.1.2 Stress-Strain Modeling of Digitized Tension Data

Preliminary checks with several data sets indicated that the model previously proposed for the modeling of stress-strain behavior in tension worked well, and the R^2 values for the model were usually higher than 0.99 (Figure 51). This model was therefore adopted for this study, and a nonlinear regression analysis was performed on every tension specimen data set. Stresses and strains were again analyzed as positive values. Two data sets were culled prior to any analysis due to excessive localized grain angles detected in these specimens following an examination of the ultimate stress and MOE values.

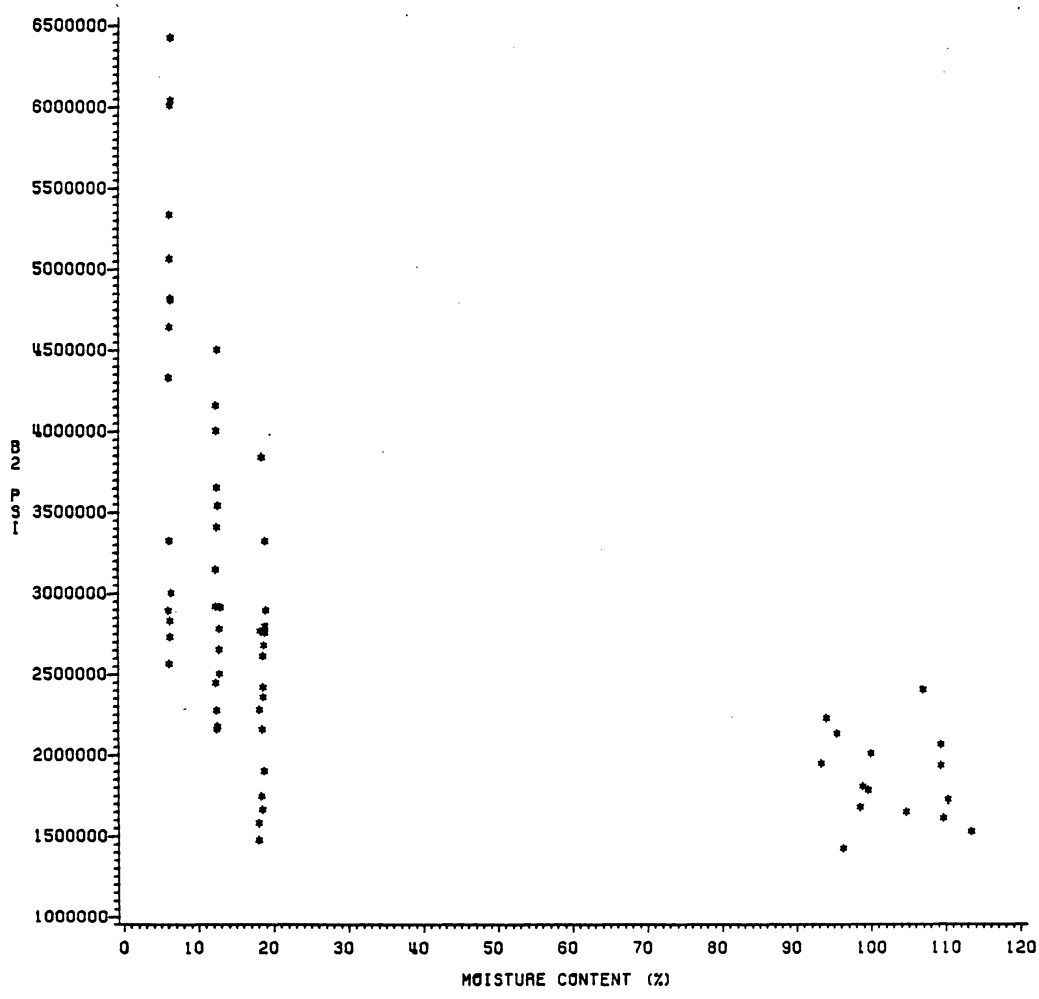

Figure 47: Compression B2 parameter values.

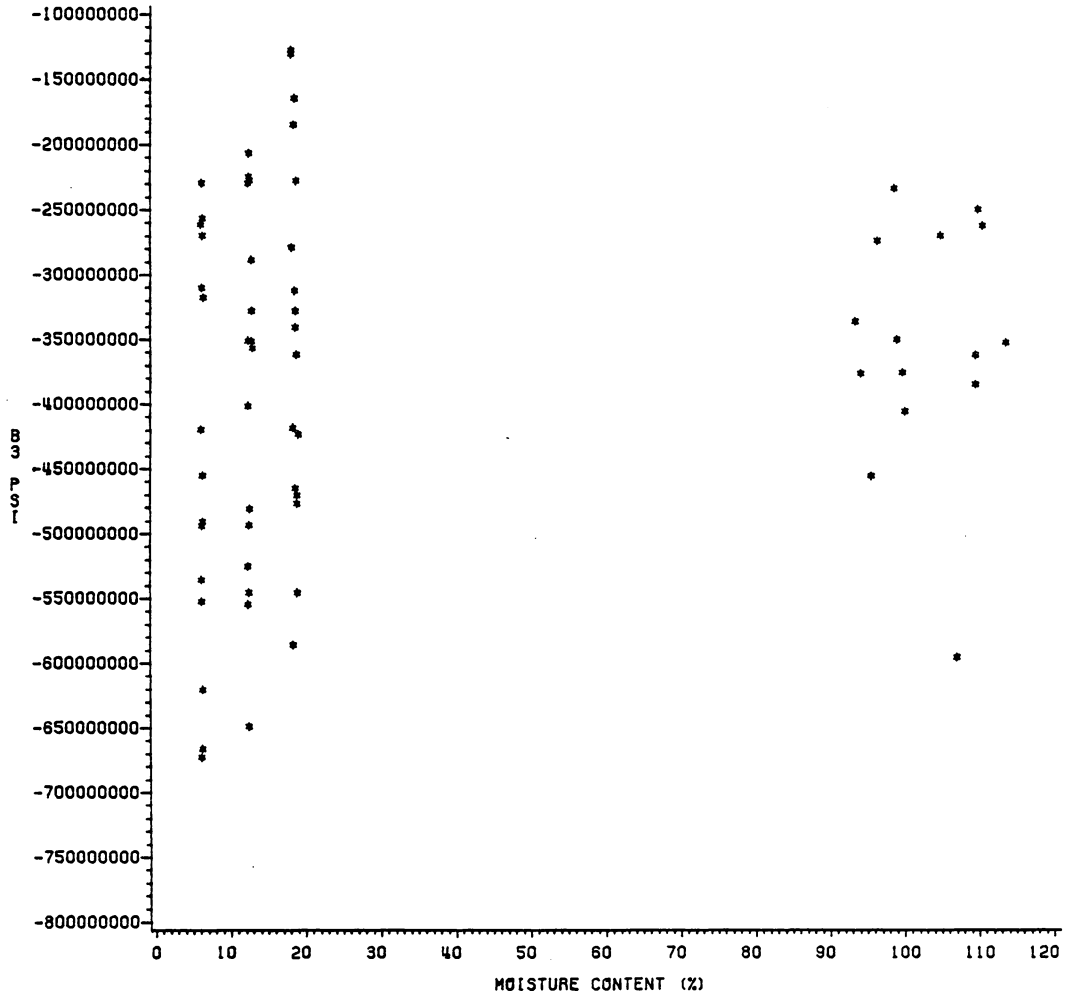

Figure 48: Compression B3 parameter values.

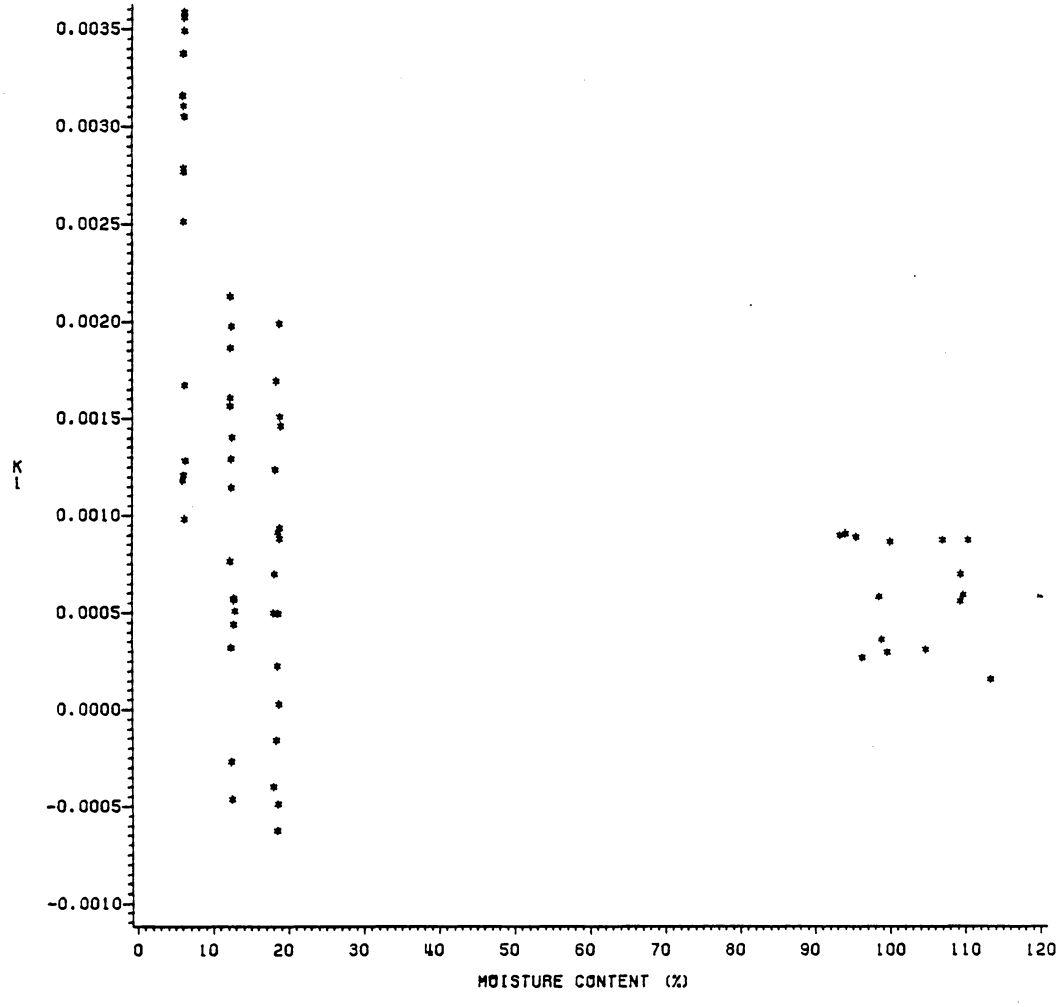

Figure 49: Strain values for the compression join point, K_1

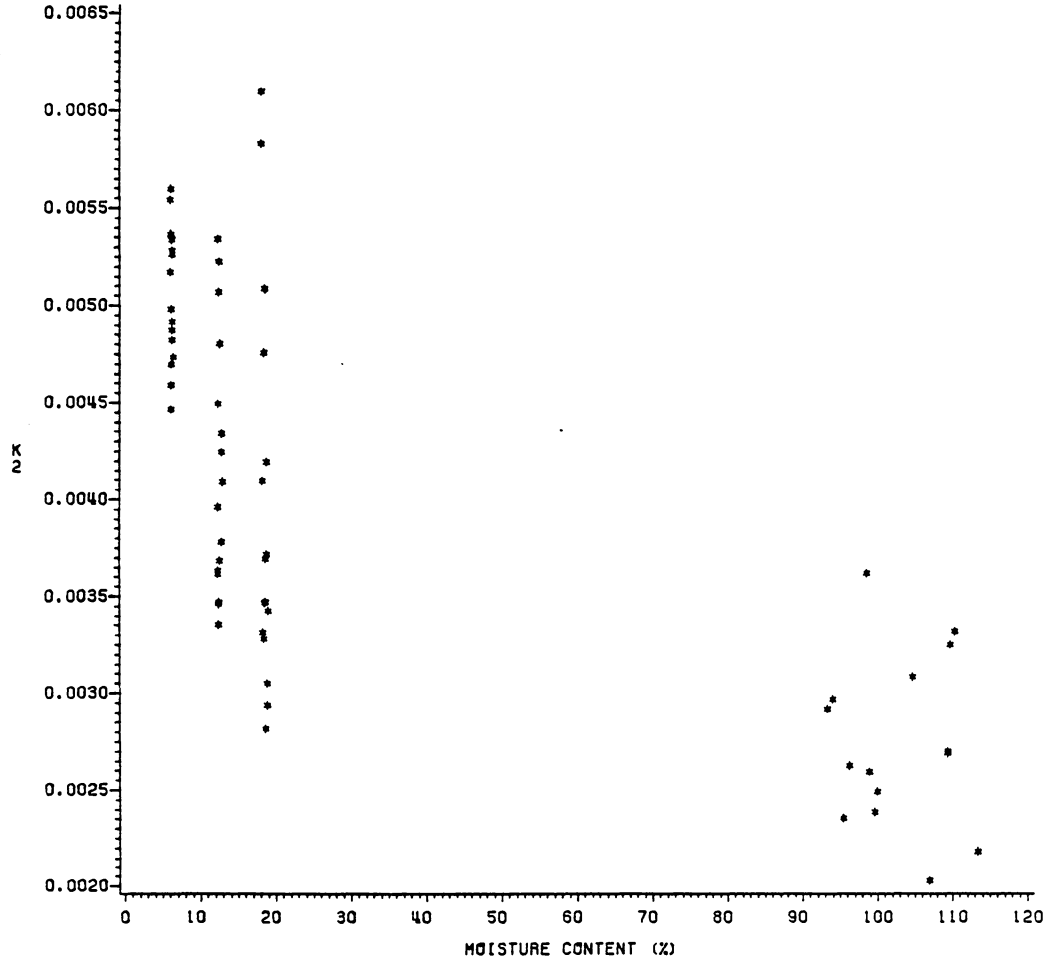

Figure 50: Strain values for the compression join point, K_2

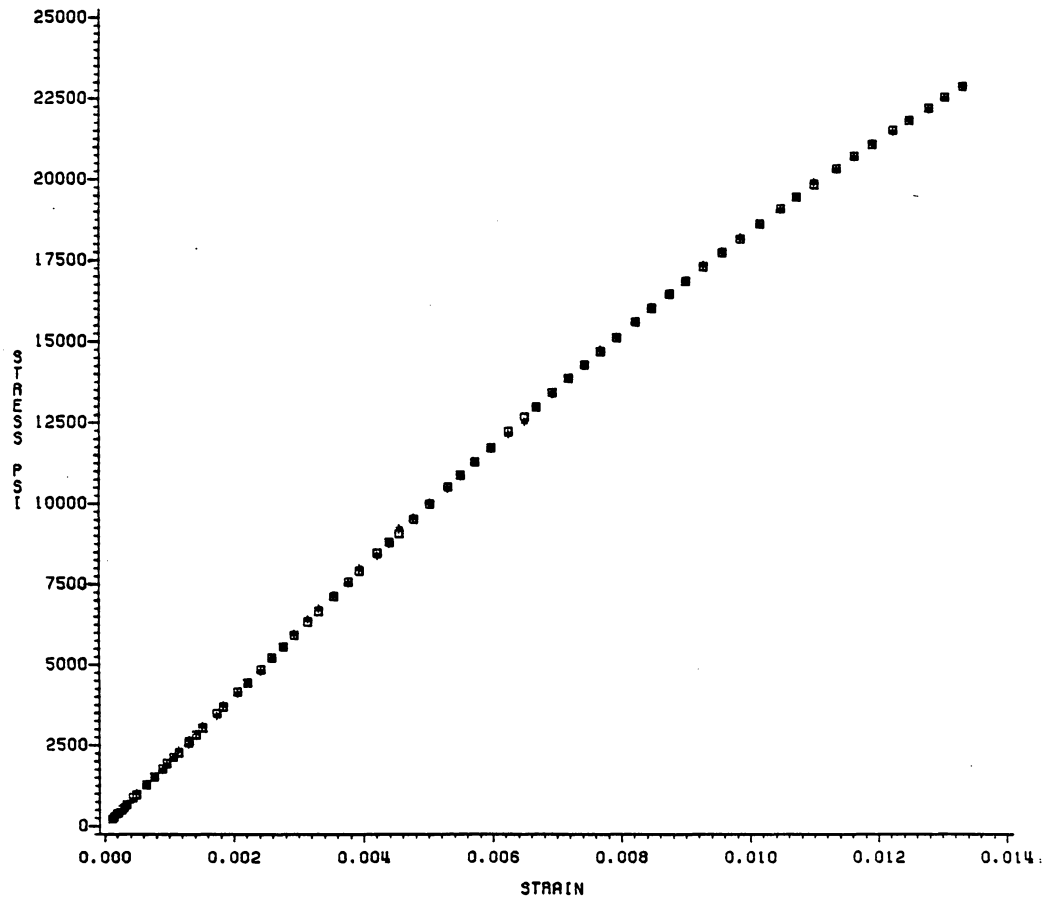

Figure 51: Overlay of predicted observations on the actual data for specimen T409. Data=asterisks, predicted points=squares.

5.1.2.1 Tension Regression Parameters and Join Points

The results of the B2 and B3 determinations for the tension specimen data are depicted in Figures 52 and 53. The B2 parameter did not appear to be dependent upon moisture content. The B3 parameter values were essentially constant between about six and eighteen percent MC, but the analyses of the green specimens yielded lower B3 values. The join point, K_1, is plotted against moisture content in Figure 54. A few specimens had negative values of strain for K_1; as explained for the compression analyses, this indicates that these specimens were more strongly curvilinear than linear from the start of the test. The join point did not appear to be influenced by moisture content.

5.1.3 Property Variation with Moisture Content

Acting on the historical assumption that green wood at or above the fiber saturation point will have the same mechanical properties regardless of the actual moisture content, it was thought desirable to determine an intersection point moisture content to use in modeling data above the fiber saturation point. Plotting the data revealed considerably different characteristics in tension and compression, however. The properties measured for tension, namely the longitudinal Young's modulus, the

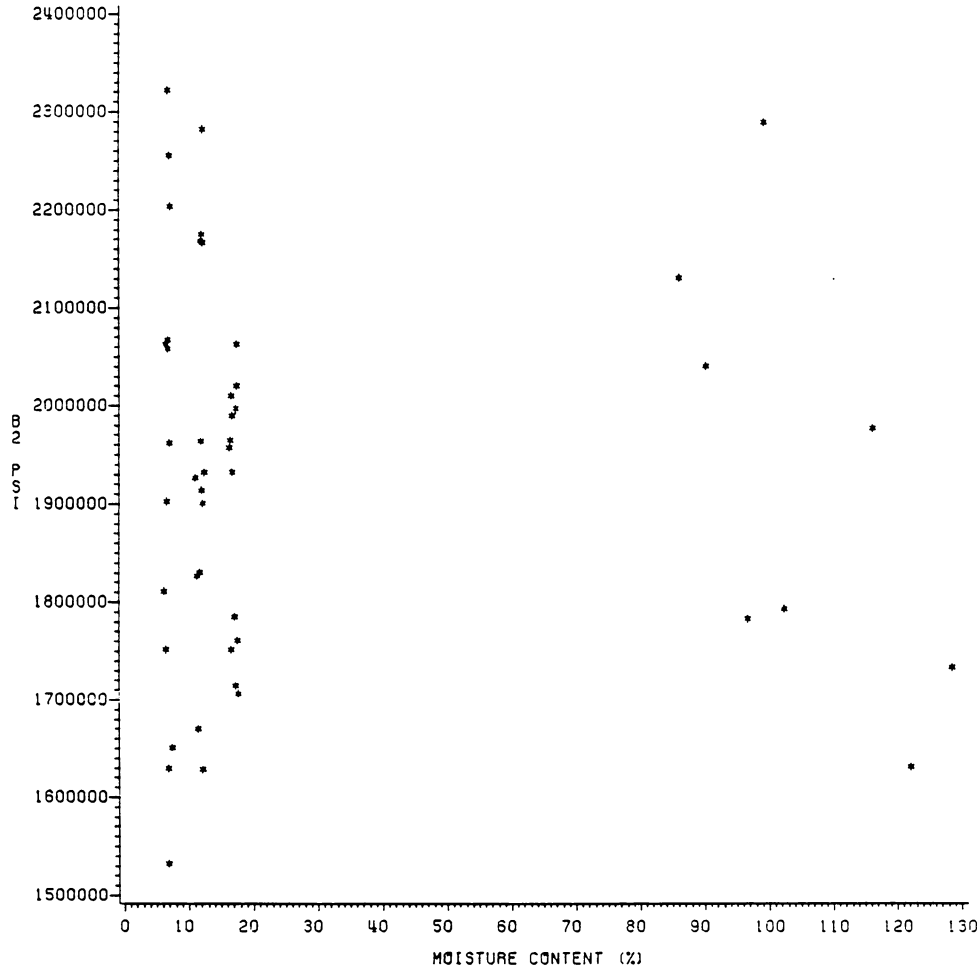

Figure 52: Tension B2 parameter values.

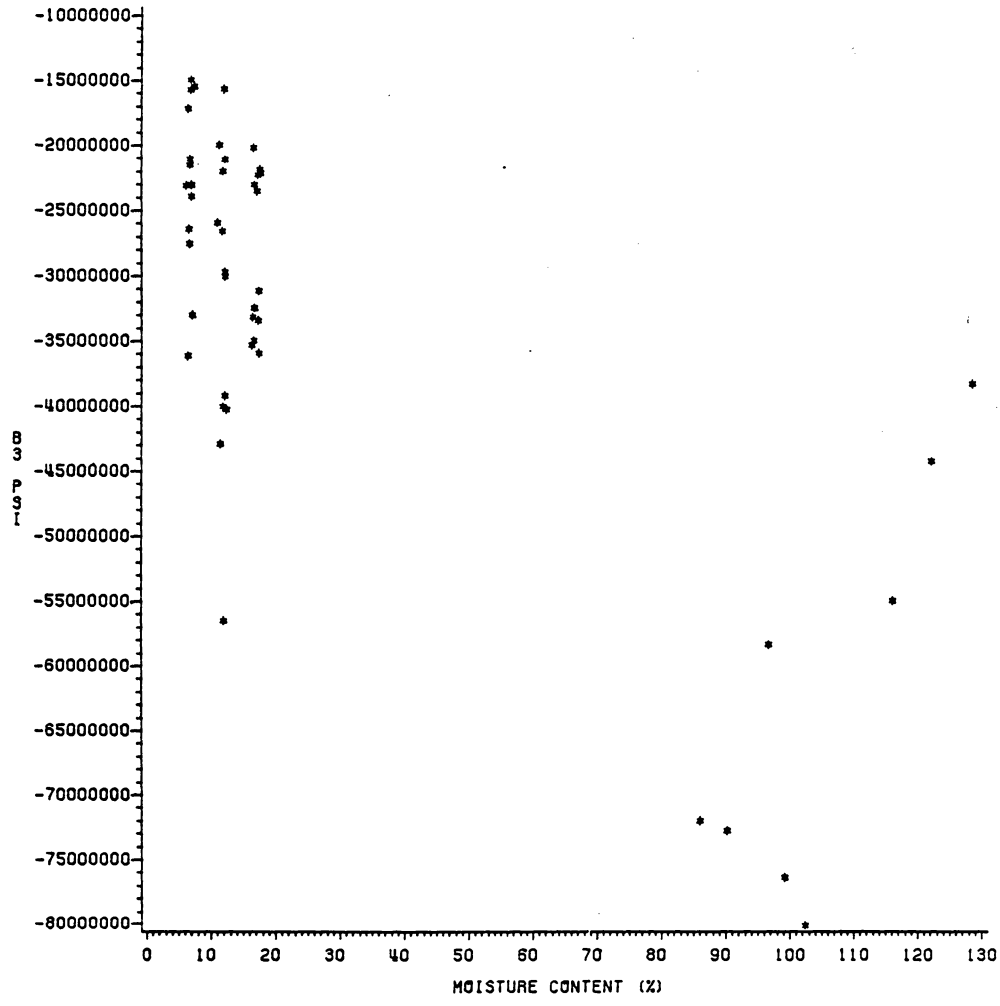

Figure 53: Tension B3 parameter values.

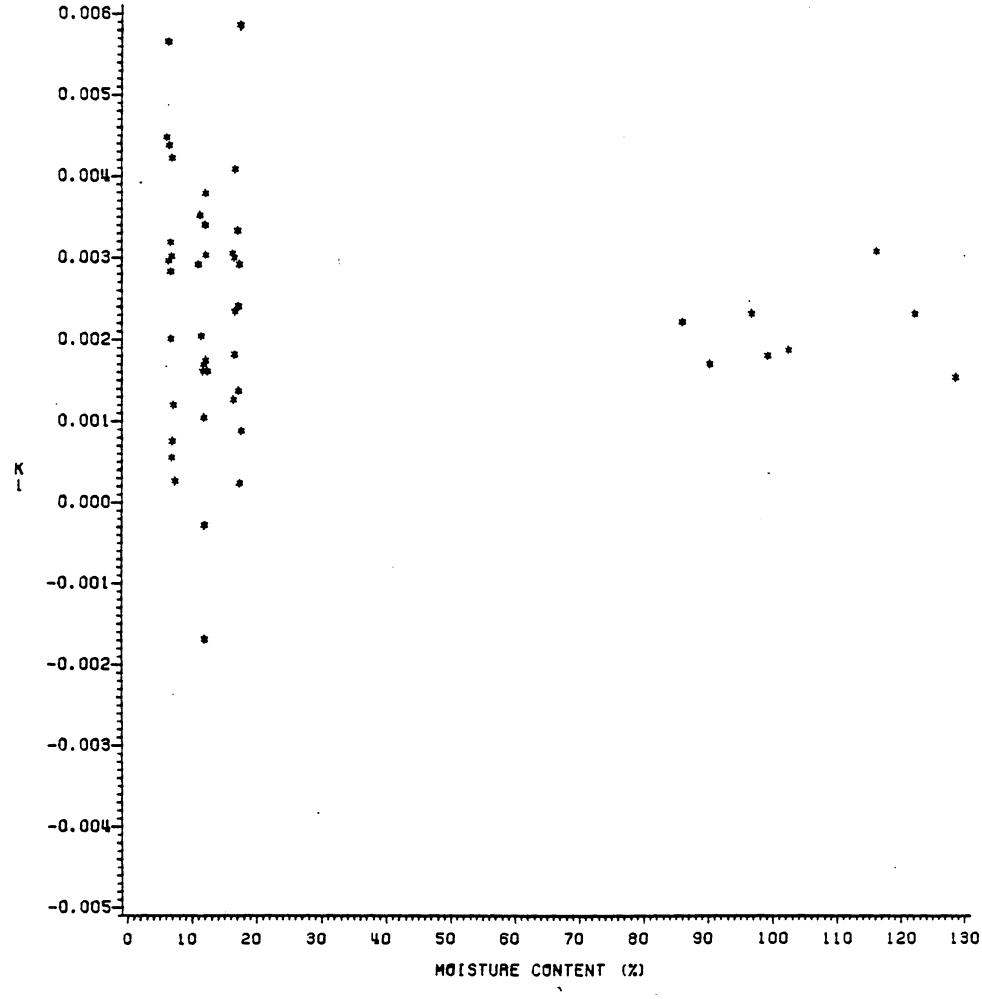

Figure 54: Strain values for the tension join point, K_1.

ultimate tensile strength, the ultimate tensile strain and the B2 and B3 model parameters were relatively insensitive to moisture content at the three lowest moisture content categories used in this project (six, twelve, and eighteen percent). This was confirmed by regression analyses of these data using various polynomial models. Young's modulus in compression exhibited a greater dependency on moisture content, but the trend was curvilinear, similar to the trend noted by Kollmann and Krech (1960) and others. Polynomial models for these compression data would likely underestimate the intersection point if they were extrapolated to the average green moisture content Young's modulus. The peak of any regression model would necessarily be close to 12% MC, and since the highest value for Young's modulus is likely to actually be between six and twelve percent MC any predictions made beyond the range of the data for which the model was determined would be biased. The data for the ultimate stress in compression and the values for the compression B2 parameter manifested strikingly different trends. The data for the three lowest moisture content categories appeared to have linear relationships with moisture content. The B2 data exhibited considerable variability, however, and it was believed that the data for maximum stress would be preferable for an intersection point

determination, as these were measured values. Therefore, these latter data were chosen to be analyzed for the intersection point determination. Linear regression was used to determine two relationships:

1. between the ultimate compression strength and moisture content, and
2. between a logarithmic transformation of the ultimate compression strength and moisture content.

The model for the non-transformed data had the smaller error sum of squares, and the linear model was selected on this basis. After calculating the average strength of the green specimens, an algebraic determination was made of the moisture content at which the regression value would equal this green strength. This moisture content, 25.6 percent, was decided upon as the approximate intersection point for the data in this study. This intersection point was assumed to be correct for all the tension and compression properties measured, even though this could not be confirmed from the data. It should also be noted that the method used to determine this point pre-supposes that the moisture content-mechanical property relationship truly has a zero slope at moisture contents in excess of this intersection point.

Tiemann (1906, 1907) defined the fiber saturation point (FSP) both as

1. the MC where mechanical properties begin to change upon drying and as
2. the MC at which the cell walls are saturated but devoid of free water.

This indicates that he viewed the fiber saturation point as being identical to an intersection point. Wilson separated the two ideas for practical purposes when he defined his own intersection point, M_p, as being that moisture content at which a logarithmic function of a specified material property intersected with the green property value. He did not contradict Tiemann's claim that the two definitions of the FSP identified a single moisture content. Tiemann's definition of the fiber saturation point as the MC at which the cell walls are saturated need not be questioned, but the data collected for this study suggest that the FSP should not be simultaneously identified with the intersection point. It seems likely that tension and compression properties vary differently with moisture content and that the intersection points may be different, possibly by a significant margin. According to Tiemann's conceptualization of the fiber saturation point, different fiber saturation points could therefore be defined for the same piece of wood depending whether it is tested in tension or compression. Obviously there can only be one moisture

content at which the cell walls become saturated, so what is being observed must be complex effects of lesser amounts of moisture on the individual cell wall layers and/or chemical constituents within the cell wall. Typically "green" properties are likely reached for some properties before the fiber physically reaches a saturated condition.[3] (It is assumed that no further mechanical property changes are possible once the fiber actually reaches this saturated state). The concept of a fiber saturation point should therefore be restricted to the definition of the physical fiber condition. On the other hand, the concept of intersection points should be expanded to encompass the hypothesis that these points need not be the same for different mechanical tests within a single species. This is likely due to the varying effects of moisture on a complex lignin-cellulose-hemi-cellulose cellular composite, and contrasts sharply with the more traditional view of moisture affecting fibrillar cellulosic (and hemi-cellulosic) components as separate entities.

Following the determination of an approximate intersection point, the Young's modulus data and the regression parameter values, as well as the ultimate tensile

[3] Since the tension data from this study appear likely to have a higher intersection point than the compression data, the compression data may be an example of this phenomenon.

strain data, were subjected to regression analysis to determine appropriate models. These analyses were conducted with the objective of predicting stress-strain diagrams in both tension and compression for yellow-poplar at any moisture content. All green moisture contents were assumed equal to 25.6% moisture content for this procedure.

Data for a few specimens were excluded from these analyses. Proc NLIN could not determine values for B2 and B3 for one compression specimen, so this specimen was not used in the analyses. A few more specimens were excluded from the tension analyses. Two specimens had to be discarded due to excessive localized grain angles detected in these specimens following an examination of the ultimate stress and Young's modulus values. Several tension specimens also yielded unusual values for B3 upon analysis (e.g., a positive value when a negative value was expected). Examination of the corresponding stress-strain diagrams revealed that many (but not all) of these specimens had either perfectly linear or gently wavy diagrams. Because the ultimate objective was to predict "typical" stress-strain diagrams, specimen data were culled only if both an unusual B3 value and and unusual stress-strain diagram were simultaneously present; data for six specimens were eliminated from consideration based on these criteria.

Before any analyses were performed, it was decided that the main purpose of the regressions would be to predict reasonable values for B2 and B3. This is a slightly different approach to regression analysis compared to the usual technique of merely checking the adequacy of fit for selected (potential) models. Montgomery and Peck (1982) state that

> It is tempting to conclude that a model that fits the data well will also be successful in the final application. This is not necessarily so. For example, a model may have been developed primarily for predicting new observations. There is no assurance that the equation that provides the best fit to existing data will be a successful predictor. Influential factors that were unknown during the model building stage may significantly affect the new observations, rending the predictions almost useless.

It was recognized that several possible models exist for any groups of data to which regression techniques may be applied. In selecting among the possible models in this dissertation, an initial screening was conducted to select those polynomial models with superior measures of goodness of fit (R^2) and lesser degrees of inherent bias (Mallows' C_p statistic). Palka's modified exponential model might have been considered for the compression Young's modulus data, but was not used in this analysis because of the small number of moisture contents in the experimental design, and also because the data did not clearly indicate the MVMC

point. In addition to the measures noted above, the error sum of squares and the mean square error (measures of model fit) were calculated. The adjusted R^2 value ($\bar{R}^2$) was also calculated for each regression to account for the varying degrees of freedom in the models considered; it is well known that the value for R^2 tends to increase as more regressors are added to the model. Finally, the PRESS statistic (predicted error sum of squares) was calculated for each model. This statistic is a measure of a model's predictive validity, and is based upon a mathematical technique which effectively splits the data set into every possible subset of n-1 observations. A regression model is then fit to each subset of n-1 points, and the resulting equation is used to predict the n-th observation in each case. The difference between the predicted and the actual observation for each model subset (e_i) is then used to form the PRESS statistic for the model as follows:

$$\text{Press} = \Sigma(e_i)^2 \qquad [5.1]$$

Fortunately, some mathematical manipulation makes it unnecessary to analyze each set of data n times, but the concept and the interpretation of the statistic remains the same. The reader is referred to Montgomery and Peck (1982) for further details.

It should be noted that all of the above measures were calculated and examined before making the final model selection. Preference was given to the model with the fewest regressors when a choice could not be made among several good model candidates on other bases. The "best" models are listed in Table 15 and were chosen from all combinations of MC, MC^2, MC^3 and specific gravity. With two exceptions, every model was significant at the 95% level. The maximum tension strain model described the data slightly less well, and there was no significant relationship found for the tension parameter, B2. In a couple of instances a factor incorporated into a selected model was not significant at the 95% level; both the fit of these models and their predictive abilities were better than the same models without these factors, however, so they were retained. Plots of the data and parameter values overlaid by the chosen models are presented in Figures 55 through 61.

5.1.4 Prediction of Stress-Strain Models at Various Moisture Contents

Once the models were determined for the longitudinal elastic constants and the various equation parameters in tension and compression, typical tension and compression stress-strain curves were mathematically reproduced at several moisture contents using equations [3.10-3.20]. The resulting curves

TABLE 15

Models selected to describe data and parameter values.

Compression

$$E_{1,c} = 143900 + 441996\ (MC\%) - 28997\ (MC\%)^2 + 534\ (MC\%)^3$$

$$B2,_c = 5719340 - 258850\ (MC\%) + 4280\ (MC\%)^2$$

$$B3,_c = -1065588500 + 3449729\ (MC\%) + 1540914880\ (SG)$$

Tension

$$E_{1,t} = 1822300 - 9.8\ (MC\%)^3$$

$$B2,_t = 1934700$$

$$B3,_t = 37045400 - 2204\ (MC\%)^3 - 150737800\ (SG)$$

$$\varepsilon_{max,t} = 0.0163 - 0.00129\ (MC\%) + 0.0000963\ (MC\%)^2 - 0.00000214\ (MC\%)^3$$

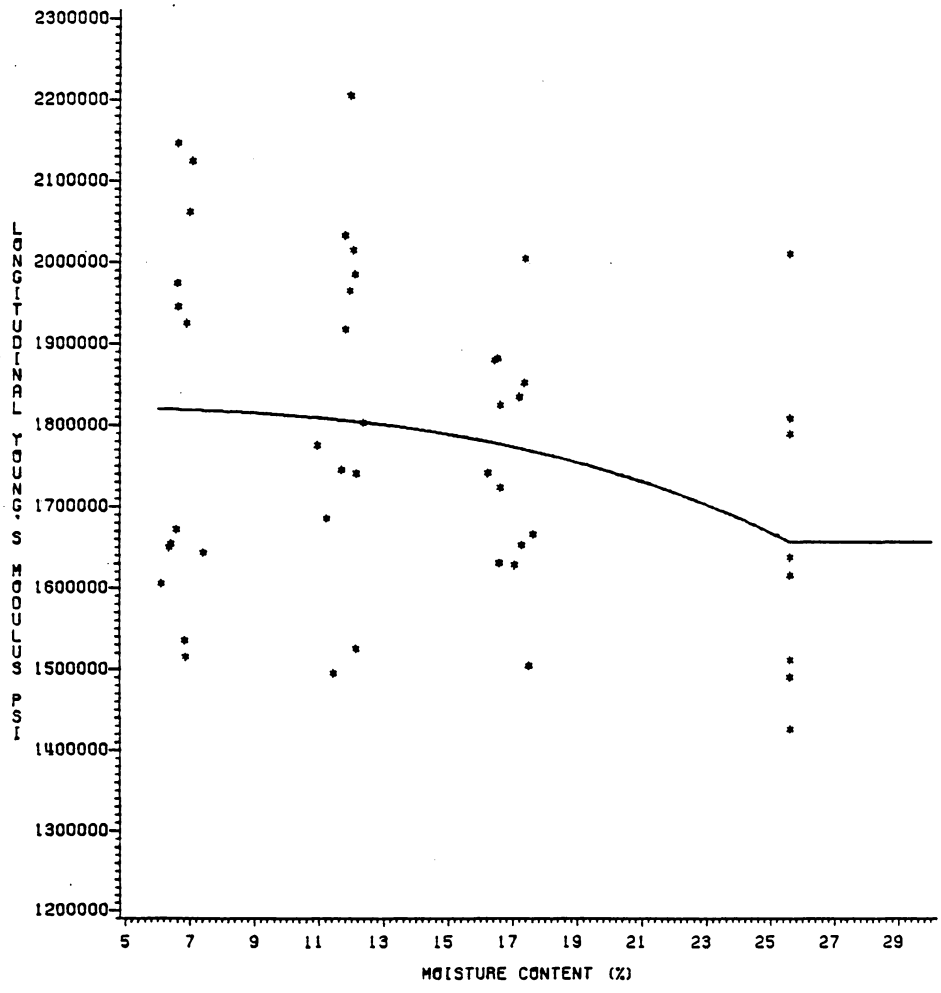

Figure 55: Young's modulus in tension overlaid by model.

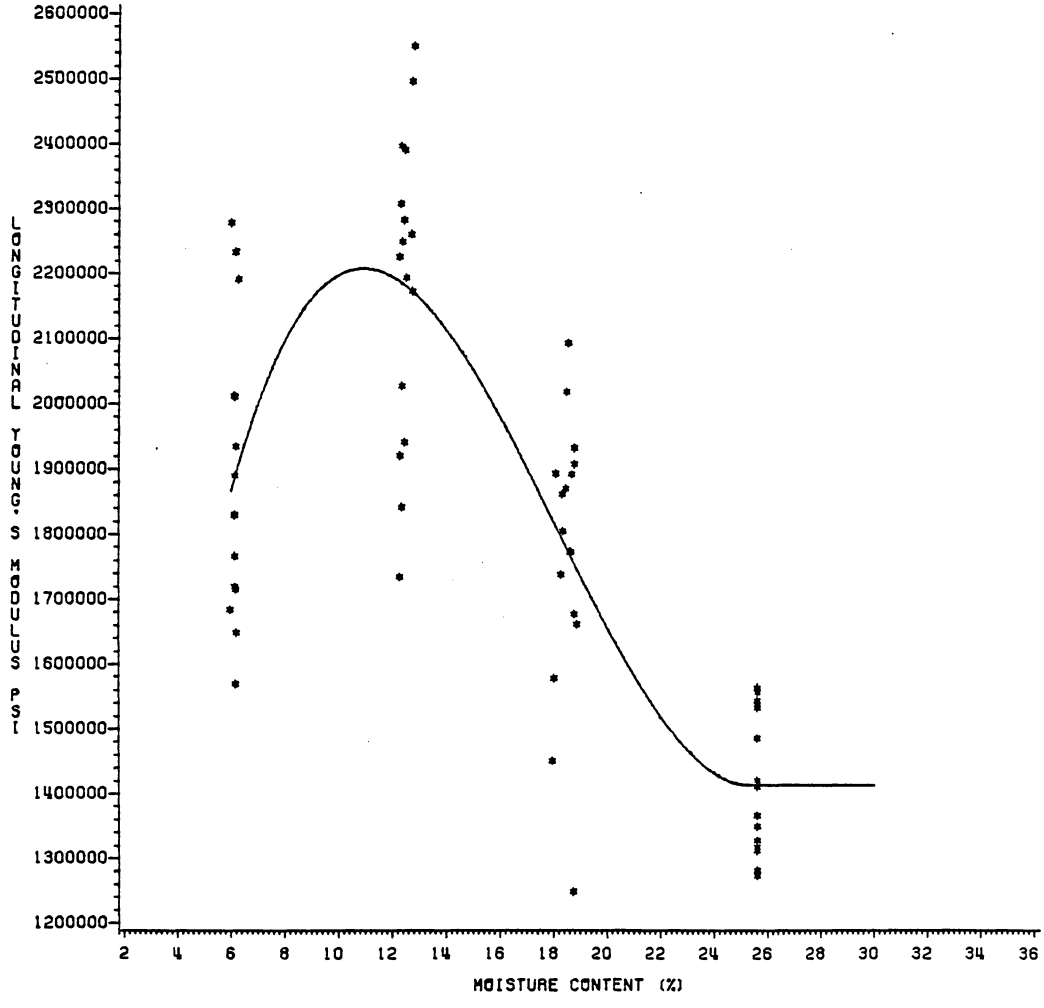

Figure 56: Young's modulus in compression overlaid by model.

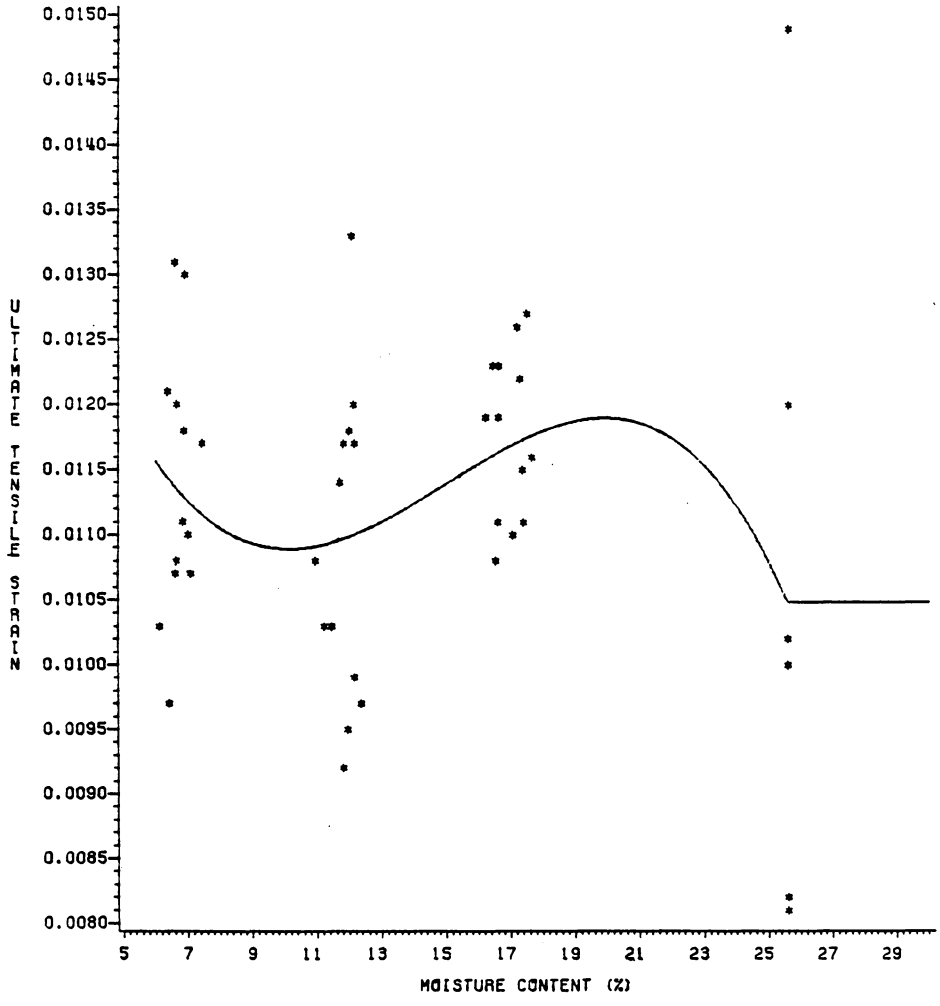

Figure 57: Maximum tension strain data overlaid by model.

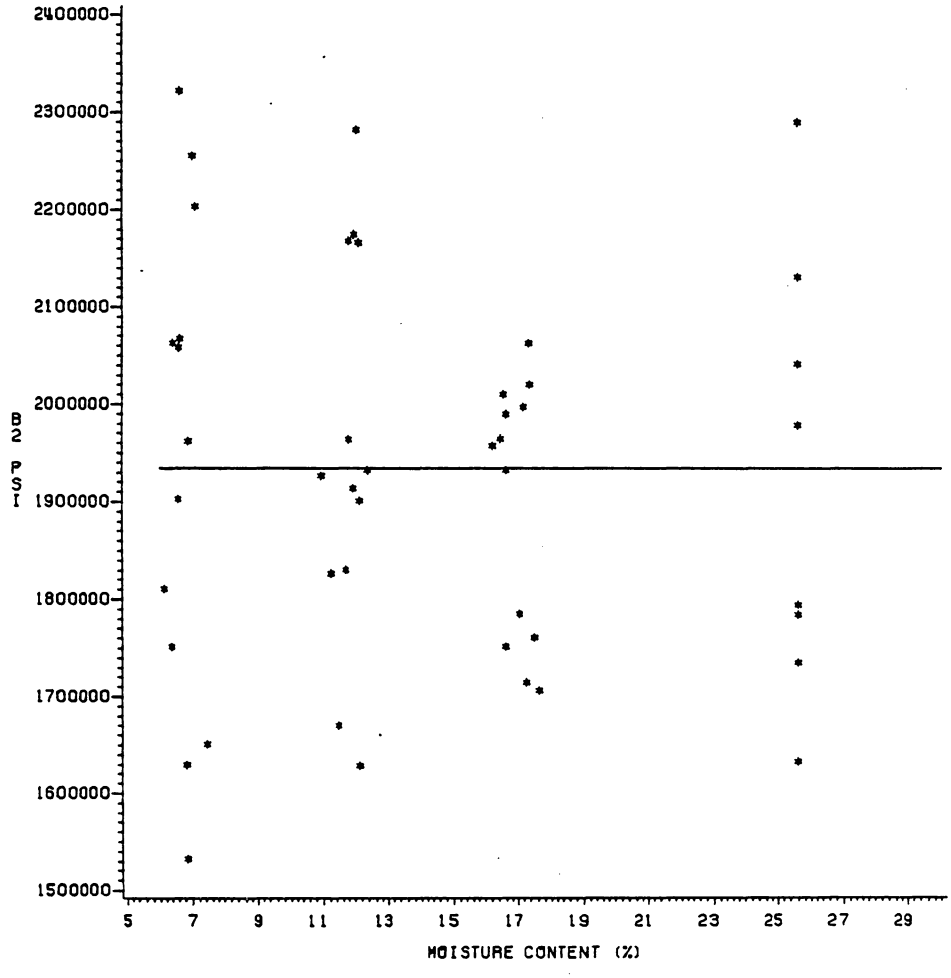

Figure 58: Tension parameter B2 values overlaid by model.

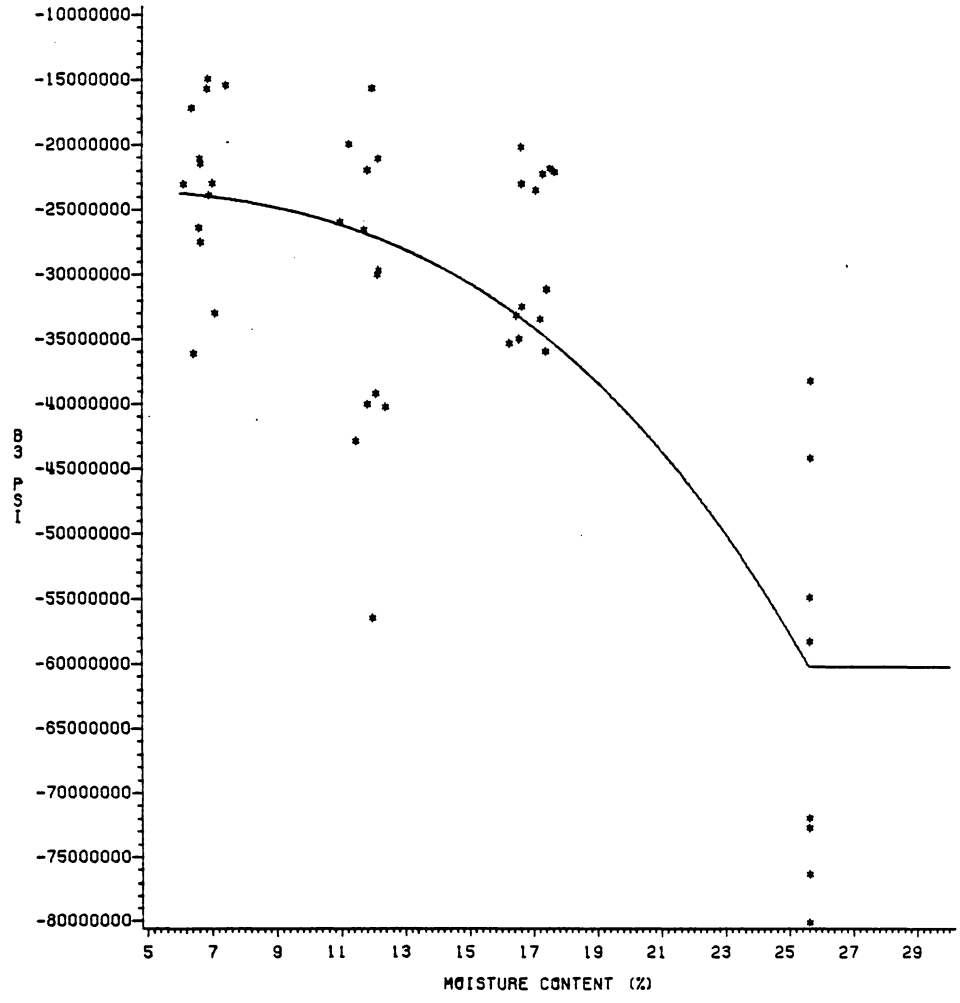

Figure 59: Tension parameter B3 values overlaid by model.

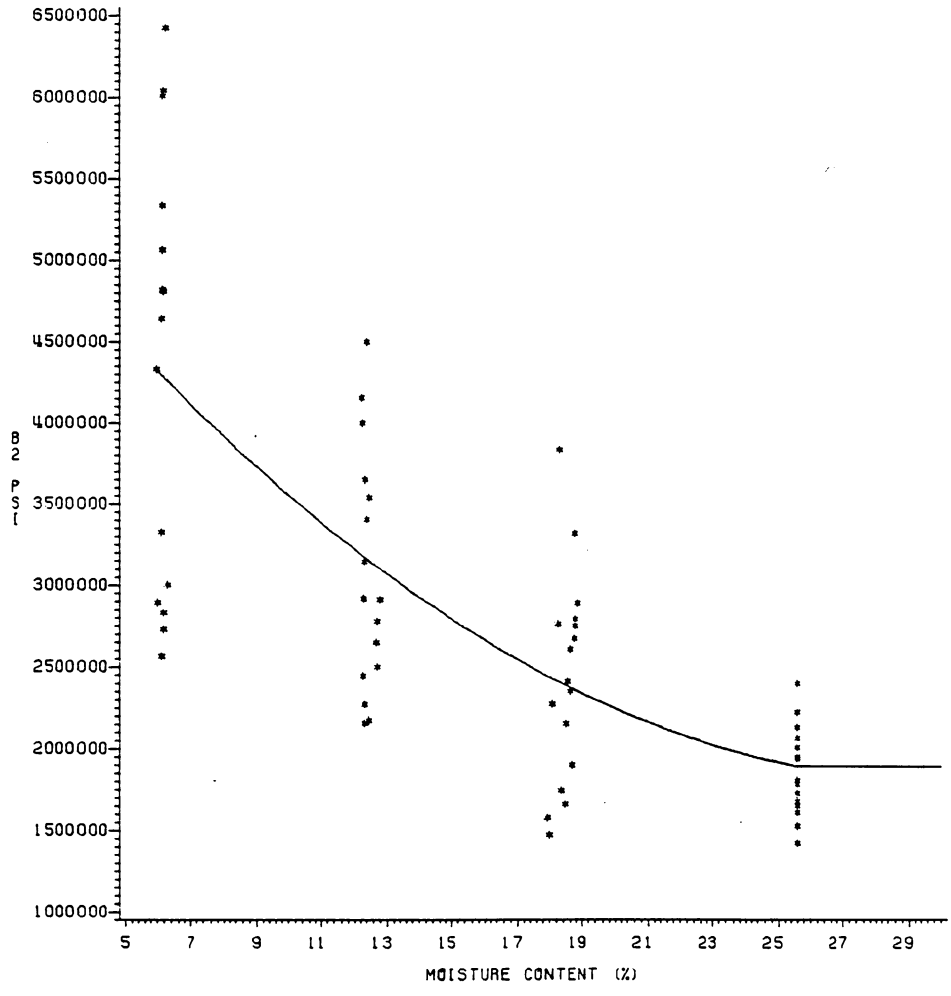

Figure 60: Compression parameter B2 values overlaid by model.

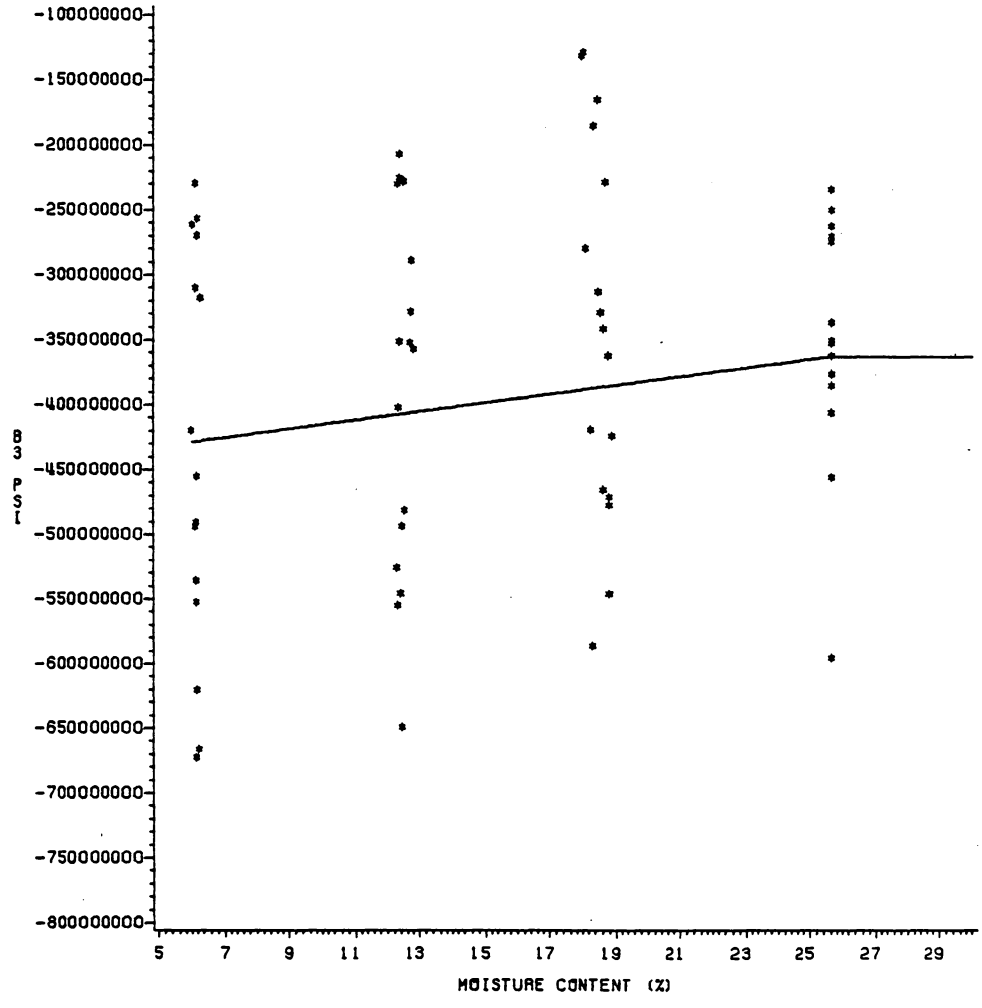

Figure 61: Compression parameter B3 values overlaid by model.

are included in this report as Figures 62 and 63. The similarity of these curves to the representative data plotted in Figures 39 and 40 is remarkable. It is possible that stress-strain curves at other moisture contents may not be predicted as accurately, but there can be little doubt that the procedure for the prediction of tension and compression stress-strain models works well overall for a wide range of moisture contents.

5.2 COMPARISON OF THE YOUNG'S MODULI IN TENSION AND COMPRESSION

Following testing, the Young's moduli in tension and compression were compared to examine the equality of these values at common moisture contents. The two selected models for the respective Young's moduli were also compared. The equality of the Young's moduli in tension and compression is often assumed (Ethington, 1960; Moe, 1961; Nwokoye, 1972; Anderson, 1981), based primarily on a relatively small number of tests showing negligible or only slight differences at only one or two moisture contents (Lamarle, 1845, 1846; Baumann, 1927; Dietz, 1942; Sliker, 1973). Others have noted different results. Stern (1944b) found that the Young's modulus in tension was greater than that in compression by nearly 25% at about nine percent moisture content. Mazur (1965) found that the average longitudinal

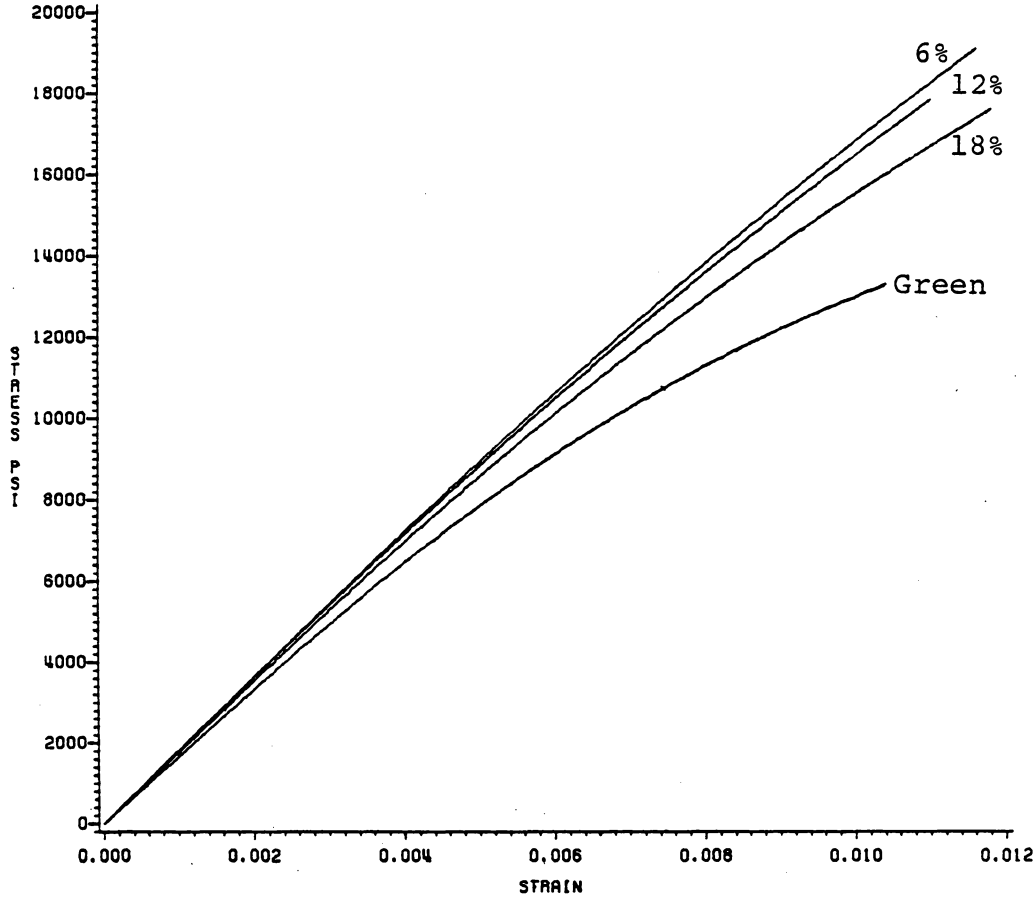

Figure 62: Overlays of predicted tension stress-strain curves

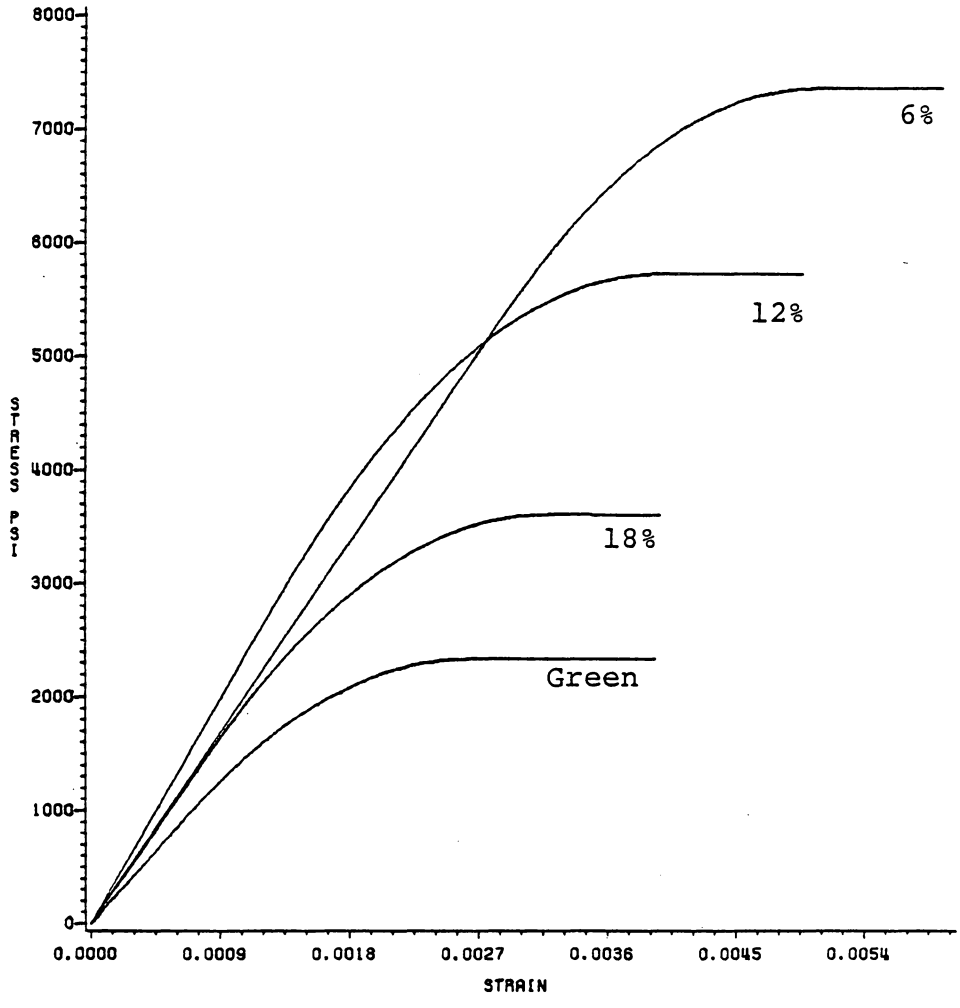

Figure 63: Overlays of predicted compression stress-strain curves

Young's modulus in compression for eastern spruce was about 18% greater than the corresponding modulus in tension at 12% MC, but he assumed that this difference was not significant. Palka (1973) states that Walker (1961) found that the longitudinal modulus was 21% greater in compression than in tension. Zakic (1976) found that the tensile modulus was almost two times as great as the modulus in compression at twelve percent moisture content. In spite of these widely varying results, however, no study appears to have compared these moduli at more than two moisture contents. As seen from a plot of the data collected for this study (Figure 64), the choice of moisture content at which the moduli are compared may be important. These data show that the tensile and compressive Young's moduli are very similar for 6% and 18% moisture content specimens. The Young's modulus in compression is greater at 12% MC, however, and the Young's modulus in tension is greater for green specimens.

Figure 65 shows a plot of the tension and compression Young's modulus data overlaid by the models selected as previously described. These models are significantly dissimilar, and the "forced" use of a single model (USFPL exponential model or other) for both does not appear to be warranted.

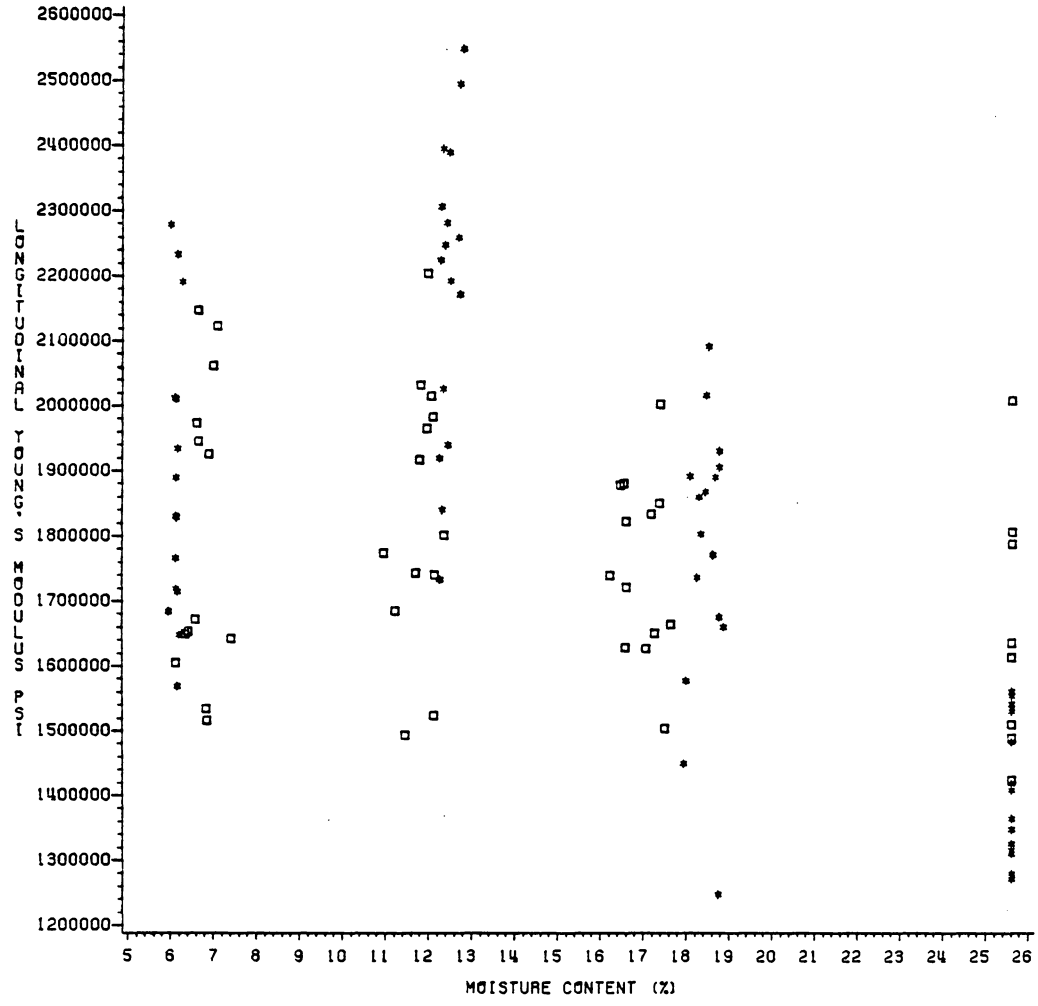

Figure 64: Tension and compression Young's modulus data. Squares=tension data, stars=compression data.

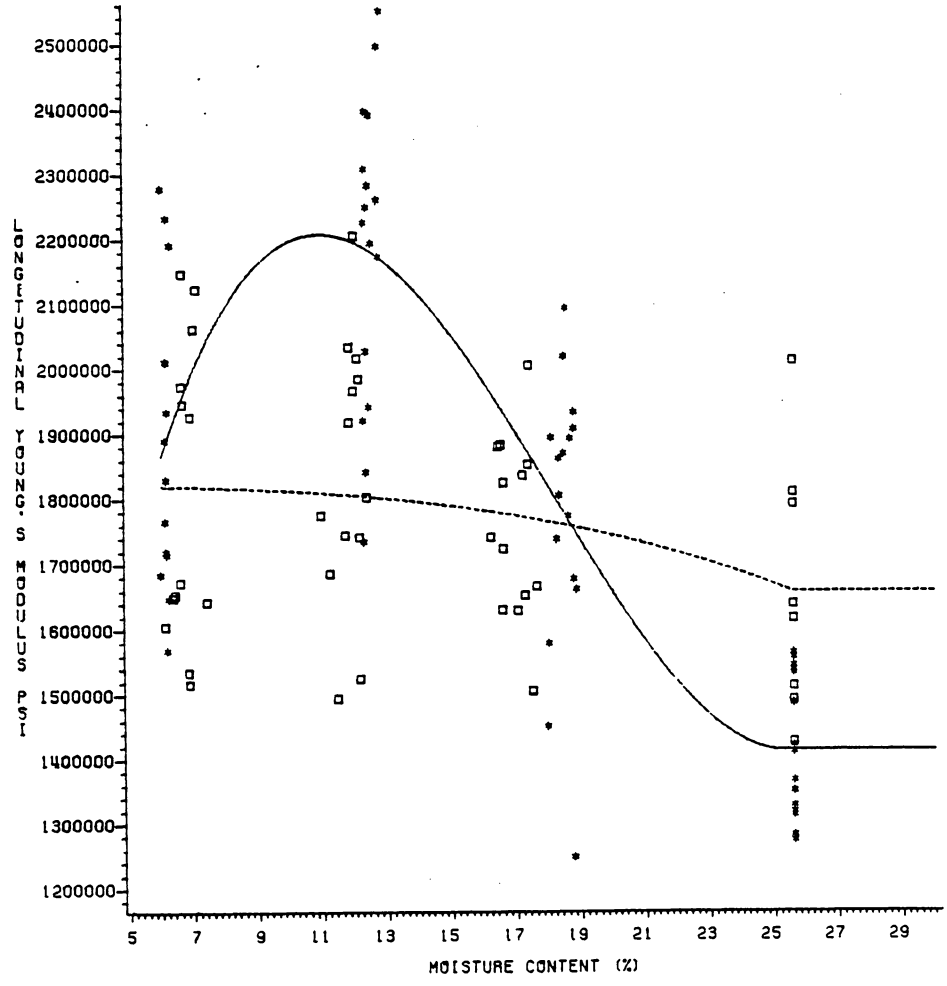

Figure 65: Tension and compression Young's modulus data overlaid by the respective models. Stars=compression data, squares=tension data. Solid line=compression model, dashed line=tension model.

5.3 COMPARISON OF OBSERVED MC GRADIENTS TO MODEL

Gradient specimens had been taken from twenty-five beams and divided into sixteen moisture content sub-sections per beam slice as described previously. After the moisture contents of these sub-sections had been determined, the data were recorded on a 4 x 4 grid corresponding to the position of each sub-section on the cross-section (Figure 66). Some slight asymmetry of the moisture content distribution was noted, but it was impossible to separate the asymmetry caused by experimental error (caused by inaccurate slicing technique, etc.) from that actually present in the specimen. Asymmetry was doubtless observed for both reasons. Most specimens had a reasonably symmetric moisture distribution, although specimens with high average moisture contents (30% or more) sometimes tended to have less uniformity in the center four blocks than did those of lower moisture contents.

A predicted moisture content for each sub-section was computed next. The cross-section centroid was taken as the (0,0) coordinate in accordance with the gradient model formulation, and the centroid coordinates of each sub-section were entered into equation [3.5] along with the average beam moisture content (determined from two specimens as described earlier) and the approximate average EMC, which

Beam Top

16.7	24.5	23.7	17.8
22.1	34.3	35.8	22.9
21.2	34.6	34.6	22.7
15.9	22.6	24.0	16.7

Figure 66: Specimen B615-3a. MC data. 1/4" blocks (nominal dimensions). Average MC=24.3%, EMC=11.5%.

was taken as 11.5%. The agreement was usually fairly close (Figure 67), although random differences between the observed and the predicted values of plus or minus one or two percent were not uncommon for sub-sections whose MC was below the intersection point. Somewhat greater deviations from the model were often noted for sub-sections whose MC was both observed and predicted to exceed the intersection point, but this was of no consequence since the assigned mechanical properties would be the same in any event.

Based on the available data, the model for the two-dimensional moisture gradient appeared to be entirely satisfactory. The slight discrepancies noted seemed to be randomly distributed, and the differences appeared to be minor. It was assumed that no significant errors would result from using this model in the finite-element program.

5.4 RESULTS OF THE BEAM TESTS

Beam test data were acquired for both equilibrated and non-equilibrated specimens of yellow-poplar. The equilibrated specimen data were observed at nominal 12, 18, 22% and green moisture contents, as noted previously. These data consisted, for the most part, of observations from material different from that tested in the uniaxial tests. Samples from each of the two groups of material were tested in the

Beam Top

16.7 17.0	24.5 23.3	23.7 23.3	17.8 17.0
22.1 23.3	34.3 36.7	35.8 36.7	22.9 23.3
21.2 23.3	34.6 36.7	34.6 36.7	22.7 23.3
15.9 17.0	22,6 23.3	24.0 23.3	16.7 17.0

Figure 67: Specimen B615-3a. MC data compared to predicted values. Observed data are recorded on the first line in each block, the predicted values are below.

green condition to determine whether they had comparable mechanical properties. Analyses of variance for the apparent MOE and MOR observations failed to reject the null hypotheses at the 95% confidence level. On this basis the two groups of wood were assumed to have equivalent mechanical properties and the data were combined.

The equilibrated MOE and MOR data obtained in this study are presented in Figures 68 and 69. The modulus of elasticity decreased only slightly between about 11% and 22% moisture content, and appeared to be significantly lower for green specimens. MOR, on the other hand, exhibited a steady decrease with moisture content.

The gradient-containing beam data were also obtained from tests of specimens drawn from the two samples of yellow-poplar. As the data were collected, it was observed that the method chosen to estimate the average beam moisture content prior to test gave only a rough idea of the actual moisture content present. An additional wood moisture specimen (one from each end of the beam) would have improved the MC estimate, but sufficient material was usually not available for this extra sample. The MC variability resulting from the estimation method used may be seen in the plots for the MOE and the MOR values for these beams (Figures 70 and 71). The average moisture content

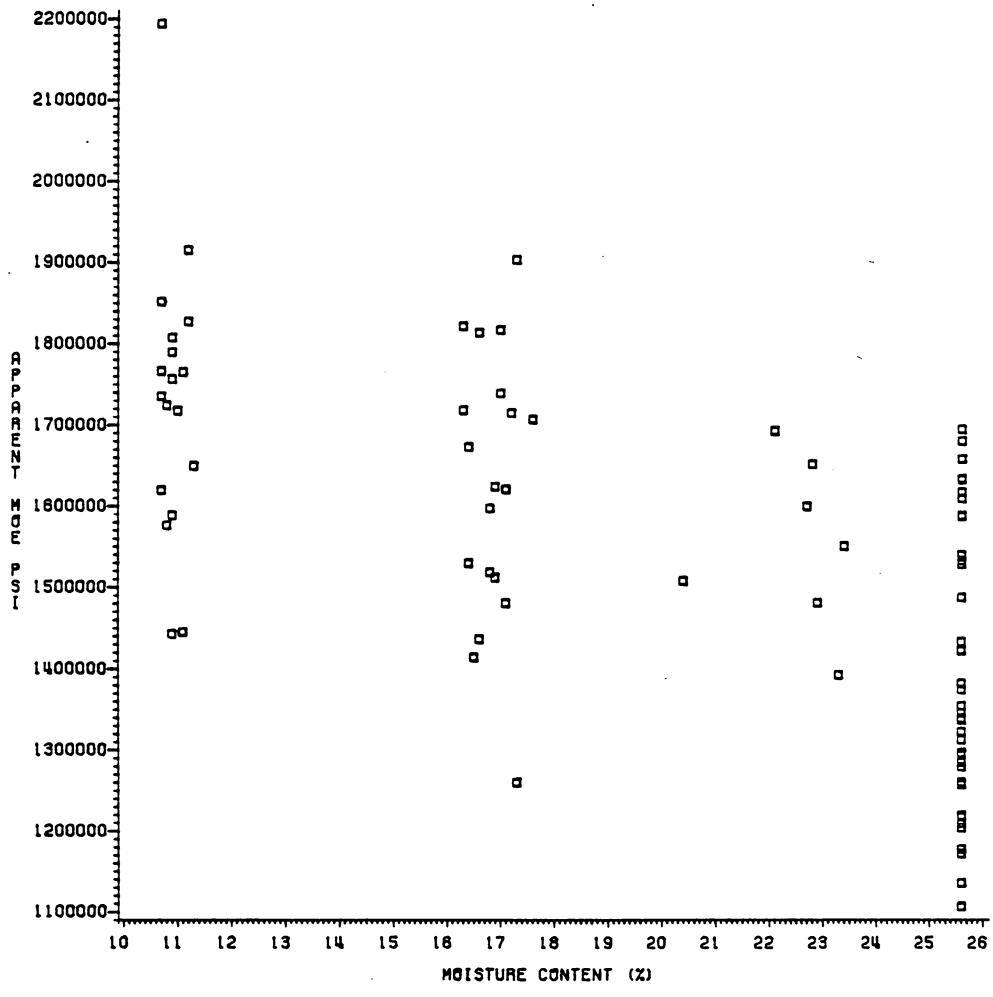

Figure 68: Modulus of elasticity data for beams with uniform moisture contents.

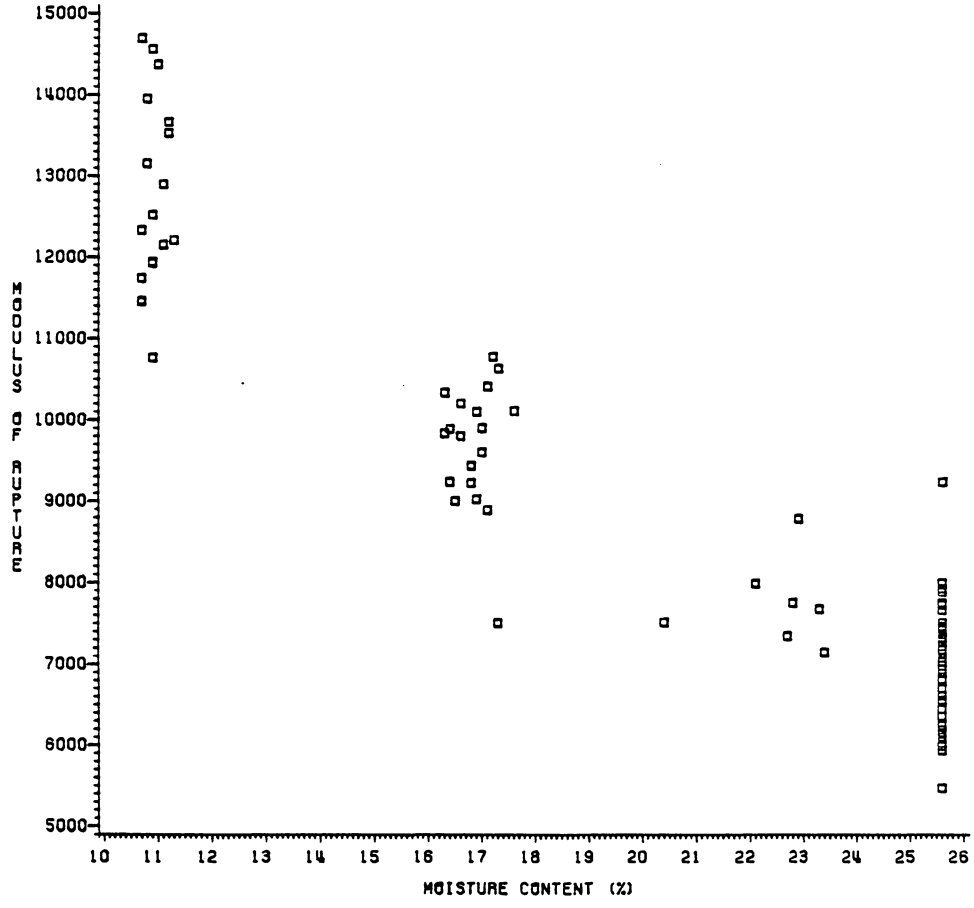

Figure 69: Modulus of rupture data for beams with uniform moisture contents.

distribution is fairly uniform from 14% to 36% instead of being concentrated at the pre-selected moisture contents.

The MOE and MOR values for both the equilibrated and non-equilibrated beams were subjected to regression analyses to determine appropriate polynomial models. Plots of the best models overlaid on the data are included in this report as Figures 72, 73, 74, and 75. The MOE data for non-equilibrated beams did not yield a statistically significant model, and the average of these values was used to describe the data. Overlays of these MOE and MOR models for the equilibrated and non-equilibrated data are included in this report (Figures 76 and 77). These relations indicate that the MOE observations for non-equilibrated beams are only slightly lower than the MOE values observed for beams equilibrated at about 12% EMC (Figure 76). As Figure 77 shows, the MOR data are approximately equal up to about 18.8% average moisture content, although the non-equilibrated MOR model predicts slightly lower values up to this moisture content. From 18.8% on, the non-equilibrated MOR model is significantly higher than the corresponding model for equilibrated data, and this model exhibits a gradual declining trend at higher moisture contents. For example, at 25% average moisture content the model for the non-equilibrated MOR data predicts that the MOR of these

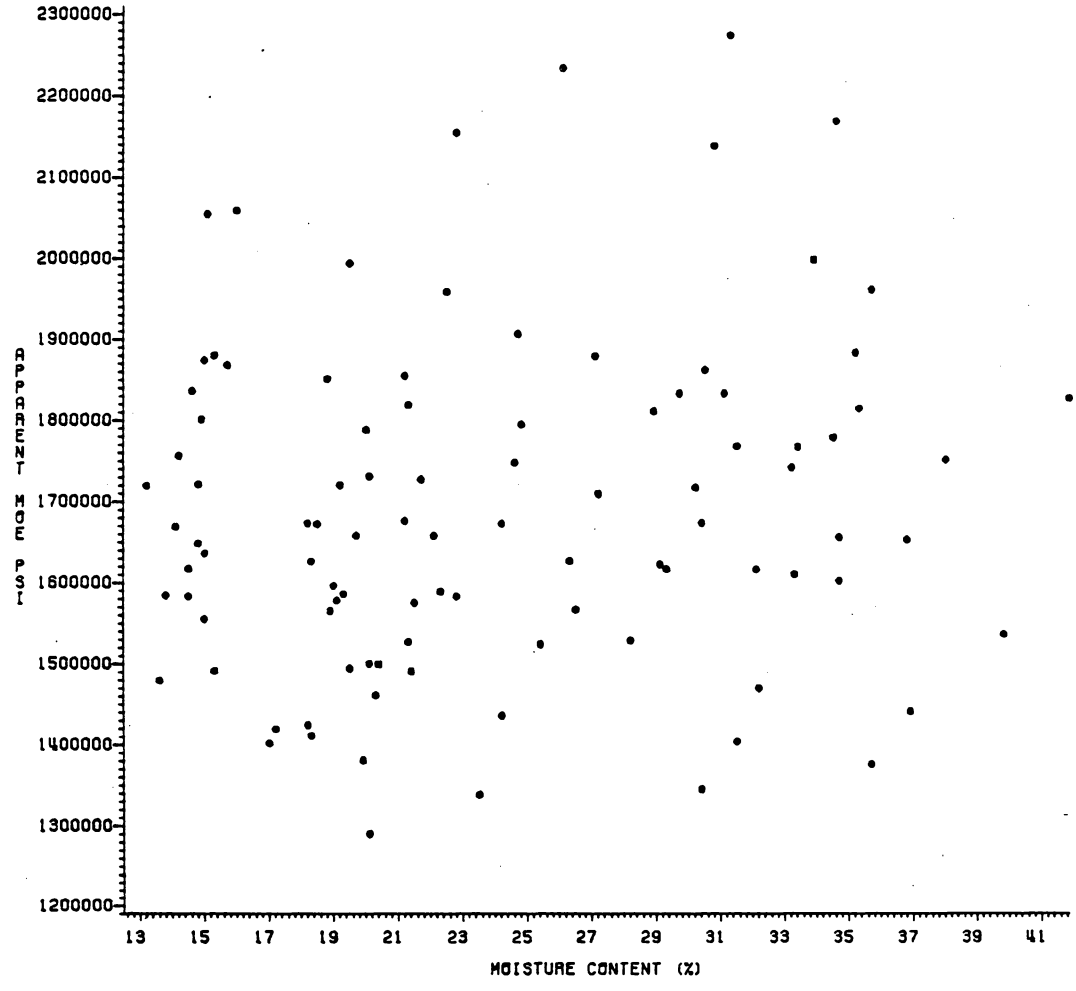

Figure 70: MOE data from non-equilibrated beams: 12% EMC.

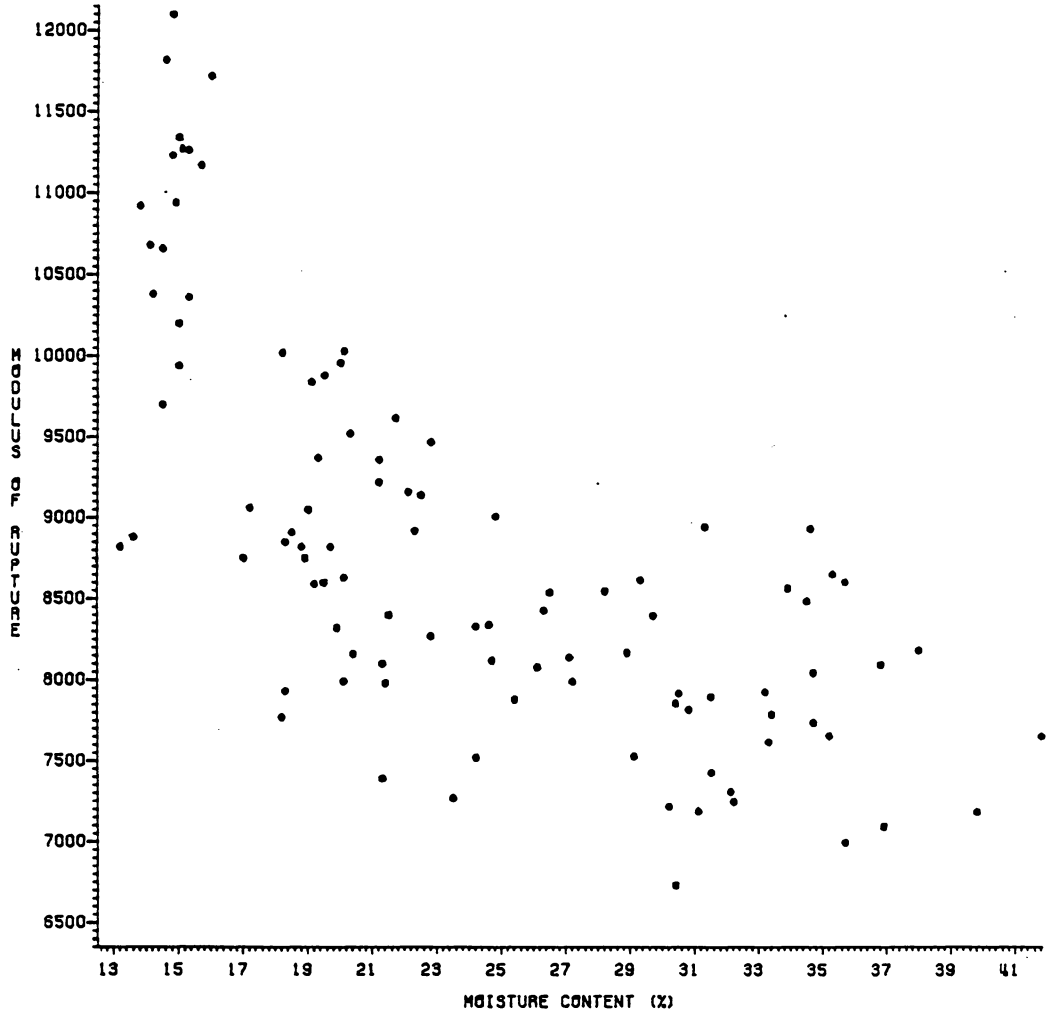

Figure 71: MOR data from non-equilibrated beams: 12% EMC.

specimens will be 28% greater than the MOR of equilibrated specimens at the same moisture content, and at 45% average moisture content the non-equilibrated specimens are predicted to be stronger than green specimens by about 16%. This trend is similar to that reported previously for beam MOR data (Wilson, 1932), but differences between equilibrated and non-equilibrated beam MOR data had previously been noted at lower moisture contents. This may be explained as due to either the influences of the species observed or to differences in the EMCs at which gradients were imposed. The EMC condition is likely to be more influential in this regard than the species. Data do not appear to have been published concerning the effects of moisture gradients on MOE prior to this report. Tiemann (1906), Wilson (1932) and Madsen, et al. (1980) were more concerned with the effects of gradients on strength than stiffness. The MOE data presented here, therefore, can not be compared to other data.

The non-equilibrated beam MOE data collected for this study deserve some additional comment at this point. As was noted above, no statistically significant relationship was able to be determined and it is, therefore, uncertain whether the chosen model (an average value) is an accurate representation of the actual trend. This model is not

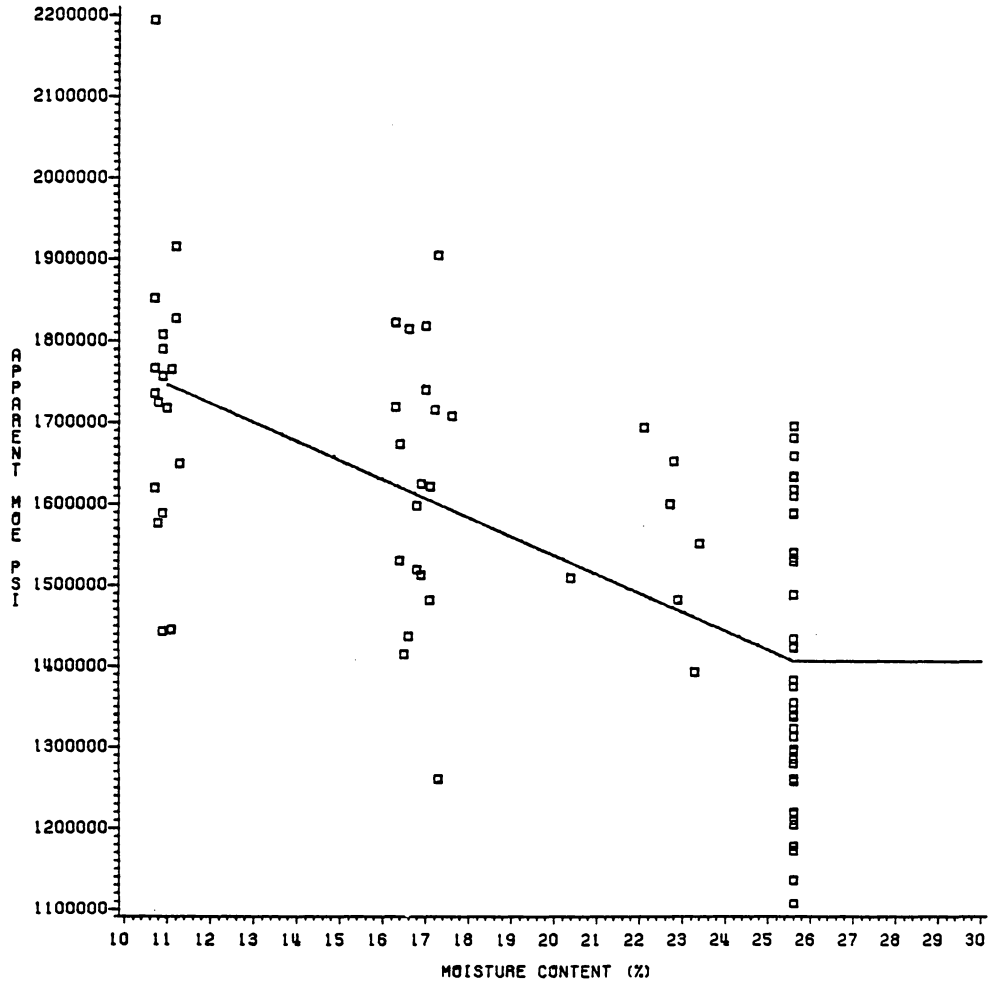

Figure 72: MOE data for equilibrated yellow-poplar beams, overlaid by model.

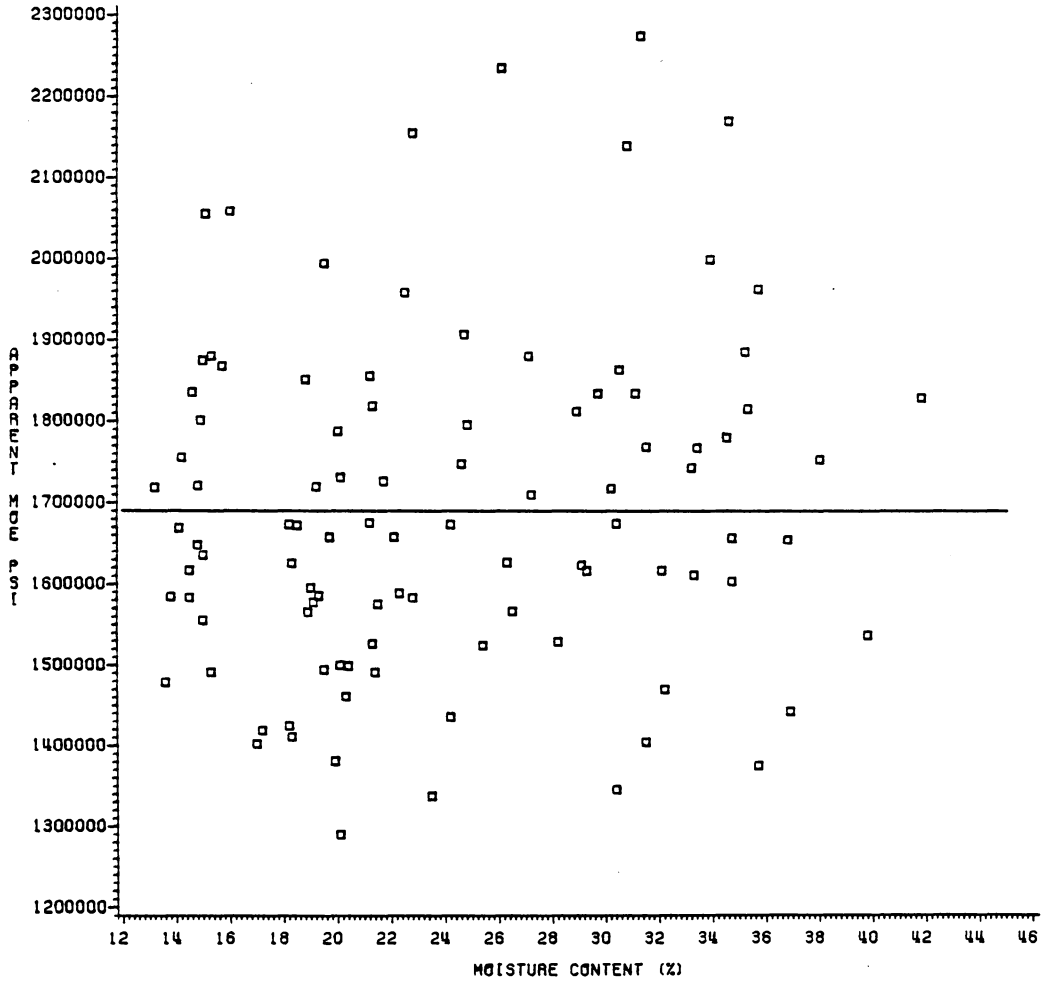

Figure 73: MOE data for non-equilibrated yellow-poplar beams, overlaid by model.

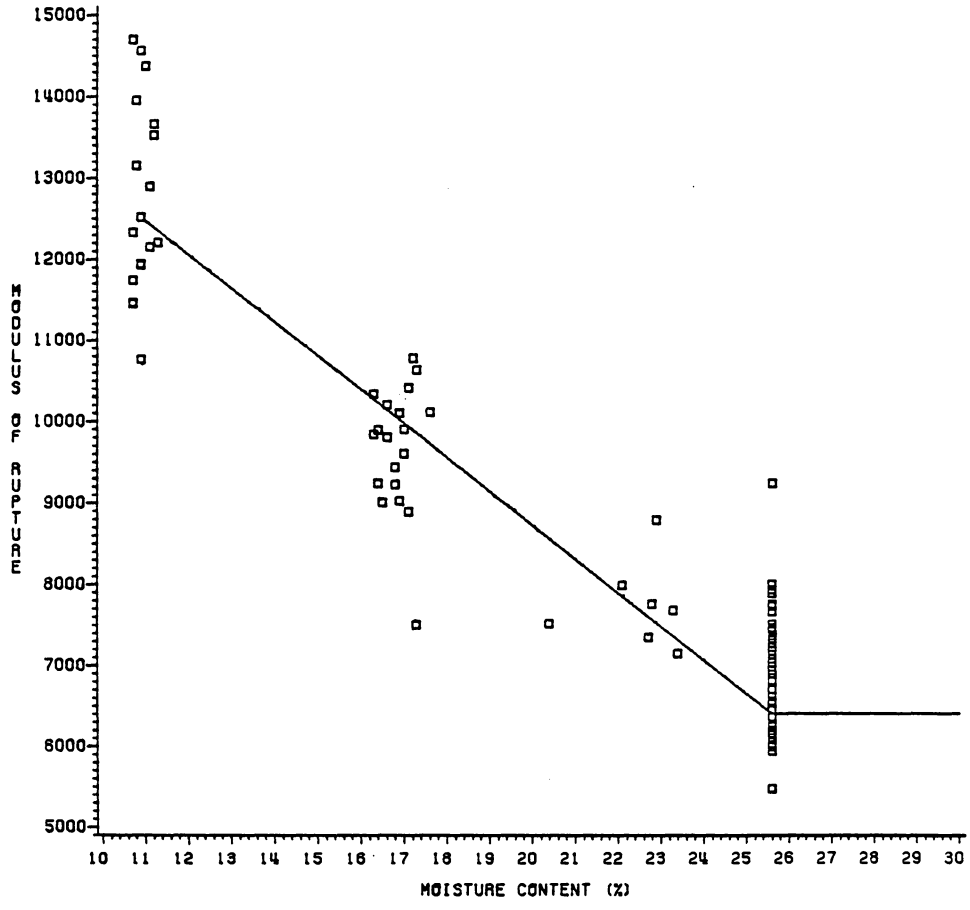

Figure 74: MOR data for equilibrated yellow-poplar beams, overlaid by model.

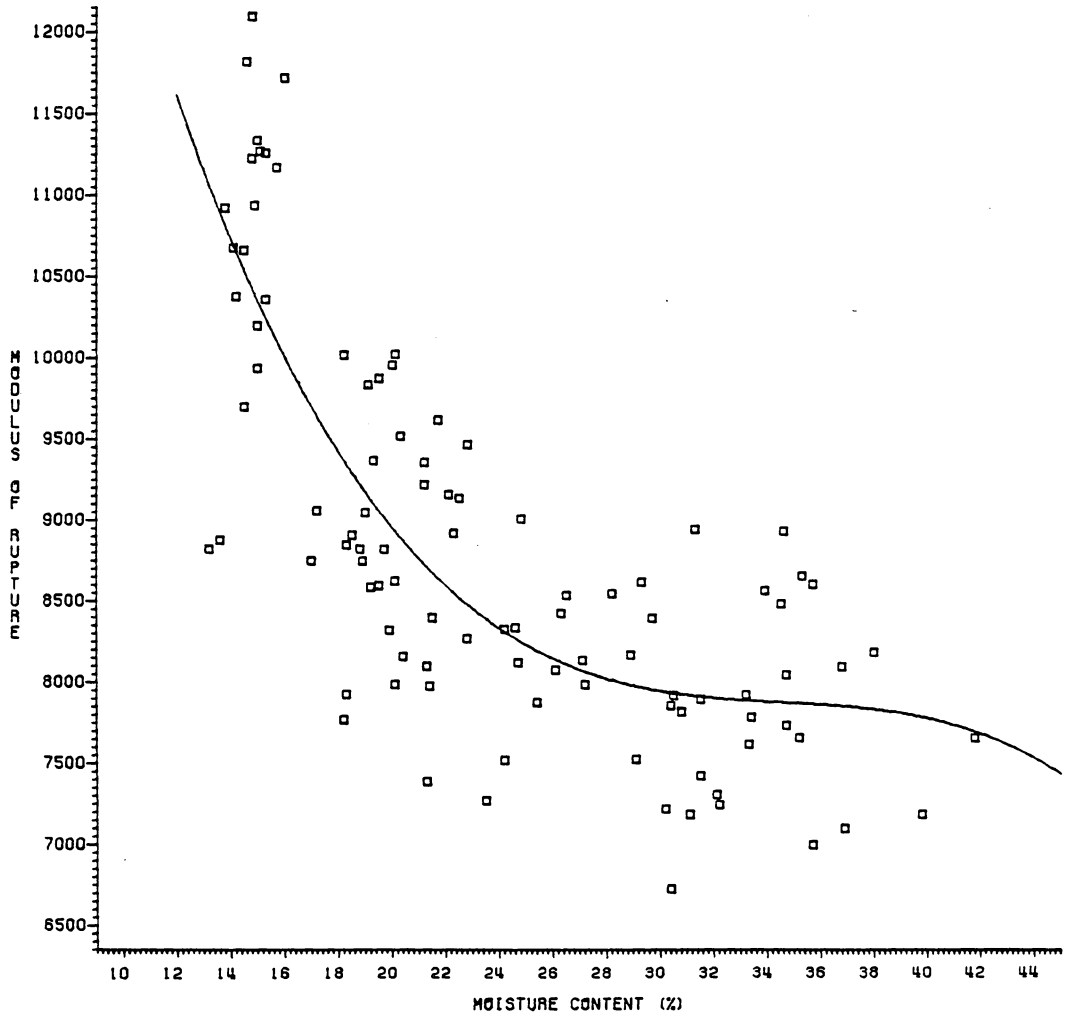

Figure 75: MOR data for non-equilibrated yellow-poplar beams, overlaid by model.

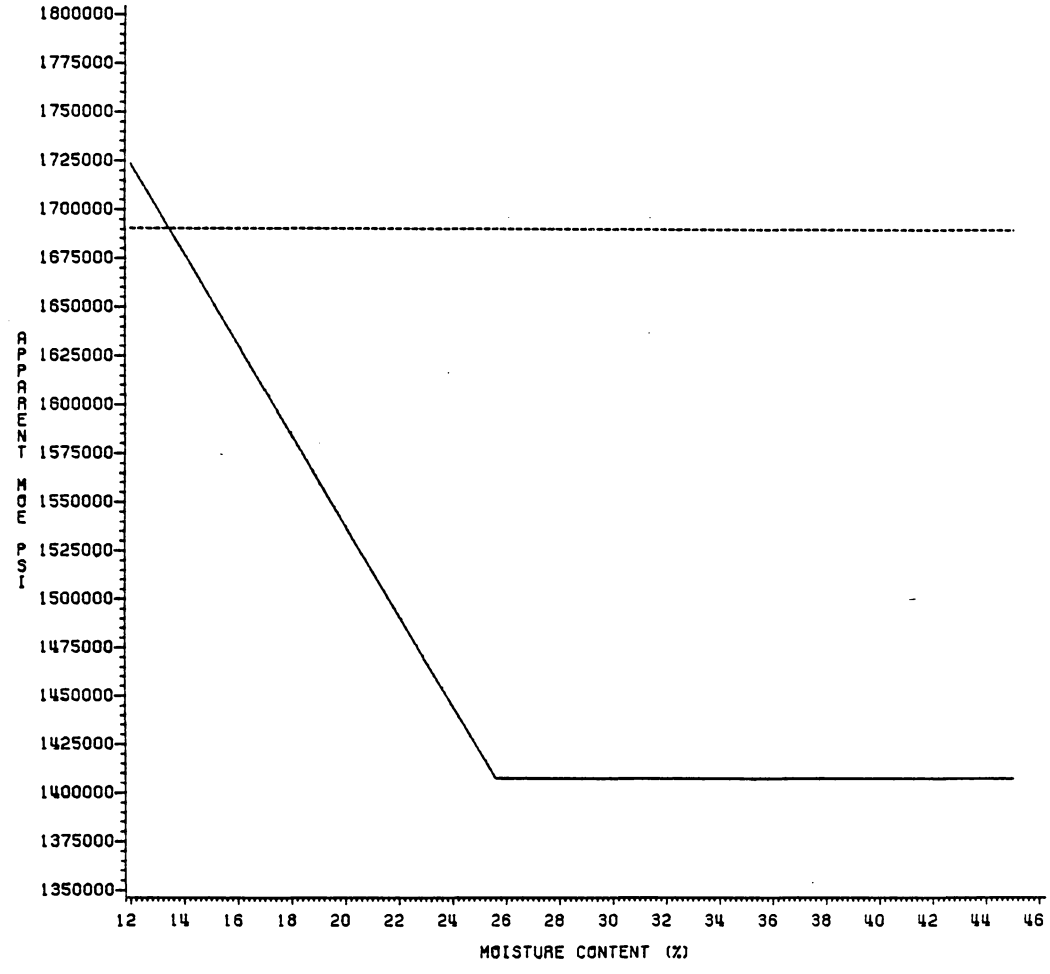

Figure 76: Overlays of MOE models for equilibrated and non-equilibrated yellow-poplar beams. Solid line=model for equilibrated data, dashed line=model for non-equilibrated data.

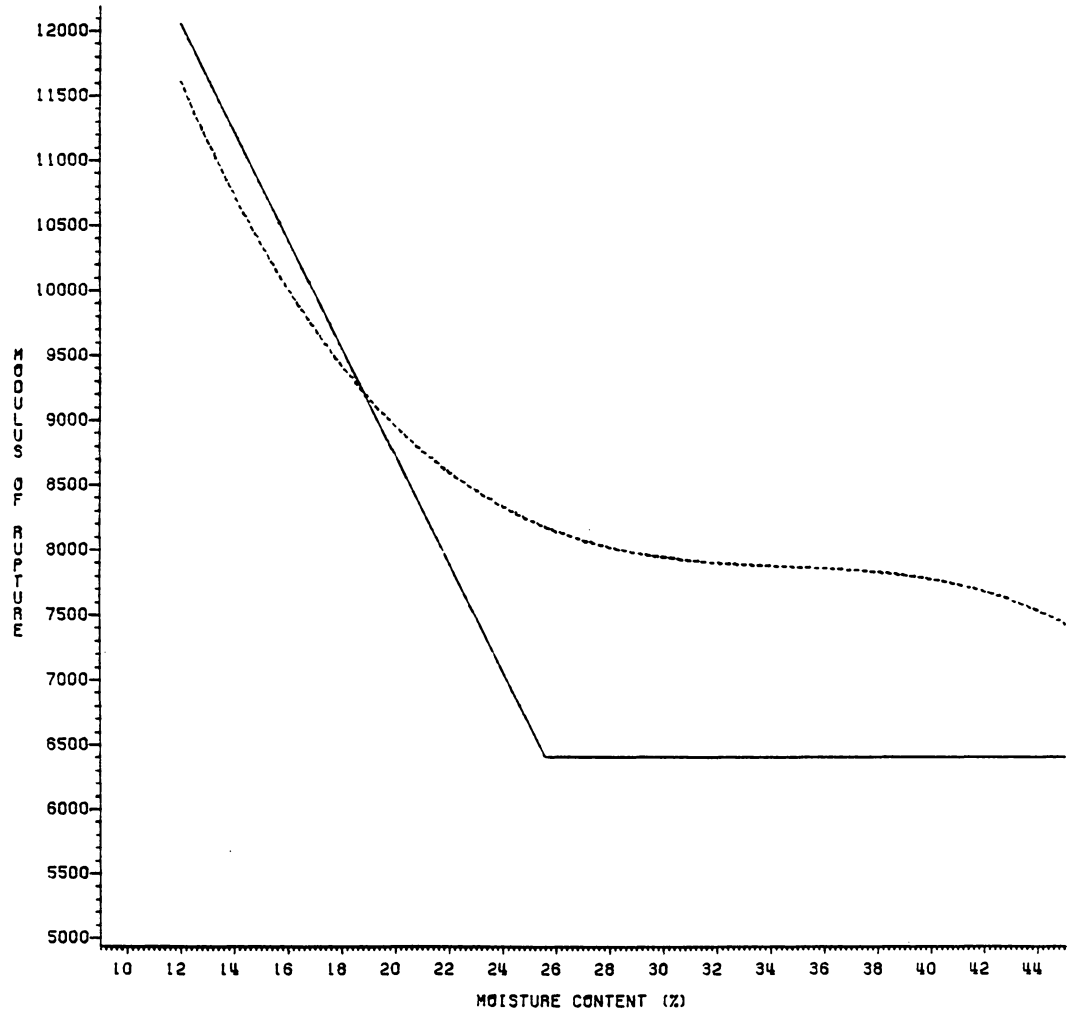

Figure 77: Overlays of MOR models for equilibrated and non-equilibrated yellow-poplar beams. Solid line=model for equilibrated data, dashed line=model for non-equilibrated data.

consistent with the expected trend described in an earlier chapter. This does not necessarily mean that the model is incorrect; there may be complex interactions (perhaps species-specific) of tension, compression and shear moduli which are not yet understood. Another possibility is that the moisture distribution at relatively high moisture contents is asymmetrical and somewhat random in nature, causing unexpected results to be observed. This would tend to account for some of the variability in the data set as well. It is this variability which makes it difficult to determine whether the trend should be correctly be represented as a horizontal line or as a downward trend. Additional testing might help to clarify whether the hypothesized trend or the data model is more correct.

5.4.1 Data Variability

To objectively judge the variability in the beam data , coefficients of variation (COV) were calculated for the equilibrated data (MOE and MOR) at each nominal moisture content, and also for the non-equilibrated data at 15% average moisture content. It was found that the COV for the equilibrated beam MOE values was approximately 10%; the COVs were slightly greater for the green specimens and slightly less for the data at 22% moisture content. The MOR COV

values were determined to be approximately 9.3%, with the same trend as was noted for the MOE data. The COVs for the non-equilibrated (15% average MC) MOE and MOR data were 9.7% and 9.2%, respectively. These COV values are approximately one-half of the values noted in Table 4-5 of the Wood Handbook (U. S. Forest Products Laboratory, 1974). According to this table, average COVs for MOE and MOR may be expected to be 22% and 16%, respectively, based on tests of approximately 50 species. A footnote to the table indicates that the magnitude of these COVs is assumed to be independent of moisture content, and the reasonableness of this assumption is supported by the data collected for this study.

With the exception of Stern's data for a single tree (filed at the Sardo Pallet Laboratory at Virginia Tech), specific small clear specimen data for yellow-poplar were not available for direct comparison. Stern's data for a single tree indicate coefficients of variation for MOE and MOR data at 9% MC of 6.8% and 6.3%, respectively. Data collected from more than one tree would be expected to exhibit greater variability.

The fact that the COVs from this study are less than those listed in the Wood Handbook may be attributed to two factors:

1. The random occurrence of dense and non-dense layers occurring in the extreme fiber region of bending specimens would greatly increase the data variability of species with definite structural "layers" such as yellow pine or oak. Yellow-poplar is a reasonably homogeneous species, and therefore would be expected to exhibit less variability in bending than many woods.
2. A limited number of logs was used in these experiments, although this is a lesser factor factor than (1) above. The variability of the data was probably increased by using several logs from several trees, although this was unavoidable.

5.4.2 The Relation Between MOE and MOR

As part of the examination of the variability of the beam data, both the equilibrated and the non-equilibrated modulus of rupture data were plotted against the corresponding modulus of elasticity data (Figures 78 and 79). Inspection of these figures showed that these have a greater interdependency than the non-equilibrated data, but it is also evident that the equilibrated data may consist of two groupings with different variabilities. As Figure 80 shows, the green and 22% MC data appear to comprise a distinct

group with a well-defined linear relationship. Drier data (from the nominal 12% and 18% moisture content categories) appear to have a wider variability. Regression analyses supported these observations. Linear models consisting of the independent variables specific gravity and modulus of elasticity provided the best empirical model for the modulus of rupture data for each group of equilibrated beam data (Figure 81), but the adjusted R, value for the green and 22% MC data was 0.680, twice that for the drier data (0.339).

The non-equilibrated data were analyzed as a single body of data. Specific gravity was a more important factor than modulus of elasticity in fitting the MOR data by an empirical expression, but together they only explained about 14% of the data variation. The model was statistically significant, but it is obviously a poor predictor of beam strength.

These analyses illustrate the perils involved in attempting to predict beam strengths from non-destructive tests. It is evident that fairly good correlation exists between MOR and MOE for green wood, but much less confidence should be placed in MOR-MOE correlations for air-dry material. Knots and any drying defects present in full-size beams are likely to increase the differences in variability between these two groups, and correlation of MOR with MOE is

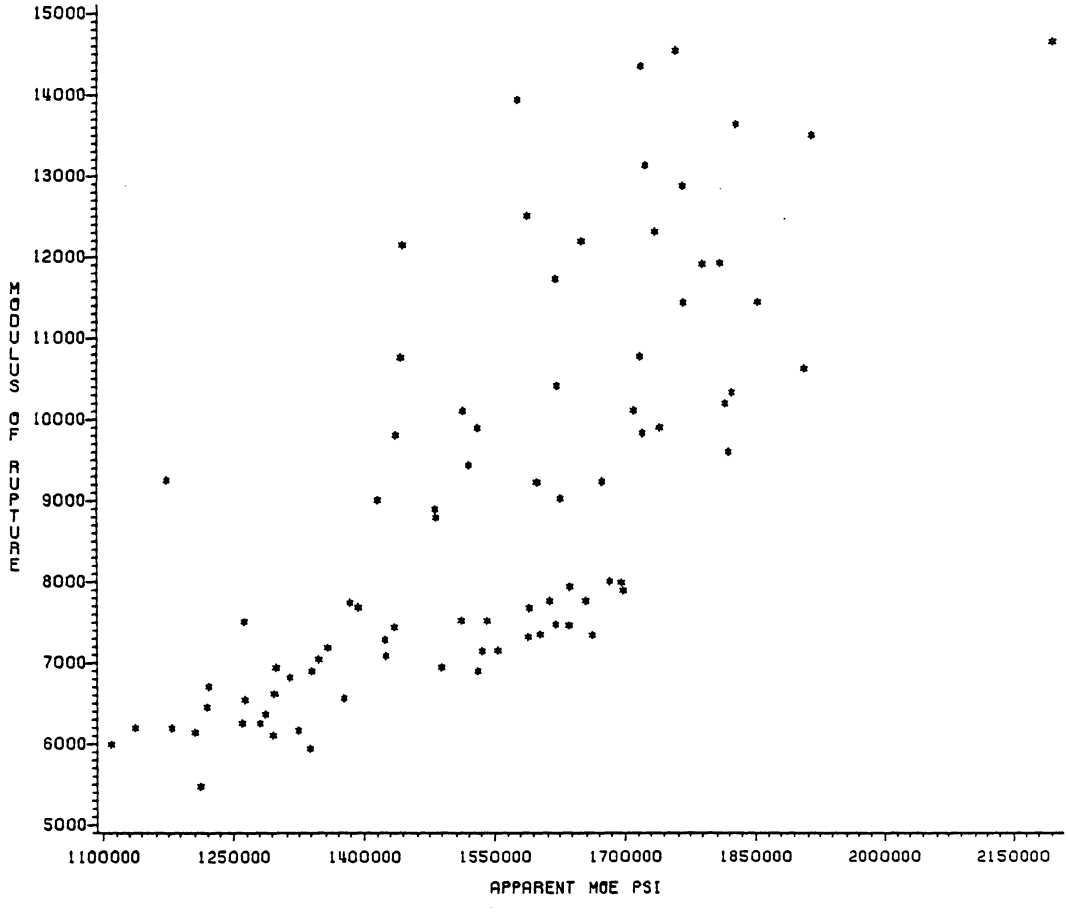

Figure 78: Equilibrated beam data: MOR versus MOE

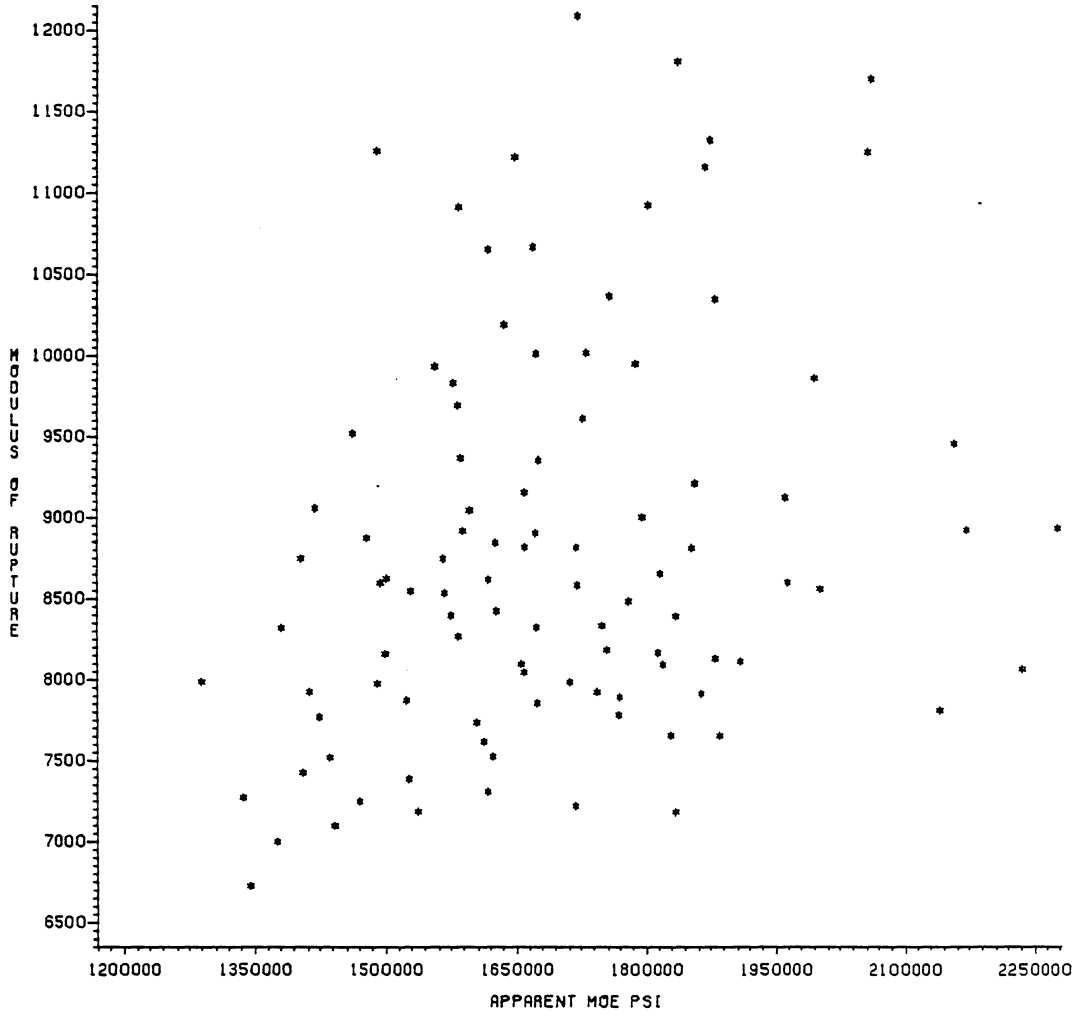

Figure 79: Non-equilibrated beam data: MOR versus MOE

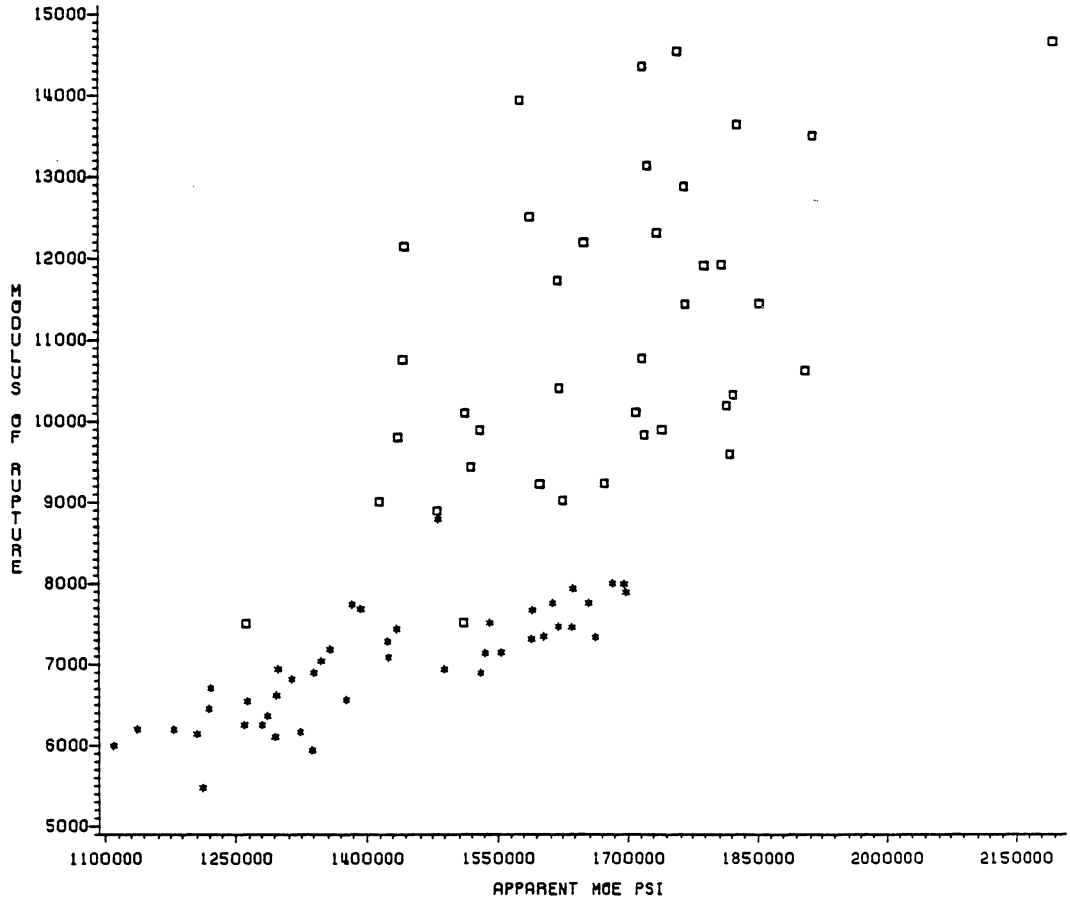

Figure 80: Equilibrated beam data: MOR versus MOE. Stars=22% MC and green data, squares=drier data.

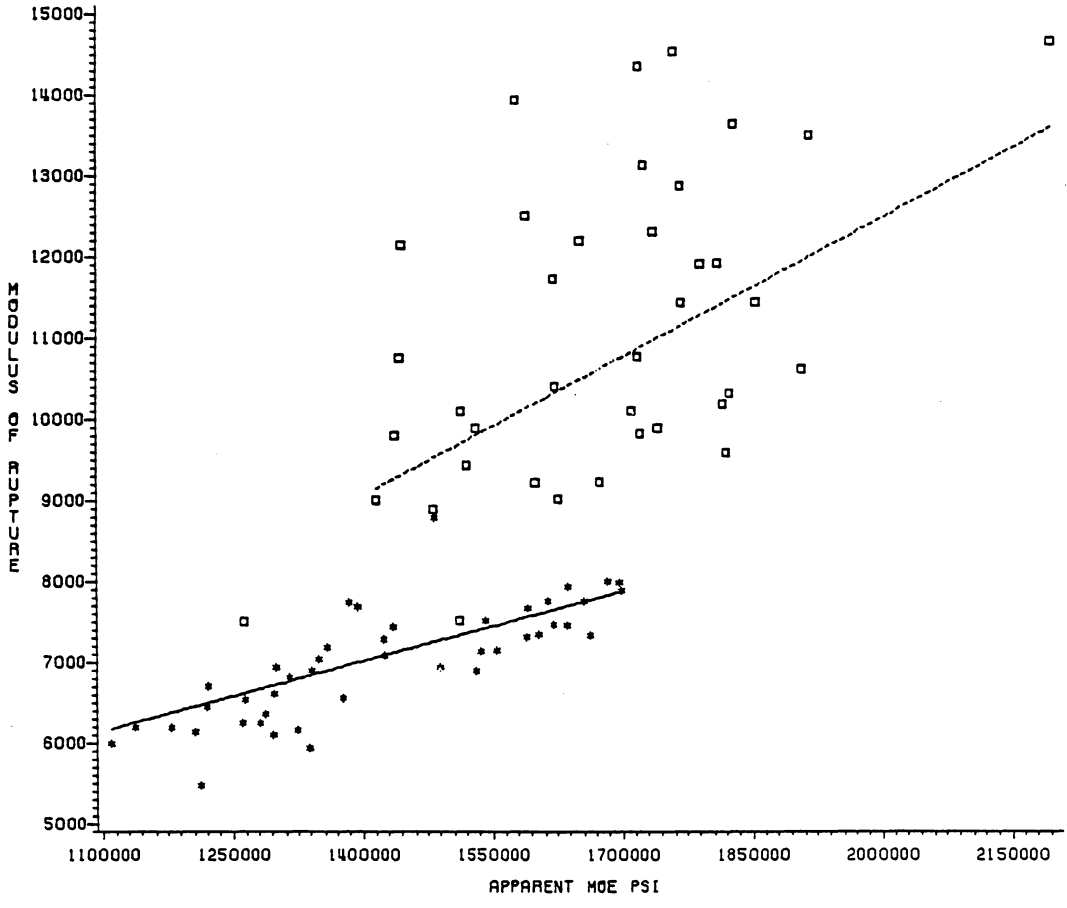

Figure 81: Equilibrated beam data: MOR versus MOE. Stars=22% MC and green data, squares=drier data.

probably insignificant in practical terms. The small clear non-equilibrated beam test data indicate that no confidence should be placed in MOR predictions when there is a chance that moisture gradients may be present. This is partly due to the increased variability of MOE and MOR observations for non-equilibrated beams as well as to the dissimilar effects of moisture content on MOE and MOR for these beams.

Chapter VI

FINITE-ELEMENT MODELING

The following sections briefly explain how isotropic models were used to verify the programs and to determine appropriate meshes for orthotropic models. Using these results, uniaxial wood specimens were modeled to failure, and this procedure is related also. Another section recounts how these intermediate steps improved the results of the beam modeling and compares the finite-element program predictions with the collected data. The final section details efforts to model nominal 2 x 6 beams.

6.1 ELASTIC MODELING OF ISOTROPIC UNIAXIAL SPECIMENS

The initial trial of the finite-element programs was the modeling of isotropic uniaxial specimens. The elastic constants for aluminum (E_i =10,000,000 psi, G_{ij}=4,000,000 psi, ν_{ij} =0.25) (Popov, 1976) were inserted into the appropriate subroutine to force their use in the program and a single-element cube was modeled. Both loads and displacements were imposed during these trials, and these were imposed along each of the three principal directions. Movements (degrees of freedom) (DF) were restricted for every node with the exception that the nodes on the surface

being "loaded" were free to move in the direction of the load or displacement imposed. These initial runs proved that the portions of the mathematical model which dealt with uniaxial stress had been correctly implemented in the programs, and also demonstrated that a very simple mesh could produce results for uniaxial models which were demonstrably correct as judged by the simple definition of Young's modulus (E=stress/strain). Expanding the mesh to several elements in each direction yielded the same results, regardless of whether the linear element program or the quadratic element program was used.

6.2 ELASTIC AND STEPWISE MODELING OF EQUILIBRATED UNIAXIAL ORTHOTROPIC SPECIMENS

Before modeling wooden beams, it was necessary to be certain that the models incorporated into the FEM programs for compression and tension stress-strain behavior worked correctly. The ability of the FEM programs to predict the correct elastic strain given a small stress was verified first in similar fashion to the checks performed on the isotropic models. The linear and quadratic element programs yielded identical results in these analyses, so only the simpler linear element program was needed to verify that the stepwise procedure implemented in these programs was functioning properly.

As part of the verification procedure, attempts were made to duplicate the uniaxial stress-strain models using the finite-element procedure. The first trials of this procedure (in compression) used fairly coarse steps (large strains), but the maximum stresses calculated were much greater than those specified by the stress-strain diagram models. The step size was reduced several times until results were obtained which were close to the values predicted by the compression stress-strain models. In the example plotted in Figure 82, an initial displacement was prescribed which was within the elastic region for the model; displacement increments of 0.00025 inches were subsequently imposed on the two-inch (with symmetry) uniaxial model. A comparison of the finite-element-predicted ultimate stress for green compression specimens to the ultimate stress calculated from the mathematical model showed that the error was slightly less than four percent. This amount of error is tolerable for uniaxial models, but at the same time it indicates quite clearly that very small vertical displacements are going to be needed to accurately model compression stresses during beam modeling. If the beam models use vertical displacement steps which are too large the result will be a stiffening of the beam model and the over-prediction of the modulus of rupture in each case.

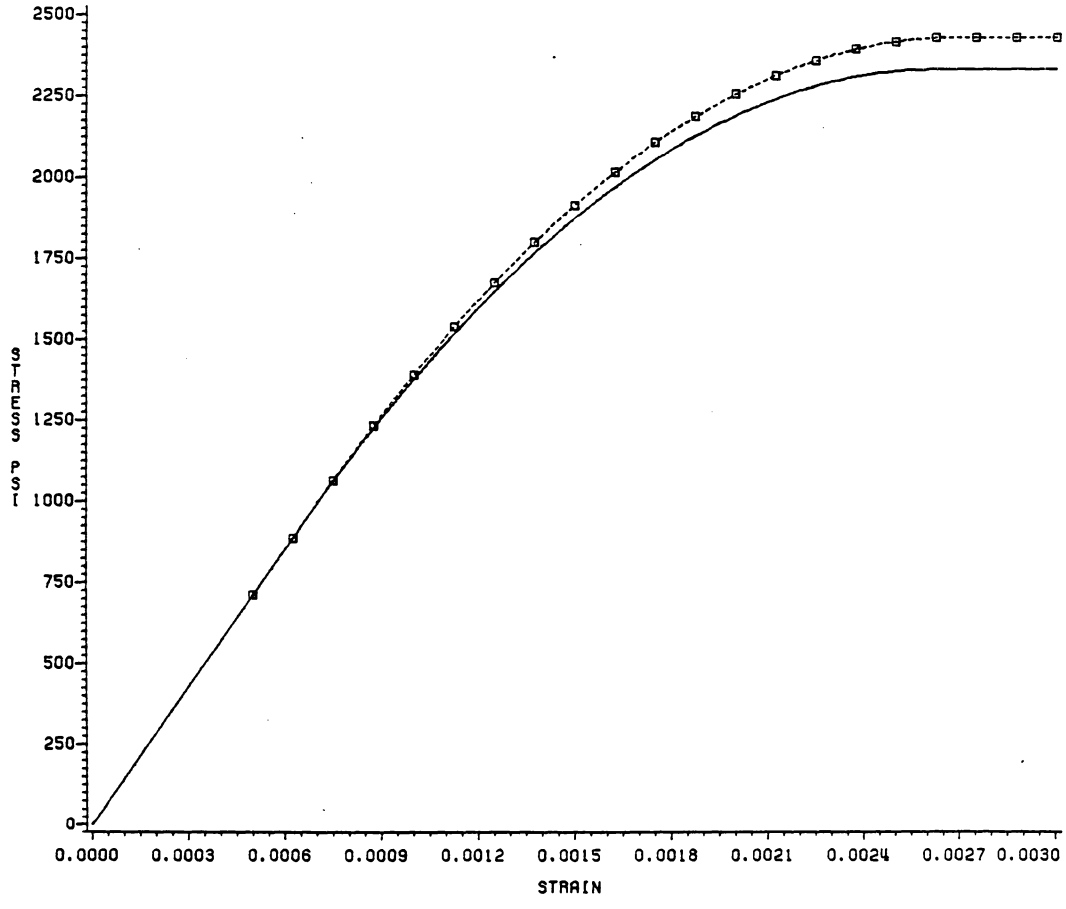

Figure 82: Stepwise FEM results for a model of green yellow-poplar in compression.

Tension modeling using the same step size as for compression was more successful (Figure 83). Due to the lesser slope, the green tension stress-strain diagram was more accurately modeled than the compression stress-strain diagram at the same moisture content. As with the compression model, better or worse results could have been achieved by using smaller or larger steps, respectively.

6.3 ELASTIC MODELING OF NON-EQUILIBRATED UNIAXIAL ORTHOTROPIC SPECIMENS

Up to this point in the finite-element studies, the degree of mesh refinement had been relatively unimportant. Neither the cross-sectional mesh nor the number of elements along the longitudinal axis significantly influenced the FEM results because of the homogeneity of the modeled material. However, gradient-containing uniaxial specimens needed to have the cross-sectional mesh defined in such a way as to reflect the changing material properties within the cross-section.

Compression specimens with four different average moisture contents (15%, 22%, 30%, and 35%) were modeled in combination with a 12% EMC condition to describe the moisture gradient. These moisture parameters were chosen to match the test conditions for gradient-containing beams. It was particularly hoped that the information obtained from

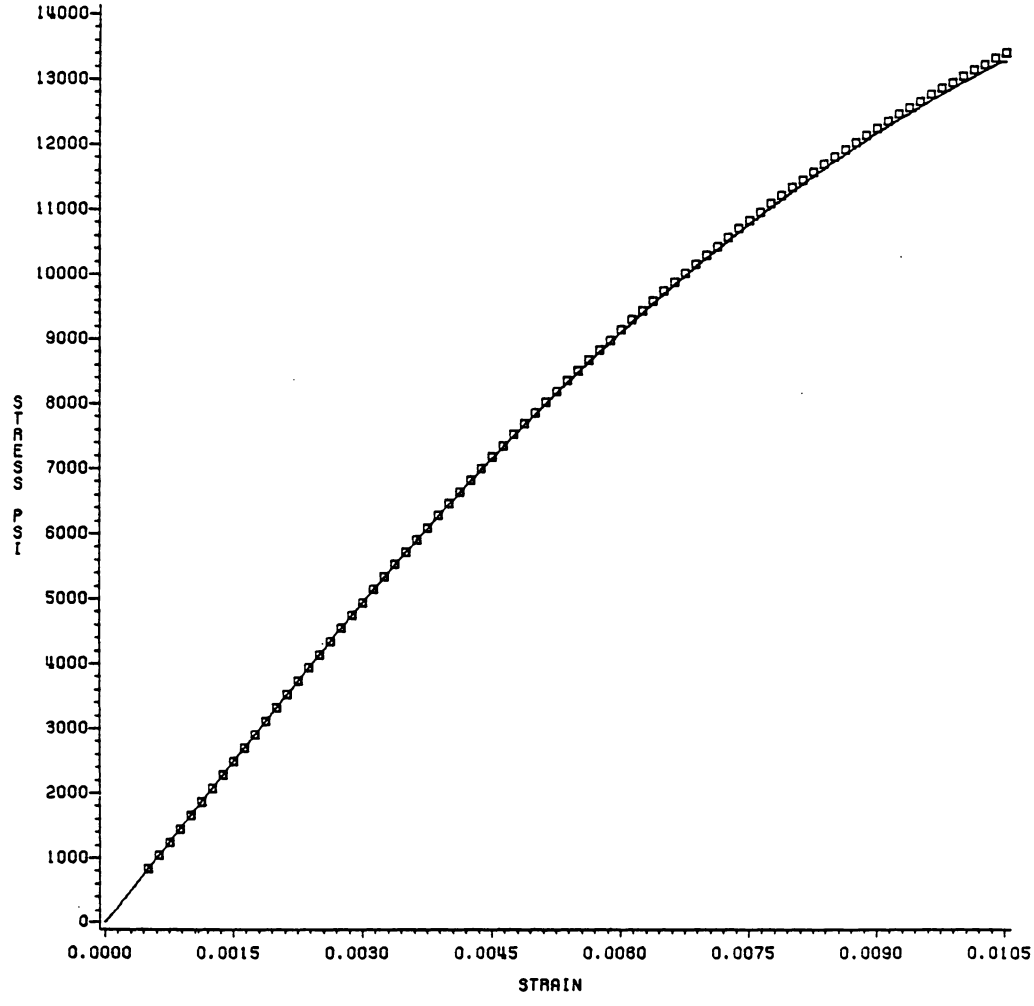

Figure 83: Stepwise FEM results for a model of green yellow-poplar in tension.

these uniaxial trials would improve the accuracy of the FEM representations of the beam data.

Six different uniform cross-section meshes (1 x 1, 2 x 2, ..., 6 x 6) were tried on 1/2 x 1/2 x 2 inch linear element models; these dimensions resulted from the restraint of 1 x 1 x 4 inch specimen models along planes of symmetry. (All subsequent references to a uniaxial cross-section refer to this reduced cross-section resulting from the use of symmetry). Imposition of a uniform load on the model cross-section would not have resulted in uniform longitudinal displacements at the cross-section surface due to the material nonhomogeneity, so uniform displacements were specified instead. These boundary conditions closely approximated the action of a laboratory test. The equivalent force resulting from the specified displacement was calculated using an option in the main program. Young's moduli were then obtained by translating the model predictions for cross-sectional forces and nodal displacements into stresses and strains. The Young's moduli in compression calculated from these analyses are depicted as a function of the mesh refinement in Figures 84, 85, 86, and 87. The influence of the cross-section mesh was of negligible importance to the 15% average moisture content model; only minor variations in the calculated moduli

resulted from using different meshes finer than 3 x 3. A 3 x 3 mesh also appeared to be adequate for the 22% average moisture content model, but the degree of mesh refinement was more important to the 30% and 35% average moisture content models, as was expected due to the steep slope of the modeled gradient. Increasing the number of elements on the cross-section tended to increase the calculated Young's moduli due to the better modeling of the drier, stiffer material at the periphery of the model domain. These models required minimum cross-sectional meshes of 5 x 5 and 6 x 6 elements respectively.

In the interest of possibly reducing the computation time and storage requirements for the 30% and 35% average moisture content models, two alternative cross-section meshes were tried using a smaller number of unequal-size elements. Each of these meshes emphasized the drier outer edges of the model domain; one mesh used was 3 x 3 elements and the second mesh used was 4 x 4 elements over the cross-section (Figures 88 and 89). The trial computer runs demonstrated that these non-uniform meshes gave similar results, and the Young's modulus estimates were close to those obtained through the use of the uniform 6 x 6 mesh (Figures 86 and 87). These modified meshes were then tried on the 15% and the 22% non-equilibrated models, but the

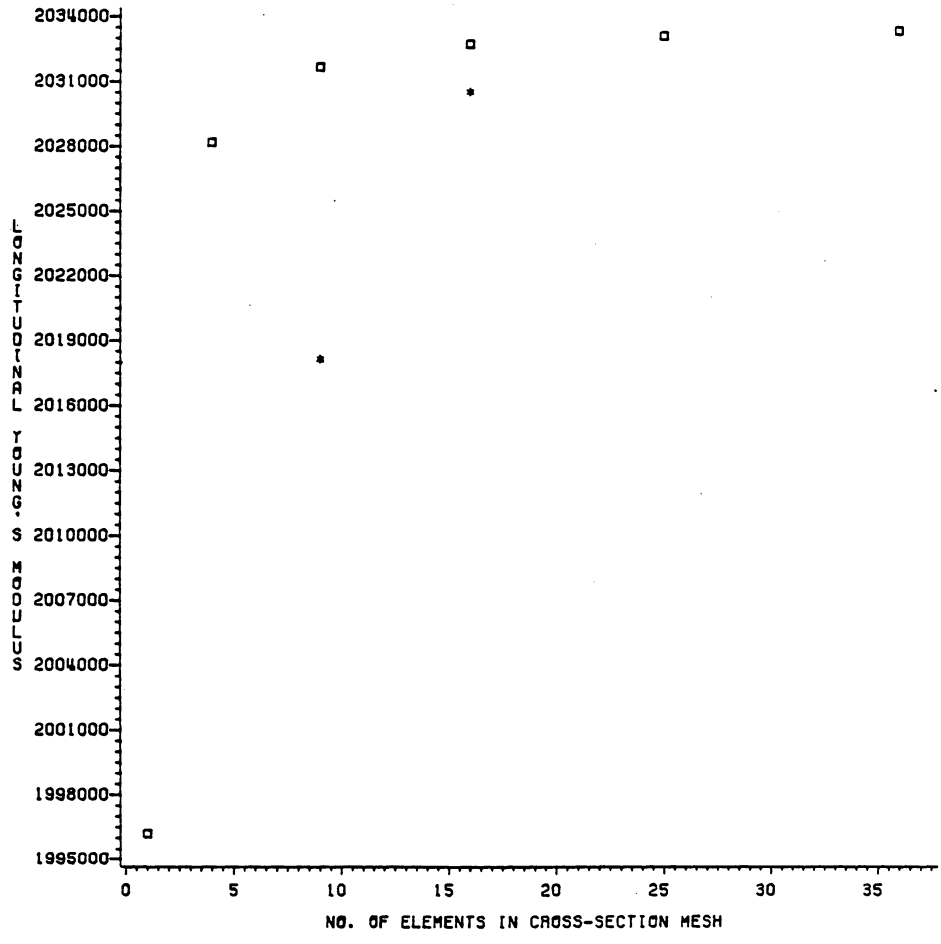

Figure 84: Compression model: convergence for 15% average MC, 12% EMC. Squares=uniform meshes, stars=non-uniform meshes.

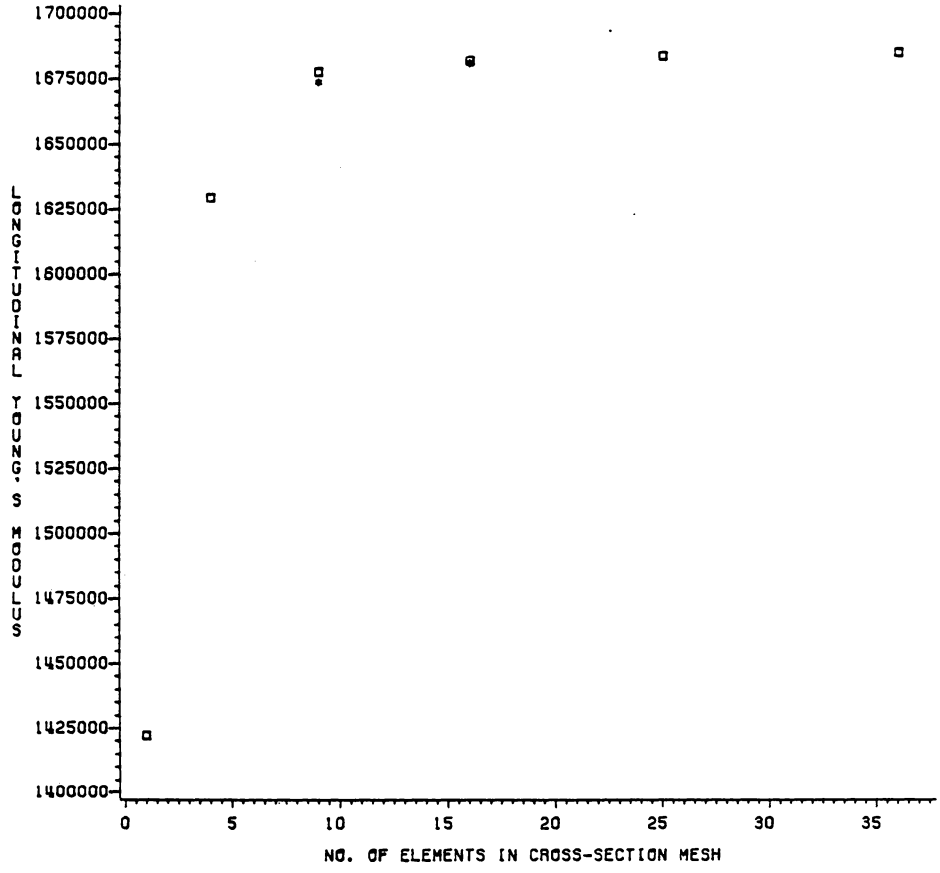

Figure 85: Compression model: convergence for 22% average MC, 12% EMC. Squares=uniform meshes, stars=non-uniform meshes.

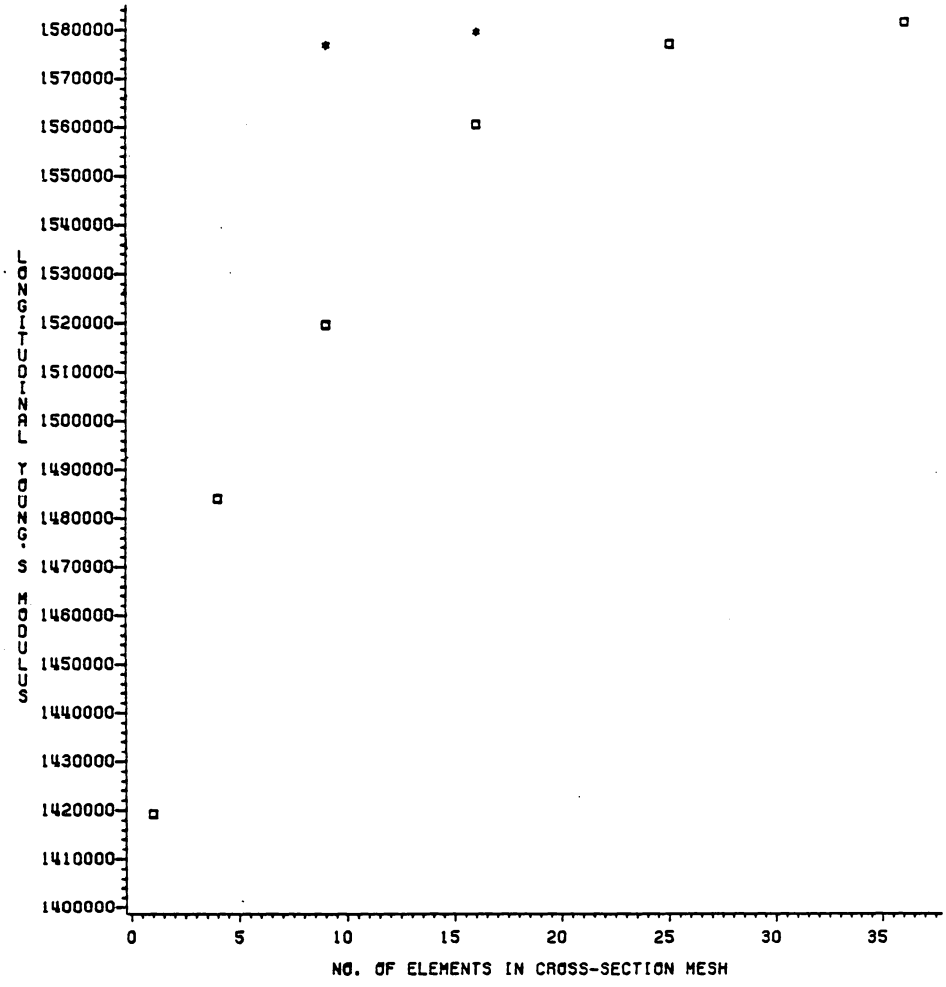

Figure 86: Compression model: convergence for 30% average MC, 12% EMC. Squares=uniform meshes, stars=non-uniform meshes.

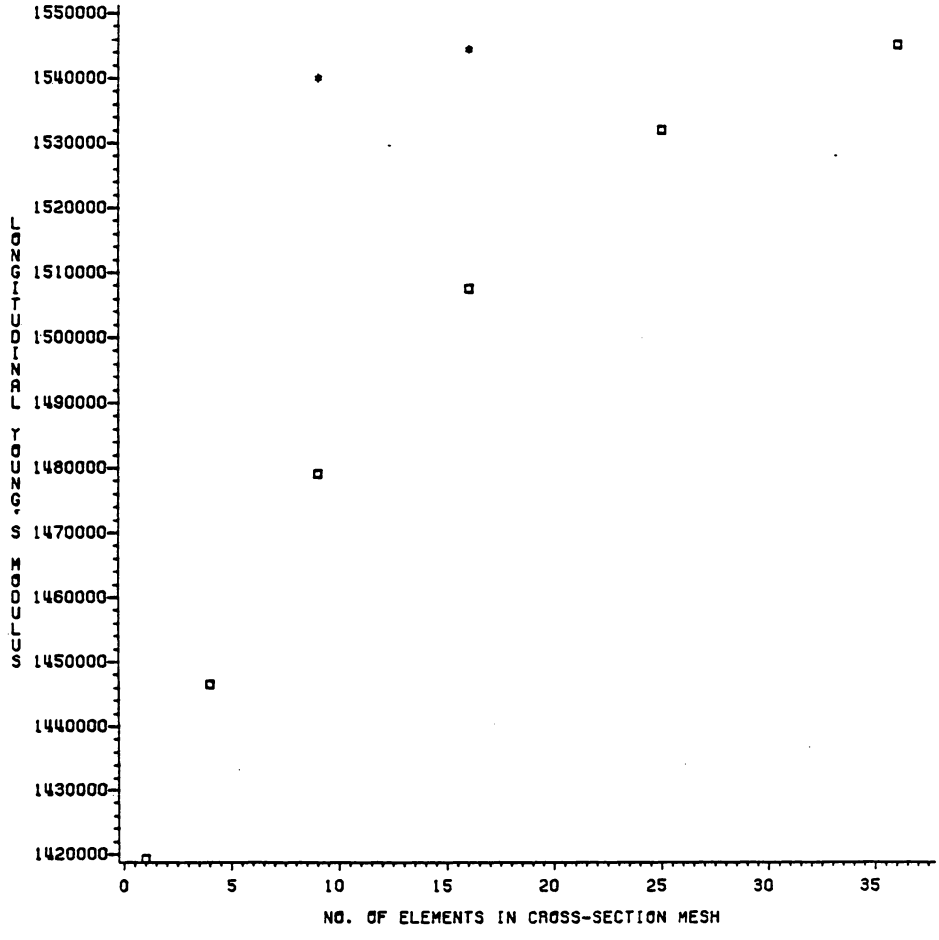

Figure 87: Compression model: convergence for 35% average MC, 12% EMC. Squares=uniform meshes, stars=non-uniform meshes.

uniform meshes performed as well or better for the same number of elements in the cross-section (Figures 84 and 85). The uniform 4 x 4 mesh was used for the 15% and 22% average moisture content models; the 4 x 4 mesh of unequal-size elements was used for the compression models at 30% and 35% average moisture content. As seen in Figure 90, the predicted longitudinal Young's modulus in compression for a non-equilibrated model is only slightly less than that of equilibrated specimens at 15% average moisture content; the non-equilibrated models, however, are considerably stiffer than their equilibrated counterparts at higher moisture contents.

The variation of the longitudinal Young's modulus in tension with moisture content, as noted previously, is considerably less than that for the compression modulus. Therefore, the cross-sectional meshes used for the compression models were judged to be more than adequate for tension modeling, and the identical meshes were used for tension modeling of non-equilibrated specimens. The average moisture contents and EMC conditions used for these tension models were the same as those used in the corresponding compression models. The model for the equilibrated Young's modulus in tension is nearly identical to the FEM predictions of the Young's moduli for non-equilibrated data

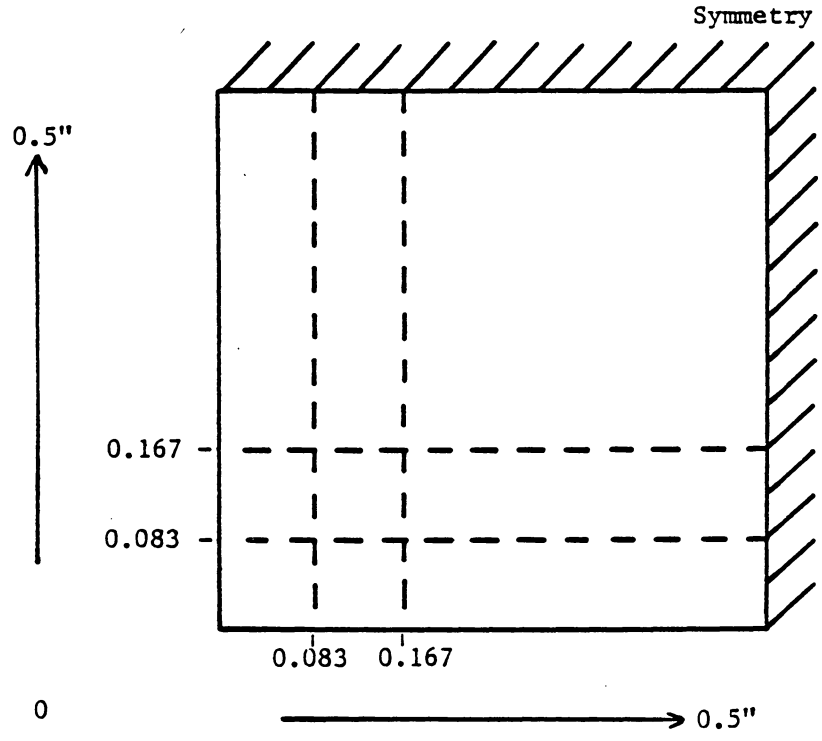

Figure 88: Non-uniform 3 x 3 cross-sectional mesh.

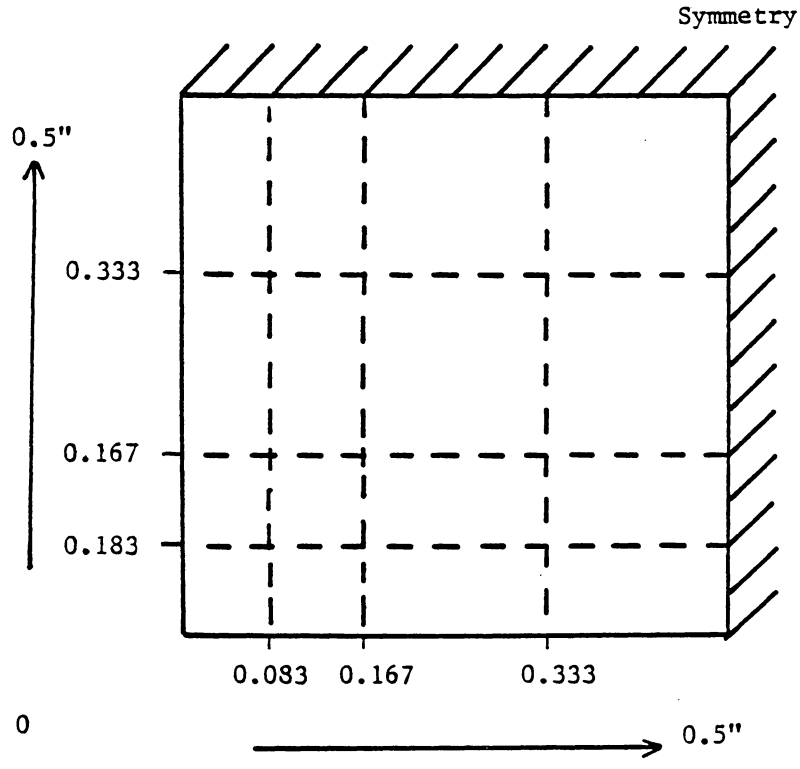

Figure 89: Non-uniform 4 x 4 cross-sectional mesh.

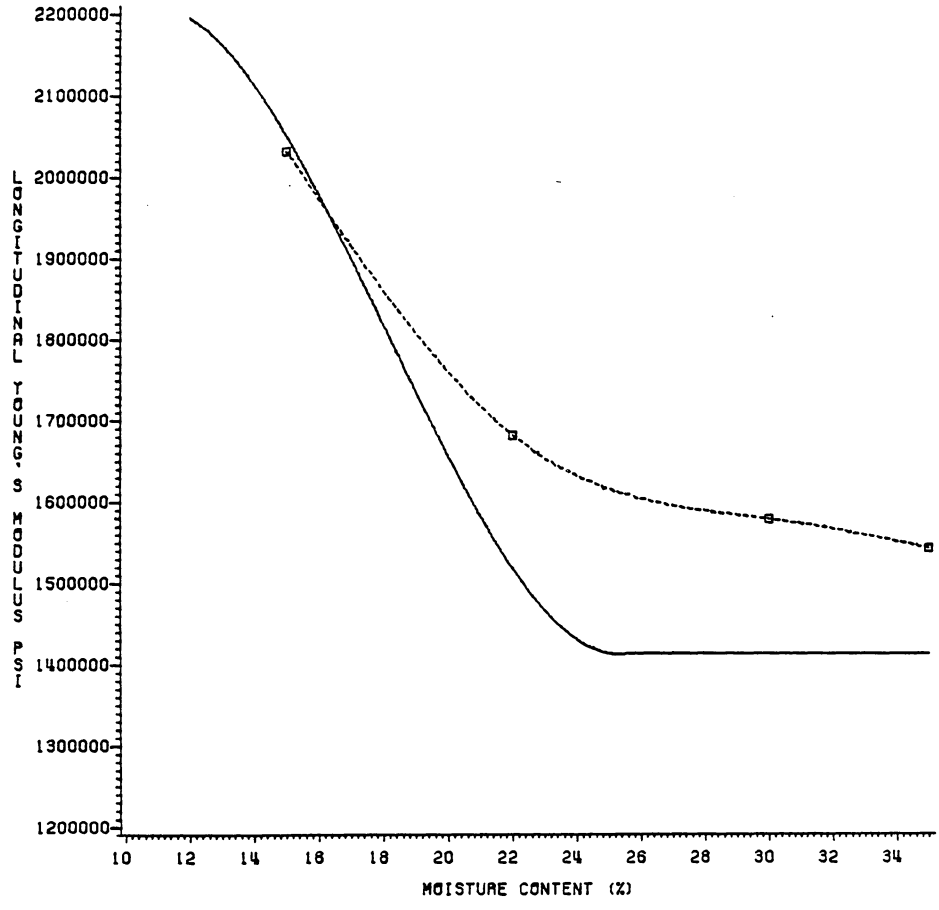

Figure 90: FEM estimates of Young's modulus for gradient specimens in compression overlaid on model for equilibrated data : 12% EMC. Solid line = model, squares = FEM predictions.

at 15% and 22% average moisture content. The finite-element model also predicts that the Young's moduli for non-equilibrated specimens will be only slightly greater than that of equilibrated specimens at higher moisture contents, but the difference does not appear to be large enough to have practical significance. The FEM predictions for the Young's moduli of non-equilibrated specimens are overlaid on a plot of the model for the equilibrated tension modulus in Figure 91.

6.4 ANALYSES OF NON-EQUILIBRATED UNIAXIAL SPECIMENS BEYOND THE ELASTIC LIMIT

Stepwise finite-element analyses were conducted in tension and compression at 15%, 22%, 30% and 35% average moisture content with a 12% EMC. The 15% and 22% average moisture content analyses were conducted using a uniform 4 x 4 element mesh on the (one-quarter) cross-section, but the 30% and 35% analyses used the unequal-size element mesh of 4 x 4 elements on the same cross-section. The step size was the same as that used for the modeling of equilibrated specimens (Figures 82 and 83), and Figures 92 and 93 show the comparisons of the maximum load predictions to the models developed for equilibrated data.

The predictions of maximum load for non-equilibrated compression models followed a similar trend to the

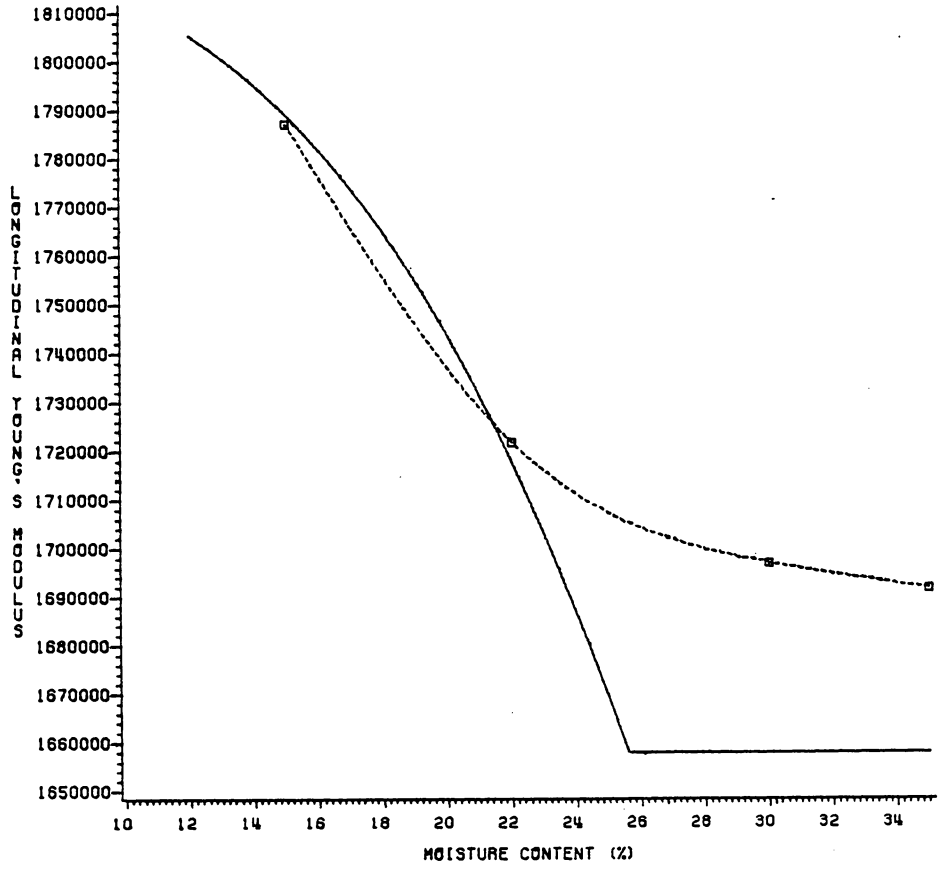

Figure 91: FEM estimates of Young's modulus for gradient specimens in tension overlaid on model for equilibrated data : 12% EMC. Solid line = model, squares = FEM predictions.

predictions of Young's modulus in compression, (Figure 92), but only small differences are predicted between equilibrated and non-equilibrated specimens up to about 22% average moisture content. Above 22% average moisture content the non-equilibrated models are predicted to be stronger than equilibrated specimens at the same moisture content, at least up to 35%. These predictions of crushing strength are in essential agreement with previous tests reported in the literature (Tiemann, 1906), although other researchers reported that differences were observable at lower average moisture contents. Additional finite-element runs using lower EMC values could probably duplicate any previous data.

Data from non-equilibrated tension specimens have not been published by other researchers, but the FEM program predicts that negligible strength differences would be observed between equilibrated and non-equilibrated tension specimens at average moisture contents below the intersection point (Figure 93).

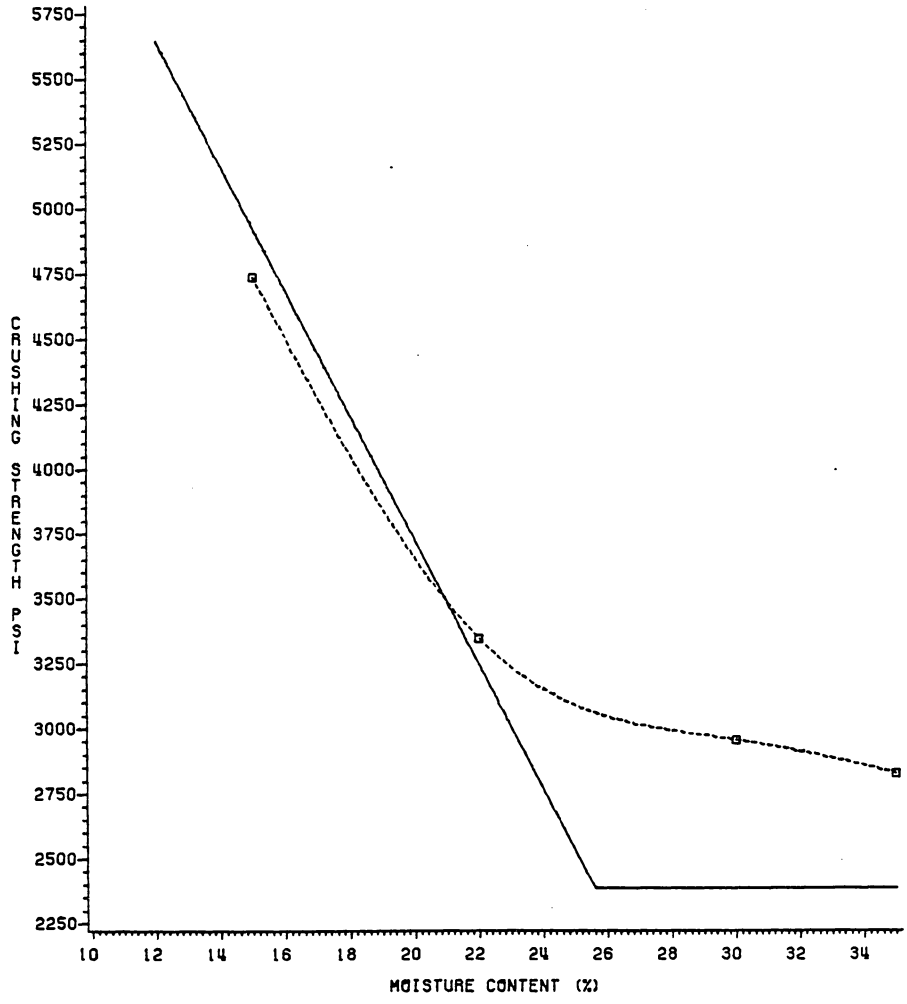

Figure 92: Predicted crushing strength for non-equilibrated compression specimens compared to a model for the collected data. Solid line = model for equilibrated data, squares = FEM predictions.

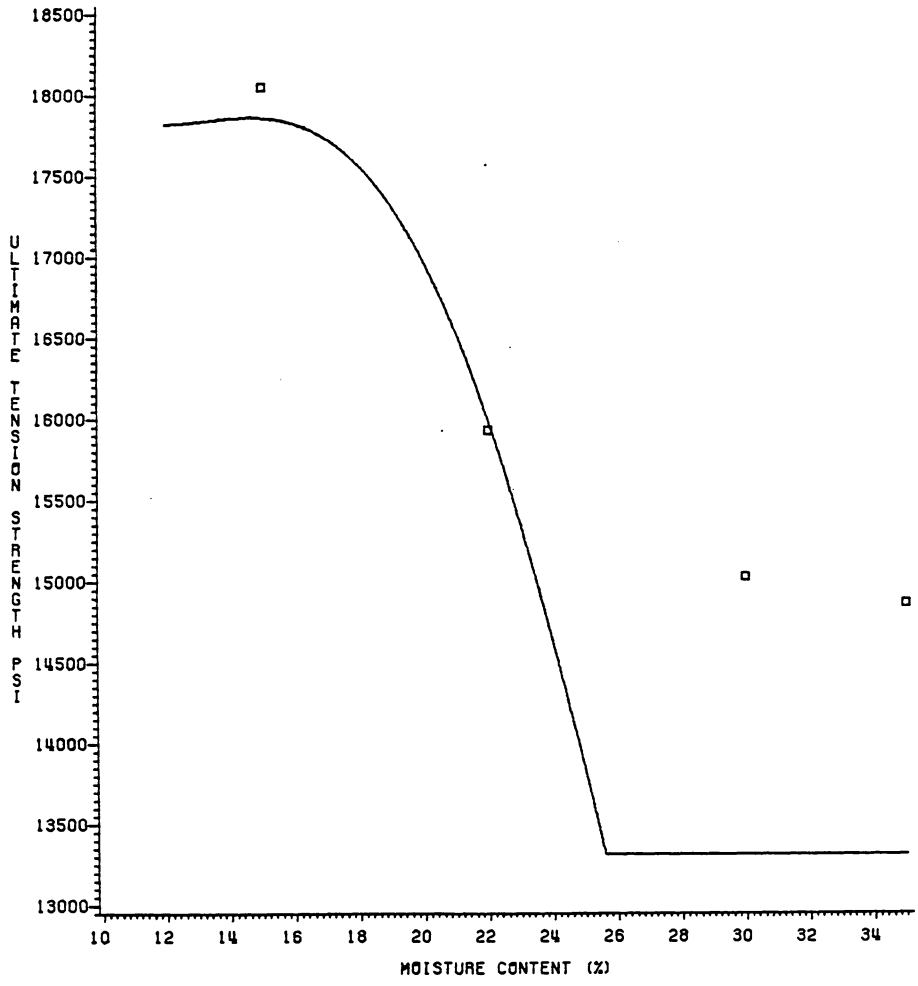

Figure 93: Predicted tensile strength for non-equilibrated tension models compared to a model for the (equilibrated) data. Solid line = model, squares = FEM predictions.

6.5 ELASTIC MODELING OF ISOTROPIC BEAMS

Beam modeling presented more challenges than simple uniaxial modeling. According to the literature cited in an earlier chapter, a finite-element program using 8-node linear elements was likely to be stiffer than a model using higher-order elements. A comparison of linear- and quadratic-element programs was desirable, and the optimum support conditions had to be determined also.

A center-loaded model of an aluminum beam was used to verify the program and to determine the effects of varying meshes, elements, and support conditions. The dimensions of the model beam were 2 x 2 x 28 inches and the elastic constants were the same as those used for aluminum previously. The following equation was used to calculate the total theoretical deflection (δ_{total}) for this beam (Bodig and Jayne, 1982)

$$\delta_{total} = \frac{Pl^3}{48EI} + \frac{0.3Pl}{AG} \qquad [6.1]$$

One restriction was placed on the mesh before the programs were run. It was arbitrarily decided that the cross-section mesh should be at least 4 elements by 4 elements (0.5 x 0.5 inches each) to simultaneously provide information about the possible meshes which could be used to

model gradient-containing orthotropic beams. (The fineness of these meshes was restrained only by the 5 megabyte storage available on the computer). Planes of symmetry were used to reduce the computer time and storage required by reducing the necessary portion of the beam to one-quarter of its original dimensions (one-half the length, one-half the width). The minimum cross-section mesh was correspondingly reduced to four elements through the depth by two elements across the width. (All subsequent references to beam cross-sections describe this reduced cross-section, and references to the number of elements along the longitudinal axis describe the half-length resulting from the use of symmetry). All movement was restrained perpendicular to each of these two planes of symmetry. This also resulted in the reduction of the imposed load to one-fourth of that required to model the whole beam.

Two load and support conditions were modeled using both the linear- and the quadratic-element programs (Figure 94). In the first, the load was placed across the top of the width of the beam at the point corresponding to the beam midpoint, and a pin support was located on the bottom of the model at one end. This is the load-support combination used by Maghsood (1970). Gerhardt (1982) used a similar load and support condition, but he modified this slightly by using a

roller support in place of the pin. A different load-support condition was advised by Dr. J. N. Reddy of the Engineering Science and Mechanics Department at Virginia Tech.[4] Both the load (or specified displacement) and the support were recommended to be placed at the neutral axis for this second load-support condition test.

Linear-element beam models were first used to compare the load-support conditions advocated by Maghsood and Reddy. Two cross-sectional meshes were used, 4 x 2 and 8 x 4 (height by width) elements (utilizing symmetry), while the number of elements in the longitudinal direction was varied from 4 to 32. As seen in Table 16, placing both the load and support according to Maghsood's usage results in a significantly stiffer model. Imposing both the load and supports at the neutral axis resulted in a more flexible model. Another set of trials was run with a roller support at the beam end instead of the pin connection. The results were nearly identical to those which resulted from the use of the pin support. The roller support condition was arbitrarily chosen for use in this study.

Comparison of the two cross-sectional meshes in Table 16 shows that cross-sectional mesh fineness was of negligible importance in determining the deflection of the isotropic

---

[4] Personal communication

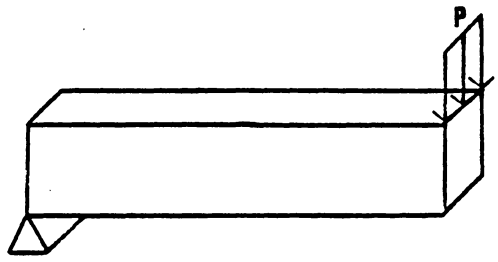

a) Load-support condition used by Maghsood (1970).

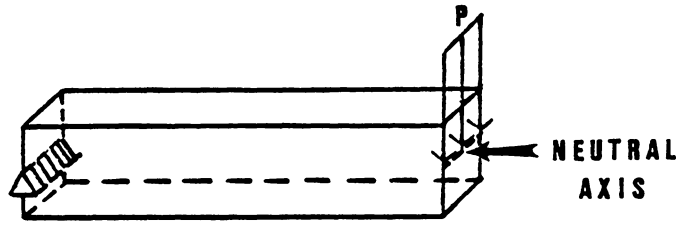

b) Load-support condition advised by Reddy.

Figure 94: Diagrams of the load-support conditions considered in this study.

TABLE 16

Comparison of load-support conditions for an isotropic center-loaded beam with different meshes: linear elements.

Mesh For Quarter-Sections (L x W x H)	Percent of Theoretical Deflection	
	Loads and Supports on Neutral Axis	Load on Top, Support on Bottom
4 x 4 x 2	44.8	26.0
8 x 4 x 2	76.3	38.0
16 x 4 x 2	92.5	44.1
32 x 4 x 2	97.7	46.4
4 x 8 x 4	44.9	26.1
8 x 8 x 4	76.6	38.2
16 x 8 x 4	93.0	44.8
32 x 8 x 4	Insufficient Storage Available	

beam. Of much greater importance is the number of elements along the beam axis; the greater the number of elements, the more closely the model predicts the theoretical deflection. When 32 linear elements were used along the longitudinal axis, the finite-element model predicted a deflection which is about 98 percent of the theoretical value.

The quadratic-element beam trials benefitted from the linear-element runs, and no comparisons were performed for the competing load-support conditions. It was also thought to be sufficient to use only the more coarse (4 x 2 element) cross-sectional mesh in these models. Several program runs showed that the deflections converged to the correct figure with far fewer elements along the beam axis. As seen in Table 17, only two quadratic elements along the beam axis resulted in the finite-element model predicting a deflection which is almost 97% of the theoretical value.

These initial beam model trials indicated that the quadratic-element program predicted accurate deflections with fewer elements than the linear element program required. Nonetheless, it became evident that the quadratic-element program would not be a practical choice for this study. The storage requirements for this program increase quickly as elements are added, and it cannot be ignored that a minimum number of elements is desirable both

TABLE 17

Convergence of model for isotropic center-loaded beam with mesh fineness along the beam axis: quadratic elements.

Mesh For Quarter-Sections (L x W x H)	Percent of Theoretical Deflections
2 x 4 x 2	96.9
4 x 4 x 2	99.7
8 x 4 x 2	100.0

to model the variation of moisture content on the cross-section and to model the variation of longitudinal strain along the beam axis. This latter requirement is especially important in analyses beyond the elastic limit, as average longitudinal strains in each element are used to define the element properties for the next step in a linear stepwise procedure. Although the linear element program incorporates a stiffer element, the accuracy is likely to be within acceptable limits and a more refined mesh is possible compared to the quadratic-element program. Therefore, the quadratic-element program was not used further and all subsequent analyses in this study were conducted using only the linear-element program.

The number of elements required to model a moisture gradient has not been discussed, and this topic will be considered in a following section. Due to storage constraints, some degree of trade-off between an optimum cross-section mesh and the number of elements along the beam axis is to be expected.

6.6 MODELING OF EQUILIBRATED ORTHOTROPIC BEAMS

6.6.1 Sensitivity Study

Although other researchers have previously determined that the longitudinal Young's modulus was the most important in finite-element modeling of wooden beams, these studies had been conducted on two-, rather than three-dimensional models. A study to determine the sensitivity of a three-dimensional model to the various elastic constants was expected to show similar results, but it was preferable to test this hypothesis since many of the elastic constants had to be estimated. Each elastic constant was in turn decreased by 25 percent and a green beam was modeled by a single linear elastic step so that the apparent modulus of elasticity could be calculated. The determination of synergistic effects due to the simultaneous variation of several elastic constants was not attempted.

Compared to a run of the original program with the elastic constants implemented as previously described, the only constant which significantly influenced the apparent MOE in bending was the longitudinal Young's modulus. The apparent MOE decreased by approximately 24 percent when the longitudinal Young's moduli were decreased by 25 percent. The shear moduli had the next greatest effect, but to a much lesser degree. A 25 percent reduction in the shear modulus

acting in the plane of the imposed load resulted in a predicted apparent MOE which was about 3 percent less than that of the original (unchanged) model. It was concluded that any inaccuracies in the estimation of the non-principal elastic constants would not significantly affect this study.

6.6.2 Moisture Content Selection and Mesh Definition

Before these analyses were conducted, the moisture contents and the mesh sizes had to be determined for the beam models. In view of the uncertainty of the relationship of the Young's modulus in compression between 6% and 12%, 12% moisture content seemed to be the lowest moisture content which could reasonably be modeled and compared to non-equilibrated beam models. A beam model at 12% moisture content could also be compared to the data collected for this study. Since beam data were also collected at 18%, 22% and green moisture content, these moisture conditions were also selected for modeling. Mesh size was limited by the computer storage available, given the necessity of maintaining about 32 linear elements along the beam axis to achieve approximately correct elastic modeling, as presented in the discussion of isotropic beam models. A uniform 6 x 3 (h x w) mesh on the (half) cross-section did not exceed the available computer storage, and the final mesh used for the equilibrated beam models was 32 x 6 x 3 (l x h x w).

6.6.3 Finite-Element Predictions of Apparent MOE for Equilibrated Beams

Following the definition of the finite-element mesh, the linear-element FEM program was used to predict the apparent moduli of elasticity at 12%, 18%, 22% and green moisture contents of beams supported on tangential faces. A comparison of the FEM program predictions to a polynomial model for the equilibrated beam MOE data is depicted in Figure 95. None of the FEM predicted values is more than 5% different from the model for the data. Based on these results, it was apparent that the finite-element program would be able to adequately model non-equilibrated beams if sufficient elements could be used on the cross-section to model the gradient. The accuracy of the FEM models of non-equilibrated beams is discussed in another section of this chapter.

6.6.4 Finite-Element Predictions of MOR for Equilibrated Beams

6.6.4.1 The Effect of Step Size on the Predicted MOR

When the linear elastic stepwise procedure was chosen for this study it was understood that the accuracy of any finite-element predictions of mechanical behavior beyond the elastic limit depended on the size of the load or displacement imposed in each step. As the plots of the

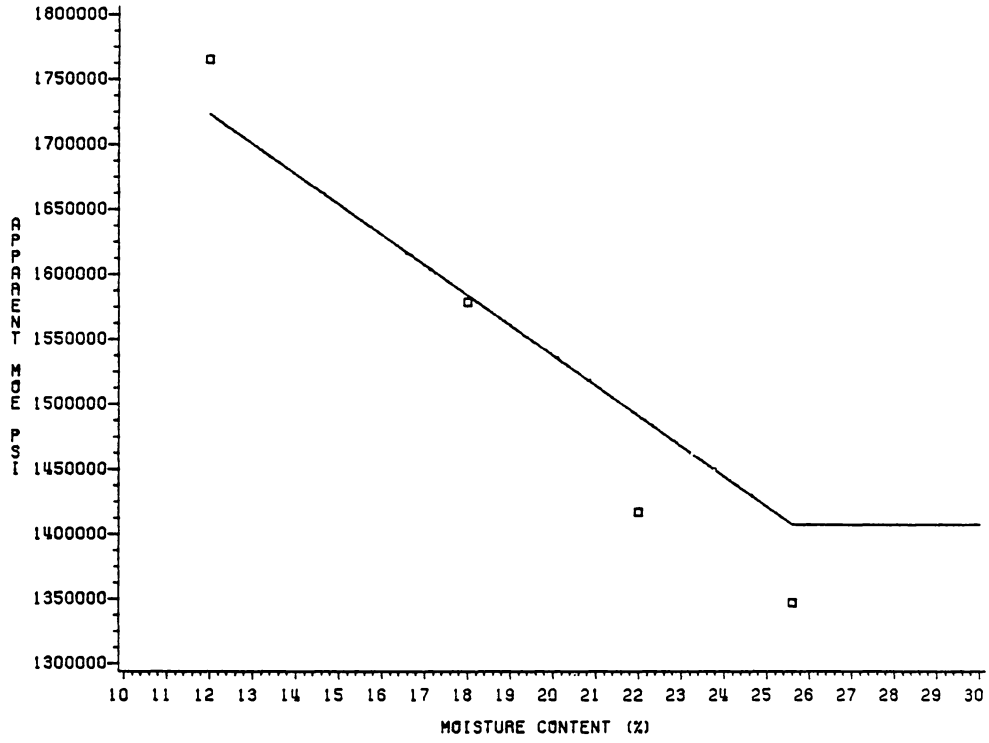

Figure 95: Predicted values for the apparent MOE at various moisture contents overlaid on a model for collected data. Solid line = model, squares = FEM predictions.

finite-element predictions of the tension and compression stress-strain curves indicate, the size of the step required to yield a chosen accuracy for a particular model cannot be determined a priori, as the degree of nonlinearity beyond the elastic limit has considerable influence. For the equilibrated beams modeled in this study, steps consisting of specified displacements were applied so that information regarding step size might be applied to non-equilibrated models; the reasons for preferring specified displacements to specified loads have been discussed previously.

A convergence study was performed to determine the optimum displacement to be imposed at each step in a beam model. A green yellow-poplar beam was modeled to failure using three displacement step sizes: 0.05, 0.025, and 0.01 inches. "Failure" was defined as a slope of the load-displacement curve less than 100 pounds per inch of vertical displacement. Together with a line representing the green MOR (from a regression analysis of the collected data), the three MOR values resulting from these analyses are plotted in Figure 96.

Although the accuracy of the finite-element procedure increases as the step size decreases, the MOR predicted using a step size of 0.01 inches is still about 14% too high compared to the regression model for the data and is just

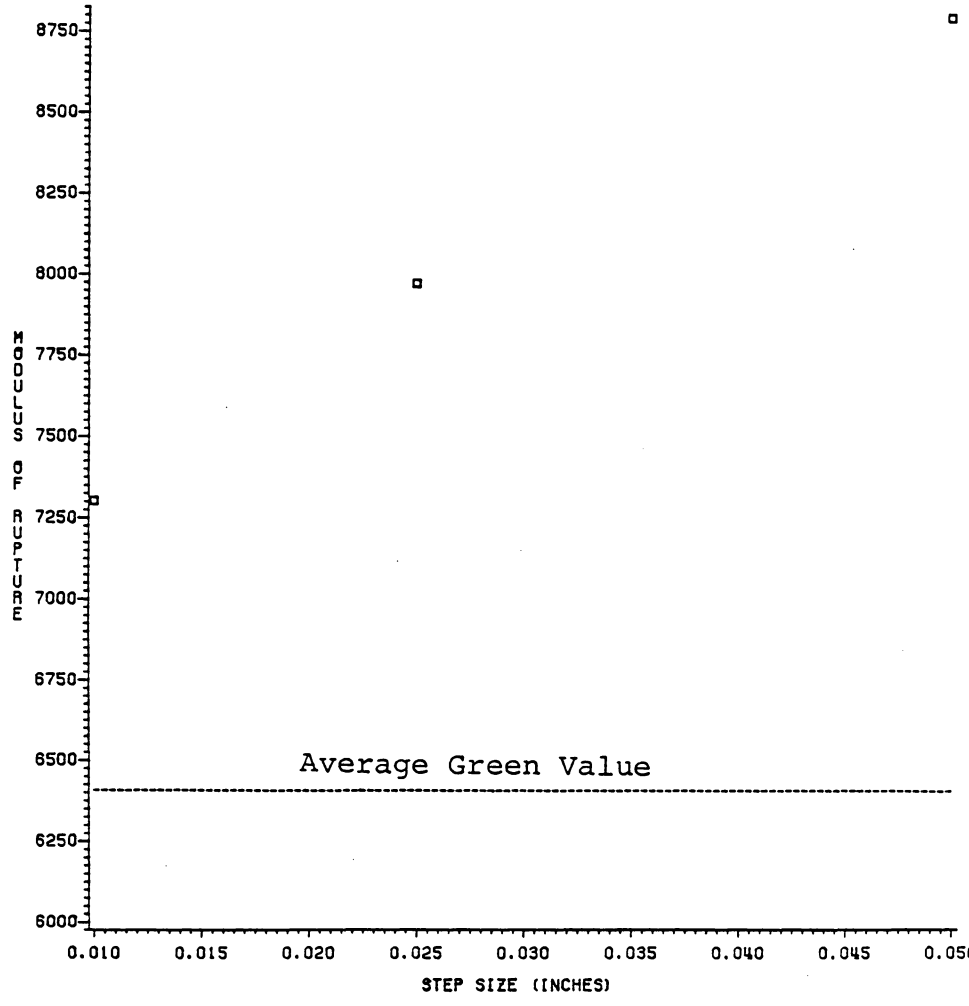

Figure 96: Comparison of the MOR for green yellow-poplar to the MOR values predicted by three FEM runs using various step sizes

barely within the range of the data collected for this study. The program required about 75 minutes of CPU time on the IBM 3084 computer when 0.01 inch steps were used, and it appeared as though reasonable results would be obtained only by halving the step size an additional one or two times with inversely proportional solution times. Although desirable, it was not practical to extend this convergence study to smaller steps.

Other boundary conditions were investigated in attempts to decrease the error in the FEM predictions. All combinations of load/displacement position (beam top or at the neutral axis) and pin/roller supports (at either the beam bottom or at the neutral axis) were attempted. No significant changes resulted in the estimated MOR values, so the original boundary conditions were retained. It was expected, therefore, that all subsequent MOR estimates would be somewhat high compared to the data collected for this study.

6.6.4.2 The Finite-Element Predictions of MOR for Equilibrated Beams

For lack of any acceptable alternative, the 0.01 inch step size was used in subsequent analyses at the other moisture contents modeled (12%, 18%, 22%). The results of the resulting MOR predictions, together with the best polynomial

regression model for the acquired beam data, are plotted in Figure 97. It is readily apparent that the accuracy of the MOR predictions varies depending on the moisture content modeled. The MOR predicted at 22% moisture content is only different from the regression model by about 4%, while it is about 12% too high at 18% MC and too high by nearly 21% at 12% moisture content. The behavior of the finite-element program at 22% moisture content is very different from that at other moisture contents. The most likely reason for this is that the shapes of the stress-stain curves predicted at this moisture content are incorrect; of the four moisture contents chosen for beam modeling, 22% is the only one at which uniaxial data were not collected and modeled. It appears probable that some parameter at this moisture content has been incorrectly specified in the uniaxial parameter regression analyses.

6.7 MODELING OF NON-EQUILIBRATED BEAMS

6.7.1 Moisture Content Selection and Mesh Definition

Since it was not practical to use the FEM program to model non-equilibrated beam behavior at every moisture content at which data were actually collected, representative average moisture contents had to be selected. Four average moisture contents (15%, 25%, 35% and 45%) were chosen for modeling

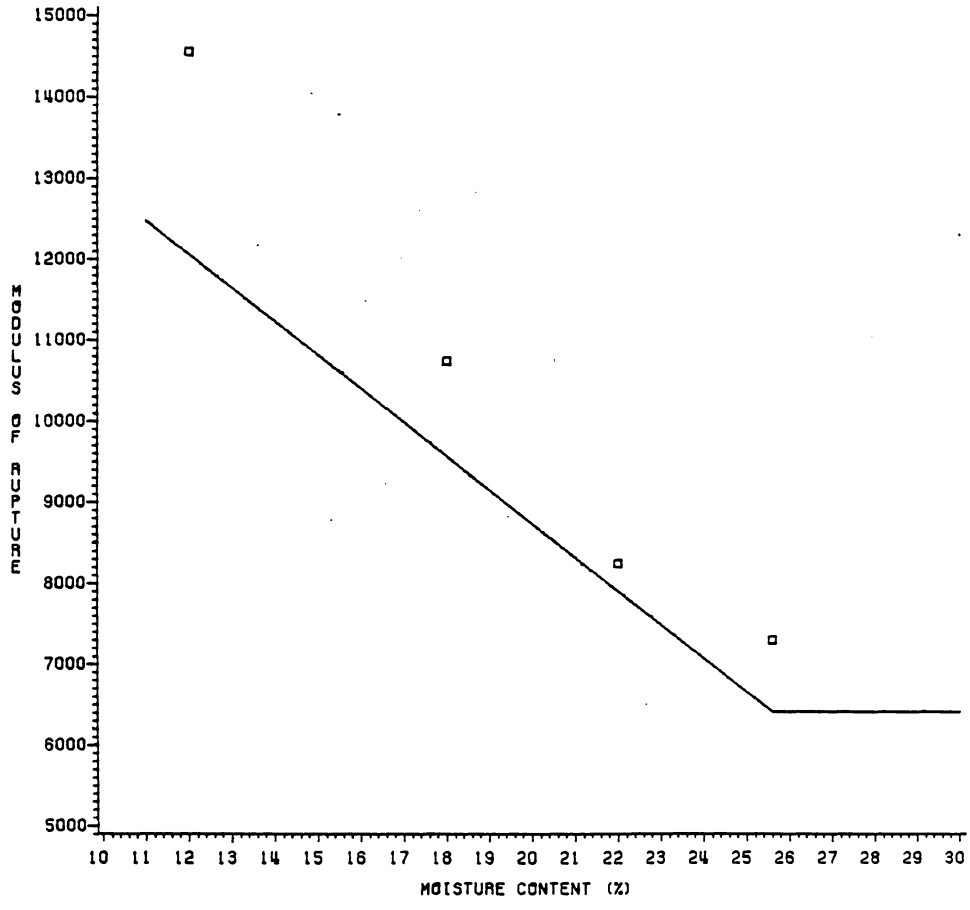

Figure 97: Comparison of equilibrated MOR model to the MOR values predicted by the finite-element program Solid line = model, squares = FEM predictions.

beams with a moisture gradient determined by a 12% EMC boundary condition.

The mesh ultimately chosen for these finite-element models was a compromise between those meshes necessary for accurate modeling of a beam in bending and accurate modeling of the two-dimensional moisture content gradient. It is first necessary to explain that the half-band width of the beam stiffness matrix was dependent entirely upon the number of elements on the cross-section (see Appendix). This implied that fewer elements might be available along the beam axis (resulting in poorer modeling of beam bending) if the representation of the moisture gradient was given priority. It was decided, therefore, to use 32 elements along the beam axis to achieve approximately 98% accurate deflection estimates and to use as many elements in the cross-section as practical given the computer storage constraints. Previous efforts had shown that a 6 x 3 (h x w) cross-sectional mesh (with symmetry) could be used without exceeding the storage capacity. Another argument for using this cross-section mesh was the result of previous comparisons of various meshes in modeling Young's modulus in compression. A cross-sectional 3 x 3 mesh of unequal-size elements was shown earlier to be close to a finer 6 x 6 mesh (on the one-quarter of the square compression model) in the

ability to predict the longitudinal Young's modulus of non-equilibrated specimens. Since the model of the 1 x 1 x 14 inch beam was twice the height and the same width as the modeled compression specimen once planes of symmetry were imposed, this 3 x 3 compression mesh could be used (as a 6 x 3 mesh (h x w)) for beam models as well (Figure 98).

Due to insufficient computer storage it was not possible to demonstrate the effectiveness of this cross-sectional mesh, but from the results of the sensitivity study in the previous section it might be inferred that models of non-equilibrated beams and compression specimens might have similar degrees of accuracy with comparable meshes. This is not likely to be strictly correct, of course, since the beam models will also be influenced by the tension properties. However, since compression properties are more sensitive to moisture content it is likely that they will influence the beam properties to a greater extent than the tension properties.

In summary of the points discussed above, it was decided to use a 32 x 6 x 3 (l x h x w) mesh to model non-equilibrated beams at average moisture contents of 15%, 25%, 35% and 45%. Due to storage limitations it was anticipated that the finite-element program would under-predict the apparent MOEs, but it was not possible to quantify the amount of error to be expected.

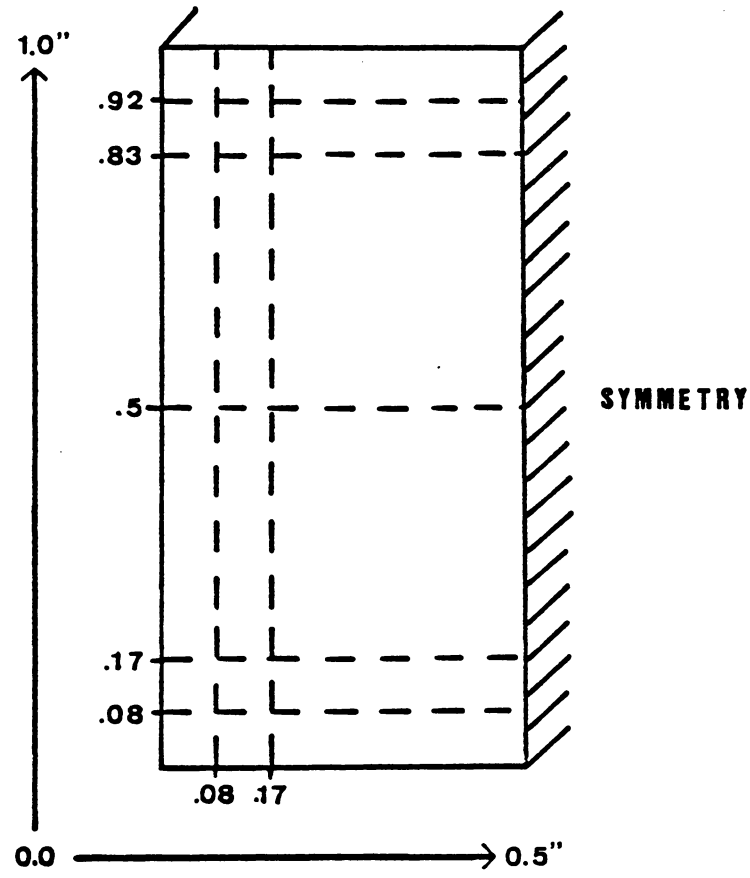

Figure 98: 6 x 3 mesh used for modeling non-equilibrated beams

6.7.2 The Apparent MOE Predictions for Non-equilibrated Beams

Predictions of apparent MOE for non-equilibrated beams at 15%, 25%, 35% and 45% average moisture content were obtained with the finite-element program using the mesh described in the previous section. These values are overlaid on a plot of the model for the collected data in Figure 99. Compared to this model, the finite-element program under-predicted the apparent MOE at 15% average moisture content by about 6%, and the differences between the data model and the FEM predictions were greater at higher average moisture contents. These differences ranged from about 10% at 25% average moisture content to approximately 12.5% at 45% average moisture content.

Two possible explanations can be advanced to account for the discrepancies between the data model and the finite-element predictions. The first hypothesis involves the possibility that the model chosen for the data is an inaccurate representation of the actual trend. The reasoning supporting this hypothesis has been discussed previously. If apparent MOE values actually decrease as average moisture content increases, then the data model error is more significant at higher moisture contents. Assuming that the data model is indeed in error, the increasing error of the FEM predictions can be accounted

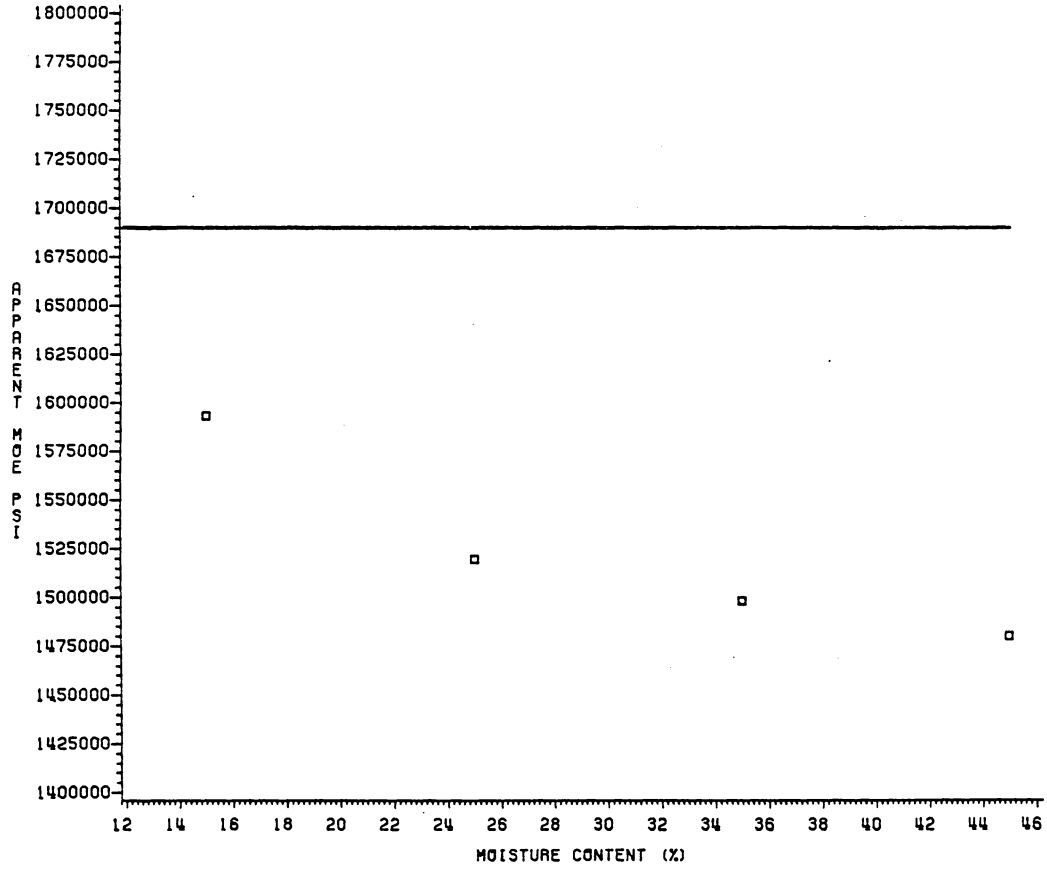

Figure 99: FEM predictions of MOE for non-equilibrated beam models compared to a model for non-equilibrated beam data. Solid line = model, squares = FEM predictions.

for. It would also be likely that the FEM model has predicted the correct trend of the data. This assumes, of course, that the moisture distribution at high average moisture contents does not have a random character. This possibility must not be discounted.

A second possible explanation for the discrepancies involves the inability of the program to accurately model the (uniform) moisture gradient. The mesh comparisons for uniaxial specimens demonstrated that a too-coarse mesh would under-predict the longitudinal modulus, and the magnitude of this effect is probably increased in bending. It is probable that the amount of under-prediction is greater as the average moisture content (and hence the slope of the moisture gradient contour) increases.

Probably both hypotheses have some validity in explaining the differences between the data model and the FEM predictions. If this is the case then the data model and the FEM predictions may be viewed as delimiters for the data trend.

In summary of the foregoing discussion, the finite-element model predicts that the apparent MOE in bending will decrease as the average moisture content increases, but there are reasons to suggest that this model may not be accurate. If the model is indeed ineffective in indicating

the data trend then some of the discrepancies between the FEM model and the data can be accounted for. Additional differences between the FEM predictions and the data probably result from inaccurate modeling of the moisture gradients, due either to relatively coarse cross-section meshes or to some random element in the actual moisture distribution.

6.7.3 The MOR Predictions for Non-equilibrated Beams

The modulus of rupture FEM predictions for non-equilibrated beams were obtained at the previously-determined average moisture contents using the 32 x 6 x 3 mesh and incremental displacement steps of 0.01 inches. Since the predictions of equilibrated beam MOR values had been up to 21% too high when this step size was used, similar results were expected with the non-equilibrated beam models. Figure 100 shows that these expectations were justified. The trend of the FEM predictions is similar to that for the data model, but the MOR values were over-estimated by approximately 20% to 27% depending on the moisture content. As with the FEM predictions of equilibrated beam MOR values, it would have been desirable to decrease this error through the use of a smaller step size, but this was not practical given the already considerable run time required by the program. Some

of the modeling error was also probably due to the cross-section mesh chosen, but this error was not quantifiable analytically.

6.8 SUMMARY AND EVALUATION OF THE FINITE-ELEMENT BEAM MODELS

The various equilibrated and non-equilibrated beam models used in this study demonstrated several things:

1. Apparent moduli of elasticity for equilibrated beams can be modeled within 5% of average data values over a range of moisture contents.
2. It is more difficult to achieve accuracy in predicting MOR for equilibrated beams. Convergence studies indicate that reasonably accurate MOR estimates are possible using the methodology employed in this study, but only at considerable expense. Reasonably accurate determinations of the MOR values for equilibrated beams resulted from using the step size chosen in this study, and the program predicted essentially correct trends.
3. The accuracy of the finite-element predictions of non-equilibrated beam MOE values is difficult to evaluate due to the uncertainty regarding the accuracy of the data model. The FEM predictions are consistent with the expected trend, but are lower

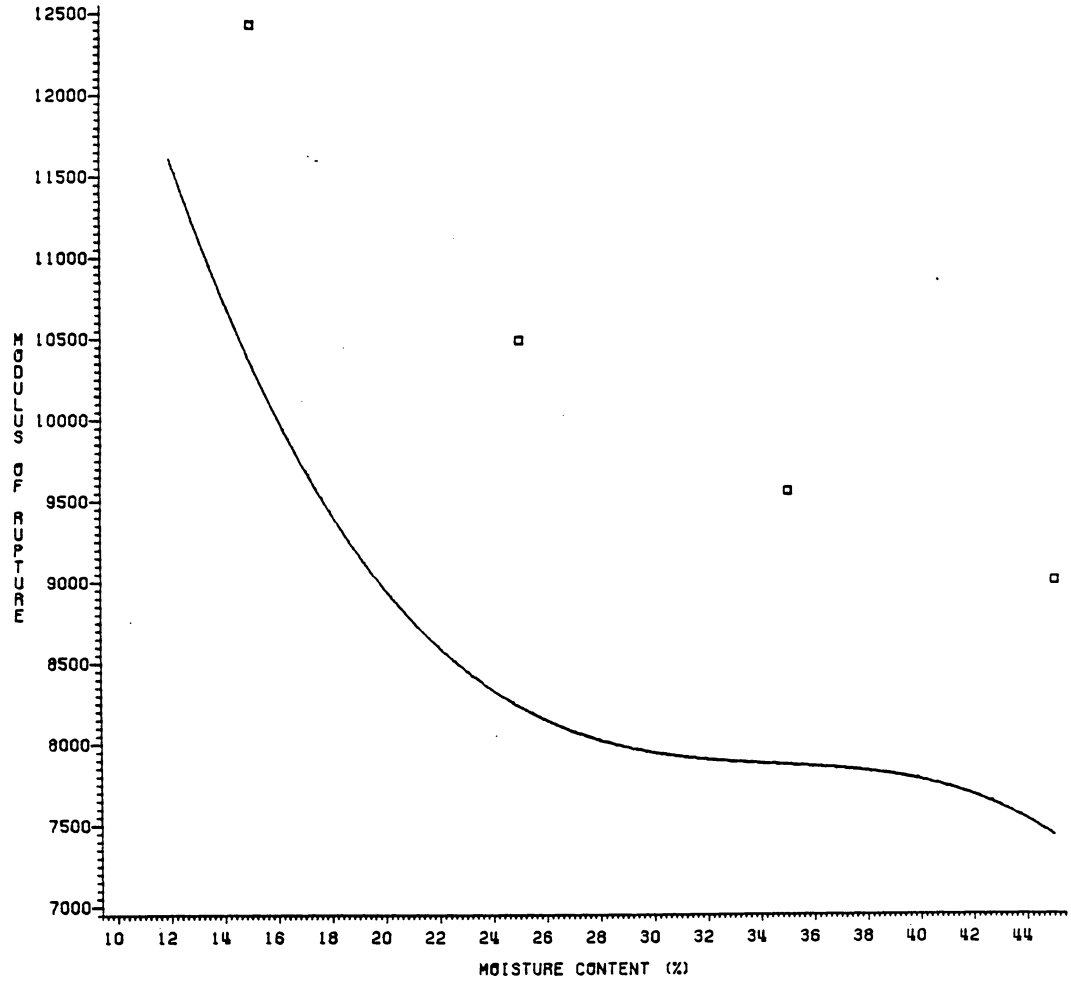

Figure 100: FEM predictions of MOR for non-equilibrated beam models compared to a model for non-equilibrated beam data. Solid line = model, squares = FEM predictions.

than the data model by about 12% at high average moisture contents. Because of the variability inherent to the data, however, it was assumed that the FEM predictions were more correct than the model in depicting the trend for the MOE. Based on an examination of the data it was also noted that the FEM program probably under-predicted the MOE values. This was attributed to ineffective modeling of the moisture gradients.

4. Modulus of rupture predictions for non-equilibrated beams were too high, primarily due to the step size/computer time constraint, but these predictions appeared to be consistent with the trend of the data model.

Overall, the finite-element program worked well, especially when one considers the number of subsidiary models which were incorporated into it. Accurate predictions of MOE and MOR could not often be made, and probably should not be expected given the inherent constraints. However, the trends of the property-average moisture content relationships were modeled with reasonable accuracy in most cases, and the constraints imposed of necessity in this study can sensibly account for the discrepancies observed between observed and predicted data.

Few significant errors would probably result from the use of this program in an environment free of these constraints.

6.9 MODELING OF 2 X 6 NON-EQUILIBRATED BEAMS

Following the completion of the finite-element modeling of the 1 x 1 x 14 inch equilibrated and non-equilibrated beam models, the finite-element program was applied to the modeling of non-equilibrated (nominal) 2 x 6 inch beams. Since no data were collected for these beams, the purpose of this investigation was to apply the methodology to a practical problem involving material of structural dimensions. Lumber tested in the national In-Grade Test Program is ostensibly evaluated in the green state. Practically, however, green test lumber often sits at the test site for varying times after cutting, inevitably resulting in moisture gradients. This effort is an attempt to estimate the effects of these gradients.

Aside from the limitations of the finite-element procedure, recognition is made of the fact that the models incorporated into the program were valid only for small clear specimens; the effects of knots and the depth effect are beyond the scope of the program. Nevertheless, it was felt that it might be instructive to apply the program to non-equilibrated 2 x 6 beams to see what trends might be

expected of the best clear material. It was known that finite-element analyses would yield results which were only qualitatively correct, but the degree of accuracy attainable was acceptable for these models.

Previous efforts had shown that MOR was most affected by moisture gradients at average moisture gradients above 20%, so non-equilibrated beams with average moisture contents of 25%, 35% and 45% were chosen for modeling at 12% EMC. A 17:1 l/d ratio was also chosen for the modeling procedure to accord with the testing procedure used by the In-Grade Testing Program. Modeling of these beams followed the procedural outline previously established for 1 x 1 x 14 inch beam models. The actual dimensions of the model were established as 5.5 x 1.5 x 93.5 inches (h x w x l) and planes of symmetry were used to reduce the model to a section one-quarter of this size (5.5 x 0.75 x 46.75 inches (h x w x l)). The support conditions chosen were those used previously; the beam was supported at the beam end by a roller at the neutral axis, and a vertical displacement was imposed across the neutral axis at the model beam midpoint. Aluminum properties were forced upon the model to aid in determining the number of elements required along the beam axis. Thirty-two linear elements resulted in 98% of the theoretical deflection, and this accuracy was acceptable.

Various meshes were then tried with uniaxial models of yellow-poplar to determine how fine a cross-sectional mesh was needed to achieve convergence in the prediction of Young's modulus. This varied slightly depending on the average moisture content of the specimen modeled, but a mesh of 6 x 5 elements (h x w) resulted in a predicted Young's modulus within 0.2 percent of the maximum value at every moisture content. Previous studies had shown that this cross-sectional mesh was comprised of too many elements for the beam model, so attempts were made to design alternative meshes which would achieve comparable results with no more than a 6 x 3 (h x w) element configuration. One mesh of unequal-size elements was found to yield Young's moduli within 0.65 percent or less of the maximum value from the afore-mentioned convergence studies, so this mesh was chosen for these studies (Figure 101).

Following the determination of the mesh for the 2 x 6 beam model, a second convergence study was conducted to determine an appropriate displacement step size to use in the linear stepwise procedure for the prediction of the modulus of rupture. Four step sizes were investigated (0.5, 0.25, 0.125 and 0.0625 inches) (Figure 102); the smallest of these (0.0625 inches) required about 83 minutes of CPU time to model a non-equilibrated beam at 25% average moisture

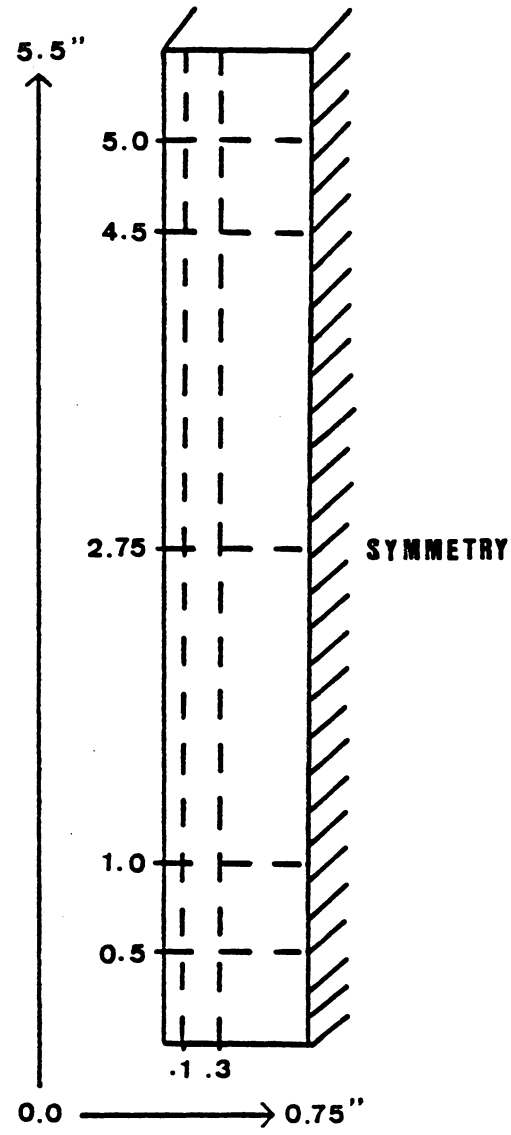

Figure 101: 6 x 3 mesh used for the nominal 2 x 6 beam models.

content. Since it was not practical to extend this study further, this step size was chosen for modeling each of the specified average moisture contents.

Together with the data models for equilibrated beam data, the FEM predictions of MOE and MOR values for non-equilibrated 2 x 6 beams are plotted in Figures 103 and 104. Since these values were not compared to 2 x 6 beam data the accuracy of the predictions is unknown, but it is interesting to note that the trends predicted by the FEM program are consistent with those predicted for the 1 x 1 x 14 inch beam models. On this basis it can be stated that moisture gradients are likely to influence both the stiffness and the strength properties of high-quality, nominally green (yellow-poplar) beams in structural sizes. If clear 2 x 6 beams act similarly to the 1 x 1 x 14 inch beams tested for this study, tests of non-equilibrated yellow-poplar beams will not yield MOE or MOR observations comparable to green beam data unless the average moisture content is greatly in excess of 45%. If these trends are applicable to the grades of lumber tested by the In-Grade Testing Program, then nominally green beams tested near the intersection point moisture content may have strength and stiffness properties which are representative of some moisture content below the intersection point. Subsequent

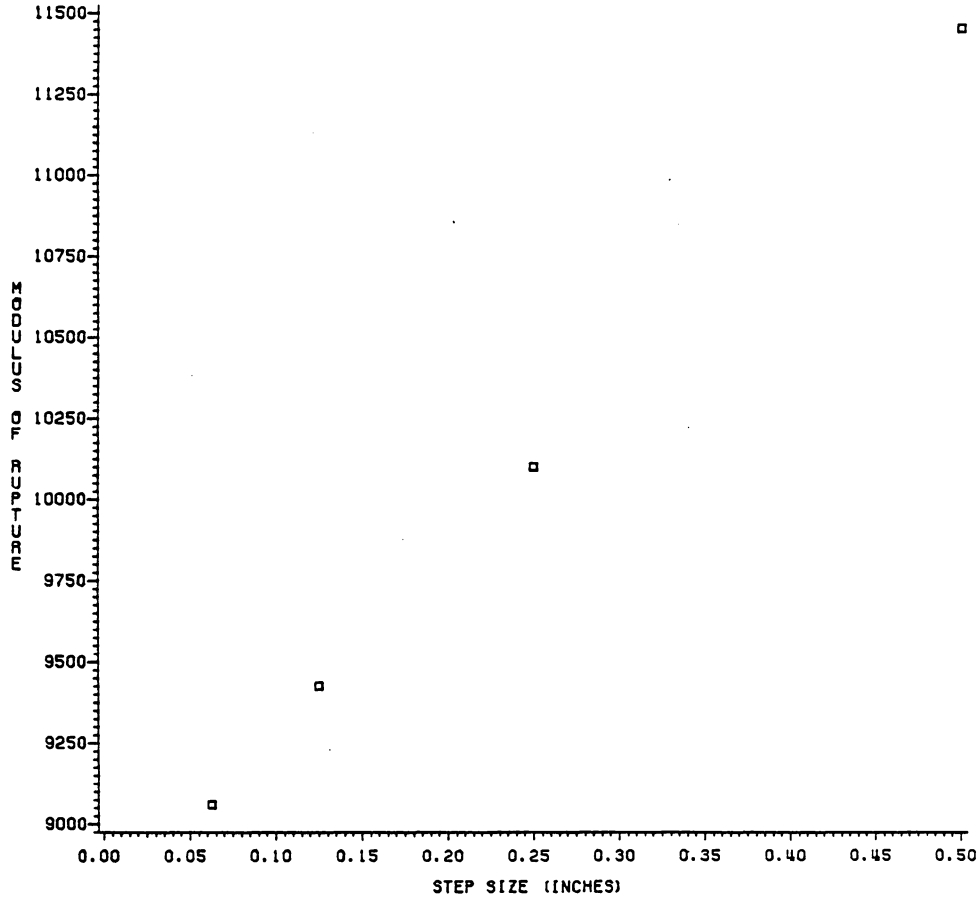

Figure 102: Convergence of the MOR estimate for 25% average MC 2 x 6 beam with different step sizes

prescriptions for seasoning adjustments based on these "green" data may be excessive.

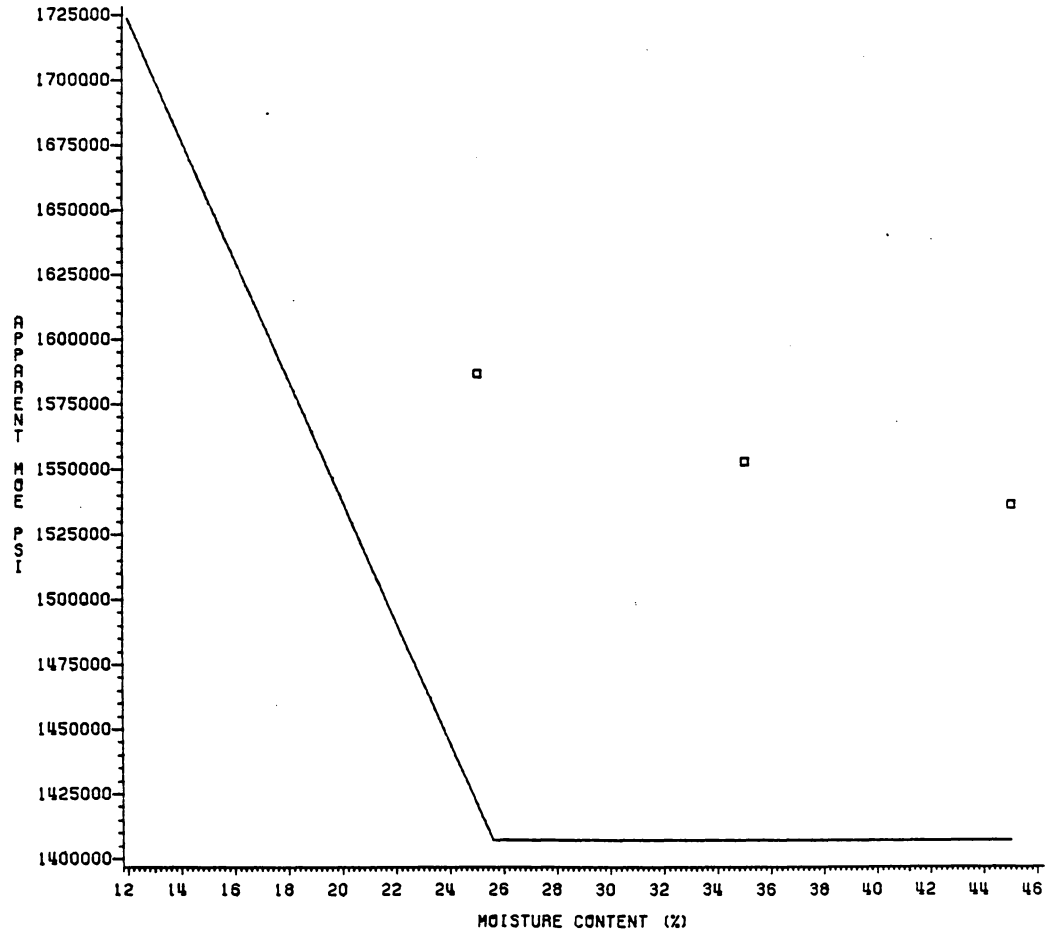

Figure 103: Comparison of the FEM predictions of MOE for non-equilibrated 2 x 6 beams to the data model for equilibrated beams. Solid line = model, squares = FEM predictions.

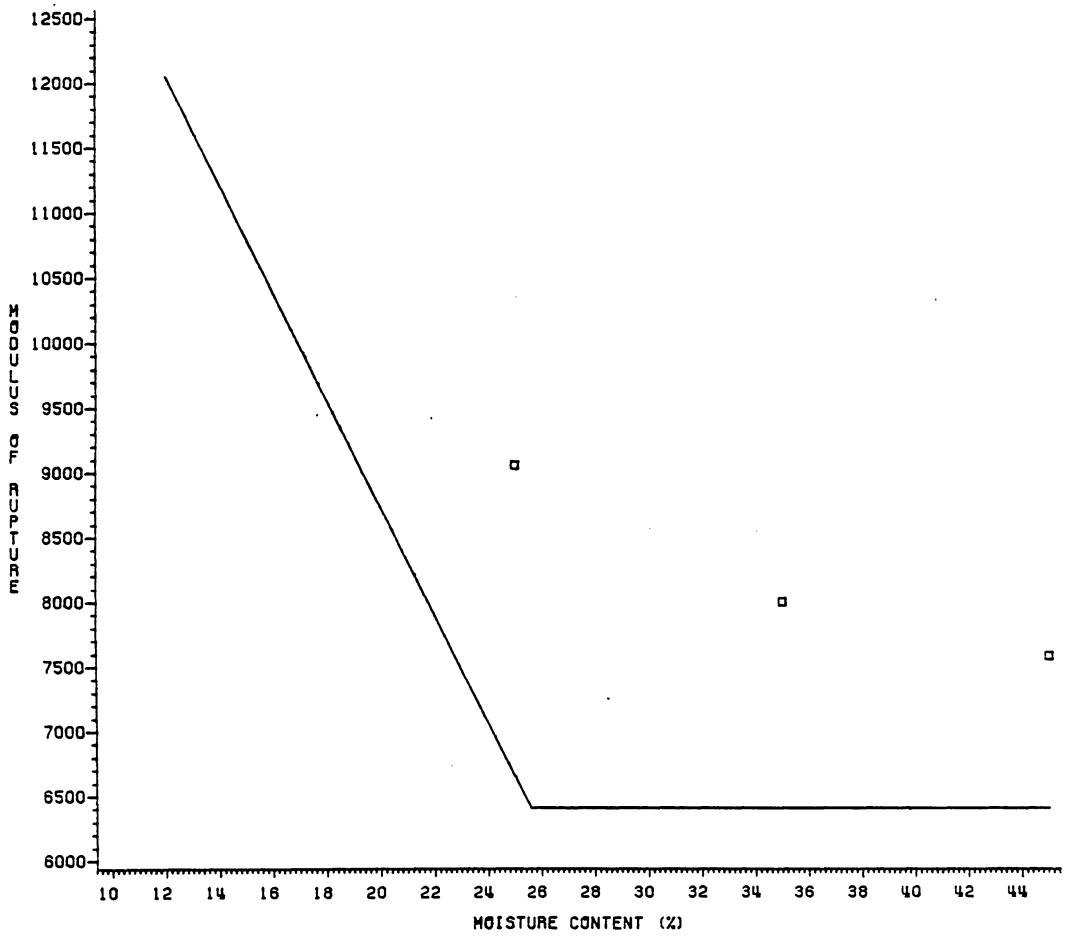

Figure 104: Comparison of the FEM predictions of MOR for non-equilibrated 2 x 6 beams to the data model for equilibrated beams. Solid line = model, squares = FEM predictions.

Chapter VII

CONCLUSIONS

7.1 SUMMARY OF THIS STUDY

A number of separate investigations were conducted during the course of this study so that the results might be incorporated into the finite-elements program. The results of these investigations are briefly summarized below.

1. A segmented mathematical model was proposed for use in modeling tension and compression stress-strain diagrams. The tension model consisted of an initial linear segment with a smooth transition to a quadratic function up to the failure point. The compression model proposed was similar in that the first and second segments were linear and quadratic functions, respectively, but a second smooth transition was added followed by a horizontal linear segment. It was shown that only three parameters were needed to describe digitized data using these models. One of these parameters was the modulus of elasticity, and the remaining two parameters for each curve were found using iterative non-linear regression techniques. The versatility and the fit of these models to data appears to surpass other models which have been previously proposed.

2. It was shown that the different uniaxial stress-strain diagrams which result from tests at various moisture contents could be regenerated by modeling the variation of the tension and compression segmented model parameters with moisture content.
3. The data collected for this study suggest that specific gravity does not materially affect the longitudinal Young's modulus in either tension or compression for clear yellow-poplar. However, specific gravity was significant in determining the uniaxial strength properties of yellow-poplar in tension and compression.
4. The term "maximum value moisture content" (or MVMC) has been proposed to identify that point around 4% to 6% moisture content where mechanical properties either stabilize or decline with decreasing moisture content.
5. Based on data available in the literature, a method has been described whereby most hardwood and softwood elastic constants can be estimated at any moisture content. Inherent in this method is the assumption that a linear relationship with moisture content is an acceptable approximation of the actual function. The slopes of these linear relationships were

determined for E_r, E_t, G_{lr}, G_{lt}, G_{rt}, ν_{lt}, ν_{rt} and ν_{tr}. The elastic constant of interest must therefore be known at only one moisture content before the amount of property change with moisture content can be estimated.

6. Several important findings arose from the tension and compression tests at various moisture contents.
   a) The equality of the longitudinal Young's moduli in tension and compression appears to depend on the moisture content at which tests are conducted. In this study, tension and compression Young's moduli were approximately equal at 6% and 18% MC; The Young's moduli in compression was the greater at 12% MC, however, while the tension modulus was greater for green specimens.
   b) Since the tension and compression Young's modulus values appear to have dissimilar relationships with moisture content, the use of a single model (e.g. USFPL "exponential formula") to describe the variation of each with moisture content is probably not justifiable.
   c) There is a lack of evidence that the "intersection point" for the mechanical property-moisture content function (historically near or equated to

the "fiber saturation point") is the same for tension and compression properties. If these intersection points are significantly different then the present-day concept of the fiber saturation point should be re-examined and possibly re-defined. Intersection points may not necessarily be identical to the fiber saturation point.

7. It has been shown that the paraboloid function used to estimate two-dimensional moisture gradients predicts values which are in good agreement with measured data below the assumed fiber saturation point.
8. Tests of small clear yellow-poplar beams demonstrated that moisture content gradients induced at 12% EMC had little effect on the MOR up to about 19% average MC. Beyond this moisture content the strength of gradient-containing beams was significantly greater than equilibrated beams when comparisons were made at the same moisture contents. The MOE data for non-equilibrated beams appear to indicate that the MOE will be approximately equal to those which would be obtained from beams equilibrated at the same EMC, but this result is suspect due to data variability. It

is also possible that a slight downward trend is present.

9. MOE-MOR correlations are significantly better for small clear green beams than for similar (equilibrated) air-dry material. The MOE is useless as a predictor of MOR when moisture gradients are present.

Following these investigations, the models resulting from analyses of the data were incorporated into a 3-D finite-element program. Two programs were actually written, one with linear elements and one with quadratic elements, but it was found that insufficient computer resources could be allocated to effectively use the quadratic-elements program. The eight-node linear-element program was used in this study. Several observations were noted from the use of this program.

10. A sensitivity study showed that the longitudinal Young's moduli in tension and compression were the most important elastic constants to describe accurately for 3-D beam modeling success.
11. The linear elastic step-by-step procedure used in this study was reasonably successful in achieving accurate uniaxial modeling beyond the elastic limit, although the accuracy was highly dependent upon the

displacement step size chosen and the curvilinearity of the function modeled. Using the same step size for comparison purposes, tension stress-strain diagrams were modeled with less error than the corresponding compression diagram for the same moisture content. Very small displacement steps were found to be necessary to avoid significant error in the FEM modeling procedure.

12. The finite-element model predicted that moisture gradients would increase both the strength and stiffness properties of uniaxial specimens beyond certain moisture contents compared to equilibrated specimens at the same average moisture levels. Based on the yellow-poplar models incorporated within the program, Young's modulus in compression was predicted to be slightly more sensitive to moisture gradients than Young's modulus in tension or the ultimate strengths in tension or compression.
13. The linear-element FEM program was able to perform well in predicting the apparent MOE for equilibrated beams. The program was also able to successfully predict the correct trend for the MOR-MC relationship, but the MOR values were over-predicted due to the displacement step size used. Convergence

studies demonstrated that the displacement step size governed the accuracy of the modeling efforts and showed that correct answers to 3-D non-linear beam problems should not be expected with this program unless extreme amounts of computer resources are utilized.

14. The finite-element program predicted that the MOE of non-equilibrated beams would decrease with higher average moisture contents. The presence or absence of this trend could not be confirmed in the data collected for this study due to the amount of variability present. However, the trend predicted by the finite-element program is consistent with expectations based on theoretical considerations. The trend for the MOR values of these beams was also predicted with reasonable fidelity, although the moduli of rupture were over-predicted due to the displacement step size used.
15. Finite-element modeling of nominal 2 x 6 beams indicated that moisture gradients have significant potential to cause increased MOE and MOR values to be observed for nominally green beams in structural sizes. These analyses are directly applicable only to clear or near-clear material, and the depth effect

was not considered. However, if the trends from these analyses are even somewhat applicable to beams with some defects, then the In-Grade Testing Program should not expect tests of "green" beams at moisture contents within 20% or 30% of the nominal intersection point to yield data which are equivalent to those obtained from freshly-cut, green material. Data resulting from tests of nominally green beams with moisture gradients may be more typical of data acquired at moisture gradients below the nominal intersection point, and currently-proposed seasoning adjustments may be excessive for these data.

The significance of the effect of moisture gradients on strength properties may, of course, be species-related; no specific amounts or percentages of change mentioned in this dissertation should be inferred as being directly applicable to anything except small clear specimens of yellow-poplar.

16. It has been demonstrated that the finite-element method can be applied to the study of beams with moisture gradients with some success, but the author is hesitant to recommend this tool for more extensive investigation of this problem due to present-day computer limitations. It may be worthwhile to repeat

this portion of the study at some future date since it has the potential to reduce the number of tests required to determine moisture gradient effects, but this should await the use of array processors and greater computer storage accessibility.

7.2 SUGGESTIONS FOR FURTHER RESEARCH

This project was not able to resolve some questions which are deserving of further study:

1. Uniaxial data similar to those collected for this study are required to assess the equality of Young's modulus in tension and compression at various moisture contents. Some previously published studies disagree with the results presented in this dissertation, and it would be worthwhile to determine if this is possibly due to some influence of species such as chemical constituents or anatomical structure.
2. The equality of the intersection points should be determined for tension and compression strength and stiffness properties.
3. The trends observed for non-equilibrated beams tested for this study were probably influenced by the tension and compression stress-strain relationships

which vary as a function of moisture content. Since these relationships are likely to vary with different species, it would be worthwhile to verify the amount of change attributable to moisture gradients for species other than yellow-poplar. Species with non-homogeneous structure such as southern pine might be expected to have different strength relationships compared to yellow-poplar when moisture gradients are present, and the influence of this heterogeneity would likely be compounded by the orientation of growth rings during testing.

4. Non-equilibrated specimens (either beam or compression) should be tested to verify the hypothesis that more severe moisture gradients (imposed at lower EMCs) will lower the average moisture content at which differences may be observed compared to equilibrated specimens.
5. Moisture gradients should be imposed in structural-size beams under controlled conditions to verify the trends resulting from the finite-element analyses in this study. It would be interesting to observe grade and depth effect interactions with moisture gradients as this was beyond the scope of the present study.

BIBLIOGRAPHY

Al-Dabbagh, A. M. 1970. Finite element stress analysis for anisotropic solids. Ph.D. dissertation in Civil Engineering, Colorado State University, Fort Collins, Colorado.

Al-Dabbagh, A., J. R. Goodman, and J. Bodig. 1972. Finite element method for wood mechanics. J. of the Struct. Div., Proceedings of ASCE, 98(ST3):569-586.

American Society for Testing and Materials. 1983. ASTM Standards. Philadelphia, Pennsylvania.

Anderson, J. A. 1981. Stress-strain relationship for defect-free timber beams. Wood Sci. 14(1):23-31.

Bach, L. 1966. Nonlinear mechanical behavior of wood in longitudinal tension. Ph. D. dissertation, State University College of Forestry at Syracuse University. Syracuse, New York.

Bateman, E., J. P. Hohf, and A. J. Stamm. 1939. Unidirectional drying of wood. Industrial and Engineering Chemistry 31(9):1150-1154.

Baumann, C. 1927. Das Holz als Baustoff. Kreidel, Munich. Original not seen. Cited by Hearmon, 1948.

Bauschinger, J. 1883. Mittheilungen aus dem Meschanish-technischen Laboratorium der konigl. Technischen Hochschule in Munchen, 9(10). Original not seen. Cited by Fernow (1892), Tiemann (1907).

Bauschinger, J. 1887. Mittheilungen aus dem Meschanish-technischen Laboratorium der konigl. Technischen Hochschule in Munchen, Vol. 16. Original not seen. Cited by Fernow (1892), Tiemann (1906).

Bazan, I. M. M. 1980. Ultimate bending strength of timber beams. Ph. D. dissertation in Civil Engineering, Nova Scotia Technical College, Halifax, Nova Scotia, Canada.

Bazhenov, V. A., L. M. Perelygin, and E. A. Semenova. 1953. Testing compression strength of wood across the grain (Ob ispytanii drevesiny na szhatie poperek volokon). Akademiya Nauk SSSR, Trudy instituta lesa. Volume 9:315-331. Israel Program for Scientific Translations, PST Cat. No. 163. OTS 60-51131. Available from National Technical Information Service, U. S. Dept. of Commerce as Document Number Number TT 6051131. Washington, D. C.

Bechtel, S. C., and C. B. Norris. 1952. Strength of wood beams of rectangular cross-section as affected by span-depth ratio. USDA Forest Service, FPL Report No. R1910. U. S. Forest Products Laboratory, Madison, Wisconsin.

Bodig, J., and J. R. Goodman. 1969. A new apparatus for compression testing of wood. Wood and Fiber 1(2):146-153.

Bodig, J., and B. A. Jayne. 1982. Mechanics of Wood and Wood Composites. Van Nostrand Reinhold, New York.

Bohlen, J. C. 1975. Compression strength adjustments for moisture in commercial Douglas-fir plywood. Forest Products Journal 25(12):26-31.

Bramhall, G. 1979. Mathematical model for lumber drying; II: The model. Wood Science 12(1):22-31.

Brokaw, M. P., and G. W. Foster. 1952. Effect of rapid loading and duration of stress on the strength properties of wood tested in compression and flexure. USDA Forest Service, FPL Report No. 1518, Forest Products Laboratory, Madison, Wisconsin.

Bryan, E. L. 1962. Maximum strength properties for particleboard. Forest Products Journal 12(2):59-64.

Brynildsen, O. 1977. Moisture effect on bending strength and stiffness of European spruce. Norsk Tre teknisk Institut, Oslo, Norway. Paper prepared for meeting of Working Party CIB W18/IUFRO S5, 02-03, London.

Byvshykh, M. D. 1959(?). Influence of temperature and moisture of wood on its elastic properties. Woodworking Industry (USSR) 8(2):13-15. Available as Translation No. 400, U. S. Forest Products Laboratory. Translated June, 1960 by D. Pronin.

Carrington, H. 1922. The elastic constants of spruce as influenced by moisture. The Aeronautical Journal 26(144):462-471.

Cech, M. Y. 1964. Development of drying stresses during high-temperature kiln-drying. Forest Products Journal 14(2):69-76.

Choong, E. T., and P. J. Fogg. 1968. Moisture movement in six wood species. Forest Products Journal 18(5):66-70.

Choong, Elvin T., and C. Skaar. 1969. Separating internal and external resistance to moisture removal in wood drying. Wood Science 1(4):200-202.

Comstock, G. 1963. Moisture diffusion coefficients in wood as calculated from adsorption, desorption, and steady-state data. Forest Products Journal 13(3):97-103.

Cook, R. D. 1981. Concepts and Applications of Finite Element Analysis. Second edition. John Wiley and Sons, New York.

Covington, S. A. 1965. The effect of drying and subsequent re-wetting on the strength properties of wood. Institute of Wood Science Journal Number 15:51-54.

Dietz, A. G. H. 1942. Stress-strain relations in timber beams of Douglas fir. ASTM Bulletin 118:19-27.

Doyle, D. V., and J. T. Drow. 1946. The elastic properties of wood: Young's moduli, moduli of rigidity, and Poisson's ratios of mahogany and khaya. USDA Forest Service, FPL Report No. 1528-C. U. S. Forest Products Laboratory, Madison, Wisconsin.

Doyle, D. V., R. S. McBurney, and J. T. Drow. 1946. The elastic properties of wood: The moduli of rigidity of Sitka spruce and their relations to moisture content. USDA Forest Service, FPL report No. 1528-B. U. S. Forest Products Laboratory, Madison, Wisconsin.

Draffin, J. O., and C. W. Muhlenbruch. 1937. ASTM report No. 96. Original not seen. Cited by Kollmann and Cote (1968).

Drow, J. T. 1957. Effect of moisture on the compression, bending, and shear strengths, and on the toughness of plywood. U. S. Forest Products Laboratory Report No. 1519. Re-issue of 1945 report.

Drow, J. T., and R. S. McBurney. 1946a. The elastic properties of wood: Young's moduli and Poisson's ratios of Sitka spruce and their relations to moisture content. USDA Forest Service, FPL Report No. 1528-A. U. S. Forest Products Laboratory, Madison, Wisconsin.

Drow, J. T., and R. S. McBurney. 1946b. The elastic properties of wood: Young's moduli, moduli of rigidity, and Poisson's ratios of yellow-poplar. USDA Forest Service , FPL Report No. 1528-G. U. S. Forest Products Laboratory, Madison, Wisconsin.

Ethington, R. L. 1960. Stiffness and bending strength of beams laminated from two species of wood. USDA Forest Service, FPL Report No. 2156. U. S. Forest Products Laboratory, Madison, Wisconsin.

Fagan, G. B. 1982. Load-support conditions and computerized test apparatus for wood pallets. M. S. thesis, Department of Forest Products, Virginia Polytechnic Institute and State University, Blacksburg, Virginia.

Fernandez, V. A., and A. Polensek. 1979. Model for predicting strength and stiffness of wood studs. Wood Science 12(2):65-72.

Fernow, B. E. 1892. Timber Physics, Part I: Preliminary report. USDA Forestry Division, Bulletin No. 6. Washington, D. C.

Fernow, B. E. 1893. Timber Physics, Part II: Progress report. USDA Forestry Division, Bulletin No. 8. Washington, D. C.

Fernow, B. E. 1896. Southern Pines - Mechanical and Physical Properties. USDA Division of Forestry, Circular No. 12.

Fernow, B. E. 1897. Summary of mechanical tests on thirty-two species of American woods. USDA Division of Forestry, Circular No. 15.

Fernow, B. E. 1898. Progress in timber physics. USDA Division of Forestry, Circular No. 18.

Fischer, S.,I. Roman, H. Harel, G. Marom, and H. D. Wagner. 1981. Simultaneous determination of shear and Young's moduli in composites. J. of Testing and Evaluation 9(5):303-307.

Galligan, W. L., D. W. Green, D. S. Gromala, and J. H. Haskell. 1980. Evaluation of lumber properties in the United States and their application to structural research. Forest Products Journal 30(10): 45-50.

Gerhards, C. C. 1968. Four-inch southern pine lumber: seasoning factors for modulus of elasticity and modulus of rupture. Forest Products Journal 19(11):27-35.

Gerhards, C. C. 1970. Further report on seasoning factor for modulus of elasticity and modulus of rupture. Forest Products Journal 20(5):40-44.

Gerhards, C. C., and J. M. McMillen (compilers). 1976. Proceedings of research conference on high-temperature drying effects on mechanical properties of softwood lumber. USDA Forest Products Laboratory, Madison, Wisconsin.

Gerhardt, T. 1982. Plane stress analysis of wood members using cubic and quadratic isoparametric finite elements. USDA Forest Service, FPL General Technical Report. U. S. Forest Products Laboratory, Madison, Wisconsin.

Gopu, V. K. A. 1980. Radial stresses in curved glulam beams. J. Struct. Div., Proceedings of ASCE 106 (ST11): 2143-2150.

Gopu, V. K. A., and J. R. Goodman. 1974. Analysis of double-tapered pitched and curved laminated beam section. Wood Science 7(1):52-60.

Gopu, V. K. A., and J. R. Goodman. 1975. Full-scale tests on tapered and curved glulam beams. J. Struct. Div., Proceedings of ASCE 101 (ST12):2609-2626.

Gurfinkel, G. 1973. Wood Engineering. Southern Forest Products Association, New Orleans, Louisiana.

Hart, C. Arthur. 1968. The Drying of Wood North Carolina Agricultural Extension Service, Ext. Cir. No. 471.

Hearmon, R. F. S. 1948. The elasticity of wood and plywood. Department of Scientific and Industrial Research, Forest Products Research Special Report No. 7. H. M. Stationery Office, London.

Hoffmeyer, P. 1978. Moisture content-strength relationship for spruce lumber subjected to bending, compression and tension along the grain. In: Proceedings, IUFRO wood engineering group meeting. Vancouver, B. C. 1978.

Hudson, D. J. 1966. Fitting segmented curves whose join points have to be estimated. J. Am. Stat. Assn. 61(316):1097-1129.

Huffman, D. R. 1977. High-temperature drying effect on the bending strength of spruce-pine-fir joists. Forest Products Journal 27(3):55-57.

Ivanov, Iu. M. 1941. Predel plasticheskogo techeniia drevesiny: Osnovaniia novoi teorii techeniia mekhanicheskoi prochnosti drevesiny (The limit of plastic flow of wood: A new theory of the mechanical strength of wood). Moscow. Available in English at the U. S. Forest Products Laboratory, Madison, Wisconsin as Translation No. 111. Translated August, 1955, by H. P. Kipp.

Ivanov, Iu. M. 1949. Novaia kharakteristika prochnosti drevesiny i metody ee opredeleniia (The new measure of the strength of wood and methods of its determination). Akademiia nauk SSR, Trudy instituta lesa (Academy of Sciences of the U. S. S. R., Transactions of the Wood Institute), Volume 4:34-45. Available in English at the U. S. Forest Products Laboratory, Madison, Wisconsin as Translation No. 24. Translated June, 1951, by H. P. Kipp.

James, W. L. 1962. Dynamic strength and elastic properties of wood. Forest Products Journal 12(6):253-260.

James, W. L. 1964. Vibration, static strength, and elastic properties of clear Douglas-fir at various levels of moisture content. Forest Products Journal 14(9):409-413.

Janka, G. 1904. Untersuchungen uber die Bautechnische Qualitat des Fichtenholzes. In Baumaterialienkunde, 17(17):262. Stuttgart. Original not seen. Cited by Tiemann (1906).

Jones, R. M. 1975. Mechanics of Composite Materials Scripta Book Co., Washington, D. C., McGraw-Hill, N.Y.

Kawai, S., K. Nakato, and T. Sadoh. 1979. Computation of drying stresses resulting from gradients in wood during drying, I. Computative method. Mokuzai Gakkaishi 25(2):103-110.

Keith, C. T. 1960. Some effects of repeated drying and wetting on wood properties. Department of Forestry, Forest Products Laboratories of Canada, FPL Technical Note No. 23.

Kellogg, R. M., and G. Ifju. 1962. Influence of specific gravity and certain other factors on the tensile properties of wood. Forest Products Journal 12(10):463-470.

Khookriansky, P. N. 1936. The effect of over-drying and subsequent moistening on the mechanical properties of normal and bent wood. Woodworking Industries (USSR) 2:53-61. Original not seen. Cited by Covington (1965).

King, E. G. Jr. 1957. Creep and other strain behavior of wood in tension parallel to the grain. Forest Products Journal 7(10):324-330.

King, E. G. Jr. 1961. Time-dependent strain behavior of wood in tension parallel to the grain. Forest Products Journal 11(13):156-165.

Koch, P., and B. Bohannan. 1966. Beam strength as affected by placement of laminae. Forest Products Journal 15(7):289-295.

Kollmann, F. F. P., and W. A. Cote. 1968. Principles of Wood Science and Technology, Volume I: Solid Wood. Springer-Verlag, New York.

Kollmann, F. F. P., and H. Krech. 1960. Dynamische Messungen der elastichen Holzeigenschaften und der Dampfung. Holz als Rohund Werkstoff 18:41-54. Original not seen. Cited by Kollmann and Cote (1968).

Krischer, O. 1942. Der Warme- und Stoffaustausch in Trocknungsgut. VDI-Forschungsheft 415. Berlin. Original not seen. Cited by Kollmann and Cote (1968).

Krueger, G. P., and L. B. Sandberg. 1974. Ultimate strength design of reinforced timber. Evaluation of design parameters. Wood Science 6(4):316-329.

Lamarle, E. 1845. Memoir on the bending of wood. Ann. Trav. publ. Belg., 3(1). Original not seen. Cited by Hearmon (1948).

Lamarle, E. 1846. Memoir on the bending of wood. Ann. Trav. publ. Belg., 4(1). Original not seen. Cited by Hearmon (1948).

Laufenberg, T. L. 1983. Characterizing the nonlinear behavior of flakeboards. Wood and Fiber Science 15(1):47-58.

Liska, J. A. 1950. Effect of rapid loading on the compressive and flexural strength of wood. USDA Forest Service, Forest Products Laboratory Report No. R1767. Re-released in 1955 as Report No. 1767.

Luxford, R. F. and L. W. Wood. 1944. Survey of strength and related properties of yellow-poplar. USDA Forest Service, Forest Products Laboratory Mimeo Report No. 1516.

McBurney, R. S., and J. T. Drow. 1956. The elastic properties of wood: Young's moduli and Poisson's ratios of Douglas-fir and their relations to moisture content. USDA Forest Service, FPL Report No. 1528-D. U.S. Forest Products Laboratory, Madison, Wisconsin.

McMillen, J. M. 1955a. Drying stresses in red oak. Forest Products Journal 5(1):71-76.

McMillen, J. M. 1955b. Drying stresses in red oak: Effect of temperature. Forest Products Journal 5(4):230-241.

Madsen, B. 1975. Moisture content-strength relationship for lumber subjected to bending. Structural Research Series, Report No. 11. Department of Civil Engineering, University of British Columbia, Vancouver, British Columbia, Canada.

Madsen, B., W. Janzen, and J. Zwaagstra. 1980. Moisture effects in lumber. Structural Research Series, Report No. 27. Department of Civil Engineering, University of British Columbia, Vancouver, British Columbia, Canada.

Maghsood, J. 1970. Finite element analysis of wood beams. Ph. D. dissertation in Agricultural Engineering, Cornell University.

Malhotra, S. K., and I. M. M. Bazan. 1980. Ultimate bending strength theory for timber beams. Wood Science 13(1):50-63.

Mark, R. 1961. Wood-aluminum beams within and beyond the elastic range. I:Rectangular sections. Forest Products Journal 11(10):477-484.

Mark,R. E., S. F. Adams, and R. C. Tang. 1970. Moduli of rigidity of Virginia pine and tulip poplar related to moisture content. Wood Science 2(4):203-211.

Markwardt, L. W. 1930. Comparative strength properties of woods grown in the United States. USDA Technical Bulletin No. 158.

Markwardt, L. J., and T. R. C. Wilson. 1935. Strength and related properties of woods grown in the United States. USDA Technical Bulletin No. 479.

Marx,C. M., and R. C. Moody. 1981a. Bending strength of shallow glued-laminated beams of a uniform grade. USDA Forest Service, Research Paper FPL 380. U. S. Forest Products Laboratory, Madison, Wisconsin.

Marx, C. M., and R. C. Moody. 1981b. Strength and stiffness of small glued-laminated beams with different qualities of tension laminations. USDA Forest Service, Research Paper FPL 381. U. S. Forest Products Laboratory, Madison, Wisconsin.

Mazur, S. J. 1965. Ultimate strength theory for rectangular wooden beams. In Symposium on Timber and Timber Structures. Transactions of the Engineering Institute of Canada. EIC-65-BR & STR 13. 8(A-16):7-11.

Moe, J. 1961. The mechanism of failure of wood in bending. International Association for Bridge and Structural Engineering. 21:163-178.

Montgomery, D. C., and E. A. Peck. 1982. Introduction to Linear Regression Analysis. John Wiley and Sons, New York.

Morgan, K., H. R. Thomas, and R. W. Lewis. 1982. Numerical modeling of stress reversal in timber drying. Wood Science 15(2):139-149.

Moschler, W. W., and R. E. Martin. 1968. Diffusion equation solutions in experimental wood drying. Wood Science 1(1):47-57.

Neely, S. T. 1898. Relation of compression-endwise to breaking load of beam. In: Progress in Timber Physics, USDA Division of Forestry Circular No. 18.

Newlin, J. A., and T. R. C. Wilson. 1919. The relation of the shrinkage and strength properties of wood to its specific gravity. USDA Bulletin No. 676.

Nwokoye, D. N. 1972. An investigation into an ultimate beam theory for rectangular timber beams - solid and laminated. Timber Research and Development Association (TRADA) Research Report E/RR/34, April, 1972. E/RR/34 TRADA, Hughenden Valley, High Wycombe, Buckinghamshire, Great Britain.

O'Halloran, M. R. 1973. Curvilinear stress-strain relationship for wood in compression. Ph. D. dissertation in Forest and Wood Sciences, Colorado State University, Fort Collins, Colorado.

Palka, L. C. 1973. Predicting the effect of specific gravity, moisture content, temperature and strain rate on the elastic properties of softwoods. Wood Science and Technology 7:127-141.

Palka, L. C. 1982. A proposed model of the effect of moisture content on the mechanical properties of sheathing-grade Douglas-fir plywood. In Structural Uses of Wood in Adverse Environments, edited by R. W. Meyer and R. M. Kellogg. Society for Wood Science and Technology. Van Nostrand Reinhold, New York. 1982.

Panshin, A. J., and C. de Zeeuw. 1980. Textbook of Wood Technology, fourth edition. McGraw-Hill Book Company, New York.

Phillips, G. E., J. Bodig, and J. R. Goodman. 1981. Flow-grain analogy. Wood Science 14(2):55-64.

Popov, E. P. 1976. Mechanics of Materials. Prentice-Hall, Inc., Englewood Cliffs, New Jersey.

Ramberg, W., and W. R. Osgood. 1943. Description of stress-strain curves by three parameters. U. S. National Advisory Committee for Aeronautics, Technical Note No. 902. U. S. Government Printing Office, Washington, D. C.

Ramos, A. N., Jr. 1961. Stress-strain distribution in Douglas-fir beams within the plastic range. USDA Forest Service, FPL Report No. 2231. U. S. Forest Products Laboratory, Madison, Wisconsin.

Reddy, J. N. 1984. An Introduction to the Finite Element Method. McGraw-Hill, New York.

Robinson, H., and D. W. Cooper. 1958. The ultimate strength in bending of solid beams of structural grade European redwood. J. Inst. Wood Sci.1(2):40-65.

Ros, M. 1936. Das Holz als Baustoff. I. Schweiz. Kongr. Forderung Holzverw. Bern, p. 274. Original not seen. Cited by Kollmann and Cote, 1968.

Rosen, H. N. 1976. Exponential dependency of the moisture diffusion coefficient on moisture content. Wood Science 8(3):174-179.

Salamon, M. 1963. Quality and strength properties of Douglas-fir dried at high temperatures. Forest Products Journal 13(8):339-344.

Salamon, M. 1969. High temperature drying and its effect on wood properties. Forest Products Journal 19(3):27-34.

Samek, J. 1970. Effect of moisture content on compression strength of sheathing-grade Douglas-fir plywood. Counc. Forest Ind. B. C., North Vancouver, B. C., Canada. Report No. 94. Original not seen. Cited by Bohlen (1975).

Sandoe, M. D., F. J. Keenan, F. C. Beall, and S. P. Fox. 1982. Tension perpendicular-to-glueline strength of hot-press and conventional glued-laminated beams. In Structural Uses of Wood in Adverse Environments, edited by R. W. Meyer and R. M. Kellogg. Society of Wood Science and Technology. Van Nostrand Reinhold, New York. 1982.

SAS Institute. 1982. Statistical Analysis System. SAS Institute, Inc., Cary, North Carolina.

Schaffer, E. L. 1980. Temperature-time dependency of longitudinal mechanical behavior of dry Douglas-fir. In General Constitutive Relations for Wood and Wood-based Materials. Syracuse University.

Schaffner, R. D. 1981. Fundamental aspects of timber seasoning. Research Report 81/1, Mechanical Engineering Department, Faculty of Engineering. University of Tasmania.

Siau, J. F. 1971. Flow in Wood. Syracuse University Press. Syracuse, New York.

Simpson, W. T. 1974. Measuring dependence of diffusion coefficient of wood on moisture concentration by adsorption experiments. Wood and Fiber 5(4):299-307.

Sliker, A. 1973. Young's modulus parallel to the grain in wood as a function of strain rate, stress level and mode of loading. Wood and Fiber, 4(4):325-333.

Sonnleithner, E. 1933. Verlauf der Feuchtigkeit innerhalb des Holzes wahrend der Trocknung. Forsch.-Ber.Holz, H.1, VDI-Verlag, Berlin. Original not seen. Cited by Kollmann and Cote (1968).

Stern, E. G. 1943. Strength properties of red spruce from West Virginia. Bulletin of the Virginia Polytechnic Institute 36(8). Engineering Experiment Station Series No. 55.

Stern, E. G. 1944a. Resistance of common hardwoods to compression perpendicular to the grain. Bulletin of the Virginia Polytechnic Institute 37(8). Engineering Experiment Station Series No. 57.

Stern, E. G. 1944b. Strength properties of yellow poplar from West Virginia. Bulletin of the Virginia Polytechnic Institute 38(2). Engineering Experiment Station Series No. 59.

Suenson, E. 1941. Die Lage der Nullinie in gebogenen Holzbalken. Holz als Roh- und Werkstoff 4:305-314. Original not seen. Cited by Kollmann and Cote, 1968.

Sugiyama, H. 1967. On the effect of the loading time on the strength properties of wood; A review of Japanese research. Wood Science and Technology 1(4):289-303.

Tang, R. C., S. F. Adams, and R. E. Mark. 1971. Moduli of rigidity and torsional strength of scarlet oak related to moisture content. Wood Science 3(4):238-244.

Tang, R. C., and N. Hsu. 1972. Dynamic Young's moduli of wood related to moisture content. Wood Science 5(1):7-14.

Thomas, H. R., R. W. Lewis, and K. Morgan. 1980. An application of the finite element method to the drying of timber. Wood and Fiber 11(4): 237-243.

Thunell, B. 1939. Ing. Vet. Akad. Stockholm, H.3. Original not seen. Cited by Kollmann and Cote, 1968.

Tiemann, H. D. 1906. Effect of moisture upon the strength and stiffness of wood. USDA Forest Service Bulletin No. 70.

Tiemann, H. D. 1907. The strength of wood as influenced by moisture. USDA Forest Service Circular No. 108.

Tiemann, H. D. 1908. The effect of the speed of testing upon the strength of wood and the standardization of tests for speed. Proceedings of the American Society for Testing and Materials 8:541-557.

Tiemann, H. D. Wood Technology: Constitution, Properties and Uses. 1942. Pitman Publishing Company, New York.

Trayer, G. W., and H. W. March. 1929. The torsion of members having sections common in aircraft construction. Technical Report No. 334 in Fifteenth Annual Report of the U. S. National Advisory Committee for Aeronautics, pp.671-719. U. S. Government Printing Office, Washington, D. C. Also available as a separate report with the same title, dated 1930.

Urbanik, T. J. 1982. Method analyzes analogue plots of paperboard stress-strain data. Tappi 65(4):104-108.

U. S. Forest Products Laboratory. 1974. Wood handbook: Wood as an engineering material. USDA Agr. Handbook 72, revised.

Walker, J. 1961. Interpretation and measurement of strains in wood. Ph. D. thesis, Purdue University, Lafayette, Indiana. Original not seen. Cited by Palka (1973).

Wengert, E. M. 1975. Prediction of moisture content in wood. Ph. D. dissertation, University of Wisconsin.

Wengert, E. M. 1979. Relationship between toughness of hardwoods and specific gravity. Wood Science 11(4):233.

Wengert, E. M., and C. Skaar. 1978. Additional consideration in measuring transverse moisture conductivity in wood. Wood Science 11(2):102-104.

Wilkinson, T. L., and R. E. Rowlands. 1981a. Influence of elastic properties on the stresses in bolted joints in wood. Wood Science 14(1):15-22.

Wilkinson, T. L., and R. E. Rowlands. 1981b. Analysis of mechanical joints in wood. Experimental Mechanics 21(11):408-414.

Wilkinson, T. L., R. E. Rowlands, and R. D. Cook. 1981. An incremental finite-element determination of stresses around loaded holes in wood plates. Computers and structures 14(1-2):123-128.

Wilson, T. R. C. 1932. Strength-moisture relations for wood. USDA Technical Bulletin No. 282.

Youngs, R. L. 1957. Mechanical properties of red oak related to drying. Forest Products Journal 7(10):315-324.

Youngs, R. L., and C. B. Norris. 1958. A method of calculating internal stresses in drying wood. USDA Forest Service, FPL Report No. 2133. U. S. Forest Products Laboratory, Madison, Wisconsin.

Zakic, B. D. 1976. Stress distribution within the plastic range in wood beams subjected to pure bending. Holzforschung und Holzverwertung 28(5):114-120.

Zienkiewicz, O. C. 1973. Introductory Lectures on the Finite Element Method. International Centre for Mechanical Sciences, Courses and Lectures No. 130. Springer-Verlag, New York.

Zienkiewicz, O. C. 1977. The Finite Element Method. Third edition. McGraw-Hill, New York.

APPENDIX A

TWOLINE

```
C .....................................................................
C
C
C                    ##############################
C                    #                            #
C                    #      T W O L I N E         #
C                    #                            #
C                    ##############################
C
C                 WATFIV, G- OR H-COMPILER COMPATIBLE
C
C .....................................................................
C
C     THIS PROGRAM WAS WRITTEN BY TERRANCE E. CONNERS, DEPARTMENT OF
C     FOREST PRODUCTS, VIRGINIA TECH (VPI & SU), MARCH, 1984.
C     PHONE: (703)-961-4524
C
C     THIS PROGRAM WAS WRITTEN TO SEARCH A BODY OF X-Y DATA FOR A BI-
C     LINEAR RELATIONSHIP AND TO DETERMINE THE BEST BI-LINEAR
C     RELATIONSHIP ON A STATISTICAL BASIS USING THE PRINCIPLE OF
C     MINIMIZATION OF RESIDUAL SUM OF SQUARES FOR THE OVERALL REGRESSION
C
C     REFERENCE: "FITTING SEGMENTED CURVES WHOSE JOIN POINTS HAVE TO BE
C                 ESTIMATED", BY DEREK J. HUDSON OF BELL LABS
C                 J AM STAT ASSN, 61(316): 1097-1129  (1966)
C
C     THIS PROGRAM ONLY SEARCHES FOR JOIN TYPES OF 1 OR 2.
C     SAS PROC NLIN WILL ACCOMODATE JOINS OF TYPE 3.
C
C .....................................................................
C
C     INPUT REQUIRED: I. TITLE OF PROBLEM, UP TO 80 CHARACTERS LONG
C
C                    II. LOWER, UPPER VALUES OF THE INDEPENDENT VARIABLE
C                        WITHIN WHICH THE JOIN POINT IS TO BE SOUGHT
C                        * (FORMAT-FREE INPUT) *
C
C                   III. TWO COLUMNS OF DATA ARE ASSUMED TO BE PRESENT
C                        A) THE INDEPENDENT VARIABLE
C                        B) THE DEPENDENT VARIABLE
C
C                           NOTE THAT A FORMAT-FREE READ STATEMENT IS
C                           IMBEDDED IN THE PROGRAM AS A COMMENT.
C                           TO USE THIS, PUT -999 0 AS THE LAST DATA
C                           CARD IN THE INPUT STACK (BESIDES JCL), AND
C                           RE-COMMENT THE FORMAT CARDS APPROPRIATELY.
C
C .....................................................................
C
C     ABOUT DIMENSION STATEMENTS:
```

```
C
C       1.  X(A),Y(A):          A=NUMBER OF DATA PAIRS IN DATA SET
C       2.  DTXLO(B),DTYLO(B): B=NUMBER OF DATA PAIRS BELOW THE UPPER
C                                 TRIAL JOIN POINT (RANGE2)
C       3.  DTXHI(C),DTYHI(C): C=NUMBER OF DATA PAIRS ABOVE THE LOWER
C                                 TRIAL JOIN POINT (RANGE1)
C       4.  RHO1(D),RHO2(D),T(D),B1STAR(D),B2STAR(D),JOINPT(D),
C           B1HAT(2,D),B2HAT(2,D):
C                               D=MAXIMUM NUMBER OF REGRESSIONS
C                                 ATTEMPTED BY PROGRAM
C       5.  DONTRY(E):          E=NUMBER OF X DATA VALUES WHICH THE PGM
C                                 WILL NOT CONSIDER DURING PART 2.
C                                 BECAUSE A GIVEN X-VALUE MAY BE LISTED
C                                 TWICE, AN ESTIMATE FOR E MIGHT BE :
C                                 (NUMBER OF X DATA VALUES BETWEEN
C                                 RANGE1 & RANGE2) TIMES AROUND 1.25
C       5.  TITLE(F):           F=CAN BE CHANGED TO ANYTHING DESIRED,
C                                 CHANGE READ & FORMAT STMT 20 ALSO.
C       6.  XPXINV,XPRIMY,CLOINV,CHIINV,CINV,CINVQ,XLOY,XHIY,TM,D,Q,
C           B1HATP,B2HATP:
C             -----DON'T CHANGE THE DIMENSIONS FOR THESE ARRAYS !!!
C
C ..................................................................
      IMPLICIT REAL*8(A-H,O-Z)
      INTEGER I,J,NUMDAT,K,J1P,JJ,J1,MINT,KSTOR,N1,N2
      REAL*8 X,Y,A,B,RANGE1,RANGE2,ORANGE,DTXLO,DTYLO,DTXHI,
     $DTYHI,SIGXI,SIGXI2,SIGDL2,FJ1,XLOBAR,XHIBAR,FJ1P,JOINPT,T,TT,TM,
     $DONTRY,RHO1,RHO2,XPXINV,B1HAT,B2HAT,B1HATP,B2HATP,FNUM,CLOINV,
     $CHIINV,XLOY,XHIY,CINV,D,Q,BIGS,B1STAR,B2STAR,CINVQ,FNUM,SYY,SYY2,
     $TSS
      DIMENSION TITLE(20),X(100),Y(100),DTXLO(100),DTYLO(100),
     $DTXHI(100),DTYHI(100),XPRIMY(2),RHO1(100),RHO2(100),
     $B1HAT(2,100),B2HAT(2,100),B2HATP(2),XPXINV(2,2),JOINPT(100),
     $T(100),DONTRY(100),CLOINV(2,2),CHIINV(2,2),XLOY(2),XHIY(2),
     $CINV(4,4),D(4),Q(4),B1STAR(100),B2STAR(100),CINVQ(4),B1HATP(2),
     $TM(4)
C
C     READ THE DATA ACCORDING TO A FORMATTED READ STATEMENT.
C     THIS WILL ALLOW THE SAME INPUT FILE TO BE USED FOR ANALYSIS OF
C     SEVERAL DIFFERENT DEPENDENT VARIABLES FOR A SINGLE INDEPENDENT
C     VARIABLE.
C     CHANGE THE FORMAT CARD FOR EACH RUN AS NECESSARY.
C
C     *************  PUT -999 0  AS THE LAST DATA CARD   ***************
C     *************  WHEN USING THE FREE-FORMAT OPTION!  ***************
C
      WRITE(6,10)
10    FORMAT(1H1,//,
     147X,40H****************************************,/,47X
     2,1H*,38X,1H*,/,47X,40H*           T W O L I N E            *,/,4
```

```
     37X,1H*,38X,1H*,/,47X,40H* A PROGRAM TO ESTIMATE THE JOIN POINT *,/
     4,47X,40H*    OF A BI-FUNCTIONAL SET OF DATA    *,/,47X,40H*    BY
     5T.E. CONNERS, DEPARTMENT OF    *,/,47X,40H* FOREST PRODUCTS, VA TE
     6CH, BLACKSBURG *,/,47X,40H* (703) 961-4524       WRITTEN 3/84    *
     7,/,47X,40H*                                      *,/,47X,40H******
     8*********************************)
      WRITE(6,15)
15    FORMAT(////,2X,'REFERENCE: "FITTING SEGMENTED CURVES WHOSE JOIN PO
     $INTS HAVE TO BE ESTIMATED"',/,13X,'BY DEREK J. HUDSON, BELL LABS',
     $/,13X,'JOURNAL OF THE AMERICAN STATISTICAL ASSOCIATION, 61(316): 1
     $097-1129  (1966)',/////)
      READ(5,20) (TITLE(I),I=1,20)
20    FORMAT(20(A4))
      WRITE(6,30) (TITLE(I),I=1,20)
30    FORMAT(///,2X,20(A4),///)
      READ(5,*) RANGE1,RANGE2
      WRITE(6,40) RANGE1,RANGE2
40    FORMAT(/,2X,'THE DATA WILL BE EXAMINED FOR JOIN POINTS BETWEEN X =
     $',1X,F6.3,1X,'AND',1X,F6.3,1X,', INCLUSIVE.',/)
      ORANGE=RANGE1
      NUMDAT=0
      K=0
      MINT=-999
      JJ=1
      DO 50 I=1,1000
C     READ(5,*) A,B
C     IF(A.EQ.-999) GO TO 55
      READ(5,51,END=55) A,B
  51  FORMAT(09X,F6.2,19X,F14.3)
      X(I)=A
      Y(I)=B
      NUMDAT=NUMDAT+1
50    CONTINUE
55    CONTINUE
      WRITE(6,60) NUMDAT
60    FORMAT(//,2X,I5,1X,'DATA POINTS HAVE BEEN ENTERED FOR ANALYSIS.',/
     $,2X,'THE FOLLOWING IS A LISTING OF THE DATA ENTERED:',//)
      WRITE(6,70)
70    FORMAT(40X,'X',16X,'Y',/)
      DO 90 I=1,NUMDAT
      WRITE(6,80) X(I),Y(I)
80    FORMAT(36X,F6.2,8X,F12.1)
90    CONTINUE
C     SORT THE DATA IN ASCENDING ORDER BY THE X-VALUE:
      NM1=NUMDAT-1
      DO 110 I=1,NM1
      IP1=I+1
      DO 100 J=IP1,NUMDAT
      IF(X(I).LE.X(J)) GO TO 100
      T1=X(I)
```

```
      T3=Y(I)
      X(I)=X(J)
      X(J)=T1
      Y(I)=Y(J)
      Y(J)=T3
100   CONTINUE
110   CONTINUE
      WRITE(6,120)
120   FORMAT(///,2X,'THE FOLLOWING IS A SORTED LIST OF THE DATA ENTERED
     $FOR ANALYSIS:',//)
      WRITE(6,70)
      DO 130 I=1,NUMDAT
      WRITE(6,80) X(I),Y(I)
130   CONTINUE
C
C     VERIFY THAT THE JOIN POINT TRIAL RANGE WAS CORRECTLY SPECIFIED
C
      N1=NUMDAT-1
      DO 131 I=1,NUMDAT
      IF(X(N1).LT.X(NUMDAT)) GO TO 132
      N1=N1-1
131   CONTINUE
132   CONTINUE
      N2=2
      DO 134 I=1,NUMDAT
      IF(X(N2).GT.X(1)) GO TO 135
      N2=N2+1
134   CONTINUE
135   CONTINUE
      IF((RANGE1.LT.X(N2)).OR.(RANGE2.GT.X(N1))) WRITE(6,140)
140   FORMAT(///,2X,'SEARCH FOR JOIN POINTS MUST BE RESTRICTED TO A SMAL
     $LER RANGE.',/,2X,'THERE ARE NO DATA POINTS OUTSIDE OF THE RANGE SP
     $ECIFIED FOR THIS RUN.',/,2X,'DATA WITH AT LEAST ONE DIFFERENT X-VA
     $LUE MUST BE OUTSIDE EACH EXTREME OF THE SEARCH RANGE.',//////)
      IF((RANGE1.LT.X(N2)).OR.(RANGE2.GT.X(N1))) GO TO 490
C
C     CALCULATE THE TOTAL ADJUSTED SUM OF SQUARES
C
      FNUM=FLOAT(NUMDAT)
      SYY=0.0
      SYY2=0.0
      DO 143 I=1,NUMDAT
      SYY=Y(I) + SYY
      SYY2=Y(I)**2 + SYY2
143   CONTINUE
      TSS=SYY2-(SYY**2)/FNUM
      WRITE(6,145) TSS
145   FORMAT(/////,2X,'TOTAL ADJUSTED SUM OF SQUARES FOR THESE DATA = ',
     $F30.2,//)
      N1P=NUMDAT-1
```

```
      IF((RANGE2.EQ.X(N1)).AND.(N1.NE.N1P)) WRITE(6,148)
148   FORMAT(///,2X,'SOME DATA SETS WITH MULTIPLE DATA AT THE HIGHEST X-
     $VALUE MAY NEED TO HAVE',/,2X,'THE UPPER JOIN POINT SEARCH RANGE RE
     $STRICTED TO BELOW THE SECOND HIGHEST',/,2X,'X-VALUE IN ORDER NOT T
     $O HAVE EXECUTION ERRORS. - DATA-DEPENDENT! -',////)
C
150   CONTINUE
C     DIVIDE DATA INTO 2 SETS FOR THE BI-LINEAR ANALYSIS
      K=K+1
      J=1
      DO 160 I=1,NUMDAT
      IF(X(I).GT.RANGE1) GO TO 170
      DTXLO(I)=X(I)
      DTYLO(I)=Y(I)
      J=J+1
160   CONTINUE
170   CONTINUE
      J1=J-1
      DO 180 I=J,NUMDAT
      DTXHI(I)=X(I)
      DTYHI(I)=Y(I)
180   CONTINUE
C     ESTIMATE PARAMETERS FOR THE 2 REGRESSIONS:
C     THIS YIELDS THE X'X MATRIX FOR REGRESSION #1.
      SIGXI=0.0
      SIGXI2=0.0
      SIGDL2=0.0
      DO 190 I=1,J1
      SIGXI=DTXLO(I) + SIGXI
      SIGXI2=DTXLO(I)**2 + SIGXI2
190   CONTINUE
      FJ1=FLOAT(J1)
      XLOBAR=SIGXI/FJ1
      DO 200 I=1,J1
      SIGDL2=(DTXLO(I)-XLOBAR)**2 + SIGDL2
200   CONTINUE
      FNUM=FLOAT(NUMDAT)
      XPXINV(1,1)=SIGXI2/(FJ1*SIGDL2)
      XPXINV(1,2)=-SIGXI/(FJ1*SIGDL2)
      XPXINV(2,1)=XPXINV(1,2)
      XPXINV(2,2)=FJ1/(FJ1*SIGDL2)
C     FORM X'Y MATRIX
      XPRIMY(1)=0.0
      XPRIMY(2)=0.0
      DO 210 I=1,J1
      XPRIMY(1)=DTYLO(I) + XPRIMY(1)
      XPRIMY(2)=DTXLO(I)*DTYLO(I) + XPRIMY(2)
210   CONTINUE
C     FORM ESTIMATES FOR BETA0 AND BET1 FOR THE LOWER SET OF DATA:
      CALL MATMLT(XPXINV,2,2,XPRIMY,1,B1HATP)
```

```
C     CALCULATE THE RESIDUAL SUM OF SQUARES FOR THIS REGRESSION:
      RHO1(K)=0.0
      B1HAT(1,K)=B1HATP(1)
      B1HAT(2,K)=B1HATP(2)
      DO 220 I=1,J1
      RHO1(K)=(Y(I)-(B1HAT(1,K)+B1HAT(2,K)*X(I)))**2 + RHO1(K)
220   CONTINUE
C     FOR REGRESSION #2:
      SIGXI=0.0
      SIGXI2=0.0
      SIGDL2=0.0
      DO 230 I=J,NUMDAT
      SIGXI=DTXHI(I)+SIGXI
      SIGXI2=DTXHI(I)**2 + SIGXI2
230   CONTINUE
      J1P=NUMDAT-J1
      FJ1P=FLOAT(J1P)
      XHIBAR=SIGXI/FJ1P
      DO 240 I=J,NUMDAT
      SIGDL2=(DTXHI(I)-XHIBAR)**2 + SIGDL2
240   CONTINUE
      XPXINV(1,1)=SIGXI2/(FJ1P*SIGDL2)
      XPXINV(1,2)=-SIGXI/(FJ1P*SIGDL2)
      XPXINV(2,1)=XPXINV(1,2)
      XPXINV(2,2)=FJ1P/(FJ1P*SIGDL2)
C     FORM THE X'Y MATRIX:
      XPRIMY(1)=0.0
      XPRIMY(2)=0.0
      DO 250 I=J,NUMDAT
      XPRIMY(1)=DTYHI(I) + XPRIMY(1)
      XPRIMY(2)=DTXHI(I)*DTYHI(I) + XPRIMY(2)
250   CONTINUE
C     FORM ESTIMATES FOR BETA0 AND BETA1 FOR THE HIGHER SET OF DATA:
      CALL MATMLT(XPXINV,2,2,XPRIMY,1,B2HATP)
C     CALCULATE THE RESIDUAL SUM OF SQUARES FOR THIS REGRESSION:
      RHO2(K)=0.0
      B2HAT(1,K)=B2HATP(1)
      B2HAT(2,K)=B2HATP(2)
      DO 260 I=J,NUMDAT
      RHO2(K)=(Y(I)-(B2HAT(1,K)+B2HAT(2,K)*X(I)))**2 + RHO2(K)
260   CONTINUE
C     CALCULATE THE JOIN POINT FOR THESE REGRESSIONS:
      JOINPT(K)=(B1HAT(1,K)-B2HAT(1,K))/(B2HAT(2,K)-B1HAT(2,K))
C     DETERMINE WHETHER OR NOT THE JOIN POINT LIES WITHIN THE REGION
C     SPECIFIED BY X(J1) AND X(J), AND SPECIFY THE VALUE FOR 'T'
C     ACCORDINGLY.
      T(K)=999.999E65
      IF((JOINPT(K).GT.X(J1)).AND.(JOINPT(K).LT.X(J))) T(K)=RHO1(K)
     $RHO2(K)
C     USE THEOREM 3A AND THE COROLLARY TO THEOREM 3D TO ELIMINATE
```

```
C     SOME POINTS FROM CONSIDERATION AS A JOIN POINT IN STEP TWO.
C     THEOREM 3A:
      IF(T(K).LT.999.999E65) DONTRY(JJ)=X(J1)
      IF(T(K).LT.999.999E65) JJ=JJ+1
      IF(T(K).LT.999.999E65) DONTRY(JJ)=X(J)
      IF(T(K).LT.999.999E65) JJ=JJ+1
C     COROLLARY TO THEOREM 3D:
      IF((JOINPT(K).GT.XLOBAR).AND.(JOINPT(K).LT.X(J1)).AND.(X(J).LT.
     $XHIBAR)) DONTRY(JJ)=X(J)
      IF((JOINPT(K).GT.XLOBAR).AND.(JOINPT(K).LT.X(J1)).AND.(X(J).LT.
     $XHIBAR)) JJ=JJ+1
      IF((X(J1).GT.XLOBAR).AND.(JOINPT(K).GT.X(J)).AND.(XHIBAR.GT.JOINPT
     $(K))) DONTRY(JJ)=X(J1)
      IF((X(J1).GT.XLOBAR).AND.(JOINPT(K).GT.X(J)).AND.(XHIBAR.GT.JOINPT
     $(K))) JJ=JJ+1
      RANGE1=X(J)
C
      IF(K.EQ.1) WRITE(6,270)
270   FORMAT('1',//,55X,'CURVE FITTING TRIALS')
      IF(K.EQ.1) WRITE(6,280)
280   FORMAT(55X,'====================')
      IF(K.EQ.1) WRITE(6,290)
290   FORMAT(//,2X,'CURVE NO.',3X,'RANGE OF ALPHA',15X,'F1(X)',28X,
     $'F2(X)',14X,'JOIN POINT',8X,'RESIDUAL SS')
      IF(K.EQ.1) WRITE(6,300)
300   FORMAT(2X,'=========',3X,'==============',3X,'====================
     $=========',4X,'============================',
     $3X,'==========',3X,'======================',/)
      WRITE(6,310) K,X(J1),X(J),B1HAT(1,K),B1HAT(2,K),B2HAT(1,K),
     $B2HAT(2,K),JOINPT(K),T(K)
310   FORMAT(4X,I4,6X,F6.2,2X,F6.2,4X,E11.4,1X,'+',1X,E11.4,'*X',5X,
     $E11.4,1X,'+',1X,E11.4,'*X',4X,F7.2,4X,F25.0)
      IF(RANGE1.LT.RANGE2) GO TO 150
C     BEFORE GOING ON TO STEP 2, APPLY THEOREM 3B TO TRY TO ELIMINATE
C     ADDITIONAL POINTS FROM CONSIDERATION AS JOIN POINTS:
      JJ=JJ-1
C     SORT TO FIND THE EQUATION NUMBER FOR THE SMALLEST VALUE OF T(K):
      NM=K-1
      DO 330 I=1,NM
      IP1=I+1
      DO 320 J=IP1,K
      IF(T(I).LE.T(J)) GO TO 320
      MINT=I
320   CONTINUE
330   CONTINUE
      IF(MINT.EQ.-999) GO TO 340
      IF(T(MINT).LT.999.999E65) JJ=JJ+1
      IF(T(MINT).LT.999.999E65) DONTRY(JJ)=X(MINT)
      IF(T(MINT).LT.999.999E65) JJ=JJ+1
      IF(T(MINT).LT.999.999E65) DONTRY(JJ)=X(MINT+1)
```

```
340   CONTINUE
C
C     COMPARE LIST OF X-VARIABLE BETWEEN THE ORIGINAL RANGE1
C     (ORANGE) AND RANGE2 WITH THE ARRAY OF X POINTS
C     WHICH IT IS OF NO VALUE TO TRY DURING STEP 2:
      DO 430 I=1,NUMDAT
      IF(X(I).LT.ORANGE) GO TO 430
      IF(X(I).GT.RANGE2) GO TO 440
      DO 350 II=1,JJ
      IF(X(I).EQ.DONTRY(II)) GO TO 430
350   CONTINUE
C     STEP 2 CALCULATIONS TO SEARCH FOR JOINS AT DATA POINTS:
      K=K+1
      DTXLOS=0.0
      DTXLO2=0.0
      DTYLOS=0.0
      DTXYLO=0.0
      DTXHIS=0.0
      DTXHI2=0.0
      DTYHIS=0.0
      DTXYHI=0.0
C     DIVIDE DATA INTO TWO SETS FOR ANALYSIS ONCE MORE:
      J=1
      DO 360 II=1,I
      DTXLO(II)=X(II)
      DTYLO(II)=Y(II)
      DTXLOS=DTXLO(II) + DTXLOS
      DTXLO2=DTXLO(II)**2 + DTXLO2
      DTYLOS=DTYLO(II) + DTYLOS
      DTXYLO=DTXLO(II)*DTYLO(II) + DTXYLO
      J=J+1
360   CONTINUE
      DO 370 II=J,NUMDAT
      DTXHI(II)=X(II)
      DTYHI(II)=Y(II)
      DTXHIS=DTXHI(II) + DTXHIS
      DTXHI2=DTXHI(II)**2 + DTXHI2
      DTYHIS=DTYHI(II) + DTYHIS
      DTXYHI=DTXHI(II)*DTYHI(II) + DTXYHI
370   CONTINUE
      FJ=FLOAT(J)
      FNUM=FLOAT(NUMDAT)
C     FORM C INVERSE MATRICES AND THE X'Y MATRICES
      DNUM=((FJ-1.0)*DTXLO2-(DTXLOS**2))
      CLOINV(1,1)=DTXLO2/((FJ-1.0)*DTXLO2-(DTXLOS**2))
      CLOINV(1,2)=-DTXLOS/((FJ-1.0)*DTXLO2-(DTXLOS**2))
      CLOINV(2,1)=CLOINV(1,2)
      CLOINV(2,2)=(FJ-1.0)/((FJ-1.0)*DTXLO2-(DTXLOS**2))
C
      CHIINV(1,1)=DTXHI2/((FNUM-FJ+1.0)*DTXHI2-(DTXHIS**2))
```

```
      CHIINV(1,2)=-DTXHIS/((FNUM-FJ+1.0)*DTXHI2-(DTXHIS**2))
      CHIINV(2,1)=CHIINV(1,2)
      CHIINV(2,2)=(FNUM-FJ+1.0)/((FNUM-FJ+1.0)*DTXHI2-(DTXHIS**2))
      XLOY(1)=DTYLOS
      XLOY(2)=DTXYLO
      XHIY(1)=DTYHIS
      XHIY(2)=DTXYHI
C     SOLVE FOR UNCONSTRAINED ESTIMATES FOR THE PARAMETERS:
      CALL MATMLT(CLOINV,2,2,XLOY,1,B1STAR)
      CALL MATMLT(CHIINV,2,2,XHIY,1,B2STAR)
C     INITIALIZE THIS MATRIX:
      DO 390 II=1,4
      DO 380 III=1,4
      CINV(II,III)=0.0
380   CONTINUE
390   CONTINUE
      CINV(1,1)=CLOINV(1,1)
      CINV(1,2)=CLOINV(1,2)
      CINV(2,1)=CLOINV(2,1)
      CINV(2,2)=CLOINV(2,2)
      CINV(3,3)=CHIINV(1,1)
      CINV(3,4)=CHIINV(1,2)
      CINV(4,3)=CHIINV(2,1)
      CINV(4,4)=CHIINV(2,2)
      D(1)=B1STAR(1)
      D(2)=B1STAR(2)
      D(3)=B2STAR(1)
      D(4)=B2STAR(2)
      Q(1)=1.0
      Q(2)=X(I)
      Q(3)=-1.0
      Q(4)=-X(I)
C     CALCULATE "S":
      CALL MATMLT(D,1,4,Q,1,S)
C     CALCULATE"TT":
      CALL MATMLT(Q,1,4,CINV,4,TM)
      CALL MATMLT(TM,1,4,Q,1,TT)
C     CALCULATE CINVQ:
      CALL MATMLT(CINV,4,4,Q,1,CINVQ)
C     CALCULATE THE BETAHATS:
      B1HAT(1,K)=D(1)-S/TT*CINVQ(1)
      B1HAT(2,K)=D(2)-S/TT*CINVQ(2)
      B2HAT(1,K)=D(3)-S/TT*CINVQ(3)
      B2HAT(2,K)=D(4)-S/TT*CINVQ(4)
C     CALCULATE THE RESIDUAL SUM OF SQUARES==BIGS FOR STEP 2
      RHO1(K)=0.0
      RHO2(K)=0.0
      J1=J-1
      DO 400 II=1,J1
      RHO1(K)=(Y(II)-(B1HAT(1,K)+B1HAT(2,K)*X(II)))**2 + RHO1(K)
```

```
400   CONTINUE
      DO 410 II=J,NUMDAT
      RHO2(K)=(Y(II)-(B2HAT(1,K)+B2HAT(2,K)*X(II)))**2 + RHO2(K)
410   CONTINUE
      BIGS=RHO1(K)+RHO2(K)
      T(K)=BIGS
      JOINPT(K)=X(I)
      WRITE(6,420) K,X(I),B1HAT(1,K),B1HAT(2,K),B2HAT(1,K),B2HAT(2,K),
     $X(I),T(K)
420   FORMAT(4X,I4,10X,F6.2,8X,E11.4,1X,'+',1X,E11.4,'*X',5X,E11.4,1X,
     $'+',1X,E11.4,'*X',5X,F6.2,4X,F25.0)
430   CONTINUE
440   CONTINUE
C     SORT THE VALUES FOR T(K) TO FIND THE SMALLEST RESIDUAL SUM OF
C     SQUARES (I.E., THE BEST FIT), THEN PRINT OUT THE EQUATIONS FOR
C     THE TWO LINES IN NON-TRUNCATED FORM.
      KSTOR=K
      NM2=K-1
      DO 470 I=1,NM2
      IP1=I+1
      DO 460 J=IP1,K
      IF(T(I).LT.T(J)) GO TO 450
      IF(T(J).LT.T(KSTOR)) KSTOR=J
      GO TO 460
450   CONTINUE
      IF(T(I).LT.T(KSTOR)) KSTOR=I
460   CONTINUE
470   CONTINUE
      WRITE(6,480) KSTOR,B1HAT(1,KSTOR),B1HAT(2,KSTOR),B2HAT(1,KSTOR),
     $B2HAT(2,KSTOR),JOINPT(KSTOR),RHO1(KSTOR),RHO2(KSTOR),T(KSTOR)
480   FORMAT(///,2X,'THE BEST FIT IS GIVEN BY EQUATION #',1X,I4,'.',/,
     $             '=======================================',//,
     $2X,'EQUATION #1 (FOR THE LOWER X VALUES) IS :',/,2X,'INTERCEPT #1
     $HAT = ',F22.10,/,2X,'BETA#1 HAT = ',6X,F22.10,//,
     $2X,'EQUATION #2 (FOR THE HIGHER X VALUES) IS :',/,
     $2X,'INTERCEPT #2 HAT = ',F22.10,/,
     $2X,'BETA#2 HAT = ',6X,F22.10,//,
     $2X,'THE JOIN POINT FOR THE TWO REGRESSIONS IS AT X =',F20.4,/,
     $2X,'THE PARTIAL RESIDUAL SUM OF SQUARES FOR F1(X) =',5X,F25.5,/,
     $2X,'THE PARTIAL RESIDUAL SUM OF SQUARES FOR F2(X) =',5X,F25.5,/,
     $2X,'THE RESIDUAL SUM OF SQUARES FOR THE COMBINED MODEL =',
     $F25.5)
      RSQUAR=1.0-T(KSTOR)/TSS
      WRITE(6,481) RSQUAR
481   FORMAT(//,2X,'THE COEFFICIENT OF DETERMINATION (R**2) FOR THE OVER
     $ALL MODEL = ',F8.5,////)
      IF ((JOINPT(KSTOR).GT.RANGE2).OR.(JOINPT(KSTOR).LT.ORANGE)) WRITE(
     $6,482)
482   FORMAT(////,2X,'WARNING !! WARNING !! THIS PROCEDURE DID NOT YIELD
     $ A JOIN POINT IN THE REGION REQUESTED !!',///)
```

```
490   CONTINUE
      STOP
      END
C.....................................................................
      SUBROUTINE MATMLT (A,M,N,B,L,C)
C     THIS SUBROUTINE MULTIPLIES MATRICES A(M,N) BY B(N,L) TO YIELD
C     MATRIX C(M,L)
      IMPLICIT REAL*8(A-H,O-Z)
      DIMENSION A(M,N), B(N,L), C(M,L)
      DO 30 I=1,M
      DO 20 J=1,L
      C(I,J)=0.0
      DO 10 K=1,N
      C(I,J)=A(I,K)*B(K,J)+C(I,J)
10    CONTINUE
20    CONTINUE
30    CONTINUE
      RETURN
      END
```

APPENDIX B

Information About the Array Dimensions Required to Run the Linear-Element FEM Program

Preliminary

NEX = No. of elements in the longitudinal (L) direction
NEY = No. of elements in the radial (R) direction
NEZ = No. of elements in the tangential (T) direction
NPX = No. of nodes in the longitudinal direction, = NEX + 1
NPY = No. of nodes in the radial direction, = NEY + 1
NPZ = No. of nodes in the tangential direction, = NEZ + 1
NDF = No. of degrees of freedom per node, = 3
NNM = No. of nodes in the mesh, = NPX x NPY x NPZ
NEQ = No. of equations in model, = NNM x NDF
NPE = Nodes per element, = 8

Arrays: Array sizes should be uniform within the program

GSTIFF (a,b)	a = No. of equations (NEQ) b = Half-band width = (NPX x NPY x NPZ + 2) x NDF If NPX $\geq$ NPY $\geq$ NPZ, HBW = (NPY x NPZ + NPZ + 2) x NDF If NPX $\geq$ NPZ $\geq$ NPY, HBW = (NPY x NPZ + NPY + 2) x NDF
GFORCE (a)	a = No. of equations (NEQ)
XCOORD (c)	c = No. of nodes along the L-axis (NPX)
YCOORD (d)	d = No. of nodes along the R-axis (NPY)
ZCOORD (e)	e = No. of nodes along the T-axis (NPZ)
X (f) Y (f) Z (f)	f = No. of nodes in the mesh (NNM)
GNOD (g,h)	g = No. of elements in the mesh (NEX x NEY x NEZ) h = No. of nodes per element (NPE), = 8
SBFNOD (i) BFVALS (i) A (i)	i = No. of specified boundary forces applied; up to 3 per node
SDFNOD (j) DFVALS (j) B (j)	j = No. of specified displacements (degrees of freedom specified); up to 3 per node
ACTMC (g) MCUSED (g)	g = No. of elements in the mesh (NEX x NEY x NEZ)
GSCOPY (k,a) RXNNOD (k)	k = No. of reaction forces requested per step a = No. of equations (NEQ)

Data Input Instructions for the Linear 3-D FEM Program

(All input is free-format unless otherwise specified)

Card No.	Mnemonics	Instructions and Comments
1	TITLE	Title card, up to an 80 character literal field.
2	TESTYP	Type of specimen modeled. Enter at least the first four letters of one of the following starting in column 1: beam, compression, tension.
2a	SYMTRY	Only used if TESTYP = beam. Must enter either a Ø or 1 in any column. A "Ø" indicates that the beam model is symmetric about the radial face and a "1" indicates that the beam model is symmetric about the tangential face.
3	INCR	Incremental analysis flag. Ø = single-step, linear analysis, 1 = multi-step analysis, linear step-by-step method.
3a	INCNUM, AUTOND	Only used if INCR = 1. INCNUM: maximum number of steps in the analysis (integer). AUTOND: when appropriate reaction forces are calculated (see below), this option can be used to automatically terminate the step-by-step model when the slope of the load-displacement curve becomes less than 100 pounds per inch displacement. Ø = option off 1 = option on
3b	DELFOR, (FORINC/ DELINC)	Only used if INCR = 1. DELFOR: a flag to specify which of either forces or displacements will be specified for certain nodes beyond the initial (linear elastic) step. 1 = forces to be applied, 2 = displacements to be specified. FORINC/DELINC: either the percent of the original force to be applied to previously loaded nodes for each step beyond the initial step (DELFOR = 1) or the additional displacement to be imposed of specified nodes for each step beyond the initial step (DELFOR = 2).

4	NEX,NEY NEZ	Three values: the (integer) number of elements in the model in the longitudinal (x), radial (y), and tangential (z) directions, respectively.
5	XCOORD	The points along the longitudinal axis at which nodes are to be placed.
6	YCOORD	The points along the radial axis at which nodes are to be placed.
7	ZCOORD	The points along the tangential axis at which nodes are to be placed.
7a	EOPSHN	Only used if TESTYP = beam. This program initially assigns a longitudinal Young's modulus to elements based on the vertical location of the element in the beam model. Assuming the elements are of equal size, if the beam model is an odd number of elements in height, the centroids of the central elements will be located on the neutral axis, and initial Young's modulus assignments (for these elements only) are delegated to the user. 1 = use the Young's modulus in tension, 2 = use the Young's modulus in compression, 3 = use the average of the tension and compression Young's moduli. After the initial step all elastic constants are determined from the direction and magnitude of the calculated strains.
8	WANTE	Mechanical property calculation flag (e.g. MOE, MOR). Ø = no, thank you 1 = yes, please
9	MCBAR,EMC, SG	MCBAR = average moisture content of model, EMC = equilibrium moisture content conditions (determines the dry, outer-layer boundary condition for the desorption moisture gradient model). Note that EMC must not be greater than MCBAR. If MCBAR = EMC then it is assumed that no gradient is present. SG = specific gravity of (yellow-poplar) model, ovendry weight/green volume basis. The program is based on data collected within the range of 0.371-0.460, although it does not abort if these limits are ignored. A warning message is printed on the output, however.
10	POSYMX POSYMY POSYMZ OVRRID	POSYM_ = number of planes of symmetry to be imposed in the longitudinal, radial and tangential directions, respectively (up to 2 each). Default planes are specified for uniaxial models. These are:

L = XCOORD(1), R = YCOORD(NEX+1) and T = ZCOORD(NEZ+1).
For beams these are:
L = XCOORD(NEX+1), R = YCOORD(NEX+1) when SYMTRY = 1, or R = YCOORD(NEY+1) when SYMTRY = 2, T = ZCOORD(NEZ+1).

OVRRID: Ø if the default planes of symmetry are acceptable,
1 if other planes of symmetry are required.

10a OVRNOD(I), OVRVAL(I)

Only used if OVRRID = 1.

OVRNOD: the L-, R-, or T-axis value at which plane of symmetry is to be placed. (Put cards in L, R, T order.)

OVRVAL: the specified displacement (usually 0.0) corresponding to the OVRNOD plane specified on the same card.

Example: POSYMX = 1, POSYMY = 2, POSYMZ = Ø, OVRRID = 1
Planes of symmetry desired at L = 0.0, R = 0.0 and 0.5. All specified displacements = 0.0.

Example Input:

```
1  2  0  1      POSYMX,...
0.0  0.0        L-plane
0.0  0.0 }      R-plane
0.5  0.0 }
```

11 NSBFX, NSBFY, NSBFZ

Number of specified boundary forces to be applied in the longitudinal, radial and tangential directions, respectively.

11a LOADX, LOADY, LOADZ, LOAD, (INCFLG)

Only used if (NSBFX+NSBFY+NSBFZ)>0. L, R, T coordinates for each node loaded, followed by the load magnitude. (+) indicates tension, (-) indicates compression (towards axis origin). Input forces to be applied in the longitudinal direction first, then the radial direction, with the forces in the tangential direction last (one node per card). If a stepwise analysis is requested and DELFOR = 1, then INCFLG must be either a "Ø" or a "1" for each node.
Ø: Don't increment the load of this node,
1: Increase the load at this node after the initial step.

12 NSDFX, NSDFY, NSDFZ

Number of specified displacements to be applied in the longitudinal, radial and tangential directions, respectively. Displacements previously specified by POSYMX, etc., must not be included here.

12a RXNREQ,
LOADX,
LOADY,
LOADZ,
LOAD,
(INCFLG)

Only used if (NSDFX+NSDFY+NSDFZ)>Ø.

RXNREQ: option to calculate reaction forces at this node resulting from specified displacements.
Ø = no, thank you,
1 = yes, please

LOADX,-Y,-Z: (L,R,T) coordinates for each node with specified displacements (not including POSYMX, etc., nodes).

LOAD: the specified displacement. (-) indicates compression (towards the axis origin), (+) indicates tension.

INCFLG: Add specified displacements to the node after the initial step (only required if DELFOR = 2)
Ø = no, thank you,
1 = yes, please

13 LOADX,
LOADY,
LOADZ

Only required if WANTE = 1.
The (L,R,T) coordinate at which the mechanical properties will be calculated at the end of each step.

```
C     ..............................................................
C
C                    ##############################
C                    #                            #
C                    #  F E M M E   F A T A L E   #
C                    #                            #
C                    ##############################
C
C     ..............................................................
C
C         3 - D   F I N I T E   E L E M E N T S   P R O G R A M
C
C     LINEAR, 8-NODE ELEMENT PROGRAM WITH NON-LINEAR CAPABILITY (STEP
C     BY STEP METHOD)
C
C     ..............................................................
C
C
C     THIS PROGRAM WAS WRITTEN BY TERRANCE E. CONNERS, DEPARTMENT OF
C     FOREST PRODUCTS, VIRGINIA TECH (VPI & SU), 703-961-4524. IT WAS
C     BASED UPON PROGRAMS WRITTEN BY DR. J.N. REDDY,DEPT. OF ENGINEERING
C     SCIENCE & MECHANICS AT VA. TECH.
C
C     THIS PARTICULAR PROGRAM WAS WRITTEN TO DEAL WITH WOOD WITH A 2-D
C     PARABOLIC MOISTURE GRADIENT ACROSS THE CROSS-SECTION.  IT CAN BE
C     USED FOR BOTH A LINEAR ANALYSIS OR A PLASTIC ANALYSIS OF YELLOW-
C     POPLAR (USES STEP-BY-STEP METHOD).  SPECIFIC EQUATIONS FOR
C     YELLOW-POPLAR PROPERTIES ARE LOCATED WITHIN SBR CKALC; EQUATIONS
C     ARE INCLUDED FOR BOTH COMPRESSION AND TENSION PROPERTIES.
C
C     NOTE: ALTHOUGH BOTH LOADS AND DISPLACEMENTS CAN BE SPECIFIED FOR
C     ====  THE INITIAL (ELASTIC) STEP, THE PROGRAM IS STRUCTURED SUCH
C           THAT EITHER LOADS OR DISPLACEMENTS CAN BE INCREMENTED FOR
C           SUCCEEDING STEPS, BUT NOT BOTH !!!
C           ALSO, THERE IS NO PROVISION FOR STARTING THE ANALYSIS WITH
C           AN INITIAL DISPLACEMENT ONLY AND INCREMENTING BY A GIVEN
C           LOAD IN SUCCEEDING STEPS (OR VICE-VERSA).
C
C     ..............................................................
C
C                      *************************
C                       M A I N   P R O G R A M
C                      *************************
C
C     ..............................................................
C
C
C     ALL REAL VARIABLES ARE DOUBLE PRECISION.
      IMPLICIT REAL*8(A-H,O-Z)
      REAL*8 BEMWID,BEMDEF,BEMLEN,MCBAR,EMC,XCOORD,SG
```

```
     1,YCOORD,ZCOORD,HAFWID,HAFDEF,X,Y,Z,GFORCE,GSTIFF,ACTMC,MCUSED
     2,BFVALS,DFVALS,ELXYZ,LFORCE,VE,W,SF,GDSF,LSTIFF,GJ,GJINV,DSF,C,REA
     3XNS,RXNSUM,DELINC,FORINC,MOE,MOI,MOR,VALUES,DELTA1,E,STRES1,TT,DF,
     4STRAIN,DOODLE,LOD1,LOD2,P1,OVRNOD,OVRVAL,MCMAX,LSUM1,LSUM2
      INTEGER GNOD,NPE,NDF,NGP,NEX,NEY,NEZ,NPX,NPY,NPZ,NNM,NEM,HBW,NW,NE
     1Q,NN,NSBFX,NSBFY,NSBFZ,NSBF,NNSBF,SBFNOD,NSDFX,NSDFY,NSDFZ,NSDF,NN
     2SDF,SDFNOD,NI,NR,I,J,K,L,M,II,JJ,KK,NCL,NC,IRES,IE,NNN,NODE,P,VECL
     3EN,SYMTRY,DIR,ORDER,A,B,X1,Y1,Z1,EOPSHN,DUMMY1,DUMMY2,EPRINT,TITLE
     4,RXN,RXNNOD,NUMRXN,BNDWID,TESTYP,BEAM1,UNIAX1,UNIAX2,IT,INCVTR
     5,INC,INCR,DELFOR,INCNUM,INCFLG,GRAD,WANTE,INTGER,NUMLOD,TABORT,END
     6EL,AAA,POSYMX,POSYMY,POSYMZ,OVRRID,COORD,CHECK,CHECK1,CHECK2,CHECK
     73,AAA1,AAA2,AAA3,AAA4,BWTYPE,AUTOND
      COMMON /LCOORD/ XCOORD
      COMMON /RCOORD/ YCOORD
      COMMON /TCOORD/ ZCOORD
      COMMON /SHAPE/ SF
      COMMON /MESH/ GNOD
      COMMON /VECTR1/ LOD1,LOD2
      COMMON /VECTR2/ RXNNOD
      COMMON /VECTR3/ VECLEN
      COMMON /GSHAPE/ GDSF
      COMMON /GLOBAL/ GSTIFF,GFORCE
      COMMON /ELEM/ LSTIFF,LFORCE
      COMMON /XYZ/ X,Y,Z
      COMMON /ELK/ ELXYZ
      COMMON /MOIST1/ ACTMC
      COMMON /MOIST2/ MCUSED,EMC,MCBAR,HAFWID,MCMAX,SG,
     1HAFDEF,N,NEM,SYMTRY,IT,GRAD,EOPSHN,TESTYP
      COMMON /SIGMA/ C,TT
      COMMON /INCRMT/ INCVTR
C     CHANGE JUST THIS FIRST DIMENSION STATEMENT FOR EACH PROBLEM: ALSO
C     CHANGE THE VALUES FOR MCUSED, ACTMC, X, Y, Z, XCOORD, YCOORD,
C     ZCOORD, GNOD, RXNNOD, GSTIFF, GFORCE, AND INCVTR IN THE
C     APPROPRIATE SUBROUTINES.
C
      DIMENSION GSTIFF(2772,102), GFORCE(2772), XCOORD(33), YCOORD(007),
     1ZCOORD(04), X(924), Y(924), Z(924), GNOD(576,8), SBFNOD(001), SDFN
     2OD(267), BFVALS(001), DFVALS(267), ACTMC(576), MCUSED(576), A(001)
     3, B(267), GSCOPY(004,2772), RXNNOD(004), INCVTR(004)
C
C     THIS NEXT DIMENSION STATEMENT WILL ONLY HAVE TO BE CHANGED IF IT
C     IS DESIRED TO HAVE MORE THAN 2 PARALLEL PLANES OF SYMMETRY
C     PERPENDICULAR TO ANY AXIS. ALSO CHANGE IN SUBROUTINE MIRROR.
      DIMENSION OVRNOD(2), OVRVAL(2)
C
C     THESE DIMENSIONS DO NOT HAVE TO BE CHANGED:
      DIMENSION ELXYZ(8,3), W(3,8), LSTIFF(24,24), LFORCE(24), SF(8), DS
     1F(3,8), GDSF(3,8), C(6,6), GJ(3,3), GJINV(3,3), NSBF(3), NSDF(3),
     2TITLE(20), NUMLOD(3)
C
```

```
      DATA NPE,NDF,NGP/8,3,2/
      DATA X1,Y1,Z1/1HL,1HR,1HT/
      DATA BEAM1,UNIAX1,UNIAX2/4HBEAM,4HTENS,4HCOMP/
      LOD1=0.0
      LOD2=0.0
      SYMTRY=0
      RXNSUM=0.0
      NUMRXN=0
      IT=1
      INCNUM=1
      INCR=0
      TABORT=0
      INC=0
      INCA=0
      INCB=0
      INCC=0
      DELTA1=0.0
      P1=0.0
      DELFOR=0
      AAA=0
      DOODLE=0.0
      DUMMY1=0
      DUMMY2=0
      LSUM1=0.0
      LSUM2=0.0
      AUTOND=0
C-----------------------------------------------------------------------
C
C     EXPLANATIONS OF SOME BASIC VARIABLES USED IN THIS PROGRAM:
C
C     X,Y,Z REFER TO THE LONGITUDINAL,RADIAL, AND TANGENTIAL DIRECTIONS,
C     RESPECTIVELY.
C
C     NEX,NEY,AND NEZ =  THE NUMBERS OF ELEMENTS IN THE X-, Y-, AND Z-
C                        DIRECTIONS, RESPECTIVELY.
C     NPX,NPY,AND NPZ =  THE NUMBER OF NODAL POINTS FOR A LINEAR,8-NODE
C                        ELEMENT IN THE X-, Y-, AND Z-DIRECTIONS,
C                        RESPECTIVELY.
C
C     NNM = NUMBER OF NODES IN THE MESH
C     NEM = NUMBER OF ELEMENTS IN THE MESH
C     NEQ = NUMBER OF EQUATIONS
C     NN = NO. OF DEGREES OF FREEDOM PER ELEMENT
C
C     X-,Y-,ZCOORD(I) = ARRAYS OF NODE POSITIONS ALONG EACH RESPECTIVE
C                       AXIS
C
C***********************************************************************
C
C       INPUT SECTION, EXCLUDING THE BOUNDARY CONDITION INPUT
```

```
C
C*********************************************************************
C
C     DESCRIPTION OF REQUIRED INPUT:
C
C     TITLE: (UP TO 80 CHARACTER STRING)
C
C     TESTYP:
C     PUT IN A CARD DESCRIBING THE TYPE OF TEST: WRITE EITHER "BEAM",
C     "TENSION", OR "COMPRESSION" (W/O THE QUOTE MARKS)
C
C     SYMTRY=1 MEANS THAT THE BEAM IS SYMMETRIC ABOUT A RADIAL PLANE
C     SYMTRY=2 MEANS THAT THE BEAM IS SYMMETRIC ABOUT A TANGENTIAL PLANE
C
C     INCR = INCREMENTAL ANALYSIS FLAG: 0=NO (1-STEP LINEAR),
C                                       1=YES (STEP-BY-STEP METHOD)
C
C     INCNUM = NO. OF STEPS IN INCREMENTAL ANALYSIS (STEP-BY-STEP)
C
C     AUTOND = AUTOMATIC TERMINATION OPTION FOR USE IN STEPWISE
C              MODELS WHEN REACTION FORCES ARE CALCULATED.
C                  0 = OPTION OFF       1 = OPTION ON
C
C     DELFOR = FLAG TO SPECIFY WHETHER A FORCE OR A DISPLACEMENT WILL BE
C              APPLIED AT EACH STEP OF THE INCREMENTAL ANALYSIS: 1=FORCE
C              2=DISPLACEMENT
C
C     FORINC, DELINC = FORCE OR DISPLACEMENT INCREMENT TO BE APPLIED AT
C              EACH STEP OF THE ANALYSIS AFTER THE FIRST (ALLOWS A
C              LARGER INITIAL FORCE OR DISPLACEMENT TO BE APPLIED,
C              THEREBY DECREASING THE NUMBER OF STEPS NECESSARY TO
C              REACH A SPECIFIC REGION OF STRESS). FORINC IS THE PERCENT
C              OF THE ORIGINAL LOAD AT LOADED NODES WHICH IS TO BE ADDED
C              TO THOSE NODES DURING INCREMENTAL ANALYSIS.  DELINC IS
C              THE AMOUNT OF ADDITIONAL DISPLACEMENT TO BE ADDED TO EACH
C              NODE (AS SPECIFIED BY INPUT).
C              ## N.B.:  FORCES OR DISPLACEMENTS WILL ONLY BE APPLIED
C              WHERE SPECIFIED BY DATA CARDS (USING INCFLG).
C
C     EOPSHN (E-OPTION) IS REQUIRED TO SPECIFY THE ELASTIC PROPERTIES
C     OF BEAM ELEMENTS AT THE NEUTRAL AXIS WHEN THERE IS AN ODD NUMBER
C     OF ELEMENTS THROUGH THE DEPTH OF THE BEAM (STEP 1 ONLY).  AFTER
C     STEP 1, PROPERTIES ARE ASSIGNED BY TYPE (DIRECTION) OF STRESS
C     OR STRAIN.
C     EOPSHN = 1: TENSION PROPERTIES WILL BE USED.
C     EOPSHN = 2: COMPRESSION PROPERTIES WILL BE USED.
C     EOPSHN = 3: THE AVERAGE OF TENSION AND COMPRESSION PROPERTIES
C                 WILL BE USED.
C
C     WANTE = 0 : NO MECHANICAL PROPERTY CALCULATIONS REQUESTED
```

```
C     WANTE = 1 : CALCULATIONS FOR MOE, MOR, ETC., WILL BE CALCULATED
C                 AS APPROPRIATE
C
C     MCBAR =  AVERAGE MOISTURE CONTENT OF THE MODELED SPECIMEN
C     EMC   =  EMC CONDITIONS TO WHICH THE MODELED SPECIMEN WAS EXPOSED
C              N.B.  THIS PGM IS BASED ON DATA COLLECTED AT MC'S AT AND
C              ####  ABOVE 6% MC.  RESULTS OF CALCULATIONS WHERE EMC IS
C                    LESS THAN 6% MC MAY BE INACCURATE !!
C
C     NOTE: TO RUN THIS PROGRAM FOR A SAMPLE W/O A MOISTURE GRADIENT,
C     ====  INPUT FOR MCBAR SHOULD EQUAL THE INPUT FOR EMC.
C
C     SG    = SPECIFIC GRAVITY OF MODELED SPECIMEN (WEIGHT OVENDRY
C             DIVIDED BY GREEN VOLUME).  LEGITIMATE VALUES (NO
C             EXTRAPOLATION) RANGE FROM 0.371 TO 0.460, INCLUSIVE.
C
C-----------------------------------------------------------------------
C     TITLE CARD DESCRIBING THE PROBLEM TO BE ANALYSED:
C
      READ (5,10) (TITLE(I),I=1,20)
10    FORMAT (20(A4))
C
      READ (5,20) TESTYP
20    FORMAT (1A4)
      IF (TESTYP.EQ.BEAM1) READ(5,*) SYMTRY
      READ (5,*) INCR
      IF (INCR.EQ.1) READ (5,*) INCNUM,AUTOND
      IF (INCR.EQ.1) READ (5,*) DELFOR,DF
      IF ((INCR.EQ.1).AND.(DELFOR.EQ.1)) FORINC=DF
      IF ((INCR.EQ.1).AND.(DELFOR.EQ.2)) DELINC=DF
      READ (5,*) NEX,NEY,NEZ
      NPX=NEX+1
      NPY=NEY+1
      NPZ=NEZ+1
      NPXY=NPX*NPY
      NNM=NPX*NPY*NPZ
      NEM=NEX*NEY*NEZ
      NEQ=NNM*NDF
      NN=NPE*NDF
C
C     READ THE MESH COORDINATES FOR THE BEAM:  FIRST THE VECTOR OF X-
C     COORDINATES (LONGITUDINAL DIRECTION), FOLLOWED BY THE Y-COOR-
C     DINATES (RADIAL DIRECTION), THEN THE Z-COORDINATES (TANGENTIAL
C     DIRECTION).
      READ (5,*) (XCOORD(I),I=1,NPX)
      READ (5,*) (YCOORD(I),I=1,NPY)
      READ (5,*) (ZCOORD(I),I=1,NPZ)
      IF (TESTYP.NE.BEAM1) SYMTRY=1
      IF ((TESTYP.EQ.BEAM1).AND.(SYMTRY.EQ.1)) DUMMY1=NEY/2
      IF ((TESTYP.EQ.BEAM1).AND.(SYMTRY.EQ.2)) DUMMY1=NEZ/2
```

```
      IF((TESTYP.EQ.BEAM1).AND.(DUMMY1.EQ.0)) DUMMY1=-1
      IF (TESTYP.EQ.BEAM1) DUMMY2=2*DUMMY1
      IF((TESTYP.EQ.BEAM1).AND.(SYMTRY.EQ.1)) DUMMY1=NEY
      IF((TESTYP.EQ.BEAM1).AND.(SYMTRY.EQ.2)) DUMMY1=NEZ
      IF ((TESTYP.EQ.BEAM1).AND.(DUMMY2.LT.DUMMY1)) READ (5,*) EOPSHN
C
C     "WANTE" IS THE FLAG FOR THE CALCULATION OF MECHANICAL PROPERTIES
C     USING DATA FOR A PARTICULAR NODAL POINT.
C NB: IT IS NECESSARY FOR REACTION FORCES TO BE CALCULATED IN ORDER
C     FOR THIS OPTION TO WORK IF ONLY DISPLACEMENTS ARE SPECIFIED
      READ (5,*) WANTE
C
C     READ IN THE VARIABLES DESCRIBING THE MOISTURE CONTENT CONDITION
C     AND THE SPECIFIC GRAVITY (GREEN VOLUME, OD WEIGHT BASIS)
C     LEGITIMATE RANGE FOR SG IS 0.371 TO 0.460
      READ (5,*) MCBAR,EMC,SG
      IF((MCBAR-EMC).GT.0.0) MCMAX=2.25*MCBAR-1.25*EMC
C           ........................................
C           :              ## ECHO ##              :
C           :                                      :
C           : PRINT THE DATA INPUT TO THE PROGRAM.  :
C           :......................................:
C
      WRITE (6,30)
30    FORMAT(1H1,/,47X,40H****************************************,/,47X
     1,1H*,38X,1H*,/,47X,40H*        F E M M E   F A T A L E       *,/,4
     27X,1H*,38X,1H*,/,47X,40H*  A 3-DIMENSIONAL NONLINEAR FINITE    *,/
     3,47X,                 40H* ELEMENTS PROGRAM FOR WOOD MECHANICS  *,/
     #,47X,1H*,38X,1H*,/
     4,47X,                 40H*    LINEAR,8-NODE ELEMENT PROGRAM     *,/
     #,47X,1H*,38X,1H*,/
     5,47X,                 40H*           BY T.E. CONNERS,           *,/
     6,47X,                 40H*    DEPARTMENT OF FOREST PRODUCTS     *,/
     7,47X,                 40H*           VIRGINIA TECH              *,/
     8,47X,                 40H*     BLACKSBURG, VIRGINIA   24061     *,/
     9,47X,                 40H*          (703) 961-4524              *,/
     !,47X,1H*,38X,1H*,/
          ,47X,                 40H*      LAST CHANGED MARCH, 1985
     #,47X,1H*,38X,1H*,/,
     $47X,40H****************************************,///)
      WRITE (6,40)
40    FORMAT (47X,40H****************************************,/,47X,40H*
     1                                   *,/,47X,40H* DATA SET-UP AND
     2 DATA PRE-PROCESSING  *,/,47X,40H*
     3      *,/,47X,40H****************************************,////)
      WRITE (6,50) (TITLE(I),I=1,20)
50    FORMAT (///,2X,20(A4),///)
      IF (TESTYP.EQ.UNIAX1) WRITE (6,60)
60    FORMAT (/,2X,26HTHIS IS A TENSION PROBLEM.,/)
      IF (TESTYP.EQ.UNIAX2) WRITE (6,70)
```

```
70    FORMAT (/,2X,30HTHIS IS A COMPRESSION PROBLEM.,/)
      IF (TESTYP.EQ.BEAM1) WRITE (6,80)
80    FORMAT (/,2X,23HTHIS IS A BEAM PROBLEM.,/)
      IF (TESTYP.NE.BEAM1) GO TO 120
      IF (SYMTRY.EQ.1) GO TO 100
      WRITE(6,90)
90    FORMAT (2X,49HSYMMETRY IS ESTABLISHED ABOUT A TANGENTIAL PLANE.,/)
      GO TO 120
100   CONTINUE
      WRITE(6,110)
110   FORMAT (2X,45HSYMMETRY IS ESTABLISHED ABOUT A RADIAL PLANE.,/)
120   CONTINUE
      IF (INCR.EQ.0) WRITE (6,130)
130   FORMAT (2X,46HA ONE-STEP LINEAR ANALYSIS HAS BEEN REQUESTED.,//)
      IF ((INCR.EQ.1).AND.(DELFOR.EQ.1)) WRITE (6,140) INCNUM
140   FORMAT (2X,39HINCREMENTAL ANALYSIS WAS REQUESTED WITH,1X,I3,1X,16H
     1LOAD INCREMENTS.,//)
      IF ((INCR.EQ.1).AND.(DELFOR.EQ.2)) WRITE (6,150) INCNUM
150   FORMAT (2X,39HINCREMENTAL ANALYSIS WAS REQUESTED WITH,1X,I3,1X,24H
     1DISPLACEMENT INCREMENTS.,//)
      IF (AUTOND.EQ.1) WRITE (6,151)
151   FORMAT (//,2X,'AUTO-TERMINATION REQUESTED.  THIS FEATURE WORKS ONL
     $Y IF REACTION FORCES ARE CALCULATED.',//)
      WRITE (6,210) NEX
210   FORMAT (2X,51HNUMBER OF ELEMENTS IN THE LONGITUDINAL DIRECTION = ,
     1I2)
      WRITE (6,220) NEY
220   FORMAT (2X,45HNUMBER OF ELEMENTS IN THE RADIAL DIRECTION = ,I2)
      WRITE (6,230) NEZ
230   FORMAT (2X,49HNUMBER OF ELEMENTS IN THE TANGENTIAL DIRECTION = ,I2
     1,//)
      WRITE (6,240) NEM
240   FORMAT (2X,9HTHERE ARE,1X,I4,1X,21HELEMENTS IN THE MESH.)
      WRITE (6,250) NNM
250   FORMAT (2X,9HTHERE ARE,1X,I4,1X,18HNODES IN THE MESH.,//)
      WRITE (6,260)
260   FORMAT (2X,75HTHESE ARE THE L-, R-, AND T-COORDINATE DATA FOR THE
     1NODES IN THIS PROBLEM :,/,2X,30H(L,R,T MEANS L,R,T DIRECTIONS))
      WRITE (6,270)
270   FORMAT (/,2X,16HL-COORDINATES = )
      WRITE (6,*) (XCOORD(I),I=1,NPX)
      WRITE (6,280)
280   FORMAT (/,2X,16HR-COORDINATES = )
      WRITE (6,*) (YCOORD(I),I=1,NPY)
      WRITE (6,290)
290   FORMAT (/,2X,16HT-COORDINATES = )
      WRITE (6,*) (ZCOORD(I),I=1,NPZ)
      WRITE (6,320) MCBAR,EMC
320   FORMAT (///,2X,30HTHE AVERAGE MC FOR THE SAMPLE=,1X,F10.5,1X,1H%,/
     1,2X,66HTHE CONDITIONS THE SAMPLE WAS EXPOSED TO CORRESPONDS TO AN
```

```
     2EMC OF ,1X,F10.5,1X,2H%.)
      IF (MCBAR.LT.EMC) WRITE (6,321)
321   FORMAT (//,2X,'EMC MUST BE LESS THAN THE AVERAGE MOISTURE CONTENT.
     $  YOU GOOFED UP THE INPUT.  PROGRAM TERMINATING.',//)
      IF (MCBAR.LT.EMC) GO TO 1400
      IF ((MCBAR.LT.6.0).OR.(EMC.LT.6.0)) WRITE(6,322)
322   FORMAT(///,1X,'#####  IMPORTANT !!!  #####    DATA WERE NOT COLLEC
     $TED AT MOISTURE CONTENTS BELOW 6%.',/,2X,'RESULTS OF THIS ANALYSIS
     $ ARE BASED ON EXTRAPOLATION AND MAY BE INACCURATE !!!')
      WRITE (6,323) SG
323   FORMAT (//,2X,'SPECIFIED SPECIFIC GRAVITY (WT OD/GREEN VOL) = ',F6
     $.3,/)
      IF ((SG.LT.0.371).OR.(SG.GT.0.460)) WRITE (6,324)
324   FORMAT (//,2X,'SG SHOULD BE WITHIN 0.371 TO 0.460 RANGE.  EXTRAPOL
     $ATION MAY LEAD TO ERRORS.  EXECUTION CONTINUING.',///)
      IF (MCBAR.EQ.EMC) GO TO 340
      WRITE (6,330)
330   FORMAT (///,2X,56H2-D PARABOLIC MOISTURE GRADIENT ASSUMED IN CALCU
     1LATIONS.,/////)
      GO TO 360
340   CONTINUE
      WRITE (6,350)
350   FORMAT (///,2X,50HMC ASSUMED TO BE UNIFORM ACROSS THE CROSS-SECTIO
     1N.,/////)
360   CONTINUE
C
C     CALL SUBROUTINE MESH3D TO GENERATE MESH AND NODE COORDINATES.
C
      CALL MESH3D (NPE,NEX,NEY,NEZ,NPX,NPY,NPZ,NNM,NEM,NPXY,BWTYPE)
C
C     COMPUTE THE HALF-BAND WIDTH OF THE GLOBAL [K] MATRIX.
C     HBW=HALF-BAND WIDTH
C     THESE METHODS OF CALCULATING THE HALF-BAND WIDTH WILL NOT WORK FOR
C     OTHER NODE-NUMBERING SCHEMES: (BWTYPE IS DEFINED IN SBR MESH3D)
      IF (BWTYPE.EQ.1) HBW=(NPXY+NPX+2)*NDF
      IF (BWTYPE.EQ.2) HBW=(NPY*NPZ + NPZ +2)*NDF
      IF (BWTYPE.EQ.3) HBW=(NPY*NPZ + NPY +2)*NDF
      WRITE (6,380) HBW
380   FORMAT (///,2X,18HHALF-BAND WIDTH = ,2X,I5,/,2X,82HMAKE SURE ALL A
     1RRAYS ARE DIMENSIONED PROPERLY, OR AN ADDRESSING ERROR WILL RESULT
     2.,//)
C*********************************************************************
C        COORDINATES FOR PLANES WITH SPECIFIED DISPLACEMENTS
C      (ESPECIALLY PLANES OF SYMMETRY WITH DISPLACEMENTS ==0.0)
C                         ARE READ IN HERE.
C
C     POSYMX,-Y,-Z==THE NO. OF PARALLEL PLANES TO HAVE SPECIFIED
C     DISPLACEMENTS IN THE L-,R-, AND T-DIRECTIONS RESPECTIVELY.
C     (MAXIMUM VALUES OF POSYMX, ETC., = 2 UNLESS OVRNOD & OVRVAL
C     ARE RE-DIMENSIONED)
```

```
C
C     NOTE THAT REACTION FORCES CANNOT BE REQUESTED WITH THIS OPTION.
C
C     WHEN OVRRID (OVERRIDE) = 0, DEFAULT PLANES ARE SET IN THE MAIN
C     PGM WHENEVER  POSYMX, POSYMY, OR POSYMZ ARE SET EQUAL TO ONE.
C     A DISPLACEMENT OF 0.0 IS SPECIFIED BY THIS OVERRIDE OPTION.
C     THE DEFAULT PLANES ARE DETERMINED BY THE MAIN PROGRAM JUST
C     BEFORE THE CALLS TO SUBROUTINE MIRROR. THE DEFAULT PLANES FOR
C     L=XCOORD(1), R=YCOORD(NPY), AND FOR T=ZCOORD(NPZ) (IN "OVRNOD"),
C     UNLESS THE TEST TYPE IS A BEAM, IN WHICH CASE THE DEFAULT FOR
C     THE L-PLANE IS XCOORD(NPX).
C
C     WHEN OVRRID = 1, PAIRS OF (L-,R-, OR T-COORDINATE, DISPLACEMENT)
C     MUST BE READ INTO THE PROGRAM, UP TO TWO PAIRS PER DIRECTION
C     (CORRESPONDS TO TWO PLANES), IN L-,R-,T-PLANE ORDER.
C
C     THE NODES AND THEIR DISPLACEMENTS ARE PRINTED JUST BEFORE THE
C     SECOND CALL TO VECTOR TO SET THE OTHER SPECIFIED DISPLACEMENTS.
C
C***********************************************************************
      READ (5,*) POSYMX,POSYMY,POSYMZ,OVRRID
C     BEMWID, BEMDEF & BEMLEN = THE BEAM DIMENSIONS.
      IF (SYMTRY.EQ.1) BEMWID=ZCOORD(NPZ)
      IF (SYMTRY.EQ.2) BEMWID=YCOORD(NPY)
      IF ((SYMTRY.EQ.1).AND.(POSYMZ.GE.1)) BEMWID=ZCOORD(NPZ)*2.0
      IF (SYMTRY.EQ.1) BEMDEF=YCOORD(NPY)
      IF ((SYMTRY.EQ.2).AND.(POSYMY.GE.1)) BEMWID=YCOORD(NPY)*2.0
      IF (SYMTRY.EQ.2) BEMDEF=ZCOORD(NPZ)
      BEMLEN=XCOORD(NPX)
      IF ((TESTYP.EQ.BEAM1).AND.(POSYMX.GE.1)) BEMLEN=XCOORD(NPX)*2.0
      IF ((TESTYP.NE.BEAM1).AND.(POSYMY.GE.1)) BEMDEF=YCOORD(NPY)*2.0
      IF ((TESTYP.NE.BEAM1).AND.(POSYMZ.GE.1)) BEMWID=ZCOORD(NPZ)*2.0
      IF ((TESTYP.NE.BEAM1).AND.(POSYMX.GE.1)) BEMLEN=XCOORD(NPX)*2.0
      HAFWID=BEMWID/2.0
      HAFDEF=BEMDEF/2.0
      WRITE (6,370) BEMWID,BEMDEF,BEMLEN
370   FORMAT (2X,24HACTUAL SAMPLE WIDTH (T)=,2X,F8.4,5X,17HACTUAL DEPTH
     1(R)=,2X,F8.4,5X,25HACTUAL SAMPLE LENGTH (L)=,2X,F8.4,////)
      MOI=BEMWID*(BEMDEF**3)/12.0
      OVRNOD(1)=XCOORD(1)
      IF(TESTYP.EQ.BEAM1) OVRNOD(1)=XCOORD(NPX)
      OVRVAL(1)=0.0
      OVRNOD(2)=0.0
      OVRVAL(2)=0.0
      IF ((OVRRID.EQ.1).AND.(POSYMX.GE.1)) READ (5,*) (OVRNOD(I),OVRVAL(
     1I),I=1,POSYMX)
      COORD=1
      VECLEN=POSYMX*NPY*NPZ+POSYMY*NPX*NPZ+POSYMZ*NPX*NPY
      IF (POSYMX.GE.1) CALL MIRROR (POSYMX,COORD,OVRNOD,OVRVAL,NDF,NPX,N
     1PY,NPZ,NNM,AAA,SDFNOD,DFVALS,BWTYPE)
```

```
      AAA1=AAA
      OVRNOD(1)=YCOORD(NPY)
      OVRVAL(1)=0.0
      IF ((OVRRID.EQ.1).AND.(POSYMY.GE.1)) READ (5,*) (OVRNOD(I),OVRVAL(
     1I),I=1,POSYMY)
      COORD=2
      IF (POSYMY.GE.1) CALL MIRROR (POSYMY,COORD,OVRNOD,OVRVAL,NDF,NPX,N
     1PY,NPZ,NNM,AAA,SDFNOD,DFVALS,BWTYPE)
      AAA2=AAA-AAA1
      OVRNOD(1)=ZCOORD(NPZ)
      OVRVAL(1)=0.0
      IF ((OVRRID.EQ.1).AND.(POSYMZ.GE.1)) READ (5,*) (OVRNOD(I),OVRVAL(
     1I),I=1,POSYMZ)
      COORD=3
      IF (POSYMZ.GE.1) CALL MIRROR (POSYMZ,COORD,OVRNOD,OVRVAL,NDF,NPX,N
     1PY,NPZ,NNM,AAA,SDFNOD,DFVALS,BWTYPE)
      AAA3=AAA-(AAA2+AAA1)
      AAA4=AAA+1
C*********************************************************************
C             SPECIFIED BOUNDARY FORCES ARE READ IN HERE              C
C                  ECHO THE BOUNDARY INFORMATION                      C
C*********************************************************************
C     NSBFX=NO. OF BOUNDARY FORCES APPLIED IN THE L (OR LONGITUDINAL)
C     DIRECTION.  NSBFY =NO. OF BOUNDARY FORCES APPLIED IN THE R (OR
C     RADIAL) DIRECTION.  NSBFZ=NO. OF BOUNDARY FORCES APPLIED IN THE T
C     (OR TANGENTIAL) DIRECTION.
      READ (5,*) NSBFX,NSBFY,NSBFZ
      WRITE (6,390) NSBFX,NSBFY,NSBFZ
390   FORMAT (//,2X,37HNO. OF BOUNDARY FORCES APPLIED IN THE,/,7X,23HLON
     1GITUDINAL DIRECTION=,20X,I5,/,7X,42HRADIAL DIRECTION (ON THE TANGE
     2NTIAL FACE)=,1X,I5,/,7X,42HTANGENTIAL DIRECTION (ON THE RADIAL FAC
     3E)=,1X,I5,/)
      NSBF(1)=NSBFX
      NSBF(2)=NSBFY
      NSBF(3)=NSBFZ
      NNSBF=NSBF(1)+NSBF(2)+NSBF(3)
      IF (NNSBF.LE.0) GO TO 530
C
C     ##########################################
C  >> RETURN TO THIS POINT AFTER EACH STEP
C     ##########################################
C
400   CONTINUE
      IF (NNSBF.LE.0) GO TO 600
      IF (IT.EQ.1) GO TO 450
      IF ((IT.EQ.2).AND.(DELFOR.EQ.1)) GO TO 410
      IF (IT.GE.2) GO TO 510
410   CONTINUE
      DO 440 I=1,INCA
      DO 420 J=1,NNSBF
```

```
      IF (SBFNOD(J).EQ.INCVTR(I)) INTGER=J
      IF (SBFNOD(J).EQ.INCVTR(I)) GO TO 430
420   CONTINUE
430   CONTINUE
      LSUM1=(FORINC/100.0) * BFVALS(INTGER)
      BFVALS(INTGER)=LSUM1
      LSUM2=LSUM2 + LSUM1
440   CONTINUE
450   CONTINUE
      IF (IT.EQ.2) GO TO 510
C     SUBROUTINE VECTOR IS CALLED TO FORM THE ARRAY OF NODES WITH SPECI-
C     FIED BOUNDARY FORCE VALUES (SBFNOD) AND THE ARRAY OF THE VALUES
C     OF THE SPECIFIED BOUNDARY FORCES AT THE ABOVE NODES (BFVALS).
C     FOR EACH LOAD, INPUT THE (L,R,T) COORDINATES, THE LOAD TO BE
C     APPLIED (ONE CARD OR LINE PER SET OF COORDINATES AND LOAD), AND
C     AN INCREMENTAL ANALYSIS FLAG IF THE NO. OF STEPS REQUESTED IS
C     GREATER THAN ONE (1 = INCREMENT LOAD AT THIS NODE, 0 = DON'T
C     INCREMENT THE LOAD AT THIS NODE).
C     INPUT COORDINATES AND LOAD FOR ALL THE LOADS IN THE L-DIRECTION
C     FIRST, THEN THE R-DIRECTION, THEN THE T-DIRECTION.
      VECLEN=NNSBF
      RXN=0
C
      CALL VECTOR (NSBF,NPX,NPXY,NNM,SBFNOD,BFVALS,RXN,NUMRXN,INC,INCR,A
     1AA,NPY,NPZ,BWTYPE)
C
      INCA=INC
      DO 460 I=1,VECLEN
      A(I)=((SBFNOD(I)-1)/NDF+1)
460   CONTINUE
      WRITE (6,470)
470   FORMAT (//)
      WRITE (6,480)
480   FORMAT (1H1,2X,36HNODES WITH SPECIFIED BOUNDARY FORCES,16X,
     119H(L,R,T) COORDINATES,15X,9HDIRECTION,6X,16HSPECIFIED FORCES)
      DO 500 I=1,VECLEN
      DIR=Z1
      IF (I.LE.(NSBFX+NSBFY)) DIR=Y1
      IF (I.LE.NSBFX) DIR=X1
      IAI=A(I)
      WRITE (6,490) A(I),X(IAI),Y(IAI),Z(IAI),DIR,BFVALS(I)
490   FORMAT (14X,I5,27X,F8.4,6X,F8.4,6X,F8.4,10X,A4,10X,F10.3)
500   CONTINUE
510   CONTINUE
      DINC=DFLOAT(INCA)
      IF (IT.GT.1) LOD1=LOD1+LSUM2
      IF (IT.EQ.1) WRITE (6,520) IT,LOD1
520   FORMAT (/,2X,48HTOTAL AMOUNT OF FORCE APPLIED BY END OF STEP NO.,1
     1X,I3,1X,1H=,2X,F12.4,/)
      IF (IT.GT.1) GO TO 600
```

```
C*********************************************************************
C               SPECIFIED DISPLACEMENTS ARE READ IN HERE             *
C             ECHO THE SPECIFIED DISPLACEMENT INFORMATION            *
C*********************************************************************
C     SUBROUTINE VECTOR IS CALLED AGAIN TO FORM THE ARRAY OF NODES WITH
C     SPECIFIED DISPLACEMENTS (SPECIFIED DEGREES OF FREEDOM) (SDFNOD)
C     AND THE ARRAY OF THE VALUES OF THE SPECIFIED DISPLACEMENTS AT THE
C     ABOVE NODES (DFVALS).
C     INPUT IS SIMILAR TO THAT FOR THE PREVIOUS CALL TO VECTOR (JUST
C     SUBSTITUTE SPECIFIED DISPLACEMENTS FOR LOADS), BUT IT IS NOW ALSO
C     NECESSARY TO PREFIX THE NODE DATA WITH AN INTEGER VALUE OF EITHER
C     "1" OR "0".  A "ONE" MEANS THAT YOU WOULD LIKE THE PROGRAM TO
C     CALCULATE THE REACTION FORCES FOR THIS NODE (IN THIS DIRECTION),
C     AND A "ZERO" MEANS THAT NO REACTION FORCE IS TO BE CALCULATED.
C
530   CONTINUE
C     PRINT THE INFORMATION ABOUT POINTS SPECIFIED BY SUBROUTINE MIRROR.
      WRITE (6,540) AAA1,AAA2,AAA3
540   FORMAT (1H1,2X,60HNO. OF POINT DISPLACEMENTS SPECIFIED USING THE P
     1LANE OPTION:,/,7X,23HLONGITUDINAL DIRECTION=,20X,I5,/,7X,42HRADIAL
     2 DIRECTION (ON THE TANGENTIAL FACE)=,1X,I5,/,7X,42HTANGENTIAL DIRE
     3CTION (ON THE RADIAL FACE)=,1X,I5,/)
      IF (AAA.EQ.0) GO TO 581
      DO 550 I=1,AAA
      B(I)=((SDFNOD(I)-1)/NDF+1)
550   CONTINUE
      WRITE (6,560)
560   FORMAT (//,2X,34HNODES WITH SPECIFIED DISPLACEMENTS,18X,19H(L,R,T)
     1 COORDINATES,15X,9HDIRECTION,6X,23HSPECIFIED DISPLACEMENTS)
      DO 580 I=1,AAA
      DIR=Z1
      IBI=B(I)
      IF (I.LE.(AAA1+AAA2)) DIR=Y1
      IF (I.LE.AAA1) DIR=X1
      WRITE (6,570) B(I),X(IBI),Y(IBI),Z(IBI),DIR,DFVALS(I)
570   FORMAT (14X,I5,27X,F8.4,6X,F8.4,6X,F8.4,10X,A4,17X,F9.4)
580   CONTINUE
581   CONTINUE
      READ (5,*) NSDFX,NSDFY,NSDFZ
      WRITE (6,590) NSDFX,NSDFY,NSDFZ
590   FORMAT (1H1,1X,32HOTHER THAN SPECIFIED PLANES, THE,/,2X,38HNO. OF
     1SPECIFIED DISPLACEMENTS IN THE ,/,7X,23HLONGITUDINAL DIRECTION=,20
     2X,I5,/,7X,42HRADIAL DIRECTION (ON THE TANGENTIAL FACE)=,1X,I5,/,7X
     3,42HTANGENTIAL DIRECTION (ON THE RADIAL FACE)=,1X,I5,/)
      NSDF(1)=NSDFX
      NSDF(2)=NSDFY
      NSDF(3)=NSDFZ
      NNSDF=NSDF(1)+NSDF(2)+NSDF(3)
      IF ((NNSDF.LE.0).AND.(INCR.EQ.1)) INCB=INCA
      IF ((NNSDF.LE.0).AND.(INCR.EQ.1)) GO TO 711
```

```
      IF ((NNSDF.LE.0).AND.(AAA.GE.1)) GO TO 711
      IF ((NNSDF.LE.0).AND.(WANTE.EQ.0)) GO TO 810
600   CONTINUE
      IF (NNSDF.LE.0) GO TO 810
      IF (IT.EQ.1) GO TO 650
      IF ((IT.EQ.2).AND.(DELFOR.EQ.2)) GO TO 610
      IF (IT.GE.2) GO TO 810
610   CONTINUE
      INCV=INCA+1
      DO 640 I=INCV,INCB
      VECLEN=NNSDF+AAA
      DO 620 J=AAA4,VECLEN
      IF (SDFNOD(J).EQ.INCVTR(I)) INTGER=J
      IF (SDFNOD(J).EQ.INCVTR(I)) GO TO 630
620   CONTINUE
630   CONTINUE
      DFVALS(INTGER)=DELINC
640   CONTINUE
      IF (IT.EQ.2) GO TO 810
650   CONTINUE
      VECLEN=NNSDF+AAA
      RXN=1
C
      CALL VECTOR (NSDF,NPX,NPXY,NNM,SDFNOD,DFVALS,RXN,NUMRXN,INC,INCR,A
     1AA,NPY,NPZ,BWTYPE)
C
      INCB=INC+INCA
660   CONTINUE
      IF(VECLEN.LT.(NNSDF+AAA)) GO TO 711
      VECLEN=NNSDF+AAA
      DO 670 I=AAA4,VECLEN
      B(I)=((SDFNOD(I)-1)/NDF+1)
670   CONTINUE
      WRITE (6,680)
680   FORMAT (//)
      WRITE (6,690)
690   FORMAT (1X,1X,34HNODES WITH SPECIFIED DISPLACEMENTS,18X,19H(L,R,T)
     1 COORDINATES,15X,9HDIRECTION,6X,23HSPECIFIED DISPLACEMENTS)
      DO 710 I=AAA4,VECLEN
      CHECK=SDFNOD(I)/3
      CHECK1=CHECK*3
      IBI=B(I)
      IF (SDFNOD(I).EQ.CHECK1) DIR=Z1
      CHECK2=CHECK1+1
      CHECK3=CHECK1+2
      IF (SDFNOD(I).EQ.CHECK2) DIR=X1
      IF (SDFNOD(I).EQ.CHECK3) DIR=Y1
      WRITE (6,700) B(I),X(IBI),Y(IBI),Z(IBI),DIR,DFVALS(I)
700   FORMAT (14X,I5,27X,F8.4,6X,F8.4,6X,F8.4,10X,A4,17X,F9.4)
710   CONTINUE
```

```
711   CONTINUE
C
      IF(NUMRXN.LE.0) GO TO 731
      WRITE (6,720) NUMRXN
720   FORMAT (////,2X,51HREACTION FORCE CALCULATIONS HAVE BEEN REQUESTED
     1 FOR,1X,I3,1X,13HNODAL POINTS.,/,2X,79HTHESE ARE THE GLOBAL NODE N
     2UMBERS FOR WHICH REACTION FORCES WILL BE CALCULATED:,/)
      DO 730 I=1,NUMRXN
      B(I)=(((RXNNOD(I)-1)/NDF)+1)
730   CONTINUE
      WRITE (6,*) (B(I),I=1,NUMRXN)
731   CONTINUE
      IF(INCB.LE.0) GO TO 751
      IF (INCR.EQ.1) WRITE (6,740) INCB
740   FORMAT (////,2X,14HTHESE ARE THE ,I3,1X,101HGLOBAL NODES AT WHICH
     1THE INCREMENTAL LOADS OR DISPLACEMENTS WILL BE APPLIED AFTER THE I
     2NITIAL STEP :,/)
      DO 750 I=1,INCB
      B(I)=(((INCVTR(I)-1)/NDF)+1)
750   CONTINUE
      IF (INCR.EQ.1) WRITE (6,*) (B(I),I=1,INCB)
751   CONTINUE
      IF ((INCR.EQ.1).AND.(DELFOR.EQ.1)) WRITE (6,760) FORINC
760   FORMAT (//,2X,68HTHE LOAD INCREMENT TO BE ADDED AT EACH STEP PAST
     1THE INITIAL STEP = ,F9.3,1X,8HPERCENT.,//)
      IF ((INCR.EQ.1).AND.(DELFOR.EQ.2)) WRITE (6,770) DELINC
770   FORMAT (//,2X,77HTHE DISPLACEMENT INCREMENT TO BE IMPOSED AT EACH
     1STEP PAST THE INITIAL STEP =,F9.5,1X,7HINCHES.,//)
780   CONTINUE
      IF (TESTYP.NE.BEAM1) INT=NPY*NPZ
      IF ((TESTYP.EQ.BEAM1).AND.(SYMTRY.EQ.1)) INT=NPZ
      IF ((TESTYP.EQ.BEAM1).AND.(SYMTRY.EQ.2)) INT=NPY
C     IF LOAD ISN'T APPLIED, AND IF ALL APPLICABLE RXN FORCES AREN'T
C     SPECIFIED, DON'T TRY TO CALCULATE THE MECHANICAL PROPERTIES.
      IF ((NUMRXN.LT.INT).AND.(WANTE.EQ.1).AND.(LOD1.EQ.0.0)) WRITE (6,7
     $90)
790   FORMAT (///,5X,48HWARNING * WARNING * WARNING * WARNING * WARNING
     1,//,2X,60HALL OF THE APPROPRIATE REACTIONS MUST BE CALCULATED IN O
     2RDER,/,2X,49HTO CALCULATE THE EFFECTIVE MECHANICAL PROPERTIES.,/,
     32X,62HEXECUTION IS CONTINUING W/O THE IMPLEMENTATION OF THIS OPTIO
     4N.,///)
      IF(WANTE.EQ.0) GO TO 810
C ***************************************************************
C     CALL SBR VECTOR ONE MORE TIME TO DESIGNATE A NODAL POINT AT WHICH
C     MOE, MOR, ETC., ARE TO BE CALCULATED AS APPROPRIATE TO THE TEST
C     (IF DESIRED).
C
C     INPUT CONSISTS OF NODE COORDINATES ONLY.
C ***************************************************************
      IF ((TESTYP.EQ.BEAM1).AND.(SYMTRY.EQ.1)) NUMLOD(1)=0
```

```
      IF ((TESTYP.EQ.BEAM1).AND.(SYMTRY.EQ.1)) NUMLOD(2)=1
      IF ((TESTYP.EQ.BEAM1).AND.(SYMTRY.EQ.1)) NUMLOD(3)=0
      IF ((TESTYP.EQ.BEAM1).AND.(SYMTRY.EQ.2)) NUMLOD(1)=0
      IF ((TESTYP.EQ.BEAM1).AND.(SYMTRY.EQ.2)) NUMLOD(2)=0
      IF ((TESTYP.EQ.BEAM1).AND.(SYMTRY.EQ.2)) NUMLOD(3)=1
C     DISPLACEMENT OF INTEREST HAS BEEN ASSUMED TO OCCUR ALONG THE
C     LONGITUDINAL AXIS FOR UNIAXIAL PROBLEMS
      IF (TESTYP.NE.BEAM1) NUMLOD(1)=1
      IF (TESTYP.NE.BEAM1) NUMLOD(2)=0
      IF (TESTYP.NE.BEAM1) NUMLOD(3)=0
      VECLEN=1
      RXN=2
C
      CALL VECTOR (NUMLOD,NPX,NPXY,NNM,NODE,VALUES,RXN,NUMRXN,INC,INCR,A
     1AA,NPY,NPZ,BWTYPE)
C
      INCC=INC+INCB
      NODEA=((NODE-1)/NDF)+1
      IF (WANTE.EQ.1) WRITE (6,800) NODEA,X(NODEA),Y(NODEA),Z(NODEA)
800   FORMAT (////,2X,22HDISPLACEMENTS AT NODE ,I3,2X,1H(,F6.3,1H,,F6.3,
     11H,,F6.3,1H),2X,75HWILL BE USED TO CALCULATE MOE,MOR, ETC., AS APP
     2ROPRIATE TO THE TYPE OF TEST,//)
810   CONTINUE
C
C     INITIALIZE ARRAYS ON THE FIRST PASS
      IF (IT.GT.1) GO TO 821
      DO 820 I=1,NEM
      ACTMC(I)=0.0
      MCUSED(I)=0.0
820   CONTINUE
821   CONTINUE
      DO 840 I=1,NEQ
      GFORCE(I)=0.0
      DO 830 J=1,HBW
      GSTIFF(I,J)=0.0
830   CONTINUE
840   CONTINUE
      WRITE (6,850) IT
850   FORMAT (1H1,46X,36H************************************,/,47X, 36H
     1*                                  *,/,47X,29H*  PROCESSING BEGINS
     2 FOR STEP,I3,4H   *,/,47X,36H*                                    *,
     3/47X,36H************************************,////)
C
      IF ((IT.GT.1).AND.(DELFOR.EQ.1)) WRITE(6,520) IT,LOD1
C
C        ######################################################
C        # LOOP TO GENERATE THE GLOBAL [K] MATRIX GOES NEXT #
C        ######################################################
C
      DO 890 N=1,NEM
```

```
      DO 860 I=1,NPE
      NI=GNOD(N,I)
      ELXYZ(I,1)=X(NI)
      ELXYZ(I,2)=Y(NI)
      ELXYZ(I,3)=Z(NI)
860   CONTINUE
C
C **  CALL THE ELEMENT STIFFNESS SUBROUTINE.
C
      CALL ELEMK (NPE,NN,NGP,NDF)
C
C **  ASSEMBLE THE ELEMENT MATRICES [LSTIFF] INTO THE GLOBAL [K]
C **  MATRIX [GSTIFF]. NEED UNALTERED LINES OF GSTIFF (==GSCOPY) FOR
C **  THE SOLUTION OF THE REACTION FORCES.
C
C **  ELEMENT MATRICES ARE ASSEMBLED INTO A BANDED MATRIX.
      DO 880 I=1,NPE
      NR=(GNOD(N,I)-1)*NDF
      DO 880 II=1,NDF
      NR=NR+1
      L=(I-1)*NDF+II
C     . . . . . .
C     LFORCE IS ONLY USED WHEN THE ELEMENT WEIGHTS NEED TO BE TAKEN INTO
C     ACCOUNT IN THE ANALYSIS.  THE PROGRAM IS CURRENTLY WRITTEN TO SET
C     LFORCE AT 0.0 FOR EACH ELEMENT.  SBR ELEMK IS WHERE THE PROGRAM
C     SHOULD BE MODIFIED TO ACCOUNT FOR BODY FORCES USING THE ELEMENT
C     DENSITY.
C     . . . . . .
      GFORCE(NR)=GFORCE(NR) + LFORCE(L)
      DO 880 J=1,NPE
      NCL=(GNOD(N,J)-1)*NDF
      DO 880 JJ=1,NDF
      M=(J-1)*NDF + JJ
      NC=NCL + JJ + 1 - NR
      IF (NC) 880,880,870
870   CONTINUE
      GSTIFF(NR,NC)=GSTIFF(NR,NC) + LSTIFF(L,M)
880   CONTINUE
890   CONTINUE
C
C     PRINT MC'S CALCULATED ON THE FIRST STEP
C
      IF ((IT.EQ.1).AND.(GRAD.EQ.1)) WRITE (6,900)
900   FORMAT (///,27X,'ELEMENT CENTROID')
      IF ((IT.EQ.1).AND.(GRAD.EQ.1)) WRITE (6,901)
901   FORMAT (2X,'ELEMENT NO.',7X,'LCOORD',6X,'RCOORD',6X,'TCOORD',10X,'
     $ACTUAL MC%',6X,'MC% USED',/)
      IF ((IT.GT.1).OR.(GRAD.EQ.0)) GO TO 905
      DO 902 I=1,NEM
      XCEN=(X(GNOD(I,1))+X(GNOD(I,2))+X(GNOD(I,3))+X(GNOD(I,4))+X(GNOD(I
```

```
     $,5))+X(GNOD(I,6))+X(GNOD(I,7))+X(GNOD(I,8)))/8.0
      YCEN=(Y(GNOD(I,1))+Y(GNOD(I,2))+Y(GNOD(I,3))+Y(GNOD(I,4))+Y(GNOD(I
     $,5))+Y(GNOD(I,6))+Y(GNOD(I,7))+Y(GNOD(I,8)))/8.0
      ZCEN=(Z(GNOD(I,1))+Z(GNOD(I,2))+Z(GNOD(I,3))+Z(GNOD(I,4))+Z(GNOD(I
     $,5))+Z(GNOD(I,6))+Z(GNOD(I,7))+Z(GNOD(I,8)))/8.0
      WRITE(6,903) I,XCEN,YCEN,ZCEN,ACTMC(I),MCUSED(I)
903   FORMAT (4X,I4,10X,F8.3,4X,F8.3,4X,F8.3,11X,F7.2,9X,F6.2)
902   CONTINUE
      WRITE(6,904)
904   FORMAT (///)
905   CONTINUE
      IF ((IT.EQ.1).AND.(GRAD.EQ.0)) WRITE(6,910) ACTMC(1)
910   FORMAT (//,2X,41HTHE MOISTURE CONTENT WAS CALCULATED TO BE,1X,F8.3
     1,1X,19H% FOR ALL ELEMENTS.)
      IF ((IT.EQ.1).AND.(GRAD.EQ.0)) WRITE (6,930) MCUSED(1)
930   FORMAT (//,2X,46HTHE MOISTURE CONTENT USED FOR ALL ELEMENTS WAS,1X
     1,F8.3,1X,2H%.,/)
C          ****************************************************
C          * THIS IS WHERE THE ARRAY ACTMC IS RE-INITIALIZED *
C          * SO THAT IT CAN BE USED AS A SCRATCH PAD FOR THE *
C          * LONGITUDINAL STRAIN INFORMATION.                *
C          ****************************************************
      IF (IT.GT.1) GO TO 950
      DO 940 I=1,NEM
      ACTMC(I)=0.0
940   CONTINUE
950   CONTINUE
      IF (NUMRXN.EQ.0) GO TO 1080
C     SAVE THE LINES OF THE GLOBAL STIFFNESS MATRIX NEEDED TO CALCULATE
C     THE REACTION FORCES.  IT IS NECESSARY TO SAVE THESE LINES BEFORE
C     MATRIX GSTIFF IS CHANGED DURING THE SOLVE PROCEDURE (SBRS BNDRY &
C     SOLVE).  THE REQUIRED LINES ARE SAVED IN MATRIX "GSCOPY".
      BNDWID=NEQ
C     INITIALIZE GSCOPY
      DO 970 I=1,NUMRXN
      DO 960 J=1,BNDWID
      GSCOPY(I,J)=0.0
960   CONTINUE
970   CONTINUE
      JJ=0
      VECLEN=NNSDF+AAA
      DO 1070 N=1,NUMRXN
      DO 980 MM=AAA4,VECLEN
      IF (RXNNOD(N).EQ.SDFNOD(MM)) LM=MM
      IF (RXNNOD(N).EQ.SDFNOD(MM)) GO TO 990
980   CONTINUE
990   CONTINUE
      LLL=((RXNNOD(N)-1)/NDF+1)
      IF (DFVALS(LM).NE.0.0) WRITE (6,1000) LLL,X(LLL),Y(LLL),Z(LLL)
1000  FORMAT (//,2X,26HERROR IN SPECIFYING NODE #,1X,I3,5X,1H(,F8.3,1H,,
```

```
     1F8.3,1H,,F8.3,1H),5X,20HAS A REACTION POINT.,/,2X,45HDISPLACEMENT
     2HAS NOT BEEN SPECIFIED TO BE 0.0)
      IF (DFVALS(LM).NE.0.0) GO TO 1070
      I=RXNNOD(N)
      JJ=JJ+1
      IF (I.GT.HBW) GO TO 1030
      J=I
      DO 1010 K=1,I
      GSCOPY(JJ,K)=GSTIFF(K,J)
      MM=K
      J=J-1
1010  CONTINUE
      K=MM
      DO 1020 J=2,HBW
      K=K+1
      GSCOPY(JJ,K)=GSTIFF(I,J)
1020  CONTINUE
      GO TO 1070
C     FOR I>HBW
1030  CONTINUE
      L=I-HBW+1
      LLLL=L
      NC=HBW
      DO 1040 M=L,I
      GSCOPY(JJ,M)=GSTIFF(LLLL,NC)
      MM=M
      NC=NC-1
      LLLL=LLLL+1
1040  CONTINUE
      M=MM+1
      L=LLLL-1
      NC=1
      DO 1050 LL=M,BNDWID
      NC=NC+1
      IF (NC.GT.HBW) GO TO 1060
      GSCOPY(JJ,LL)=GSTIFF(L,NC)
1050  CONTINUE
1060  CONTINUE
1070  CONTINUE
1080  CONTINUE
C
C        ********************************************
C        *  ASSEMBLED MATRIX EQUATIONS ARE NOW READY *
C        *  FOR IMPLEMENTATION OF THE BOUNDARY       *
C        *  CONDITIONS.                              *
C        ********************************************
C
      IF (NNSBF.EQ.0) GO TO 1100
      DO 1090 I=1,NNSBF
      II=SBFNOD(I)
```

```
      GFORCE(II)=-BFVALS(I)+GFORCE(II)
1090  CONTINUE
1100  CONTINUE
      VECLEN=NNSDF+AAA
      IF (VECLEN.EQ.0) GO TO 1120
      DO 1110 I=1,VECLEN
      IE=SDFNOD(I)
      VE=DFVALS(I)
C
      CALL BNDRY (NEQ,HBW,IE,VE)
C
1110  CONTINUE
1120  CONTINUE
C
C     CALL SUBROUTINE 'SOLVE' TO DETERMINE THE GENERALIZED DISPLACEMENTS
C     THE SOLUTION IS RETURNED IN ARRAY 'GFORCE'.
      IRES=0
C
      CALL SOLVE (NEQ,HBW,IRES)
C
C     PRINT THE DISPLACEMENTS HERE:
      WRITE (6,1130) IT
1130  FORMAT (1H1,/,49X,27HDISPLACEMENTS FOR STEP NO. ,I3,6H ONLY:,/)
      WRITE (6,1140)
1140  FORMAT (2X,8HNODE NO.,19X,19HL, R, T COORDINATES,41X,21HL, R, T DI
     1SPLACEMENTS,/)
      WRITE (6,1150)
1150  FORMAT (18X,1HL,15X,1HR,15X,1HT,19X,7HDELTA L,18X,7HDELTA R,18X,7H
     1DELTA T,/)
      WRITE (6,1160) (I,X(I),Y(I),Z(I),GFORCE(3*I-2),GFORCE(3*I-1),GFORC
     1E(3*I),I=1,NNM)
1160  FORMAT (4X,I3,10X,F6.3,10X,F6.3,10X,F6.3,10X,F15.8,10X,F15.8,10X,F
     115.8)
C     IF WANTE = 1, DELTA1 IS THE SUM OF THE DISPLACEMENTS AT
C     THE SPECIFIED NODE.
      IF (WANTE.EQ.1) DELTA1=GFORCE(NODE)+DELTA1
C
C     ***********************************************
C     COMPUTE STRAINS AND STRESSES FOR EACH ELEMENT:
C     ***********************************************
C
      DO 1180 N=1,NEM
      DO 1170 I=1,NPE
      NI=GNOD(N,I)
      L=NI*NDF-2
      W(1,I)=GFORCE(L)
      W(2,I)=GFORCE(L+1)
      W(3,I)=GFORCE(L+2)
      ELXYZ(I,1)=X(NI)
      ELXYZ(I,2)=Y(NI)
```

```
      ELXYZ(I,3)=Z(NI)
1170  CONTINUE
C     CKALC MUST BE CALLED TO PROVIDE THE [C] MATRIX FOR SBR STRESS.
C     EPRINT IS USED TO SUPPRESS THE PRINTING OF E SUB 1, ETC., FOR EACH
C     ELEMENT.
      EPRINT=0
C
      CALL CKALC (EPRINT)
C
C     SOLVE FOR THE STRESSES IN THE ELEMENT: STRESSES ARE PRINTED IN THE
C     SUBROUTINE.
C
      CALL STRESS (N,NPE,W,IT,TABORT)
C
      IF(TABORT.EQ.1) WRITE(6,1171) N
1171  FORMAT(/,2X,'ELEMENT ',I4,1X,'HAS FAILED IN LONGITUDINAL TENSION.'
     $,/,12X,'PROGRAM CONTINUING.',/)
      TABORT=0
1180  CONTINUE
      IF ((NUMRXN.EQ.0).AND.(WANTE.EQ.1).AND.(LOD1.EQ.0.0)) GO TO 1350
      IF (NUMRXN.EQ.0) GO TO 1271
C
C********************* SOLVE FOR REACTION FORCES ***********************
C
C     DISPLACEMENTS ARE IN GFORCE, UNALTERED GSTIFF IS IN GSCOPY.
      WRITE (6,1190) IT
1190  FORMAT (////,22X,40HREACTION FORCE CALCULATIONS FOR STEP NO.,1X,I3
     1,1H:,/)
      WRITE (6,1200)
1200  FORMAT (/,22X,8HNODE NO.,8X,19H(L,R,T) COORDINATES,10X,15HFORCE DI
     1RECTION,5X,11HRXN. FORCES)
      JJ=0
      VECLEN=NNSDF+AAA
      ENDRXN=0.0
      DO 1270 N=1,NUMRXN
      DO 1210 MM=AAA4,VECLEN
      LM=MM
      IF ((RXNNOD(N).EQ.SDFNOD(MM)).AND.(DFVALS(MM).EQ.0.0)) GO TO 1220
1210  CONTINUE
      GO TO 1260
1220  CONTINUE
      IF (DFVALS(LM).NE.0.0) GO TO 1260
      I=RXNNOD(N)
      JJ=JJ+1
      REAXNS=0.0
      J=1
      DO 1230 L=1,BNDWID
      REAXNS=GSCOPY(JJ,L)*GFORCE(J)+REAXNS
      J=J+1
1230  CONTINUE
```

```
C     UP TO THIS POINT, HAVE ONLY CALCULATED THE INTERNAL FORCES--
C     HAVE TO REVERSE THE SIGN TO GET THE REACTION FORCES
      REAXNS=-REAXNS
      RXNSUM=REAXNS+RXNSUM
      ENDRXN=REAXNS + ENDRXN
      ORDER=(((RXNNOD(N)-1)/NDF)+1)
      CHECK=SDFNOD(MM)/3
      CHECK1=CHECK*3
      IF (SDFNOD(I).EQ.CHECK1) DIR=Z1
      CHECK2=CHECK1+1
      CHECK3=CHECK1+2
      IF (SDFNOD(MM).EQ.CHECK2) DIR=X1
      IF (SDFNOD(MM).EQ.CHECK3) DIR=Y1
      WRITE (6,1240) ORDER,X(ORDER),Y(ORDER),Z(ORDER),DIR,REAXNS
1240  FORMAT (24X,I4,3X,3(F8.4,3X),9X,A4,6X,F15.4)
      IF (N.EQ.NUMRXN) WRITE (6,1250) IT,RXNSUM
1250  FORMAT (//,22X,44HTOTAL REACTION FORCE AT THE END OF STEP NO. ,I3,
     13H = ,F12.4,///)
1260  CONTINUE
1270  CONTINUE
1271  CONTINUE
C
C     THE FOLLOWING LINES DETERMINE THE APPROPRIATE VALUE TO USE FOR
C     THE LOAD IN THE MOE EQUATION.  THE APPLIED LOAD IS USED WHEN
C     AVAILABLE IN PREFERENCE TO THE CALCULATED REACTION FORCE.
C
      IF ((WANTE.NE.1).AND.(RXNSUM.EQ.0.0)) GO TO 1350
      IF (WANTE.NE.1) GO TO 1370
      IF ((NUMRXN.LT.INT).AND.(LOD1.EQ.0.0)) GO TO 1370
      DOODLE=RXNSUM*2.0
      IF (POSYMX.GE.1) DOODLE=RXNSUM*4.0
      IF (LOD1.NE.0.0) DOODLE=LOD1*2.0
      IF ((LOD1.NE.0.0).AND.(POSYMX.GE.1)) DOODLE=LOD1*4.0
C     MOE IN EQUATION BELOW IS THE APPARENT MODULUS OF ELASTICITY,
C     UNCORRECTED FOR ANY VERTICAL DISPLACEMENT AT SUPPORTS.
      IF ((IT.EQ.1).AND.(TESTYP.EQ.BEAM1)) MOE=DABS((DOODLE*BEMLEN/BEMDE
     1F)/(4.0*DELTA1*BEMWID)*((BEMLEN/BEMDEF)**2))
      IF (TESTYP.EQ.BEAM1) MOR=DABS((3.0*DOODLE*BEMLEN)/(2.0*BEMWID*(BEM
     $DEF**2)))
      IF ((TESTYP.NE.BEAM1).AND.(LOD1.EQ.0.0)) STRES1=(-RXNSUM/(ZCOORD(N
     $PZ)*YCOORD(NPY)))
      IF ((TESTYP.NE.BEAM1).AND.(LOD1.NE.0.0)) STRES1=(LOD1/(ZCOORD(NPZ)
     $*YCOORD(NPY)))
      IF (TESTYP.NE.BEAM1) STRAIN=DELTA1/X(NODEA)
      IF ((TESTYP.NE.BEAM1).AND.(IT.EQ.1)) E=DABS(STRES1/STRAIN)
      IF (TESTYP.EQ.BEAM1) WRITE (6,1280) IT
1280  FORMAT (///,48X,31HSUMMARY AT THE END OF STEP NO. ,I3,1H:,//,2X,9H
     1NODE NO. ,10X,8HLOAD (#),10X,15HDEFLECTION (IN),14X,8HAPP. MOE,13X
     2,16HMOR AT THIS STEP,/)
      IF ((TESTYP.EQ.BEAM1).AND.(IT.EQ.1)) WRITE (6,1290) NODEA,DOODLE,D
```

```
     1ELTA1,MOE,MOR
1290  FORMAT (4X,I3,10X,F9.2,10X,F15.8,10X,F15.1,12X,F15.1)
      IF ((TESTYP.EQ.BEAM1).AND.(IT.GT.1)) WRITE (6,1300) NODEA,DOODLE,D
     1ELTA1,MOR
1300  FORMAT (4X,I3,10X,F9.2,10X,F15.8,15X,10HSEE STEP 1,12X,F15.1)
      IF ((TESTYP.NE.BEAM1).AND.(LOD1.EQ.0.0)) WRITE (6,1310) IT
1310  FORMAT (///,48X,31HSUMMARY AT THE END OF STEP NO. ,I3,1H:,//,2X,29
     1HDISPLACEMENT (IN) AT NODE NO.,10X,6HSTRAIN,10X,7HRXN (#),10X,6HST
     2RESS,15X,1HE)
      IF ((TESTYP.NE.BEAM1).AND.(LOD1.NE.0.0)) WRITE(6,1311) IT
1311  FORMAT (///,48X,31HSUMMARY AT THE END OF STEP NO. ,I3,1H:,//,2X,29
     1HDISPLACEMENT (IN) AT NODE NO.,10X,6HSTRAIN,9X,9HFORCE (#),9X,
     26HSTRESS,15X,1HE)
      IF ((TESTYP.NE.BEAM1).AND.(IT.EQ.1).AND.(LOD1.EQ.0.0)) WRITE (6,13
     $20) DELTA1,NODEA,STRAIN,RXNSUM,STRES1,E
      IF ((TESTYP.NE.BEAM1).AND.(IT.EQ.1).AND.(LOD1.NE.0.0)) WRITE (6,13
     $20) DELTA1,NODEA,STRAIN,LOD1,STRES1,E
1320  FORMAT (/,5X,F10.6,10X,I3,10X,F9.6,7X,F10.2,7X,F10.2,7X,F12.1,///)
      IF ((TESTYP.NE.BEAM1).AND.(IT.GT.1).AND.(LOD1.EQ.0.0)) WRITE (6,13
     $30) DELTA1,NODEA,STRAIN,RXNSUM,STRES1
      IF ((TESTYP.NE.BEAM1).AND.(IT.GT.1).AND.(LOD1.NE.0.0)) WRITE (6,13
     $30) DELTA1,NODEA,STRAIN,LOD1,STRES1
1330  FORMAT (/,5X,F10.6,10X,I3,10X,F9.6,7X,F10.2,7X,F10.2,10X,10HSEE ST
     1EP 1,///)
1340  CONTINUE
C     *#*#*#*#*#*#*#*#*#*#*#*#*#*#*#*#*#*#*#*#*#*#*#*#*#*#*#*#*#*#*#*#*#*#
C
C                          AUTO-TERMINATION
C                            (UPON REQUEST)
C
C     PROGRAM WILL END IF NO MORE THAN 10# OF REACTION FORCE IS ADDED
C     BETWEEN STEPS EQUALLING 0.1" DISPLACEMENT, AS THE RUN IS
C     ESSENTIALLY COMPLETED.  (SLOPE OF 100# PER INCH DISPLACEMENT)
C     (COMPUTATION BASED ON SLOPE BETWEEN 2 STEPS).
C
C     REACTION FORCE USED IS THE TOTAL FORCE FOR THE ENTIRE MODEL AFTER
C     ADJUSTMENTS ARE MADE FOR THE QUARTER-SYMMETRY COMMONLY USED.
C
C     *#*#*#*#*#*#*#*#*#*#*#*#*#*#*#*#*#*#*#*#*#*#*#*#*#*#*#*#*#*#*#*#*#*#
      ENDVAR=DABS(ENDRXN)
C     ASSUMES QUARTER-SYMMETRY WAS USED IN SPECIFYING THE DOMAIN:
      ENDVAR=ENDVAR * 4.0
      IF (DELFOR.EQ.2) ENDVAR=DABS(ENDVAR/DELINC)
      IF ((ENDVAR.LE.100.0).AND.(AUTOND.EQ.1).AND.(DELFOR.EQ.2).AND.(IT.
     $GT.1))  GO TO 1380
      GO TO 1370
1350  CONTINUE
      IF (IT.EQ.1) WRITE (6,1360)
1360  FORMAT (///,2X,71H# # # # # NO REACTION FORCES WERE REQUESTED FOR
     1THIS PROBLEM # # # # # ,///)
```

```
1370  CONTINUE
      IT=IT+1
      IF (IT.LE.INCNUM) GO TO 400
      GO TO 1400
1380  CONTINUE
      WRITE (6,1390)
1390  FORMAT (///,2X,51HPROGRAM TERMINATING DUE TO DECREASING LOAD CAPAC
     1ITY,///)
1400  CONTINUE
      STOP
      END
C*******************************************************************************
C                E N D   O F   M A I N   P R O G R A M
C*******************************************************************************
      SUBROUTINE ELEMK (NPE,NN,NGP,NDF)
C     THIS SUBROUTINE CALCULATES THE ELEMENT CONTRIBUTION TO THE GLOBAL
C     [K] MATRIX.
C     SF = ELEMENT SHAPE FUNCTIONS
C     GDSF = GLOBAL DERIVATIVES OF THE SHAPE FUNCTIONS
C            GDSF(I,J) = DERIVATIVES OF SF(J) WITH RESPECT TO X(I), ETC.
C     GAUSS = ARRAY OF POINTS FOR GAUSS-LEGENDRE QUADRATURE
C     WT = ARRAY OF GAUSSIAN WEIGHTS CORRESPONDING TO THE GAUSSIAN PTS.
C     SXX(I,J),SYY(I,J),SXY(I,J),ETC. = INTEGRAL OF THE TWO PARTIAL
C              DERIVATIVES IN THE FINITE ELEMENT FORMULATION--EXAMPLE:
C              THE INTEGRAL OF THE PARTIAL DERIVATIVE OF (PSI SUB I WITH
C              RESPECT TO X) * THE PARTIAL DERIVATIVE OF (PSI SUB J WITH
C              RESPECT TO Y) = SXY(I,J).
C
C     CONST = THE NUMBER RESULTING FROM THE MULTIPLICATION OF THE DETER-
C             MINANT OF THE JACOBIAN MATRIX TIMES THE APPROPRIATE GAUSS
C             WEIGHTS AS PART OF THE GAUSS QUADRATURE PROCEDURE.
C     LSTIFF = FINAL ARRAY OF PARTIAL ELEMENT STIFFNESS MATRICES FOLLOW-
C              ING GAUSS QUADRATURE OVER THE DESIRED NUMBER OF GAUSS
C              POINTS.
C
      IMPLICIT REAL*8 (A-H,O-Z)
      REAL*8 LFORCE,LSTIFF,MCUSED,MCBAR,HAFDEF,MCMAX,SG
      INTEGER SYMTRY,EPRINT,IT,GRAD,TESTYP,EOPSHN
      COMMON /ELEM/ LSTIFF,LFORCE
      COMMON /ELK/ ELXYZ
      COMMON /MOIST1/ ACTMC
      COMMON /MOIST2/ MCUSED,EMC,MCBAR,HAFWID,MCMAX,SG,
     1HAFDEF,N,NEM,SYMTRY,IT,GRAD,EOPSHN,TESTYP
      COMMON /SIGMA/ C,TT
      COMMON /GSHAPE/ GDSF
      DIMENSION MCUSED(576), ACTMC(576)
      DIMENSION GAUSS(4,4), WT(4,4), SXX(8,8), SYY(8,8), SZZ(8,8), SXY(8
     1,8), SXZ(8,8), SYZ(8,8), ELXYZ(8,3), C(6,6), GDSF(3,8), LSTIFF(24,
     224), LFORCE(24)
      DATA GAUSS/4*0.0D0,-.577350269189626D0,.577350269189626D0,2*0.0D0,
```

```
     1-.774596669241483D0,0.0D0,.774596669241483D0,0.0D0,-.8611363115940
     253D0,-.339981043584856D0,.339981043584856D0,.861136311594053D0/
      DATA WT/2.0D0,3*0.0D0,2*1.0D0,2*0.0D0,.555555555555556D0,.88888888
     18888889D0,.555555555555556D0,0.0D0,.347854845137454D0,2*.652145154
     2862546D0,.347854845137454D0/
      DO 20 I=1,NPE
      DO 10 J=1,NPE
      SXX(I,J)=0.0
      SYY(I,J)=0.0
      SZZ(I,J)=0.0
      SXY(I,J)=0.0
      SXZ(I,J)=0.0
      SYZ(I,J)=0.0
10    CONTINUE
20    CONTINUE
C     HERE IS WHERE LFORCE IS INITIALIZED.  MAKE ANY CHANGES (TO ACCOUNT
C     FOR DENSITY, ETC., WHEN USING BODY FORCES) WITHIN THIS SUBROUTINE.
      DO 30 I=1,NN
      LFORCE(I)=0.0
30    CONTINUE
      DO 80 NI=1,NGP
      DO 70 NJ=1,NGP
      DO 60 NK=1,NGP
      XI=GAUSS(NI,NGP)
      ETA=GAUSS(NJ,NGP)
      ZETA=GAUSS(NK,NGP)
C     CALCULATE GDSF AND THE DETERMINANT OF THE JACOBIAN MATRIX.
      CALL SF3DL (NPE,XI,ETA,ZETA,DET)
      CONST=DET*WT(NI,NGP)*WT(NJ,NGP)*WT(NK,NGP)
C     CALCULATE SXX(I,J),ET CETERA.
      DO 50 I=1,NPE
      DO 40 J=1,NPE
      SXX(I,J)=GDSF(1,I)*GDSF(1,J)*CONST+SXX(I,J)
      SYY(I,J)=GDSF(2,I)*GDSF(2,J)*CONST+SYY(I,J)
      SZZ(I,J)=GDSF(3,I)*GDSF(3,J)*CONST+SZZ(I,J)
      SXY(I,J)=GDSF(1,I)*GDSF(2,J)*CONST+SXY(I,J)
      SXZ(I,J)=GDSF(1,I)*GDSF(3,J)*CONST+SXZ(I,J)
      SYZ(I,J)=GDSF(2,I)*GDSF(3,J)*CONST+SYZ(I,J)
40    CONTINUE
50    CONTINUE
60    CONTINUE
70    CONTINUE
80    CONTINUE
      DO 100 I=1,NN
      DO 90 J=1,NN
      LSTIFF(I,J)=0.0
90    CONTINUE
100   CONTINUE
C     CALCULATE THE VALUES OF THE [C] MATRIX FOR THE ELEMENT.
C     EPRINT IS USED TO CONTROL THE PRINTING OF E FOR EACH ELEMENT
```

```
      EPRINT=1
      CALL CKALC (EPRINT)
      II=1
      DO 120 I=1,NPE
      JJ=1
      DO 110 J=1,NPE
      LSTIFF(II,JJ)=C(1,1)*SXX(I,J)+C(6,6)*SYY(I,J)+C(5,5)*SZZ(I,J)
      JJ1=JJ+1
      LSTIFF(II,JJ1)=C(1,2)*SXY(I,J)+C(6,6)*SXY(J,I)
      JJ2=JJ+2
      LSTIFF(II,JJ2)=C(1,3)*SXZ(I,J)+C(5,5)*SXZ(J,I)
      II1=II+1
      LSTIFF(II1,JJ)=C(6,6)*SXY(I,J)+C(1,2)*SXY(J,I)
      LSTIFF(II1,JJ1)=C(6,6)*SXX(I,J)+C(2,2)*SYY(I,J)+C(4,4)*SZZ(I,J)
      LSTIFF(II1,JJ2)=C(2,3)*SYZ(I,J)+C(4,4)*SYZ(J,I)
      II2=II+2
      LSTIFF(II2,JJ)=C(5,5)*SXZ(I,J)+C(1,3)*SXZ(J,I)
      LSTIFF(II2,JJ1)=C(4,4)*SYZ(I,J)+C(2,3)*SYZ(J,I)
      LSTIFF(II2,JJ2)=C(5,5)*SXX(I,J)+C(4,4)*SYY(I,J)+C(3,3)*SZZ(I,J)
      JJ=NDF*J+1
110   CONTINUE
      II=NDF*I+1
120   CONTINUE
      RETURN
      END
C     ..................................................................
      SUBROUTINE MESH3D (NPE,NEX,NEY,NEZ,NPX,NPY,NPZ,NNM,NEM,NPXY,BWTYPE
     $)
C     'MESH GENERATION FOR 3-D LINEAR ELEMENTS'
C
C     THIS SUBROUTINE CALCULATES THE BOOLEAN CONNECTIVITY MATRIX (GNOD)
C     AND MINIMIZES THE HALF BANDWIDTH FOR THE INDIVIDUAL ANALYSIS.
C     THIS SUBROUTINE ALSO GENERATES THE ELEMENT AND GLOBAL MESH NODE
C     NUMBERS AND COORDINATES FOR EVERY CORNER OF EVERY 8-NODE ELEMENT.
      IMPLICIT REAL*8 (A-H,O-Z)
      INTEGER I,J,K,M,N,NEXY,NPXY,NPYZ,NEYZ,GNOD,BWTYPE
      COMMON /XYZ/ X,Y,Z
      COMMON /LCOORD/ XCOORD
      COMMON /RCOORD/ YCOORD
      COMMON /TCOORD/ ZCOORD
      COMMON /MESH/ GNOD
      DIMENSION X(924), Y(924), Z(924), XCOORD(33), YCOORD(07), ZCOORD(0
     14), GNOD(576,8)
      NPYZ=NPY*NPZ
      NPXY=NPX*NPY
      NEXY=NEX*NEY
      NEYZ=NEY*NEZ
      BWTYPE=1
      IF((NPX.GE.NPY).AND.(NPY.GE.NPZ)) BWTYPE=2
      IF((NPX.GE.NPZ).AND.(NPZ.GE.NPY)) BWTYPE=3
```

```
      IF(BWTYPE.EQ.2) GO TO 150
      IF(BWTYPE.EQ.3) GO TO 300
C
C     ########################   BWTYPE = 1   ############################
C
C     GNOD(I,J) IS THE GLOBAL NODE NUMBER ASSIGNED TO THE J-TH LOCAL
C     NODE OF THE I-TH ELEMENT.
C
C     NUMBER ELEMENT NUMBER ONE. LOCAL NODE 8 = GLOBAL NODE 1 AT (0,0,0)
C     PICTURE OF ELEMENT:  2-4 MEANS GLOBAL NODE 2, LOCAL NODE 4 (ETC.)
C
C     Y               7-6=> .:-------: <=8-2
C     ¢                    ' |     ' |
C     |             3-5=> '.......' <=4-1          NUMBERED AS THOUGH
C     |     Z             |  |    |  |             THIS WAS THE ONLY
C     |   .'           5-7=> :____|__: <=6-3       ELEMENT, HENCE THE
C     | .'                | .'    | .'            GLOBAL NUMBERING
C     |========> X        |.......|'
C                      1-8     2-4
C
      GNOD(1,8)=1
      GNOD(1,4)=2
      GNOD(1,3)=GNOD(1,4)+NPXY
      GNOD(1,2)=GNOD(1,3)+NPX
      GNOD(1,1)=GNOD(1,4)+NPX
      GNOD(1,5)=GNOD(1,8)+NPX
      GNOD(1,7)=GNOD(1,8)+NPXY
      GNOD(1,6)=GNOD(1,7)+NPX
C     NUMBER THE NODES IN THE X (OR LONGITUDINAL) DIRECTION
      N=1
      IF (NEX.EQ.1) GO TO 30
      DO 20 I=2,NEX
      N=N+1
      DO 10 J=1,NPE
      GNOD(I,J)=GNOD(I-1,J)+1
10    CONTINUE
20    CONTINUE
C     NUMBER THE NODES IN THE Y (OR RADIAL) DIRECTION
30    CONTINUE
      IF (NEY.EQ.1) GO TO 70
      DO 60 J=2,NEY
      DO 50 I=1,NEX
      N=N+1
      M=N-NEX
      DO 40 K=1,NPE
      GNOD(N,K)=GNOD(M,K)+NPX
40    CONTINUE
50    CONTINUE
60    CONTINUE
      NEXY=NEX*NEY
```

```
C     NUMBER THE NODES IN THE Z (OR TANGENTIAL) DIRECTION
70    CONTINUE
      IF (NEZ.EQ.1) GO TO 110
      DO 100 J=2,NEZ
      DO 90 K=1,NEXY
      N=N+1
      M=N-NEXY
      DO 80 I=1,NPE
      GNOD(N,I)=GNOD(M,I)+NPXY
80    CONTINUE
90    CONTINUE
100   CONTINUE
C     ASSIGN (L,R,T) COORDINATES TO THE ASSOCIATED GLOBAL NODE
C     NUMBER, N.
110   CONTINUE
      DO 140 K=1,NPZ
      DO 130 J=1,NPY
      DO 120 I=1,NPX
      N=1+(I-1)+(J-1)*NPX+(K-1)*NPXY
      X(N)=XCOORD(I)
      Y(N)=YCOORD(J)
      Z(N)=ZCOORD(K)
120   CONTINUE
130   CONTINUE
140   CONTINUE
      GO TO 450
150   CONTINUE
C
C     ########################   BWTYPE = 2   ############################
C
C     GNOD(I,J) IS THE GLOBAL NODE NUMBER ASSIGNED TO THE J-TH LOCAL
C     NODE OF THE I-TH ELEMENT.
C
C     NUMBER ELEMENT NUMBER ONE. LOCAL NODE 8 = GLOBAL NODE 1 AT (0,0,0)
C     PICTURE OF ELEMENT:  2-7 MEANS GLOBAL NODE 2, LOCAL NODE 7 (ETC.)
C
C     Y               4-6=> .:-------: <=8-2
C     ¢                    ' |     ' |
C     |             3-5=> '.......' <=7-1          NUMBERED AS THOUGH
C     |     Z              |  |    |  |            THIS WAS THE ONLY
C     |   .'            2-7=> :____|__: <=6-3      ELEMENT, HENCE THE
C     | .'                 | .'    | .'            GLOBAL NUMBERING
C     |========> X         |.......|'
C                       1-8     5-4
C
      GNOD(1,8)=1
      GNOD(1,7)=2
      GNOD(1,5)=GNOD(1,8)+NPZ
      GNOD(1,6)=GNOD(1,5)+1
      GNOD(1,4)=GNOD(1,8)+NPYZ
```

```
      GNOD(1,3)=GNOD(1,4)+1
      GNOD(1,1)=GNOD(1,4)+NPZ
      GNOD(1,2)=GNOD(1,1)+1
C     NUMBER THE NODES IN THE Z ( TANGENTIAL ) DIRECTION
      N=1
      IF (NEZ.EQ.1) GO TO 180
      DO 170 I=2,NEZ
      N=N+1
      DO 160 J=1,NPE
      GNOD(I,J)=GNOD(I-1,J)+1
160   CONTINUE
170   CONTINUE
C     NUMBER THE NODES IN THE Y (OR RADIAL) DIRECTION
180   CONTINUE
      IF (NEY.EQ.1) GO TO 220
      DO 210 J=2,NEY
      DO 200 I=1,NEZ
      N=N+1
      M=N-NEZ
      DO 190 K=1,NPE
      GNOD(N,K)=GNOD(M,K)+NPZ
190   CONTINUE
200   CONTINUE
210   CONTINUE
C     NUMBER THE NODES IN THE X (OR LONGITUDINAL) DIRECTION
220   CONTINUE
      IF (NEX.EQ.1) GO TO 260
      DO 250 J=2,NEX
      DO 240 K=1,NEYZ
      N=N+1
      M=N-NEYZ
      DO 230 I=1,NPE
      GNOD(N,I)=GNOD(M,I)+NPYZ
230   CONTINUE
240   CONTINUE
250   CONTINUE
260   CONTINUE
C     ASSIGN (L,R,T) COORDINATES TO THE ASSOCIATED GLOBAL NODE
C     NUMBER, N.
      N=0
      DO 290 K=1,NPX
      DO 280 J=1,NPY
      DO 270 I=1,NPZ
      N=N + 1
      X(N)=XCOORD(K)
      Y(N)=YCOORD(J)
      Z(N)=ZCOORD(I)
270   CONTINUE
280   CONTINUE
290   CONTINUE
```

```
      GO TO 450
300   CONTINUE
C
C     ########################   BWTYPE = 3   ############################
C
C     GNOD(I,J) IS THE GLOBAL NODE NUMBER ASSIGNED TO THE J-TH LOCAL
C     NODE OF THE I-TH ELEMENT.
C
C     NUMBER ELEMENT NUMBER ONE. LOCAL NODE 8 = GLOBAL NODE 1 AT (0,0,0)
C     PICTURE OF ELEMENT:  2-5 MEANS GLOBAL NODE 2, LOCAL NODE 5 (ETC.)
C
C     Y               4-6=> .:-------: <=8-2
C     ¢                    ' |     ' |              NUMBERED AS THOUGH
C     |             2-5=> '.......' <=6-1           THIS WAS THE ONLY
C     |     Z             |  |    |  |             ELEMENT, HENCE THE
C     |   .'            3-7=> :____|__: <=7-3       GLOBAL NUMBERING
C     | .'                 | .'    | .'
C     |========> X         |.......|'
C                       1-8     5-4
C
      GNOD(1,8)=1
      GNOD(1,5)=2
      GNOD(1,4)=GNOD(1,8)+NPYZ
      GNOD(1,1)=GNOD(1,4)+1
      GNOD(1,3)=GNOD(1,4)+NPY
      GNOD(1,2)=GNOD(1,3)+1
      GNOD(1,7)=GNOD(1,8)+NPY
      GNOD(1,6)=GNOD(1,7)+1
C     NUMBER THE NODES IN THE Y (OR RADIAL) DIRECTION
      N=1
      IF (NEY.EQ.1) GO TO 330
      DO 320 I=2,NEY
      N=N+1
      DO 310 J=1,NPE
      GNOD(I,J)=GNOD(I-1,J)+1
310   CONTINUE
320   CONTINUE
C     NUMBER THE NODES IN THE Z (OR TANGENTIAL) DIRECTION
330   CONTINUE
      IF (NEZ.EQ.1) GO TO 370
      DO 360 J=2,NEZ
      DO 350 I=1,NEY
      N=N+1
      M=N-NEY
      DO 340 K=1,NPE
      GNOD(N,K)=GNOD(M,K)+NPY
340   CONTINUE
350   CONTINUE
360   CONTINUE
C     NUMBER THE NODES IN THE X (OR LONGITUDINAL) DIRECTION
```

```
370   CONTINUE
      IF (NEX.EQ.1) GO TO 410
      DO 400 J=2,NEX
      DO 390 K=1,NEYZ
      N=N+1
      M=N-NEYZ
      DO 380 I=1,NPE
      GNOD(N,I)=GNOD(M,I)+NPYZ
380   CONTINUE
390   CONTINUE
400   CONTINUE
C     ASSIGN (L,R,T) COORDINATES TO THE ASSOCIATED GLOBAL NODE
C     NUMBER, N.
410   CONTINUE
      N=0
      DO 440 K=1,NPX
      DO 430 J=1,NPZ
      DO 420 I=1,NPY
      N=N + 1
      X(N)=XCOORD(K)
      Y(N)=YCOORD(I)
      Z(N)=ZCOORD(J)
420   CONTINUE
430   CONTINUE
440   CONTINUE
450   CONTINUE
C
C     PRINTING OF THE BOOLEAN CONNECTIVIY MATRIX IS SUPPRESSED
C
C     WRITE (6,460)
C 460 FORMAT (48X,18HLOCAL NODE NUMBERS,/,39X,1H1,4X,1H2,4X,1H3,4X,1H4,4
C    1X,1H5,4X,1H6,4X,1H7,4X,1H8,//,22X,11HELEMENT NO.,12X,23HASSOCIATED
C    2 GLOBAL NODES)
C     DO 480 I=1,NEM
C     WRITE (6,470) I,(GNOD(I,J),J=1,NPE)
C 470 FORMAT (26X,I3,8X,8(I3,2X))
C 480 CONTINUE
      RETURN
      END
C     ..................................................................
      SUBROUTINE CKALC (EPRINT)
C
C     THIS SUBROUTINE HAS THREE SECTIONS:
C           1) ESTIMATE THE MOISTURE CONTENT OF THE ELEMENT
C              (IF MC DISTRIBUTION IS NON-UNIFORM, MC IS ASSUMED TO
C               HAVE A 2-D PARABOLIC GRADIENT OVER THE CROSS-SECTION)
C           2) ESTIMATE THE ELASTIC CONSTANTS AT THE ESTIMATED MC
C           3) CALCULATE THE 'C' MATRIX
C
      IMPLICIT REAL*8 (A-H,O-Z)
```

```
      REAL*8 ACTMC,MCUSED,XBAR,YBAR,ZBAR,C,B1,B1P,B2,B2P,
     1ESUB1,ESUB2,ESUB3,GSUB12,GSUB13,GSUB23,NU12,NU13,NU21,
     2NU23,NU31,NU32,DELTA,EMC,MCBAR,MCMAX,EBARC,EBART,
     3CC,HAFDEF,TT,EDUMMY,EELEV,NU1211,NU1311,NU2311,NU3211,
     4E2DEL,E3DEL,G12DEL,G13DEL,G23DEL,NU12DL,NU13DL,NU23DL,NU32DL,
     5E2DRY,E3DRY,G12DRY,G13DRY,G23DRY,NU12DY,NU13DY,NU23DY,NU32DY,
     6E1,E2,E3,G12,G13,G23,ERATIO,SG,K1,K2
      INTEGER SYMTRY,GRAD,EPRINT,IT,EOPSHN,TESTYP,EMETHD
      INTEGER UNIAX1,UNIAX2,BEAM1
      COMMON /MOIST1/ ACTMC
      COMMON /MOIST2/ MCUSED,EMC,MCBAR,HAFWID,MCMAX,SG,
     1HAFDEF,N,NEM,SYMTRY,IT,GRAD,EOPSHN,TESTYP
      COMMON /SIGMA/ C,TT
      COMMON /ELK/ ELXYZ
      DIMENSION ACTMC(576), MCUSED(576)
      DIMENSION C(6,6), ELXYZ(8,3)
      DATA BEAM1,UNIAX1,UNIAX2/4HBEAM,4HTENS,4HCOMP/
      ESUB1=0.0
      EMETHD=0
      XBAR=0.0
      YBAR=0.0
      ZBAR=0.0
      IF (IT.GT.1) GO TO 40
      GRAD=1
C     DETERMINE THE KIND OF GRADIENT: 2-D PARABOLIC OR EQUILIBRATED.
C
      IF (MCBAR.EQ.EMC) GO TO 30
C
C     ###################
C     M.C. CALCULATIONS:
C     ###################
C
C     METHOD OF CALCULATION DEPENDS ON THE ORIENTATION OF THE PIECE:
      IF (SYMTRY.EQ.2) GO TO 10
C     SYMMETRY ABOUT THE RADIAL FACE:
C
C       ELEMENT CROSS-SECTION      :--------------:          | Y
C       WITH LOCAL NODE NUMBERS    | 1          2 |          |
C                                  |              |          |
C                                  |              |          |
C                                  | 4          3 |          '-------->
C                                  |______________|                  Z
C
C
C     FIND THE AVERAGE Z-COORDINATE FOR THE ELEMENT (CORRESPONDS TO
C     THE AVE. DIMENSION OF THE ELEMENT IN THE TANGENTIAL DIRECTION)
C     ZBAR CORRESPONDS TO XBAR IN 2-D WHEN SYMTRY = 1.
      ZBAR=HAFWID-((ELXYZ(1,3)+ELXYZ(2,3))/2.0)
      XBAR=ZBAR
C     FIND THE AVERAGE Y-COORDINATE FOR THE ELEMENT (CORRESPONDS TO
```

```
C     THE AVE. DIMENSION OF THE ELEMENT IN THE RADIAL DIRECTION)
C     YBAR CORRESPONDS TO YBAR IN 2-D WHEN SYMTRY = 1.
      YBAR=DABS(((ELXYZ(1,2)+ELXYZ(4,2))/2.0)-HAFDEF)
C     DETERMINE THE TYPE OF ELASTIC PROPERTIES TO BE USED FOR STEP 1
C     (WHETHER COMPRESSION OR TENSION PROPERTIES ARE USED FOR BEAMS
C     DEPENDS ON THE POSITION OF THE ELEMENT IN THE MODELED SPECIMEN)
      IF ((TESTYP.EQ.BEAM1).AND.(YBAR.LT.HAFDEF)) EMETHD=1
      IF ((TESTYP.EQ.BEAM1).AND.(YBAR.GT.HAFDEF)) EMETHD=2
      IF ((TESTYP.EQ.BEAM1).AND.(YBAR.EQ.HAFDEF)) EMETHD=EOPSHN
      IF (TESTYP.EQ.UNIAX1) EMETHD=1
      IF (TESTYP.EQ.UNIAX2) EMETHD=2
      GO TO 20
10    CONTINUE
C     SYMMETRY ABOUT THE TANGENTIAL FACE:
C
C       ELEMENT CROSS-SECTION      :--------------:          | Z
C       WITH LOCAL NODE NUMBERS    | 4          1 |          |
C                                  |              |          |
C                                  |              |          |
C                                  |              |          |
C                                  | 3          2 |          '-------->
C                                  |______________|                 Y
C
C
C     YBAR CORRESPONDS TO XBAR IN 2-D WHEN SYMTRY = 2.
      YBAR=HAFWID-((ELXYZ(1,2)+ELXYZ(4,2))/2.0)
C     ZBAR CORRESPONDS TO YBAR IN 2-D WHEN SYMTRY = 2.
      ZBAR=DABS(HAFDEF-DABS((ELXYZ(1,3)+ELXYZ(2,3))/2.0))
      XBAR=YBAR
      YBAR=ZBAR
C     DETERMINE THE TYPE OF ELASTIC PROPERTIES TO BE USED FOR STEP 1
C     (AS ABOVE)
      IF ((TESTYP.EQ.BEAM1).AND.(YBAR.LT.HAFDEF)) EMETHD=1
      IF ((TESTYP.EQ.BEAM1).AND.(YBAR.GT.HAFDEF)) EMETHD=2
      IF ((TESTYP.EQ.BEAM1).AND.(YBAR.EQ.HAFDEF)) EMETHD=EOPSHN
      IF (TESTYP.EQ.UNIAX1) EMETHD=1
      IF (TESTYP.EQ.UNIAX2) EMETHD=2
20    CONTINUE
C
C     ---------------------------
C     START THE M.C. CALCULATIONS:
C     ---------------------------
C     ACTMC=CALCULATED ACTUAL MC OF ELEMENT (DURING THE FIRST STEP)
C     MCUSED(N)=MC USED IN CALCULATIONS; = ACTMC IF ACTMC < INTERSECTION
C     POINT MOISTURE CONTENT (DEFINED FOR THIS ANALYSIS TO BE 25.60%),
C     AND = 25.60 IF ACTMC > 25.60
C
      IF ((IT.EQ.1).AND.(EPRINT.EQ.1)) ACTMC(N)=2.25*(MCBAR-EMC)*(1.0-(X
     1BAR**2)/(HAFWID**2))*(1.0-(YBAR**2)/(HAFDEF**2)) + EMC
      IF ((IT.EQ.1).AND.(EPRINT.EQ.1)) MCUSED(N)=ACTMC(N)
      IF (((IT.EQ.1).AND.(EPRINT.EQ.1)).AND.(ACTMC(N).GT.25.60)) MCUSED(
```

```
     1N)=25.60
C
      GO TO 40
30    CONTINUE
C
C     FOR SAMPLES WITHOUT A GRADIENT:
C     -------------------------------
      GRAD=0
      IF ((TESTYP.EQ.BEAM1).AND.(SYMTRY.EQ.1)) YBAR=DABS(((ELXYZ(2,2) -
     1ELXYZ(3,2))/2.0) + ELXYZ(3,2))
      IF ((TESTYP.EQ.BEAM1).AND.(SYMTRY.EQ.1)) ZBAR=DABS(((ELXYZ(2,3) -
     1ELXYZ(1,3))/2.0) + ELXYZ(1,3))
      IF ((TESTYP.EQ.BEAM1).AND.(SYMTRY.EQ.2)) YBAR=DABS(((ELXYZ(2,2) -
     1ELXYZ(3,2))/2.0) + ELXYZ(3,2))
      IF ((TESTYP.EQ.BEAM1).AND.(SYMTRY.EQ.2)) ZBAR=DABS(((ELXYZ(2,3) -
     1ELXYZ(1,3))/2.0) + ELXYZ(2,3))
C
      IF ((TESTYP.EQ.BEAM1).AND.(SYMTRY.EQ.1).AND.(YBAR.LT.HAFDEF)) EMET
     1HD = 1
      IF ((TESTYP.EQ.BEAM1).AND.(SYMTRY.EQ.1).AND.(YBAR.GT.HAFDEF)) EMET
     1HD = 2
      IF ((TESTYP.EQ.BEAM1).AND.(SYMTRY.EQ.1).AND.(YBAR.EQ.HAFDEF)) EMET
     1HD = EOPSHN
      IF ((TESTYP.EQ.BEAM1).AND.(SYMTRY.EQ.2).AND.(ZBAR.LT.HAFDEF)) EMET
     1HD = 1
      IF ((TESTYP.EQ.BEAM1).AND.(SYMTRY.EQ.2).AND.(ZBAR.GT.HAFDEF)) EMET
     1HD = 2
      IF ((TESTYP.EQ.BEAM1).AND.(SYMTRY.EQ.2).AND.(ZBAR.EQ.HAFDEF)) EMET
     1HD = EOPSHN
      IF (TESTYP.EQ.UNIAX1) EMETHD=1
      IF (TESTYP.EQ.UNIAX2) EMETHD=2
C
      IF ((IT.EQ.1).AND.(EPRINT.EQ.1)) ACTMC(N)=MCBAR
      IF (MCBAR.LE.25.60) MCUSED(N)=MCBAR
      IF (MCBAR.GT.25.60) MCUSED(N)=25.60
C
40    CONTINUE
C
C     ####################
C     CALCULATE E VALUES:
C     ####################
C
C     CALCULATE E SUB L AT MOISTURE CONTENT OF THE ELEMENT:
C
C     THIS SUBROUTINE USES ONE POSSIBLE APPROACH TO CALCULATE THE ELAS-
C     TIC PARAMETERS OF WOOD WITH A MOISTURE GRADIENT.  E-SUB-L IS FIRST
C     CALCULATED FROM THE APPROPRIATE REGRESSION EQUATIONS FOR E BASED
C     ON TESTING BY T.E. CONNERS    (TESTS ON YELLOW POPLAR ONLY !!)
C     THE OTHER ELASTIC PARAMETERS ARE THEN ESTIMATED FROM THE DATA
C     GIVEN IN FPL REPORT 1528-G (12/46) FOR YELLOW-POPLAR AT 11% MC
```

```
C     AND FROM OTHER DATA IN THE LITERATURE FOR VARIOUS SPECIES.
C     POISSON'S RATIOS ARE A FUNCTION OF MC IN THIS SUBROUTINE ALSO.
C
C     ###################################################################
C
C     CALCULATION OF THE LONGITUDINAL YOUNG'S MODULUS IN COMPRESSION
C     AT VARIOUS STRAINS IS BASED UPON THE SLOPE OF A SEGMENTED MODEL
C     FOR THE STRESS-STRAIN DIAGRAM.
C
C     EBARC IS THE AVERAGE YOUNG'S MODULUS FOR A GIVEN MOISTURE CONTENT
C     FROM ZERO STRAIN TO A JOIN POINT WITH THE NEXT MODEL SEGMENT (K1).
C
      EBARC=143908.0 + 441996.0*MCUSED(N) -28997.4*(MCUSED(N)**2)
     $      534.3*(MCUSED(N)**3)
C
C     ESTIMATE THE PARAMETERS B2 AND B3 FOR THE COMPRESSION MODEL:
C
      B2=5719344.0 - 258848.0*MCUSED(N) + 4281.8*(MCUSED(N)**2)
C
      B3= -1065588539.0 + 3449729.0*MCUSED(N) + 1540914880.0*SG
      B3=-B3
C
C
C     TWO PARAMETERS NEED TO BE DEFINED IN TERMS OF B2 AND B3
C     SO THAT THE MODEL FOR STRESS-STRAIN BEHAVIOR IN COMPRESSION
C     CAN BE COMPLETE. K1 IS THE JOIN POINT BETWEEN A LINEAR AND A
C     QUADRATIC MODEL AT LOW STRAIN VALUES, K2 IS THE JOIN POINT
C     BETWEEN BETWEEN THE QUADRATIC MODEL AND THE LINE AT PMAX.
C
      K1= (EBARC-B2)/(2*B3)
      K2= -B2/(2*B3)
C
C     AFTER MCUSED(N) IS DEFINED ON THE FIRST PASS THROUGH THIS SBR (ON
C     THE FIRST STEP), ACTMC(N) BECOMES A SCRATCH PAD HOLDING THE
C     ACCUMULATED STRAINS FOR EACH ELEMENT.
C
      IF ((EMETHD.EQ.2).OR.((IT.GT.1).AND.(ACTMC(N).GE.K1).AND.(ACTMC(N)
     $.LE.0.0))) E1=EBARC
      IF ((ACTMC(N).LT.K1).AND.(IT.GT.1))
     $   E1= B2 + 2.0*B3*ACTMC(N)
C
C     LONGITUDINAL YOUNG'S MODULUS IN COMPRESSION AT FAILURE = 1.0
      IF ((ACTMC(N).LE.K2).AND.(IT.GT.1)) E1=1.0
C
C     ###################################################################
C
C     CALCULATION OF THE LONGITUDINAL YOUNG'S MODULUS IN TENSION
C     AT VARIOUS STRAINS IS BASED UPON THE SLOPE OF A SEGMENTED MODEL
C     FOR THE STESS-STRAIN DIAGRAM.
C
```

```
C     EBART IS THE AVERAGE YOUNG'S MODULUS IN TENSION FOR A GIVEN M.C.
C     FROM ZERO STRAIN TO A JOIN POINT WITH THE NEXT MODEL SEGMENT (K1).
C
      EBART=1822346 - 9.8*(MCUSED(N)**3)
C
C     ESTIMATE THE PARAMETERS B2P AND B3P FOR TENSION:
C
      B2P = 1934676.0
      B3P = 37045444.0 - 2203.5*(MCUSED(N)**3) - 150737800.0*SG
C
C     SIMILAR CIRCUMSTANCES AS FOR COMPRESSION, BUT
C     NO K2 (PER SE) FOR TENSION MODEL (SEE TT BELOW) :
      K1= (EBART - B2P)/(2*B3P)
C
      IF ((EMETHD.EQ.1).OR.((IT.GT.1).AND.(ACTMC(N).LE.K1).AND.(ACTMC(N)
     $.GT.0.0))) E1=EBART
      IF ((IT.GT.1).AND.(ACTMC(N).GE.K1)) E1=B2P + 2.0*B3P*ACTMC(N)
C
C     THE FAILURE STRAIN IN TENSION FOR THIS ELEMENT = TT
C
      TT = 0.016334 - 0.00129434*MCUSED(N)
     $     0.00009634534*(MCUSED(N)**2) - 0.0000021399*(MCUSED(N)**3)
C
C     LONGITUDINAL YOUNG'S MODULUS IN TENSION AT FAILURE = 1.0
      IF ((ACTMC(N).GE.TT).AND.(IT.GT.1)) E1=1.0
C
C     ######################################################################
C
C     CALCULATE AN AVERAGE E SUB L TO USE AT NEUTRAL AXIS OF BEAMS
C     WHENEVER AN ODD NO. OF ELEMENTS IS PRESENT IN THE LOADING
C     DIRECTION ON THE FIRST STEP. (AVE. OF TENSION,COMPRESSION E SUB L)
C
      IF ((EMETHD.EQ.3).AND.(IT.EQ.1)) E1= (EBARC + EBART)/2.0
C
C     NO SPECIFIC DATA EXIST FOR YELLOW-POPLAR E2 & E3 EXCEPT AT 11% MC.
C     SOME DATA ARE AVAILABLE FOR SHEAR MODULI IN MARK, ET AL., AND COM-
C     PARE FAVORABLY WITH VALUES FOUND IN FPL REPORT #1528-G FOR 11% MC.
C     POISSON'S RATIOS FOR Y-P ARE ALSO ONLY AVAILABLE AT 11% MC IN FPL
C     REPORT #1528-G.
C
C     PROCEDURE:
C     TO BE CONSISTENT FOR ALL THE ELASTIC CONSTANTS, ESTIMATE E2 & E3,
C     THE SHEAR MODULI AND THE POISSON'S RATIOS AT 11% MC.
C     THE RATE OF CHANGE OF THE ELASTIC CONSTANTS HAVE BEEN APPROXIMATED
C     BASED ON A PROPERTY AT SOME MAXIMUM VALUE MOISTURE CONTENT (MVMC)
C     AND ADJUSTMENTS ARE MADE TO ACCOUNT FOR MC BASED ON THE
C     APPROXIMATION OF THIS RATE OF CHANGE, THE PROPERTY VALUE AT MVMC,
C     AND THE PROPERTY VALUE AT 11%.  MC IS ASSUMED TO BE A LINEAR
C     INFLUENCE ON THESE ELASTIC CONSTANTS.
C
```

```
C     THE E2 & E3 VALUES WERE TAKEN FROM FPL REPORT 1528-G (1946), AS
C     WERE THE VALUES FOR THE POISSON'S RATIOS.
C     G SUB IJ VALUES WERE TAKEN FROM FPL REPORT 1528-G AND FROM
C     MARK, ET AL., WOOD SCIENCE 2(4):203-211 (1970).
C
C     E2,E3 DO NOT APPEAR TO BE PROPORTIONAL TO DENSITY ACCORDING TO FPL
C     REPORTS, SERIES #1528:A-G.
C     G SUB IJ MAY OR MAY NOT BE PROPORTIONAL TO DENSITY ACCORDING TO
C     KOLLMANN AND COTE PAGE 307.
C     BODIG AND JAYNE, P. 384 ASSUME E2 & E3 ARE PROPORTIONAL TO S.G.,
C     BUT THIS PROPORTIONALITY IS PROBABLY ONLY VALID WHEN A WIDE RANGE
C     OF S.G. EXISTS.
C     FPL REPORTS #1528 ALSO INDICATE THAT S.G. DOES NOT AFFECT THE
C     POISSON'S RATIOS.
C     MY ANALYSES FOR E SUB L INDICATE THAT S.G. IS SOMEWHAT IMPORTANT
C     FOR PREDICTING THE SHAPE OF THE STRESS-STRAIN DIAGRAM BEYOND THE
C     ELASTIC LIMIT FOR COMP. & TENS., BUT OTHER REGRESSORS WERE MORE
C     EFFECTIVE IN PREDICTING THE YOUNG'S MODULI AT VARIOUS M.C.'S.
C     OVERALL, I DECIDED THAT S.G. IS NOT A SIGNIFICANT REGRESSOR OR
C     MODIFIER FOR THE ELASTIC CONSTANTS.
C
C     THE FOLLOWING E SUB I VALUES ARE FROM FPL REPORT #1528-G (AVERAGED
C     DATA):
C
C     WITH THE EXCEPTION OF E1, THE ASSUMPTION HAD TO BE MADE THAT THE
C     ELASTIC CONSTANTS HAVE THE SAME VALUES IN EITHER COMPRESSION
C     OR TENSION.
C
      ESUB2=129000.0
      ESUB3= 60000.0
      GSUB12=105000.0
      GSUB13= 97000.0
      GSUB23= 16000.0
C     THESE POISSON'S RATIOS ARE ALSO SPECIFIC FOR YELLOW-POPLAR AT 11%
      NU1211=0.318
      NU1311=0.392
      NU2311=0.703
      NU3211=0.329
C
C     ELASTIC CONSTANTS ARE ASSUMED TO CHANGE AS SOON AS THE M.C.
C     DROPS BELOW AN INTERSECTION POINT (PERHAPS FSP); ASSUMED ALSO THAT
C     THE ELASTIC CONSTANT VERSUS MC CURVE IS APPROXIMATELY LINEAR.
C     THE AMOUNT OF CHANGE IN THE ELASTIC CONSTANT CAN THEN BE
C     DEFINED LINEARLY AS A FUNCTION OF THE CHANGE IN M.C.
C     ALL EQUATIONS ARE WITH REFERENCE TO THE PROPERTY AT THE MVMC
C     (= MAXIMUM  PROPERTY VALUE EXCEPT FOR SOME POISSON'S RATIOS)
C     (MVMC = MAXIMUM VALUE MOISTURE CONTENT)
C
C     E SUB I CHANGES ARE BASED ON YOUNG'S RED OAK DATA, DATA FROM
C     CARRINGTON'S SPRUCE (1922), AND D.FIR AND SITKA SPRUCE DATA FROM
```

```
C     FPL REPORTS #1528-A&D.
      E2DEL=-0.0283002303
      E3DEL=-0.0296368095
C     GIJDEL ARE SPECIFIC FOR YELLOW-POPLAR, BASED ON MARK, ET AL. AND
C     FPL REPORT #1528-G.
C     THESE ARE NOT ESTIMATES BASED ON OTHER SPECIES.
      G12DEL=-0.0209330144
      G13DEL=-0.0188235294
      G23DEL=-0.0289855072
C     POISSON'S ESTIMATES ARE BASED ON CARRINGTONS'S SPRUCE DATA & FPL
C     REPORTS #1528-A&D
      NU12DL=-0.0110545944
      NU13DL=+0.0189257296
      NU23DL=+0.0219786258
      NU32DL=+0.0169128189
C
C     THE ELASTIC CONSTANTS AT THE LOWEST MC'S AT WHICH THEY ARE
C     SENSITIVE TO MOISTURE CONTENT CHANGES (MAXIMUM VALUE MOISTURE
C     CONTENTS) HAVE ALREADY BEEN CALCULATED:
C
      E2DRY= 173745.0
      E3DRY=  82157.0
      G12DRY=130382.0
      G13DRY=122329.0
      G23DRY= 20073.0
      NU12DY=0.3536
      NU13DY=0.3344
      NU23DY=0.5858
      NU32DY=0.2851
C
C     CALCULATE THE VALUES OF THE ELASTIC CONSTANTS AT THE MC SPECIFIED
C     FOR THE ELEMENT:  (EXCEPT FOR E1, CALCULATED TOP OF THIS SECTION)
C
      IF (MCUSED(N).GT.24.15) A=24.15
      IF (MCUSED(N).LE.24.15) A=MCUSED(N)
      E2=E2DRY + (A-1.9)*E2DEL*E2DRY
      IF (MCUSED(N).LT.1.9) E2=E2DRY
C
      IF (MCUSED(N).GT.24.15) A=24.15
      IF (MCUSED(N).LE.24.15) A=MCUSED(N)
      E3=E3DRY + (A-1.9)*E3DEL*E3DRY
      IF (MCUSED(N).LT.1.9) E3=E3DRY
C
      IF (MCUSED(N).GT.22.6) A=22.6
      IF (MCUSED(N).LE.22.6) A=MCUSED(N)
      G12=G12DRY + (A-1.7)*G12DEL*G12DRY
      IF (MCUSED(N).LT.1.7) G12=G12DRY
C
      IF (MCUSED(N).GT.20.0) A=20.0
      IF (MCUSED(N).LE.20.0) A=MCUSED(N)
```

```
      G13=G13DRY + (A-0.0)*G13DEL*G13DRY
      IF (MCUSED(N).LT.0.0) G13=G13DRY
C
      IF (MCUSED(N).GT.22.0) A=22.0
      IF (MCUSED(N).LE.22.0) A=MCUSED(N)
      G23=G23DRY + (A-4.0)*G23DEL*G23DRY
      IF (MCUSED(N).LT.4.0) G23=G23DRY
C
      IF (MCUSED(N).GT.24.15) A=24.15
      IF (MCUSED(N).LE.24.15) A=MCUSED(N)
      NU12=NU12DY + (A-1.9)*NU12DL*NU12DY
      IF (MCUSED(N).LT.1.9) NU12=NU12DY
C
      IF (MCUSED(N).GT.24.15) A=24.15
      IF (MCUSED(N).LE.24.15) A=MCUSED(N)
      NU13=NU13DY + (A-1.9)*NU13DL*NU13DY
      IF(MCUSED(N).LT.1.9) NU13=NU13DY
C
      IF (MCUSED(N).GT.24.15) A=24.15
      IF (MCUSED(N).LE.24.15) A=MCUSED(N)
      NU23=NU23DY + (A-1.9)*NU23DL*NU23DY
      IF(MCUSED(N).LT.1.9) NU23=NU23DY
C
      IF (MCUSED(N).GT.24.15) A=24.15
      IF (MCUSED(N).LE.24.15) A=MCUSED(N)
      NU32=NU32DY + (A-1.9)*NU32DL*NU32DY
      IF(MCUSED(N).LT.1.9) NU32=NU32DY
C
C     USE SYMMETRY OF THE COMPLIANCE MATRIX
C     TO CALCULATE REMAINING POISSON'S RATIOS:
      NU21=(NU12*E2)/E1
      NU31=(NU13*E3)/E1
C
C     ONLY NU12 AND NU13 ASSUMED TO DECREASE AS E1 DECREASES:
C
      IF ((IT.GT.1).AND.(ACTMC(N).GT.0.0)) ESUB1=EBART
      IF ((IT.GT.1).AND.(ACTMC(N).LE.0.0)) ESUB1=EBARC
      IF (IT.GT.1) ERATIO=E1/ESUB1
      IF (IT.GT.1) NU12=ERATIO*NU12
      IF (IT.GT.1) NU13=ERATIO*NU13
C
C     IF THE MODELED DISPLACEMENT IN TENSION FROM THE PREVIOUS STEP
C     EXCEEDED THE ALLOWABLE DISPLACEMENT, ALL MODULI ARE REDUCED
C     BECAUSE THE MATERIAL HAS RUPTURED:
      IF ((IT.GT.1).AND.(ACTMC(N).GE.TT)) E2=ERATIO * E2
      IF ((IT.GT.1).AND.(ACTMC(N).GE.TT)) E3=ERATIO * E3
      IF ((IT.GT.1).AND.(ACTMC(N).GE.TT)) G12=ERATIO * G12
      IF ((IT.GT.1).AND.(ACTMC(N).GE.TT)) G13=ERATIO * G13
      IF ((IT.GT.1).AND.(ACTMC(N).GE.TT)) G23=ERATIO * G23
      IF ((IT.GT.1).AND.(ACTMC(N).GE.TT)) NU12=ERATIO * NU12
```

```
      IF ((IT.GT.1).AND.(ACTMC(N).GE.TT)) NU13=ERATIO * NU13
      IF ((IT.GT.1).AND.(ACTMC(N).GE.TT)) NU21=ERATIO * NU21
      IF ((IT.GT.1).AND.(ACTMC(N).GE.TT)) NU23=ERATIO * NU23
      IF ((IT.GT.1).AND.(ACTMC(N).GE.TT)) NU31=ERATIO * NU31
      IF ((IT.GT.1).AND.(ACTMC(N).GE.TT)) NU32=ERATIO * NU32
C
C     'EDUMMY' IS USED ONLY FOR PRINTING MATERIAL PROPERTIES.
      EDUMMY=1.0D0
      IF (((IT.GT.1).AND.(ACTMC(N).LE.TT)).OR.(IT.EQ.1)) EDUMMY=E1
C        REMEMBER: ACTMC(N) IS THE STORAGE SPACE FOR THE ACCUMULATED
C        --------  LONGITUDINAL STRAIN FOR ELEMENT N.
C
C     ########################################
C     CALCULATE THE [C] MATRIX FOR ELEMENT 'N'
C     ########################################
C
      DELTA=(1-NU12*NU21-NU23*NU32-NU31*NU13-2.0*NU21*NU32*NU13)/(E1*
     1E2*E3)
      DO 60 I=1,6
      DO 50 J=1,6
      C(I,J)=0.0
50    CONTINUE
60    CONTINUE
      C(1,1)=(1-NU23*NU32)/(E2*E3*DELTA)
      C(1,2)=(NU12+NU32*NU13)/(E1*E3*DELTA)
      C(1,3)=(NU13+NU12*NU23)/(E1*E2*DELTA)
      C(2,1)=C(1,2)
      C(2,2)=(1-NU13*NU31)/(E1*E3*DELTA)
      C(2,3)=(NU23+NU21*NU13)/(E1*E2*DELTA)
      C(3,1)=C(1,3)
      C(3,2)=C(2,3)
      C(3,3)=(1-NU12*NU21)/(E1*E2*DELTA)
      C(4,4)=G23
      C(5,5)=G13
      C(6,6)=G12
C
C     PRINT THE VALUES OF E SUB 1, ETC., FOR EACH ELEMENT.
C
      IF ((N.EQ.1).AND.(EPRINT.EQ.1)) WRITE (6,70)
70    FORMAT (////,54X,23HELASTIC PROPERTIES USED)
      IF ((N.EQ.1).AND.(EPRINT.EQ.1)) WRITE (6,80)
80    FORMAT (//,2X,9H STEP NO.,3X,7HEL. NO.,8X,7HE SUB L,10X,7HE SUB R,
     110X,7HE SUB T,8X,8HG SUB LR,8X,8HG SUB LT,9X,8HG SUB RT,/,28X,9HNU
     2 SUB LR,8X,9HNU SUB LT,8X,9HNU SUB RL,6X,9HNU SUB RT,7X,9HNU SUB T
     3L,8X,9HNU SUB TR,/)
      IF ((N.EQ.1).AND.(GRAD.EQ.0).AND.(EPRINT.EQ.1).AND.(IT.EQ.1).AND.(
     1TESTYP.NE.BEAM1)) WRITE(6,90) IT,E1,E2,E3,G12,G13,G23
90    FORMAT (5X,I3,9X,3HALL,6X,F12.1,4X,F12.1,4X,F12.1,4X,F12.1,4X,F12.
     11,4X,F12.1)
      IF (((N.GE.1).AND.(GRAD.EQ.1).AND.(EPRINT.EQ.1).AND.(IT.GE.1)).OR.
```

```
     1((N.GE.1).AND.(GRAD.EQ.0).AND.(EPRINT.EQ.1).AND.(IT.GT.1)).OR.
     2((EPRINT.EQ.1).AND.(TESTYP.EQ.BEAM1)))
     3WRITE(6,100) IT,N,EDUMMY,E2,E3,G12,G13,G23
100   FORMAT (5X,I3,8X,I4,6X,F12.1,4X,F12.1,4X,F12.1,4X,F12.1,4X,F12.1,4
     1X,F12.1)
      IF(((EPRINT.EQ.1).AND.(IT.EQ.1).AND.(GRAD.EQ.1)).OR.
     1((IT.GT.1).AND.(EPRINT.EQ.1)).OR.((EPRINT.EQ.1).AND.(TESTYP.EQ.BEA
     2M1))) WRITE(6,110) NU12,NU13,NU21,NU23,NU31,NU32
110   FORMAT(31X,6(F6.3,10X),/)
      IF ((EPRINT.EQ.1).AND.(IT.EQ.1).AND.(GRAD.EQ.0).AND.(N.EQ.1).AND.(
     1TESTYP.NE.BEAM1)) WRITE(6,120) NU12,NU13,NU21,NU23,NU31,NU32
120   FORMAT(31X,6(F6.3,10X))
      RETURN
      END
C     .....................................................................
      SUBROUTINE SF3DL (NPE,XI,ETA,ZETA,DET)
C     THIS SUBROUTINE EVALUATES THE SHAPE FUNCTIONS AND THEIR DERIVA-
C     TIVES AT THE GAUSSIAN POINTS FOR AN ISOPARAMETRIC EIGHT-NODE
C     (LINEAR) THREE-DIMENSIONAL ELEMENT.
C     ELNODE IS AN ARRAY OF THE (XI,ETA,ZETA) COORDINATES FOR AN ELEMENT
C     DSF=DERIVATIVES OF THE SHAPE FUNCTION WITH RESPECT TO THE LOCAL
C     COORDINATE SYSTEM.  ELXYZ=GLOBAL COORDINATES FOR THE ELEMENT.
C     GJ=JACOBIAN TRANSFORMATION MATRIX BASED ON GLOBAL COORDINATES.
C     GJINV=INVERSE OF THE [GJ] MATRIX.  GDSF=DERIVATIVES OF THE SHAPE
C     FUNCTION WITH RESPECT TO THE GLOBAL COORDINATE SYSTEM (L,R,T).
      IMPLICIT REAL*8(A-H,O-Z)
      COMMON /SHAPE/ SF
      COMMON /GSHAPE/ GDSF
      COMMON /ELK/ ELXYZ
      DIMENSION ELNODE(8,3), DSF(3,8), GJ(3,3), GJINV(3,3), SF(8), GDSF(
     13,8), ELXYZ(8,3)
      DATA ELNODE/2*1.0D0,2*-1.0D0,2*1.0D0,3*-1.0D0,2*1.0D0,2*-1.0D0,2*1
     11.0D0,5*-1.0D0,4*1.0D0/
C     COORDINATES OF EACH LOCAL NODE:
      DO 10 I=1,NPE
      XP=ELNODE(I,1)
      YP=ELNODE(I,2)
      ZP=ELNODE(I,3)
      XIO=1.0+XI*XP
      ETAO=1.0+ETA*YP
      ZETAO=1.0+ZETA*ZP
C     SF(I)=SHAPE FUNCTIONS
      SF(I)=(XIO*ETAO*ZETAO)/8.0
C     DERIVATIVES OF THE SHAPE FUNCTION WITH RESPECT TO XI,ETA,ZETA
      DSF(1,I)=(XP*ETAO*ZETAO)/8.0
      DSF(2,I)=(XIO*YP*ZETAO)/8.0
      DSF(3,I)=(XIO*ETAO*ZP)/8.0
10    CONTINUE
C     MULTIPLY [DSF]*[ELXYZ] TO GET [GJ]
      CALL MATMLT (DSF,3,NPE,ELXYZ,3,GJ)
```

```
C     COMPUTE THE DETERMINANT OF THE JACOBIAN TRANSFORMATION MATRIX AND
C     INVERT THE JACOBIAN MATRIX.
      CALL INVDET (GJ,GJINV,DET)
C     MULTIPLY [GJINV]*[DSF] TO GET [GDSF]
      CALL MATMLT (GJINV,3,3,DSF,NPE,GDSF)
      RETURN
      END
C     ..................................................................
      SUBROUTINE MATMLT (A,M,N,B,L,C)
C     THIS SUBROUTINE MULTIPLIES MATRICES A(M,N) BY B(N,L) TO YIELD
C     MATRIX C(M,L)
      IMPLICIT REAL*8(A-H,O-Z)
      DIMENSION A(M,N), B(N,L), C(M,L)
      DO 30 I=1,M
      DO 20 J=1,L
      C(I,J)=0.0
      DO 10 K=1,N
      C(I,J)=A(I,K)*B(K,J)+C(I,J)
10    CONTINUE
20    CONTINUE
30    CONTINUE
      RETURN
      END
C     ..................................................................
      SUBROUTINE INVDET (A,B,DET)
C     THIS SUBROUTINE CALCULATES THE DETERMINANT AND THE INVERSE OF A
C     3 X 3 MATRIX. [A] IS THE MATRIX TO BE INVERTED, [B] IS ITS INVERSE
      IMPLICIT REAL*8(A-H,O-Z)
      DIMENSION A(3,3), B(3,3)
      G(Z1,Z2,Z3,Z4)=Z1*Z2-Z3*Z4
      F(Z1,Z2,Z3,Z4)=G(Z1,Z2,Z3,Z4)/DET
      C1=G(A(2,2),A(3,3),A(2,3),A(3,2))
      C2=G(A(2,3),A(3,1),A(2,1),A(3,3))
      C3=G(A(2,1),A(3,2),A(2,2),A(3,1))
      DET=A(1,1)*C1+A(1,2)*C2+A(1,3)*C3
      B(1,1)=F(A(2,2),A(3,3),A(3,2),A(2,3))
      B(1,2)=-F(A(1,2),A(3,3),A(1,3),A(3,2))
      B(1,3)=F(A(1,2),A(2,3),A(1,3),A(2,2))
      B(2,1)=-F(A(2,1),A(3,3),A(2,3),A(3,1))
      B(2,2)=F(A(1,1),A(3,3),A(3,1),A(1,3))
      B(2,3)=-F(A(1,1),A(2,3),A(1,3),A(2,1))
      B(3,1)=F(A(2,1),A(3,2),A(3,1),A(2,2))
      B(3,2)=-F(A(1,1),A(3,2),A(1,2),A(3,1))
      B(3,3)=F(A(1,1),A(2,2),A(2,1),A(1,2))
      RETURN
      END
C     ..................................................................
      SUBROUTINE MIRROR (POSYM,COORD,OVRNOD,OVRVAL,NDF,NPX,NPY,NPZ,NNM,A
     1AA,SDFNOD,DFVALS,BWTYPE)
C     THIS SUBROUTINE IS A CONVENIENCE ROUTINE TO IMPOSE A SPECIFIED
```

```
C     DISPLACEMENT UPON AN ENTIRE PLANE (OR PLANES) WHEN NO REACTION
C     FORCES ARE TO BE CALCULATED AT THE NODES IN THE PLANE.  THIS
C     ROUTINE IS ESPECIALLY USEFUL, THEREFORE, FOR IMPOSING A
C     SPECIFIED DISPLACEMENT OF 0.0 AT THE PLANES OF SYMMETRY.  THE
C     SUBROUTINE MUST BE MODIFIED IF MORE THAN 2 PARALLEL PLANES OF
C     SYMMETRY ARE DESIRED IN ANY DIRECTION (RE-DIMENSION OVRNOD,OVRVAL)
C
C     THIS SUBROUTINE ONLY WORKS WITH 3-D LINEAR ELEMENTS AND MATCHES
C     THE NODE-NUMBERING SCHEMES USED IN SUBROUTINE 'MESH3D'.
C
      IMPLICIT REAL*8(A-H,O-Z)
      REAL*8 OVRNOD,OVRVAL,DFVALS,XCOORD,YCOORD,ZCOORD
      INTEGER SDFNOD,AAA,POSYM,COORD,VECLEN,NPX,NPY,NPZ,NNM,NPXY,NODE
      INTEGER BWTYPE,NPYZ
      COMMON /VECTR3/ VECLEN
      COMMON /LCOORD/ XCOORD
      COMMON /RCOORD/ YCOORD
      COMMON /TCOORD/ ZCOORD
      DIMENSION XCOORD(33), YCOORD(07), ZCOORD(04)
      DIMENSION OVRNOD(2), OVRVAL(2)
      DIMENSION SDFNOD(VECLEN), DFVALS(VECLEN)
      NPXY=NPX*NPY
      NPYZ=NPY*NPZ
      IF (COORD.NE.1) GO TO 80
      DO 70 J=1,POSYM
      DO 60 I=1,NPX
      IF (XCOORD(I).NE.OVRNOD(J)) GO TO 60
      IF (BWTYPE.NE.1) GO TO 20
      DO 10 K=I,NNM,NPX
      AAA=AAA+1
      NODE=(K-1)*NDF+COORD
      SDFNOD(AAA)=NODE
      DFVALS(AAA)=OVRVAL(J)
10    CONTINUE
20    CONTINUE
      IF (BWTYPE.NE.2) GO TO 40
      M=(I-1)*NPYZ+1
      N=I*NPYZ
      DO 30 K=M,N
      AAA=AAA+1
      NODE=(K-1)*NDF+COORD
      SDFNOD(AAA)=NODE
      DFVALS(AAA)=OVRVAL(J)
30    CONTINUE
40    CONTINUE
      IF (BWTYPE.NE.3) GO TO 70
      M=(I-1)*NPYZ+1
      N=I*NPYZ
      DO 50 K=M,N
      AAA=AAA+1
```

```
      NODE=(K-1)*NDF+COORD
      SDFNOD(AAA)=NODE
      DFVALS(AAA)=OVRVAL(J)
50    CONTINUE
      GO TO 70
60    CONTINUE
70    CONTINUE
80    CONTINUE
      IF (COORD.NE.2) GO TO 190
      DO 180 J=1,POSYM
      DO 170 I=1,NPY
      IF (YCOORD(I).NE.OVRNOD(J)) GO TO 170
      IF (BWTYPE.NE.1) GO TO 110
      M=NPX*(I-1)+1
      N=NPX*I
      DO 100 L=1,NPZ
      DO 90 K=M,N
      AAA=AAA+1
      NODE=(K-1)*NDF+COORD
      SDFNOD(AAA)=NODE
      DFVALS(AAA)=OVRVAL(J)
90    CONTINUE
      M=M+NPXY
      N=M+NPX-1
100   CONTINUE
110   CONTINUE
      IF (BWTYPE.NE.2) GO TO 140
      M=(I-1)*NPZ+1
      N=M+NPZ-1
      DO 130 L=1,NPX
      DO 120 K=M,N
      AAA=AAA+1
      NODE=(K-1)*NDF+COORD
      SDFNOD(AAA)=NODE
      DFVALS(AAA)=OVRVAL(J)
120   CONTINUE
      M=M+NPYZ
      N=M+NPZ-1
130   CONTINUE
140   CONTINUE
      IF (BWTYPE.NE.3) GO TO 180
      M=I
      N=NPYZ
      DO 160 L=1,NPX
      DO 150 K=M,N,NPY
      AAA=AAA+1
      NODE=(K-1)*NDF+COORD
      SDFNOD(AAA)=NODE
      DFVALS(AAA)=OVRVAL(J)
150   CONTINUE
```

```
      M=N+I
      N=N+NPYZ
160   CONTINUE
      GO TO 180
170   CONTINUE
180   CONTINUE
190   CONTINUE
      IF (COORD.NE.3) GO TO 280
      DO 270 J=1,POSYM
      DO 260 I=1,NPZ
      IF (ZCOORD(I).NE.OVRNOD(J)) GO TO 260
      IF (BWTYPE.NE.1) GO TO 210
      M=NPXY*(I-1)+1
      N=M+NPXY-1
      DO 200 K=M,N
      AAA=AAA+1
      NODE=(K-1)*NDF+COORD
      SDFNOD(AAA)=NODE
      DFVALS(AAA)=OVRVAL(J)
200   CONTINUE
210   CONTINUE
      IF (BWTYPE.NE.2) GO TO 230
      M=I
      N=NPY*NPZ*(NPX-1)+(NPY-1)*NPZ+I
      DO 220 K=M,N,NPZ
      AAA=AAA+1
      NODE=(K-1)*NDF+COORD
      SDFNOD(AAA)=NODE
      DFVALS(AAA)=OVRVAL(J)
220   CONTINUE
230   CONTINUE
      IF (BWTYPE.NE.3) GO TO 270
      M=(I-1)*NPY+1
      DO 250 II=1,NPX
      INT=M-1+NPY
      DO 240 K=M,INT
      AAA=AAA+1
      NODE=(K-1)*NDF+COORD
      SDFNOD(AAA)=NODE
      DFVALS(AAA)=OVRVAL(J)
240   CONTINUE
      M=M+NPYZ
250   CONTINUE
      GO TO 270
260   CONTINUE
270   CONTINUE
280   CONTINUE
      RETURN
      END
C     ..................................................................
```

```
      SUBROUTINE VECTOR (NUMLOD,NPX,NPXY,NNM,NODES,VALUES,RXN,NUMRXN,INC
     1,INCR,AAA,NPY,NPZ,BWTYPE)
C
C     THIS ROUTINE IS FOR 3-D LINEAR 8-NODE ELEMENTS.  THE NODE
C     NUMBERING SCHEME USED IN THE PROGRAM IS PASSED IN BY BWTYPE.
C
C     THIS SUBROUTINE FORMS THE ARRAYS NECESARY FOR THE IMPLEMENTATION
C     OF THE BOUNDARY CONDITIONS.  THIS SUBROUTINE IS CALLED FOR THE
C     BOUNDARY FORCES AS WELL AS FOR THE SPECIFIED DISPLACEMENTS.
C     "LOAD" IN THE SUBROUTINE APPLIES EQUALLY TO LOADS OR DISPLACEMENTS
C     NUMLOD(I)=NO. OF LOADS APPLIED IN THE X-DIRECTION FOR I=1
C               NO. OF LOADS APPLIED IN THE Y-DIRECTION FOR I=2
C               NO. OF LOADS APPLIED IN THE Z-DIRECTION FOR I=3
C     LOADX=X-COORDINATE AT WHICH THE LOAD IS APPLIED
C           (SIMILAR FOR LOADY & LOADZ)
C
C     FOR EACH LOAD, INPUT THE (X,Y,Z) COORDINATES AND THE LOAD TO BE
C     APPLIED (ALL ON ONE CARD OR LINE).  INPUT COORDINATES AND LOAD FOR
C     ALL THE LOADS IN THE X-DIRECTION FIRST, THEN THE Y-DIRECTION, THEN
C     THE Z-DIRECTION.
C
C     IF THE NODE IS TO HAVE ADDITIONAL FORCES OR DISPLACEMENTS IMPOSED
C     ON IT DURING THE COURSE OF A STEPWISE ANALYSIS, THE INPUT LINE
C     MUST HAVE A '1' AS THE LAST VALUE (FOR VARIABLE INCFLG).  IF
C     ADDITIONAL FORCES OR DISPLACEMENTS ARE TO BE IMPOSED DURING THE
C     ANALYSIS, BUT NOT TO THIS INDIVIDUAL NODE, THE INPUT LINE MUST
C     HAVE A ZERO ('0') AS THE LAST VALUE (FOR VARIABLE INCFLG).
C
      IMPLICIT REAL*8 (A-H,O-Z)
      REAL*8 LOADX,LOADY,LOADZ,LOAD,VALUES,LOD1,LOD2
      INTEGER VECLEN,NUMLOD(3),NODNUM,PLACE,I,J,K,L,NPX,NPXY,NNM,AAA
      INTEGER NODES,P,RXN,NUMRXN,RXNREQ,RXNNOD,INCVTR,INCFLG,INC,INCR
      INTEGER NPYZ,NPY,NPZ,BWTYPE
      COMMON /XYZ/ X,Y,Z
      COMMON /VECTR1/ LOD1,LOD2
      COMMON /VECTR2/ RXNNOD
      COMMON /VECTR3/ VECLEN
      COMMON /INCRMT/ INCVTR
      DIMENSION X(924), Y(924), Z(924), RXNNOD(004), INCVTR(004)
      DIMENSION VALUES(VECLEN), NODES(VECLEN)
C     LOD1 = SUM OF FORCES APPLIED, LOD2 = SUM OF DISPLACEMENTS APPLIED
      PLACE=0
      IF (RXN.EQ.1) PLACE=AAA
      L=1
      INC=0
      INCFLG=0
      NPYZ=NPY*NPZ
10    CONTINUE
      IF (NUMLOD(L).EQ.0) GO TO 330
      P=NUMLOD(L)
```

```
      DO 320 II=1,P
      RXNREQ=0
      IF ((RXN.EQ.0).AND.(INCR.EQ.0)) READ (5,*) LOADX,LOADY,LOADZ,LOAD
      IF ((RXN.EQ.0).AND.(INCR.EQ.1)) READ (5,*) LOADX,LOADY,LOADZ,LOAD,
     1INCFLG
      IF ((RXN.EQ.1).AND.(INCR.EQ.0)) READ (5,*) RXNREQ,LOADX,LOADY,LOAD
     1Z,LOAD
      IF ((RXN.EQ.1).AND.(INCR.EQ.1)) READ (5,*) RXNREQ,LOADX,LOADY,LOAD
     1Z,LOAD,INCFLG
      IF (RXN.EQ.2) READ (5,*) LOADX,LOADY,LOADZ
      IF (RXN.EQ.0) LOD1=LOAD+LOD1
      IF (RXN.EQ.1) LOD2=LOAD+LOD2
      IF (BWTYPE.NE.1) GO TO 30
      DO 20 I=1,NPX
      IF (LOADX.EQ.X(I)) GO TO 110
20    CONTINUE
30    CONTINUE
      IF (BWTYPE.NE.2) GO TO 50
      DO 40 I=1,NNM,NPYZ
      IF (LOADX.EQ.X(I)) GO TO 110
40    CONTINUE
50    CONTINUE
      IF (BWTYPE.NE.3) GO TO 70
      DO 60 I=1,NNM,NPYZ
      IF (LOADX.EQ.X(I)) GO TO 110
60    CONTINUE
70    CONTINUE
      IF (RXN.EQ.0) WRITE (6,80) LOADX,LOADY,LOADZ,LOAD
      IF (RXN.EQ.1) WRITE (6,90) RXNREQ,LOADX,LOADY,LOADZ,LOAD
      IF (RXN.EQ.2) WRITE (6,100) LOADX,LOADY,LOADZ
80    FORMAT (//,2X,43HL-COORDINATE DID NOT MATCH UP IN THIS LINE:,2X,4(
     1F8.4,3X))
90    FORMAT (//,2X,43HL-COORDINATE DID NOT MATCH UP IN THIS LINE:,2X,I1
     1,3X,4(F8.4,3X))
100   FORMAT (//,2X,43HL-COORDINATE DID NOT MATCH UP IN THIS LINE:,2X,3(
     1F8.4,3X))
110   CONTINUE
      IF (BWTYPE.NE.1) GO TO 130
      DO 120 J=I,NPXY,NPX
      IF (LOADY.EQ.Y(J)) GO TO 210
120   CONTINUE
130   CONTINUE
      IF (BWTYPE.NE.2) GO TO 150
      DO 140 J=I,NNM,NPZ
      IF (LOADY.EQ.Y(J)) GO TO 210
140   CONTINUE
150   CONTINUE
      IF (BWTYPE.NE.3) GO TO 170
      DO 160 J=I,NNM
      IF (LOADY.EQ.Y(J)) GO TO 210
```

```
160   CONTINUE
170   CONTINUE
      IF (RXN.EQ.0) WRITE (6,180) LOADX,LOADY,LOADZ,LOAD
      IF (RXN.EQ.1) WRITE (6,190) RXNREQ,LOADX,LOADY,LOADZ,LOAD
      IF (RXN.EQ.2) WRITE (6,200) LOADX,LOADY,LOADZ
180   FORMAT (//,2X,43HR-COORDINATE DID NOT MATCH UP IN THIS LINE:,2X,4(
     1F8.4,3X))
190   FORMAT (//,2X,43HR-COORDINATE DID NOT MATCH UP IN THIS LINE:,2X,I1
     1,3X,4(F8.4,3X))
200   FORMAT (//,2X,43HR-COORDINATE DID NOT MATCH UP IN THIS LINE:,2X,3(
     1F8.4,3X))
210   CONTINUE
      IF (BWTYPE.NE.1) GO TO 230
      DO 220 K=J,NNM,NPXY
      IF (LOADZ.EQ.Z(K)) GO TO 310
220   CONTINUE
230   CONTINUE
      IF (BWTYPE.NE.2) GO TO 250
      DO 240 K=J,NNM
      IF (LOADZ.EQ.Z(K)) GO TO 310
240   CONTINUE
250   CONTINUE
      IF (BWTYPE.NE.3) GO TO 270
      DO 260 K=J,NNM,NPY
      IF (LOADZ.EQ.Z(K)) GO TO 310
260   CONTINUE
270   CONTINUE
      IF (RXN.EQ.0) WRITE (6,280) LOADX,LOADY,LOADZ,LOAD
      IF (RXN.EQ.1) WRITE (6,290) RXNREQ,LOADX,LOADY,LOADZ,LOAD
      IF (RXN.EQ.2) WRITE (6,300) LOADX,LOADY,LOADZ
280   FORMAT (//,2X,43HT-COORDINATE DID NOT MATCH UP IN THIS LINE:,2X,4(
     1F8.4,3X))
290   FORMAT (//,2X,43HT-COORDINATE DID NOT MATCH UP IN THIS LINE:,2X,I1
     1,3X,4(F8.4,3X))
300   FORMAT (//,2X,43HT-COORDINATE DID NOT MATCH UP IN THIS LINE:,2X,3(
     1F8.4))
310   CONTINUE
      NODNUM=K
      PLACE=PLACE+1
      NODES(PLACE)=(3*(NODNUM-1)+L)
      IF (RXN.NE.2) VALUES(PLACE)=LOAD
      IF (INCFLG.EQ.1) INC=INC+1
      IF ((INCR.EQ.1).AND.(INCFLG.EQ.1)) INCVTR(INC)=NODES(PLACE)
      IF ((RXN.EQ.1).AND.(RXNREQ.EQ.1)) NUMRXN=NUMRXN+1
      IF ((RXN.EQ.1).AND.(RXNREQ.EQ.1)) RXNNOD(NUMRXN)=NODES(PLACE)
320   CONTINUE
330   CONTINUE
      L=L+1
      IF (L.LE.3) GO TO 10
      RETURN
```

```
      END
C     ..................................................................
      SUBROUTINE STRESS (N,NPE,W,IT,TABORT)
C     THIS SUBROUTINE CALCULATES THE STRAINS AND STRESSES FOR EACH ELE-
C     MENT IN A THREE DIMENSIONAL PROBLEM, SMALL STRAINS ASSUMED.
      IMPLICIT REAL*8(A-H,O-Z)
      REAL*8 ACTMC,TT
      INTEGER TABORT
      COMMON /SIGMA/ C,TT
      COMMON /ELK/ ELXYZ
      COMMON /SHAPE/ SF
      COMMON /GSHAPE/ GDSF
      COMMON /MOIST1/ ACTMC
      DIMENSION ACTMC(576)
      DIMENSION W(3,8), S(3,3), C(6,6), ELXYZ(8,3), SF(8), GDSF(3,8)
      TABORT=0
      XI=0.0
      ETA=0.0
      ZETA=0.0
      CALL SF3DL (NPE,XI,ETA,ZETA,DET)
      X=0.0
      Y=0.0
      Z=0.0
      DUDX=0.0
      DUDY=0.0
      DUDZ=0.0
      DVDX=0.0
      DVDY=0.0
      DVDZ=0.0
      DWDX=0.0
      DWDY=0.0
      DWDZ=0.0
      DO 6 I=1,3
      DO 5 J=1,3
      S(I,J)=0.0
5     CONTINUE
6     CONTINUE
      DO 10 I=1,NPE
      X=X+ELXYZ(I,1)*SF(I)
      Y=Y+ELXYZ(I,2)*SF(I)
      Z=Z+ELXYZ(I,3)*SF(I)
C     CALCULATION OF THE STRAIN COMPONENTS FOLLOWS:
      DUDX=DUDX+W(1,I)*GDSF(1,I)
      DUDY=DUDY+W(1,I)*GDSF(2,I)
      DUDZ=DUDZ+W(1,I)*GDSF(3,I)
      DVDX=DVDX+W(2,I)*GDSF(1,I)
      DVDY=DVDY+W(2,I)*GDSF(2,I)
      DVDZ=DVDZ+W(2,I)*GDSF(3,I)
      DWDX=DWDX+W(3,I)*GDSF(1,I)
      DWDY=DWDY+W(3,I)*GDSF(2,I)
```

```
      DWDZ=DWDZ+W(3,I)*GDSF(3,I)
10    CONTINUE
C
C     USE THE ARRAY FOR ACTUAL MOISTURE CONTENTS AS A SCRATCH PAD ONCE
C     THE ACTUAL MOISTURE CONTENTS HAVE BEEN PRINTED OUT.  THIS ARRAY
C     IS USED TO KEEP TRACK OF THE TOTAL LONGITUDINAL STRAINS FOR EACH
C     ELEMENT. ACTMC IS RE-INITIALIZED IN MAIN AFTER THE M.C.'S ARE
C     PRINTED OUT. THIS IS WHERE TENSION STRAIN IS CHECKED TO SEE IF
C     IT EXCEEDS MAXIMUM LIMITS (FROM EXPERIMENTS)
C
      ACTMC(N)=DUDX+ACTMC(N)
      IF (ACTMC(N).GT.TT) TABORT=1
C     CALCULATE STRESS AS THOUGH ELEMENT FAILS AT END OF
C     LOAD/DISPLACEMENT INCREMENT - USER WARNED THAT ELEMENT
C     HAS FAILED DURING THE APPROPRIATE INCREMENT IN MAIN PGM.
C     NOTE: RESULTS WILL NOT BE CONSERVATIVE
C
C     STRESS COMPUTATION FOR 3-D ORTHOTROPIC MATERIALS FOLLOWS:
C     AGAIN, IT IS ASSUMED THAT 1=LONGITUDINAL DIRECTION, 2=RADIAL
C     DIRECTION, AND 3=TANGENTIAL DIRECTION, AS IN SBR CKALC.
      S(1,1)=C(1,1)*DUDX+C(1,2)*DVDY+C(1,3)*DWDZ
      S(2,2)=C(1,2)*DUDX+C(2,2)*DVDY+C(2,3)*DWDZ
      S(3,3)=C(1,3)*DUDX+C(2,3)*DVDY+C(3,3)*DWDZ
      S(2,3)=C(4,4)*(DVDZ+DWDY)
      S(1,3)=C(5,5)*(DWDX+DUDZ)
      S(1,2)=C(6,6)*(DUDY+DVDX)
      IF (N.EQ.1) WRITE (6,20)
20    FORMAT (1H1,24X,20HCENTROID COORDINATES)
      IF (N.EQ.1) WRITE (6,30)
30    FORMAT (2X,8HSTEP NO.,3X,7HEL. NO.,5X,4HLBAR,4X,4HRBAR,4X,4HTBAR,5
     1X,9HSTRESS LL,4X,9HSTRESS RR,4X,9HSTRESS TT,4X,9HSTRESS LR,4X,9HST
     2RESS LT,4X,9HSTRESS RT,/)
      WRITE (6,40) IT,N,X,Y,Z,S(1,1),S(2,2),S(3,3),S(1,2),S(1,3),S(2,3)
40    FORMAT (4X,I3,8X,I3,4X,F7.3,1X,F7.3,1X,F7.3,5X,F9.1,4X,F9.1,4X,F9.
     11,4X,F9.1,4X,F9.1,4X,F9.1)
      RETURN
      END
C     ................................................................
      SUBROUTINE BNDRY (NEQ,HBW,IE,SVAL)
C     THIS SUBROUTINE IMPOSES THE PRESCRIBED BOUNDARY CONDITIONS ON THE
C     SYSTEM MATRIX (BANDED SYMMETRIC MATRIX).  IN THIS SUBROUTINE,
C     GSTIFF IS THE SYSTEM MATRIX (GLOBAL STIFNESS MATRIX)
C     GFORCE IS THE LOAD VECTOR
C     IE IS THE LABEL OF THE VARIABLE THAT IS PRESCRIBED
C     SVAL IS THE VALUE OF THE PRESCRIBED VARIABLE
      IMPLICIT REAL*8(A-H,O-Z)
      INTEGER HBW
      COMMON /GLOBAL/ GSTIFF,GFORCE
      DIMENSION GSTIFF(2772,102), GFORCE(2772)
      IT=HBW-1
```

```
      I=IE-HBW
      DO 10 II=1,IT
      I=I+1
      IF (I.LT.1) GO TO 10
      J=IE-I+1
      GFORCE(I)=GFORCE(I)-GSTIFF(I,J)*SVAL
      GSTIFF(I,J)=0.0
10    CONTINUE
      GSTIFF(IE,1)=1.0
      GFORCE(IE)=SVAL
      I=IE
      DO 20 II=2,HBW
      I=I+1
      IF (I.GT.NEQ) GO TO 20
      GFORCE(I)=GFORCE(I)-GSTIFF(IE,II)*SVAL
      GSTIFF(IE,II)=0.0
20    CONTINUE
      RETURN
      END
C     ..................................................................
      SUBROUTINE SOLVE (NEQ,NBW,IRES)
C     THIS SUBROUTINE SOLVES A BANDED SYMMETRIC SYSTEM OF EQUATIONS.
C     THE BANDED MATRIX IS INPUT THROUGH GSTIFF(NEQ,NBW) IN COMMON.
C     THE RIGHT HAND SIDE IS GFORCE(NEQ) IN COMMON.
C     NEQ IS THE NO. OF EQUATIONS (= ACTUAL NO. OF ROWS)
C     NBW IS THE HALF BANDWIDTH OF THE SYSTEM (=HBW IN MAIN PGM).
C     IN RESOLVING, IRES>0, LEFT HAND SIDE ELIMINATION IS SKIPPED.
      IMPLICIT REAL*8(A-H,O-Z)
      COMMON /GLOBAL/ GSTIFF,GFORCE
      DIMENSION GSTIFF(2772,102), GFORCE(2772)
      MEQNS=NEQ-1
      IF (IRES.GT.0) GO TO 40
      DO 30 NPIV=1,MEQNS
      NPIVOT=NPIV+1
      LSTSUB=NPIV+NBW-1
      IF (LSTSUB.GT.NEQ) LSTSUB=NEQ
      DO 20 NROW=NPIVOT,LSTSUB
C     INVERT ROWS AND COLUMNS FOR ROW FACTOR
      NCOL=NROW-NPIV+1
      FACTOR=GSTIFF(NPIV,NCOL)/GSTIFF(NPIV,1)
      DO 10 NCOL=NROW,LSTSUB
      ICOL=NCOL-NROW+1
      JCOL=NCOL-NPIV+1
10    GSTIFF(NROW,ICOL)=GSTIFF(NROW,ICOL)-FACTOR*GSTIFF(NPIV,JCOL)
20    GFORCE(NROW)=GFORCE(NROW)-FACTOR*GFORCE(NPIV)
30    CONTINUE
      GO TO 70
40    DO 60 NPIV=1,MEQNS
      NPIVOT=NPIV+1
      LSTSUB=NPIV+NBW-1
```

```
      IF (LSTSUB.GT.NEQ) LSTSUB=NEQ
      DO 50 NROW=NPIVOT,LSTSUB
      NCOL=NROW-NPIV+1
      FACTOR=GSTIFF(NPIV,NCOL)/GSTIFF(NPIV,1)
50    GFORCE(NROW)=GFORCE(NROW)-FACTOR*GFORCE(NPIV)
60    CONTINUE
C     BACK SUBSTITUTION
70    DO 90 IJK=2,NEQ
      NPIV=NEQ-IJK+2
      GFORCE(NPIV)=GFORCE(NPIV)/GSTIFF(NPIV,1)
      LSTSUB=NPIV-NBW+1
      IF (LSTSUB.LT.1) LSTSUB=1
      NPIVOT=NPIV-1
      DO 80 JKI=LSTSUB,NPIVOT
      NROW=NPIVOT-JKI+LSTSUB
      NCOL=NPIV-NROW+1
      FACTOR=GSTIFF(NROW,NCOL)
80    GFORCE(NROW)=GFORCE(NROW)-FACTOR*GFORCE(NPIV)
90    CONTINUE
      GFORCE(1)=GFORCE(1)/GSTIFF(1,1)
      RETURN
      END
```

The vita has been removed from the scanned document